OPEN ACCESS

African Journal of **Biotechnology**

July 2019
ISSN 1684-5315
DOI: 10.5897/AJB
www.academicjournals.org

ACADEMIC JOURNALS
expand your knowledge

About AJB

The African Journal of Biotechnology (AJB) is a peer reviewed journal which commenced publication in 2002. AJB publishes articles from all areas of biotechnology including medical and pharmaceutical biotechnology, molecular diagnostics, applied biochemistry, industrial microbiology, molecular biology, bioinformatics, genomics and proteomics, transcriptomics and genome editing, food and agricultural technologies, and metabolic engineering. Manuscripts on economic and ethical issues relating to biotechnology research are also considered.

Indexing

CAB Abstracts, CABI's Global Health Database, Chemical Abstracts (CAS Source Index) Dimensions Database, Google Scholar, Matrix of Information for The Analysis of Journals (MIAR), Microsoft Academic, Research Gate

Open Access Policy

Open Access is a publication model that enables the dissemination of research articles to the global community without restriction through the internet. All articles published under open access can be accessed by anyone with internet connection.

The African Journals of Biotechnology is an Open Access journal. Abstracts and full texts of all articles published in this journal are freely accessible to everyone immediately after publication without any form of restriction.

Article License

All articles published by African Journal of Biotechnology are licensed under the Creative Commons Attribution 4.0 International License. This permits anyone to copy, redistribute, remix, transmit and adapt the work provided the original work and source is appropriately cited. Citation should include the article DOI. The article license is displayed on the abstract page the following statement:

This article is published under the terms of the Creative Commons Attribution License 4.0
Please refer to https://creativecommons.org/licenses/by/4.0/legalcode for details
about Creative Commons Attribution License 4.0

Memberships and Standards

Academic Journals strongly supports the Open Access initiative. Abstracts and full texts of all articles published by Academic Journals are freely accessible to everyone immediately after publication.

Crossref is an association of scholarly publishers that developed Digital Object Identification (DOI) system for the unique identification published materials. Academic Journals is a member of Crossref and uses the DOI system. All articles published by Academic Journals are issued DOI.

Similarity Check powered by iThenticate is an initiative started by CrossRef to help its members actively engage in efforts to prevent scholarly and professional plagiarism. Academic Journals is a member of Similarity Check.

CrossRef Cited-by Linking (formerly Forward Linking) is a service that allows you to discover how your publications are being cited and to incorporate that information into your online publication platform. Academic Journals is a member of CrossRef Cited-by.

Academic Journals is a member of the International Digital Publishing Forum (IDPF). The IDPF is the global trade and standards organization dedicated to the development and promotion of electronic publishing and content consumption.

Contact

Editorial Office: ajb@academicjournals.org

Help Desk: helpdesk@academicjournals.org

Website: http://www.academicjournals.org/journal/AJB

Submit manuscript online http://ms.academicjournals.org

Academic Journals
73023 Victoria Island, Lagos, Nigeria
ICEA Building, 17th Floor,
Kenyatta Avenue, Nairobi, Kenya.

Editor-in-Chief

Editorial Board Members

Table of Content

Molecular characterization of some bacteria isolated from munitions contaminated sites in Kachia Military Firing Range, Kaduna State, Nigeria 585
A. I. Alhaji, B. C. Onusiriuka, D. B. Maikaje, J. A. Appah, P. A. Vantsawa, Y. Magaji, A. A. Haroun, E. E. Oaikhena and E. O. Oladapo

Genetic diversity in some Ghanaian and Malian sorghum [Sorghum bicolor (L) Moench] accessions using SSR markers 591
Andrews Danquah, Isaac K. A. Galyuon, Emmanuel P. Otwe and Daniel K. A. Asante

Effective method to control Vibrio mimicus infection in channel catfish Ictalurus punctatus 603
Yan-Wei Li, Xiang Zhang , Yi-Jie Cai, Shu-Yin Chen, Hong-Yan Sun and Xue-Ming Dan

Morphological and molecular screening of rice accessions for salt tolerance 612
Uyoh E. A., Ntui V. O., Umego C., Ita E. E. and Opara C.

Enhancement of phytoremediation efficiency of Acacia mangium using earthworms in metal-contaminated soil in Bonoua, Ivory Coast 622
BONGOUA-DEVISME Affi Jeanne, AKOTTO Odi Faustin, GUETY Thierry, KOUAKOU Sainte Adélaïde Ahya Edith, NDOYE Fatou and DIOUF Diégane

Review of microfluidics approaches to mimic the kidney
Zach Odeh and Hongli Lin 632

Role of mucous cell and p53 protein in gastroprotective activity of methanolic extracts of Ageratum conyzoides Linn in rats 640
Omotoso D. R., Ajeigbe K. O., Owonikoko W. M., Okwuonu U. C., Akinola A. O., Daramola O. O., Adagboyin O. and Bienonwu E. O.

Modified protocol for RNA isolation from different parts of field-grown jute plant suitable for NGS data generation and quantitative real-time RT-PCR 647
Rasel Ahmed, Md. Sabbir Hossain, Md. Samiul Haque, Md. Monjurul Alam and Md. Shahidul Islam

DNA barcoding of Ghanaian fish species: Status and prospects 659
Gyamfua Afriyie, Shunkai Huang, Zhongdian Dong, Yusong Guo, Felix K. A. Kuebutornye, Christian Ayisi Larbi, Berchie Asiedu and Zhongduo Wang

Genomic sequencing and recombinant expression of proinsulin isolated from cow and buffalo in Pakistan 664
Farheen Aslam, Hooria Younas and Saima Iftikhar Bajwa

Optimization studies of chitin and chitosan production from Penaeus notialis shell waste 670
Amoo K. O., Olafadehan O. A. and Ajayi T. O.

Somatic embryogenesis and regeneration of Kenyan wheat (Triticum aestivum L.) genotypes from mature embryo explants 689
Mark Ochieng Adero, Easter David Syombua, Lydia Kwamboka Asande, Nelson Onzere Amugune, Eliud Sagwa Mulanda and Godwin Macharia

Vol. 18(27), pp. 585-590, July, 2019
DOI: 10.5897/AJB2019.16766
Article Number: E88069F61407
ISSN: 1684-5315

http://www.academicjournals.org/AJB

ACADEMIC JOURNALS
expand your knowledge

African Journal of Biotechnology

Full Length Research Paper

Molecular characterization of some bacteria isolated from munitions contaminated sites in Kachia Military Firing Range, Kaduna State, Nigeria

A. I. Alhaji[1], B. C. Onusiriuka[1], D. B. Maikaje[2], J. A. Appah[1], P. A. Vantsawa[1], Y. Magaji[1], A. A. Haroun[1], E. E. Oaikhena[1*] and E. O. Oladapo[1]

[1]Department of Biological Sciences, Nigerian Defence Academy, Kaduna, Kaduna State, Nigeria.
[2]Department of Microbiology, Faculty of Science, Kaduna State University, Kaduna, Kaduna State, Nigeria.

Received 8 February, 2019; Accepted 1 April, 2019

Environmental pollution is principally caused by human activities that usually result in the release of man–made pollutants such as biological, chemical and radioactive in such states as solid, liquid and gaseous substances into the biosphere via, land, water and air. Globally, the increasing rate of environmental contamination by ammunition/explosives resulting from their increasing deployments in the rising spites of military conflicts and training has certainly become a matter of great concern for every nation. The aim of this research was to molecularly characterize some isolated bacteria from an apparent munitions contaminated sites in Kachia Military Firing Range, Kaduna State. DNA from each isolated bacteria was extracted and 16s rRNA Gene amplified from each isolated bacteria DNA using thermo cycler. The amplified genes were run on Agarose gel plate and visualized. Amplified gene bands were sequenced and Basic Local Alignment Search Tool (BLAST). 16s rRNA gene sequences result aligned with BLAST search of NCBI databases that revealed the presence of *Lysinibacillus pakistanensis, Eschericia coli, Achromobacter spanius, Achromobacter animicus, Escherichia fergusonii and Shigella* sp. The results identified bacteria that were isolated from munitions contaminated sites and that could also be useful for their bioremediation potential against munitions contaminant.

Key words: Environment, pollution, contamination, bacteria, bioremediation.

INTRODUCTION

Globally, the increasing rate of environmental contamination by ammunition/explosives resulting from their increasing deployments in the rising spites of military conflicts and training has certainly become a matter of great concern for every nation. Therefore, there is an urgent need to make provisions for efficient and effective mediation measures to save the affected nation(s) from the danger of environmental contamination by ammunition/explosive toxic substances. Environmental regulations have however not been established for trinitrotoluene (TNT), royal demolition explosive (RDX) and high melting explosive (HMX) in many countries including Nigeria (Rya et al., 2007). United States Environmental Protection Agency (EPA) classified TNT

*Corresponding author. E-mail: oaikhenaeni@yahoo.com.

as a possible human carcinogenic (class C). Explosives are being used by different military formations in test firing, during training of military personnel's which take place in all the military firing ranges across the country in Nigeria and the Nigerian Army School of Artillery (NASA) Kachia, Kaduna State which is the area of study in this research. The formations that carried out training and firing ranges in NASA includes the Nigerian Defence Academy (NDA), Nigerian Air Force Base (NAF), Nigerian Army School of Infantry (NASI) Armed Forces Staff and Command College, Jaji and Defence Industrial Corporation (DICON). So far, no current practice is taking place by the military of Armed Forces of Nigeria for the remediation of the contaminated soil apart from the normal cleaning and burning of the munitions contaminated sites.

The primary human exposure pathways for explosive contaminated soils are dust inhalation, soils ingestion and dermal absorption (Craig et al*.,* 1995). Inhalation of air and consumption of farm products may increase the liveliness of shooters transporting heavy metals and explosives on their hands, hair, skin, clothing, shoes and shooting equipment from the range into their vehicles and homes. Also, wind interaction and rain run offs flow through to the stream in the site of firing range leading to the contamination of air, ground water, soil, plants, animals and other ecological parameters within the sites and its vicinity. In order for a contaminated site to be treated properly, the magnitude, impacts and risks the pollutants impose on the ecological parameters and human health must be assessed. Clean up of the soil and groundwater in such sites is necessary to prevent the spread of contaminants and subsequent injury to the ecosystems. Contaminated soil that contains heavy metals or volatile organic compounds (*VOCs*) have in the past been remediated utilizing the techniques of land farming, soil washing, or soil flushing (described under soil reclamation section) (Fall, 2003).

The chemical, mechanical and thermal treatments (incineration) of lands and water bodies to destroy hazardous wastes have proved to be economically and environmentally unsustainable, hence the shift of focus to biological methods which are cost-effective, environmentally sustainable as well as socially acceptable (Rittmann et al., 1994).

Microorganisms have developed many different strategies for removal and degrading of these xenobiotic compounds; also, oxidative or reductive pathways for the degradation of nitroaromatics have been widely studied (Spain, 1995). Microorganisms with distinctive features of catabolic potential and/or their products such as enzymes and bio surfactant direct use is a novel approach to enhance and boost their remediation efficacy (Le et al., 2017). Microorganisms used for remediation of polluted environment can either be bacteria, fungi, algae or combination of different species. Bacteria rely on various enzymes such as mono and dioxygenases, nitroreductases, haloreductases and esterase to degrade chemicals. These enzymes often need to be induced by the pollutant for degradation to occur (Axtell, 1998). In general, those enzymes metabolize contaminants and are located within the cell. The aim of the research was to molecularly characterize bacteria isolated from munitions contaminated sites in Kachia Military Firing Range, Kaduna.

MATERIALS AND METHODS

Study site

The study was conducted in the permanent military shooting/ training range located at 5 km east of Kachia town in Kaduna State. The range was established in 1965 and it covers an area of about 24.95 km^2 that lies between longitudes 9° 55' N and 7° 58' E, with an elevation of 732 m above sea level (Figure 1). The topography is undulating and the vegetation is Guinea Savannah. The area where the munitions/explosives are fired (the impact area) is a valley consisting of about four large rocks as objectives where the fired munitions/explosives land and explode.

Sampling points

Four sampling points selected for the study are locations 1, 2, 3 and 4. Location 1 and 2 are approximately 200 m from the table top, that is, where the small arms are fired such as Kalashinokov, FN, Grenade, GPMG, SMG and Pistols. The soil in Location 1 and 2 is made of 50% silt and a flat ground with shrubs and drainage that flows through to the farm lands near the sites. Location 3 is approximately 9000 m away from the table top and lies between 9° 53' 44.71" Northings and 7° 53' 17.87" Easting's while Location 4 is ahead of Location 3 and is about 10,000 m from the table top where heavy weapons are aimed at. The impact area of Location 3 and 4 are mainly largely rocks containing high concentration of explosive due to the extensive use of bombardment by the artillery weapons, 155 mm nortwizer, and other heavy weapons.

Soil sampling

This was done at particular sampling areas using soil iron auger. Four locations within NASA shooting/training range Kachia were earmarked as sampling sites for this study. Samples for bacteria analysis were kept in a cool box refrigerated with ice pack to retain the original microbial activities.

Screening for explosive/munitions degrading bacteria

Nutrient agar media preparation

Nutrient Agar (Antec/USA) was prepared by dissolving 28 g of the agar in 1 L of distilled water in a conical flask. The conical flaks with the media was autoclaved at 121°C at 15 Pressure Per Square inch (PSI) for 15 min, cooled to 40°C before dispensing into sterile petri dishes.

Isolation of possible explosives degrading bacteria

Thirty gram samples of soil from selected positive screening tests were placed into flasks and amended with 1% cometabolite

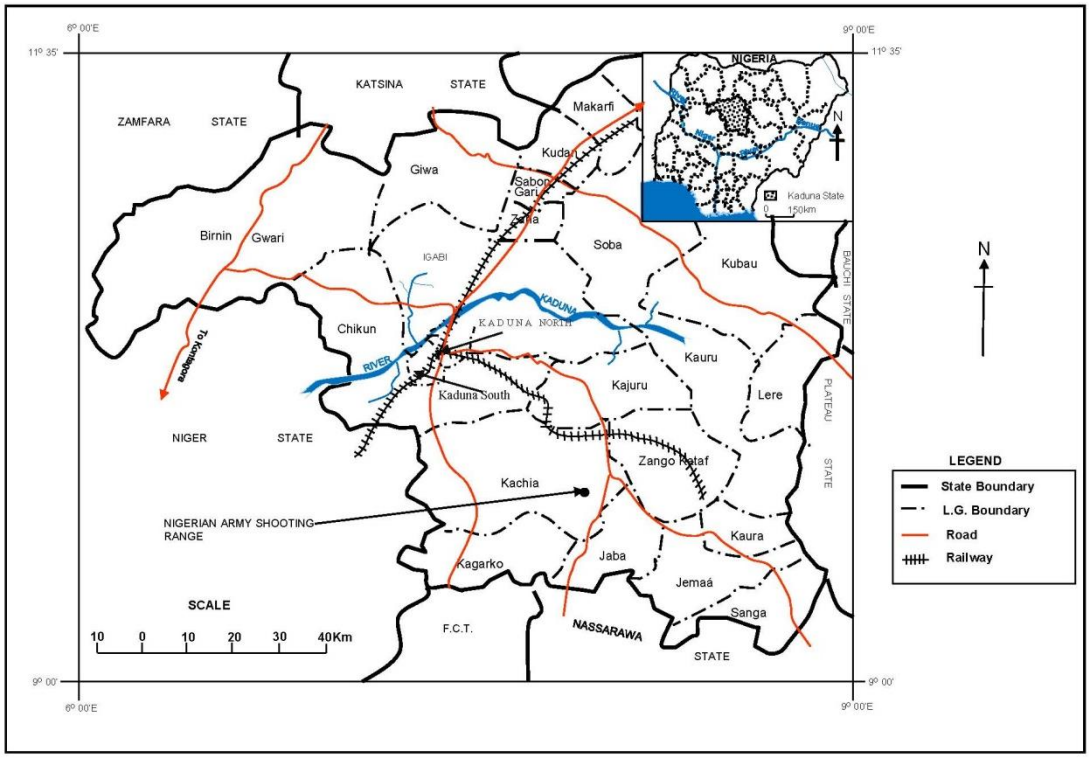

Figure 1. Map of Kaduna State Showing study area (Nigerian Army Shooting Range). Source: Geography Department NDA Kaduna.

(Sodium acetate) and 5 ml of distilled water. Flasks were plugged and incubated at 28°C. After one week of incubation, samples of the acetate primed sterile water were plated onto basal salts medium supplemented with 15 g/L yeast extract that cannot solidify medium Nutrient Agar and the cometabolite at a concentration of 20 g/L and 60 g/ml nystatin to suppress fungal growth. Plates were incubated at 28°C for two weeks. Representative colonies were picked from each plate and transferred to liquid culture media containing 100 mg/L TNT and incubated for 10 days at 28°C on a gyrorotary shaker at 150 rpm. Bacteria Isolates were identified by molecular characterization.

Isolation of genomic DNA from bacteria

Bacteria with proven bioremediation capacity were selected and their DNA isolated. DNA of bacteria strains isolated was extracted from 1 ml of bacteria culture; the culture was pelleted by centrifuging at 12,000 rpm for 2 min. Further, the pellet was treated with lyses solution and proteinase K and incubated at 60°C for 30 min. Nucleic acid was precipitated with isopropanol by centrifuging at 10,000 rpm for 10 min, washed with 1 ml of a 70% (v/v) ethanol solution and dissolved in 0.1 ml of a TE buffer (Tris-EDTA buffer). The purity and quantity of DNA were examined by recording its agarosegel electrophoresis (Jyothi et al*.,* 2012; Thenmozhil et al*.,* 2013).

Polymerase chain reaction amplification of 16S rRNA gene

The PCR reaction mixture containing 10 X PCR buffer, 25 mM, Magnesium chloride, 25 mM dNTP's, 10 pm/ul Primer concentrations and template DNA were used for the amplification of the 16s rRNA gene for each isolates. PCR conditions were optimized using 96-well PCR thermocycler. The PCR Program began with an initial 5-min denaturation step at 94°C: 35 cycles of 94°C for 45 s, annealing (1 min at 55°C), and 10 min extension step at 72°C. All reaction mixtures were preserved at 4°C until it was time for analysis as reported by Kloos et al. (2006).

The amplified 16S rRNA gene of each isolates was further characterized using gel electrophoresis.

Sequence determination of 16s rRNA gene

The amplified 16s rRNA gene of each isolate was processed for sequencing and characterization. The sequencing Kit (Applied Biosystems) with the product was analyzed with ABI prism DNA sequence (ABI). The gene sequence of each isolate obtained in this study was compared with known 16s rRNA gene sequences in the Gene Bank database as described by Jyothi et al. (2012).

RESULTS

16S rRNA gene amplification from bacteria isolates

16s rRNA gene band size of 100bp was observed for each bacteria on the agarose gel isolates from each munition contaminated site (Figure 1). The positive results were obtained as shown in the following DNA samples BB1, BB2, BB3, BB6, BB9, BB10 and BB11

Table 1. Blast results of 16S rRNA sequenced gene for bacteria identification.

Organism code	Accession number	Length	Identity (%)	Identified organism
BB1	MK064218.1	216	100	*Achromobacter animicus*
BB2	MH934930.1	167	99	*Lysinibacillus pakistanensis*
BB3	GU594305.1	392	98	*Escherichia coli*
BB6	KX980487.1	331	100	*Escherichia fergusonii*
BB8	MH934930.1	156	99	*Lysinibacillus pakistanensis*
BB10	JQ428795.1	391	95	*Achromobacter spanius*
BB11	MF104544.1	322	98	*Shigella* sp

while the others have negative results. Meanwhile, the identity of the isolates were further confirmed by 16S rRNA sequencing and BLAST bacterial samples.

16S rRNA gene sequences result

The bacterial 16S rRNA genes were sequenced and the sequenced results were BLAST (Basic Local Alignment Search Tool) using NCBI databases. The sequences aligned showed 100% result similarity with *Achromobacter animicus and Esherichia fergusonii,* 99% similarity with *Lysinibacillus pakistanensis,* 98% similarity with *Esherichia coli,* while *Achromobacter spanius* had 95% similarity. In this result, different species of bacteria strains involved in munition/explosive degradation were highlighted (Table 1).

DISCUSSION

Different metal types are used in munition bodies for steel casing and copper driving band that can lead to accelerated galvanic corrosion, although authigenic mineral precipitation and biological overgrowth may slow corrosion rates (Jurczak and Fabisiak, 2017). Even at low concentration, toxic and mutagenic effects of some explosives to various organisms ranging from microorganisms and humans have been described (Ayoub et al., 2010). Microorganisms have developed many different strategies to remove and degrade these xenobiotic compounds and oxidative or reductive pathways for the degradation of nitro aromatics.

Out of the 14 isolates, 16S rRNA gene was amplified from seven bacteria isolates (Plate 1) and sequenced (Figure 2). The gene sequence from each of the isolates were BLAST (Basic Local Alignment Search Tool) using NCBI databases and identified as *L. pakistanensis, E. coli, A. spanius, A. animicus, E. fergusonii and Shigella* sp (Table 1). The result showed similarity of 100, 99, 98 and 95% with the uploaded gene in the NCBI database gene bank. The differences in genetic makeup might be due to the mutation of their genes caused by the adaptation of the organisms to the environmental change. This work conformed to that of Rajbanshi (2008) who isolated *E. coli, Klebsiella* sp*., Enterobacter* sp*., Flavobacterium* sp*., Bacillus* sp*., Arcobacter* sp*. and Psendomonas* sp*.* as heavy metal tolerant bacteria in treatment plant in Nepali.

Among the seven bacteria isolates, three of the genera, viz; *Achromobacter* sp., *Escherichia* sp. and *Lysinibacillus* sp. were predominant when compared to the other bacteria isolate from the munition contaminated soil samples. This finding is in agreement with Philip et al*.,* (2000) and Gunasekaran et al*.* (2003), whose report revealed that *Bacillus* sp. showed maximum tolerance to Zinc, Copper, Cadium, Nickel, Lead, and Arsenic. The result is also similar with the study that was carried out by Kitts et al*.* (1994) and Kafilzadeh et al*.* (2011) respectively where bacteria strains were isolated indigenously from ammunition contaminated site and identified as follows: *Bacillus, Citrobacter, Escherichia, Klesbsiella, Enterobacter, Achromobacter* and *Shigella*

The dominant groups of bacteria isolated from munition contaminated soil samples were gram negative bacteria and this result corroborates with the report of Kaplan and Kitts (2004). In general, the gram negative bacteria have been reported as the most effective group of hydrocarbon degrading bacteria. Lipopolysaccharide produced in the bacterial membranes of gram negative bacteria supports the formation and stabilization in aqueous system and contributes by increasing the attack surface on the pollutant for subsequent assimilation (Van Hamme et al., 2003).

Bacteria are known to mineralize explosive by primary reduction of nitro group that are amenable to reduction of electrons. It is the combination of these oxidants together with the carbon skeleton that gives an explosive the capability for explosive autocatalytic oxidation. The isolated bacteria can be used to bioremediate munition contaminants in varying degrees and may be used as consortia for bioremediation of soils contaminated with heavy metals and explosive products.

Conclusion

Bioremediation is a rapidly establishing technology for contaminated soil and ground water treatment. For some compounds, it may be the best technology for treatment,

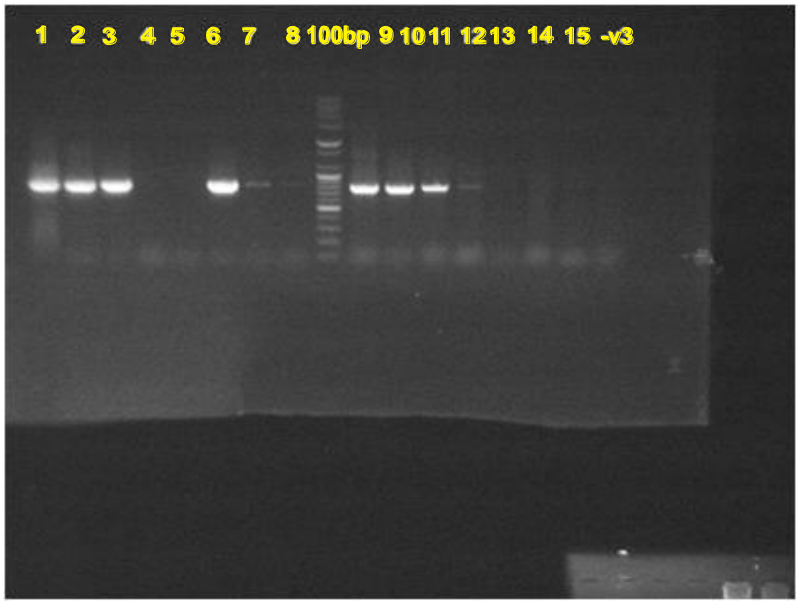

Plate 1. 16S rRNA gene amplification from the isolated munition/explosive degrading bacteria. Lane of 100bp-DNA marker (ladder) lane 1- BB1, Lane 2-BB2. Lane 3- BB3, Lane 6- BB6, Lane 9- BB9, Lane 10-BB10 and Lane 11-BB11.

BB1
ACGCTAGCGGGATGCCTTACACATGCAAGTCGAACGGCAGCACGGACTTCGGTCTGGTGGCGAGTGGCGAACGGGTGAGTAATGTATCGGA
ACGTGCCTAGTAGCGGGGGATAACTACGCGAAAGCGTAGCTAATACCGCATACGCCCTACGGGGGAAAGCAGGGGATCGCAAGACCTTGCA
CTATTAGAGCGGCCGATATCGGATTAGCTAGTTG

BB2
GCCTAATACATGCAAGTCGAGCGATCAGAGAAGGAGCTTGCTCCTTATGACGTTAGCGGCGGACGGGTGAGTAACACGTGGGCAACCTACCC
TATAGTTTGGGATAACTCCGGGAAACCGGGGCTAATACCGAATAATCTATGTCACCTCATGGTGACATACTGAAA

BB3
TCGCTGACGAGTGGCGGACGGGTGAGTAACGTCTGGGAAACTGCCTGATGGAGGGGGATAACTACTGGAAACGGTAGCTAATACGCGATAA
CGTCGCAAGACCAAAGAGGGGGACCTTCGGGCCTCTTGCCATCGGATGTGCCCAGATGGGATTAGCTAGTAGGTGGGGTAACGGCTCACCT
AGGCGACGATCCCTAGCTGGCTTGAGAGGATGACCAGCCACACTGGAACTGAGACACGGTCCAGACTCCTACGGGAGGCAGCAGTGGGGAA
TATTGCACAATGGGCGCAAGCCTGATGCAGCCATGCCGCGTGTATGAAGAAGGCCTTCGGGTTGTAAAGTACTTTCANCGGGGAGGAAGGG
GAGTAAAGTTAATACCTTGTCTCATTGA

BB6
TACTGGAAACGGCAGCCAATACCGCATAACGTCGCAAGACCAAAGAGGGGGACCCTTTCGGGCCTCTTGCCATCGGATGTGCCCAGATGGG
ATTAGCTAGTAGGTGGGGTAACGGCTCACCTAGGCGACGATCCCTAGCTGGTCTGAGAGGATGACCAGCCACACTGGAACTGAGACACGGT
CCAGACTCCTACGGGAGGCAGCAGTGGGGAATATTGCACAATGGGCGCAAGCCTGATGCAGCCATGCCGCGTGTATGAAGAAGGCCTTCGG
GTTGTAAAGTACTTTCANCGGGGAGGAAGGGAGTAAAGTTAATACCTTTGCTCATTGA

BB8
GCGAACGAGAAGGAGCTTGCTCCTTTGACGTTAGCGGCGGACGGGTGAGTAACACGTGGGCAACCTACCCTATAGTTTGGGATAACTCCGG
GAAACCGGGGCTAATACCGAATAATCTATGTCCCCTCATGGTGACATACTGAAAGACGGTTTCCG

BB10
CCTAACACATGCAAGTCAGAACGGCTACGCACGAGACGTATCGGTCTGGTGGCAGAGTGGCGAACGGGTGAGTAATGTATCGGAACGTGCC
TAGTAGCGTGGGGATAACAACGCGACAAGCGTAGCTAATACCGCATACGCCCTACGGGGGAAAGCAGGGGATCGCAAGACCTTGCACTATTA
GAGCGGCCGATATCGGATTAGCTAGTTGGTGGGGTAACGGCTCACCAAGGCGACGATCCGTAGCTGGTTTGAGAGGACGACCAGCCACACT
GGGACTGACGACACGGCCCAGACTCCTACGGGAGGCAGCAGTGGGGAATTCTTGGACAATGGGGGAAACCCTTGATCCCCGCCCTTCCCGC
GTTGTGCGATTCGACCCGCTTTCTTG

BB11
CGGTAACAGGAANCANGCTTGCTGCTTCGCTGACGAGTGGNGGACGGGTGACTAATGTCTGGGAAACTGCCTGATGGAGGGGGATAACTAC
TGGAAACGGTAGCTAATACCGCATAACGTCGCAAGACCAAAGAGGGGGACCTTCGGGCCTCTTGCCATCGGATGTGCCCAGATGGGATTAGC
TAGTAGCTGGGGTAACGGCTCACCTAGGCGACGATCCCTAGCTGGTCTGAGAGGATGACCAGCCACACTGGAACTGAGACACGGTCCANAC
TCCTACGGGAGGCAGCAGTGGGGAATATTGCACAATGGGCGCAAGTCC

Figure 2. Sequence results of 16S rRNA sequenced bacteria gene.

particularly in sites where it is difficult to access the contamination such as in deeper aquifers. It was observed from this study that munitions-explosives degrading bacteria are ever-present in the study site and they can be isolated as indigenous bacteria. It is observed from this study that bacterial strain isolated from contaminated soil can be good heavy metal and explosives degraders. Therefore, isolated bacteria can be capable of bioremediation of munition contaminants in varying degrees and should be used as consortia for bioremediation of soils contaminated with heavy metals and explosive products.

CONFLICT OF INTERESTS

The authors have not declared any conflict of interests.

REFERENCES

Axtell CA (1998). Bioremediation of soil contaminated with explosives. Msc Thesis, University of Northern Lowe.

Ayoub K, van Hullebusch ED, Cassir M, Bermond A (2010). Application of advanced oxidation processes for TNT removal: a review. Journal 0f Hazardous Materials 178(1):10-28.

Craig H, Nelson MD,Sisk WE, Dana WH (1995). Bioremediation of Explosives contaminated Soils: A status Review In: proceedings of the 10th Annual Conference on Hazardous Waste Research 164.

Fall (2003). Restoration and Reclamation Review (1996-2003). Student Journal for the university of Minnesota'sn Restoration and Reclamation Ecology Class (Hort 5015/5071). Http://hdl.handle.net/11299/55448

Gunasekaran K, Tsai C, Kumar S, Zamuy D, Nussinov R (2003). Extended disordered proteins, targeting function with fewer scaffolds. Trends Biochemical Science 28(2):81-85.

Jurczak W, Fabisiak J (2017). Corrosion of ammunition dumped in the Baltic Sea. Journal of *Konbin* 41(1):227-246.

Jyothi K, Surendra KB, Nancy CK, Kashyap A (2012). Identification and isolation of Hydrocarbon Explosives Degrading Bacteria by Molecular Characterization. Helix 2:105-111.

Kafilzadeh F, Parvaneh S, Hooshang J, Ayaghoob T (2011). Isolation and identification of Hydrocarbens and toxic metals in degrading Bacteria by molecular characterization. Helix 2:105-111.

Kaplan CW, Kitts CL (2004). Bacterial succession in a petroleum land treatment unit. Applied Environmental Microbiology 70(3):1777-1786.

Kitts CL, Cunningham DP, Unkefer PJ (1994). Isolation of three hexahydro- 1,3,5-trinitro- 1,3,5-triazine degrading species of the family Enterobacteriaceae from nitriamine explosive-contaminated soil. Applied Environmental Microbiology 60(12):4608-4611.

Kloos K, Munch JC, Scholater M (2006). A new method for the detection of Alkane Homologens genes (ALKB) in soil based on PCR *Hybridization.* Journal of Microbiology Method 66(3):486-496.

Le TT, Son MH, Nam HI, Yoon H, Kang GH, Chang YS (2017). Transformation of hexabromocyclododecane in contaminated soil in association with microbial diversity. Journal of Hazardous Materials 325:82-89.

Philip L, Iyengar L, Venkobacter L (2000). Site of interaction of copper on Bacillus polymyxa. Water, Air and Soil Pollution 119:11-21.

Rajbanshi A (2008). Study on heavy Metal Resistant Bacteria in Guheswori Sewage Treatment Plant. Our Nature 6(1):52-57

Rittmann BE, Eric S, Brian AW (1994). *In situ* Bioremediation (second edition). *In Situ* Bioremediation, second edition. Noyes Publications, Park Ridge, New Jersey pp. 61-63, 205, 219-220.

Rya H, Han JK, Jung JW (2007). Human health risk assessment of explosives and heavy metals at a military gunnery range. Environmental Geochemistry Health 29(4):59-269.

Spain JC (1995). Biodegraration of nitroaromatic compounds. Annual Microbiology 49:523-555

Thenmozhil R, Arumugan K, Nagasathya A, Thajuddin N, Paneerselvam A (2013). Studies on mycroremediation of used engine oil contaminated Soil Samples. Advances in Applied Science Research 4 (2):110-118.

Van Hamme JD, Singh A, Ward OP (2003). Recent advances in petroleum microbiology. Microbiology and Molecular Biology Reviews 67(4):503-549.

Vol. 18(27), pp. 591-602, July, 2019
DOI: 10.5897/AJB2019.16767
Article Number: C8FC9A961409
ISSN: 1684-5315

http://www.academicjournals.org/AJB

ACADEMIC JOURNALS
expand your knowledge

African Journal of Biotechnology

Full Length Research Paper

Genetic diversity in some Ghanaian and Malian sorghum [*Sorghum bicolor* (L) Moench] accessions using SSR markers

Andrews Danquah[1]*, Isaac K. A. Galyuon[1,2], Emmanuel P. Otwe[1] and Daniel K. A. Asante[1]

[1]Department of Molecular Biology and Biotechnology, School of Biological Sciences, College of Agriculture and Natural Sciences, University of Cape Coast, Ghana.
[2]Department of Mathematics and Science, College of Distance Education, University of Cape Coast, Cape Coast, Ghana.

Received 9 February 2019; Accepted 26 June 2019

The study was carried out to assess genetic diversity among forty-one sorghum accessions obtained from Savanna Agricultural Research Institute (SARI), Nyankpala, Northern Region of Ghana and the germplasm collection of Department of Molecular Biology and Biotechnology, University of Cape Coast. Genetic diversity and relationship among the forty-one accessions were evaluated using 22 microsatellite primers. The 22 markers generated 92 alleles, with a mean of 4.2, indicating an average range of diversity. The average polymorphic information content (PIC) was 0.44, indicating that the microsatellites were informative. The cluster analysis grouped the 41 cultivars into seven distinct clusters. The most genetically distinct genotypes were Edipipii, Jibare and Belkozia, which did not cluster with any other line. The similarity between the sorghum accessions ranged from 77 to 100%. Observed heterozygosity ranged from 0 to 0.17 with an average of 0.03 per locus. Results of this study indicated that the landraces were related, and were probably exchanged between farmers in the collection regions, with some duplication found in the material, indicating that there must have been a common source of material somewhere in the history of the breeding programmes. Nonetheless, the Edipipii, Jibare and Belkozia could be exploited in breeding programmes to transfer desirable traits into elite Ghanaian sorghum cultivars.

Key words: Sorghum, simple sequence repeats (SSRs), genetic diversity, polymorphic information content (PIC).

INTRODUCTION

Sorghum is one of the most important food and feed crops in the arid and semi-arid regions of the world (Sanchez et al., 2002), and especially the northern regions of Ghana. Grain sorghum is the fifth most planted cereal crop in the world and represents the only viable food grain for many of the world's most food-insecure people (Zhihong et al., 2008). While the global population will increase from about seven to nine billion by 2050,

*Corresponding author. E-mail: andrews.danquah@ucc.edu.gh.

most of the increase will occur in sub-Saharan Africa, where population growth is among the highest in the world (Haub, 2013). This will increase the risk of food insecurity in sub-Saharan Africa (United Nations Development Programme (UNDP), 2012). Feeding more people with less water is a major challenge facing humanity (Foley et al., 2011), requiring crops that are highly adapted to dry environments.

Climate change can have a big impact on Africa's food availability and security. A report by the IPCC (2014) indicates that, over the next 100 years, the average temperature in Africa will rise by 3 to 4°C resulting in the continent becoming generally drier than it is currently (Africa Harvest, 2007). Despite the threat of climate change and global warming leading to variable and drier climate, there is still no clear policy and government commitment for the development of sorghum, which can be used as a model for developing crops for a changing climate.

Analysis of genetic diversity in crops is important for crop improvement and provides essential information to enable more efficient use of available genetic resources (Mohammadi and Prasanna, 2003). Additionally, it is a platform for stratified sampling of breeding populations by grouping populations into subgroups with similar genetic characteristics (Mohammadi and Prasanna, 2003). Accurate assessment of the levels and patterns of diversity can be invaluable in the analysis of genetic variability in cultivars (Smith, 1984; Cox et al., 1986), identification of diverse parental combinations to create segregating progenies with maximum genetic variability for further selection (Barrett and Kidwell, 1998) and in introgressing desirable genes from diverse germplasm into the available genetic base (Thompson et al., 1998). Understanding of genetic relationships among inbred or pure lines can be useful for the planning of crosses, assigning lines to specific heterotic groups and for precise identification with respect to plant varietal protection (Mohammadi and Prasanna, 2003). Presently, there is an incomplete national core collection of sorghum germplasm and insufficient information on the genetic variability of sorghum varieties cultivated by farmers in Ghana. Limited genetic information is therefore available to establish the identity of these accessions in the national collection and develop a national core collection for sorghum. Studying the extent and structure of genetic diversity in germplasm accessions, through characterization, is essential for better understanding of the evolutionary trends, management of gene-banks and development of strategies for the collection and conservation of the germplasm. The use of molecular markers, particularly DNA-based polymorphisms, which detect variation at the DNA sequence level (Smith and Smith, 1992), has become an increasingly useful and powerful tool in the assessment of genetic similarity and manipulation of important agronomic traits in breeding stocks (Lee, 1995). For any effective breeding and selection programme, there is the need to assess the support breeding programmes with exotic genetic resources or not. Therefore, this study sought to assess the genetic diversity of Ghanaian and Malian sorghum germplasm using SSR markers in order to provide information necessary to improve the current accessions through breeding and selection for desirable characteristics.

MATERIALS AND METHODS

Sorghum seeds were obtained from the Department of Molecular Biology and Biotechnology of the School of Biological Sciences, College of Agriculture and Natural Sciences, University of Cape Coast. Seeds of 7 cultivars (Dorado, Kapaala, Kadaga, Naga White, Bawku Red, GO-1 and GO-2), originally obtained by the Department from the Savannah Agricultural Research Institute (SARI), Manga Station in Bawku, were used. Seeds of 34 sorghum accessions were also obtained from the sorghum germplasm collection currently held at the Savanna Agriculture Research Institute (SARI) - Nyankpala in the Northern Region of Ghana, making a total of 41 sorghum accessions. Passport data for these accessions were recorded (Table 1). These cultivars were selected because they had 90 to 100% germination rates and are cultivated in the semi-arid regions of Africa.

DNA extraction

The sorghum seedlings were germinated in Petri-dishes lined with moistened Whatman No.1 filter papers and incubated at 30°C. After germination, the young shoots were harvested and stored at -20°C for DNA extraction. DNA was extracted using the ZR Plant/Seed DNA MiniPrep™ Extraction Kit D6020 (ZYMO RESEARCH CORP.; IRVINE, CA-USA) using manufacturer's protocol.

Polymerase chain reaction (PCR) amplification of SSRs

Twenty-five pairs of SSR primers were procured from Inqaba Biotechnical Industries (Pty) Ltd. The primer pairs chosen have been used in other sorghum genetic diversity studies (Ali et al., 2008; Pei et al., 2010). Of these, 22 displayed polymorphism in a preliminary study and these were used for genetic diversity analysis (Table 2). Details of the primer sequences and type of microsatellite repeats are publicly available (http://sorgblast2.tamu.edu/SorghumGenome/Mapping/Markers/SSR.html#217). PCR reactions were conducted in a TECHNE TC 512 PCR System in 25 µl reaction mixtures in 96-well plates. The mixture contained 12.5 µl One Taq Quick-Load 2x Master Mix with Standard Buffer (NEW ENGLAND BIOLABS) comprising 20mM Tris-HCl (pH 8.9 at 25°C), 1.8 mM $MgCl_2$, 22 mM NH_4Cl, 22 mM KCl, 0.2 mM dNTPs, 5% glycerol, 0.06% IGEPAL*CA-630 (Rhodia Operations), 0.05% Tween*20 (Uniqema Ameracas LLC), Xylene Cyanol FF, Tartrazine, 25 units/ml One Taq DNA Polymerase; and 0.5 µl of the 10 µM Forward Primer, 0.5 µl of the 10 µM Reverse Primer, 10.5 µl Nuclease-Free water and 1 µl genomic DNA. The PCR programme consisted of an initial denaturation for 30 s (s) at 94°C and then 30 cycles of denaturation for 30 s at 94°C, annealing at 57°C (55 or 60°C) for 60 s, depending on the annealing temperature for the primer, and extension at 72°C for 60 s. The last PCR cycle was followed by a 5 min extension at 72°C and then put on hold at 10°C, at infinity (∞). The amplified products were stored at -20°C until they were needed to run gels (Table 2).

Table 1. Sorghum accessions collected from SARI – Nyankpala and Manga Stations.

ACC No.	District	Location	Local name	Desirable trait
SARSORG 04	Sissala West	Sorbelle	Chodiri	Striga resistant
SARSORG 05	Sissala West	Sorbelle	Buyele Kadapula	Striga tolerant
SARSORG 06	Sissala West	Sorbelle	Kadaga	Medium maturing
SARSORG 14	Sissala West	Zini	Gongo	No fertilizer application
SARSORG 16	Jirapa Lambusie	Pina	Dorado	Early maturing and drought tolerant
SARSORG 26	Lawra	Kuwari/ Eremon	Jibare	Can be cultivated on marginal land
SARSORG 39	Wa Central	Kampaala	Charie	
SARSORG 40	Sawla Tuna Kalba	Gindabuo	Kapaala	Drought tolerant, higher yield and early maturing
SARSORG 55	Savelugu Nantom	Kanshegu	Kazegu	Early maturity
SARSORG 57	Savelugu Nantom	Tiego-zoo	Kapiela	
SARSORG 65	Central Gonja	Sankpagla	Kapagnin-sablinli (Kazinli)	High yielding
SARSORG 66	Central Gonja	Sankpagla	Kapagninzie (Kukohibua)	Early maturity
SARSORG 69	Central Gonja	Sankpagla	Mankariga	Weeds tolerant
SARSORG 75	Central Gonja	Mankpang	Ayu	
SARSORG 87	Nanumba South	Nyankpani	Edipii	
SARSORG 108	Saboba	Wandamdo	Bonaje	Drought tolerant
SARSORG 111	Saboba	Nankpando	Edepipii	
SARSORG 112	Chereponi	Achuma	Nganikokole	
SARSORG 124	Karaga	Kariboyili	Bankanyinkpe	
SARSORG 130	East Mamprusi	Nyingari	Kazegupieli	Striga tolerant
SARSORG 132	East Mamprusi	Nyingari	Baninga	
SARSORG 137	West Mamprusi	Wungu-Naabofong	Nangruma	Striga tolerant
SARSORG 138	West Mamprusi	Wungu-Naabofong	Belko	Striga tolerant
SARSORG 145	Talensi Nabdam	Tindong	Cheto	Drought tolerant
SARSORG 148	Bolga Municipal	Gowrie	Kundabua	
SARSORG 153	Bongo	Feo	Naga white	Early maturing
SARSORG 167	Kassena Nankana East	Doba	Baninga	Striga tolerant
SARSORG 169	Bunkpurugu-Yunyoo	Kauk	Demonau	
SARSORG 175	Garu-Tempane	Denugu	Belkozia	
SARSORG 176	Bunkpurugu-Yunyoo	Kauk	Demonjack	
SARSORG 178	Garu-Tempane	Kuka-Zuli	Belko-peelik	
SARSORG 186	Bawku West	Kusasi	Bawku red	High yielding
SARSORG 187	Bawku West	Googo	GO-1	
SARSORG 195	Savelugu-Nantom	Nanton	Kalazie	High yielding
SARSORG 200	Nanumba North	Toanayili	Idimai (red)	Striga tolerant, high yielding
SARSORG 204	Gushegu/karaga	Zantili	Bochachi	High yielding
SARSORG 219	Bawku Municipality	Bankango	Amoro (1)	High yielding
SARSORG 220	Bawku Municipality	Narango	Amoro (2)	
MALISOR 92-1		Segou	Seguifa	
IS 15401			Soumalemba	
		Koutiala	Dua-G	
			GO-2	

Gel electrophoresis of PCR products

Gel electrophoresis was run using a 2.5% agarose gel. The gel contained 6.25 g of agarose, weighed using a Mettler Toledo Electronic Balance (PG-203), dissolved in 250 ml TAE in a conical flask (volume of flask is required) and the mouth covered with cotton wool. The mixture was then heated in a microwave (Panasonic NN-SM322M) to dissolve finally and allowed to cool to about 60°C and 5 µl of ethidium bromide added. This was swirled gently to avoid bubbling and when cooled, the solution was poured into a mould with comb placed on a level surface and allowed to cool and solidify. The comb was gently removed and the gel was transferred into an electrophoretic tank (BIO RAD Mini-Sub® Cell GT) filled with 1X TAE buffer. PCR products of 10 µl were loaded into each well and run at 90 V for 45 min. The gel was then observed under an UV transilluminator (model M-15, UVP Inc., USA) and photomicrographs processed and printed using a Canon IXUS camera.

Analysis of PCR products

Scoring of SSR bands

Bands on the processed contact film or scanned images were used for scoring the size of SSR bands obtained. For each gel, the distance travelled by each marker size of the DNA ladder was measured. The size of the DNA fragments was determined relative to the size standard from the Quick-Load® 50 bp DNA Ladder (NEW ENGLAND BioLabs® Inc.). Allelic data for each locus was recorded as fragment size in comparison with a standard 50 bp DNA ladder and also as binary data coded as 1 or 0 for the presence or absence for each allele.

Analysis of data, genotyping and determination of genetic diversity

Bands for the same SSR locus with different molecular weights were scored as alleles. Alleles for each SSR locus were scored for each sorghum line. Where an allele was present it was scored as one (1) and zero (0) when absent. The binary data matrix generated from this scoring was used to calculate a similarity matrix using the Nei and Lei (1979) coefficient. Cluster analysis was conducted using the Unweighted Paired Group Method using Arithmetic Averages (UPGMA) as defined by Sneath and Sokal (1973) to produce dendrograms of genetic similarities using the Numerical Taxonomy and Multivariate Analysis System software (NTSTSpc) version 2.1 (Exeter Software, New York) and Paleontological Statistics software.

Genetic diversity for each marker was calculated according to the following equation of Nei (1973):

Genetic diversity = $1- \Sigma P_{ij}^2$,

Where; P_{ij} is the frequency of j^{th} allele for the i^{th} locus summed across all the alleles of the locus. Calculated in this manner, the genetic diversity is synonymous with the term polymorphic information content (PIC) described by Anderson et al. (1993).

RESULTS

Performance of SSRs markers

The major allele frequency, number of alleles produced, gene diversity, heterozygosity and the PIC values of the 22 SSR loci examined are presented in Table 3. Samples of DNA profile generated by two of the primers, Xtxp57 and Xtxp321 are shown in Figure 1.

A total of 92 alleles were detected among the 41 genotypes. The number of alleles per locus ranged from 2 (*Xtxp278* and *Xtxp283*) to 7 (*Xtxp319*) and the mean number of alleles was 4.2. The observed heterozygosity (H_o) ranged from 0.0 (*Xtxp*57, *Xtxp*321, *Xtxp*256, *Xtxp*211, *Xtxp278, Xtxp283, Xtxp230, Xtxp296, Xtxp298* and *Kaf2e*) to 0.17 (*Xtxp*270), with an average of 0.03 per locus. Seven loci (*Xtxp145, Xtxp196, Xtxp319, Xtxp270, Xtxp289, Xtxp295,* and *Xtxp285)* had observed heterozygosity values at each locus across all accessions higher than the average.

The PIC values for the microsatellite loci ranged from 0.05 (*Xtxp278*) to 0.78 (*Xtxp319*) with a mean of 0.45 (Table 3). Based on their individual PIC values, seven of the primer pairs were moderately informative (0.25<PIC<0.5), while nine primer pairs were highly informative (PIC>0.5). Even though the mean number of alleles per locus detected in the 41 sorghum accessions was 4.2, the average PIC value of 0.45 gave an indication that the microsatellite markers were informative (Table 3). *Xtxp319* had the lowest major allele frequency (0.27) and *Xtxp278* had the highest (0.98) with a mean of 0.63.

Genetic diversity among the 41 sorghum genotypes

PCR products from these 22 pairs of SSR primers were used to evaluate genetic diversity in the 41 sorghum lines. Genetic relationships between the lines studied, based on the cluster analysis, are presented in a dendrogram (Figure 2). The set of markers used was able to uniquely classify the 41 lines into seven distinct groups, indicating that genetic diversity existed among them. The most genetically distinct genotypes were ‘Edepipii’, ‘Jibare’ and ‘Belkozia’, which did not cluster with any other line.

The largest group consisted of 19 genotypes in cluster five with ‘Demonau’ and ‘GO-1’ at one end and ‘Amoro_2’ at the other (Figure 2). This group was subdivided into five, but there was minimal diversity between these lines with the first subgroup containing ‘Kazegupiele’ and ‘Mankariga’ with coefficient of 1 showing close similarity among them. ‘Cheto’ also clustered with ‘Kazegupiele’ and ‘Mankariga’ at 0.88 coefficient of similarity. The other members in the group are ‘Demonau’ and ‘GO-1’, which clustered at a similarity coefficient of 0.95, quite similar to each other.

The rest in the group were ‘Kapagninsablini’ and‘Gongo’, which also clustered with ‘Demonau’ and ‘GO-1’. The second sub-group was‘ Buyele_Kadapale’ and ‘Kalazie’, which had a coefficient of 1 showing close

Table 2. Sequence of SSR primers and their annealing temperatures used for genetic diversity analysis among the sorghum genotypes.

Primer name	Primer sequence 5^1 - 3^1	Annealing temperature (°C)
Xtxp57	Forward: GGAACTTTTGACGGGTAGTGC Reverse: CGATCGTGATGTCCCAATC	60
Xtxp321	Forward: TAACCCAAGCCTGAGCATAAGA Reverse: CCCATTCACACATGAGACGAG	60
Kaf2e	Forward: TCGGCGAGCATCTTACA Reverse: TACGTAGGCGGTTGGATT	57
Xtxp258	Forward: CACCAAGTGTCGCGAACTGAA Reverse: GCTTAGTGTGAGCGCTGACCAG	62
Xtxp145	Forward: GTTCCTCCTGCCATTACT Reverse: CTTCCGCACATCCAC	57
Xtxp107	Forward: CAAAGTGAGCGTGGTC Reverse: GGACAGGGATAACATAACATA	56.7
Xtxp196	Forward: CAGCGAGTGCAAGGA Reverse: CGAAGCTGGCGAAGT	56.2
Xtxp319	Forward: TAGACATCTGAATTAAGGAGC Reverse: CATGCCCCTGAAAGAGA	57
Xtxp211	Forward: TCAACGGCCAATGATTTCTAAC Reverse: AGGTTGCGAATAAAAGGTAATGTG	59
Xtxp278	Forward: GGGTTTCAACTCTAGCCTACCGAACTTCCT Reverse: ATGCCTCATCATGGTTCGTTTTGCTT	63
Xtxp205	Forward: CCTGCCGTGTCTTCC Reverse: TATATGCATGCCGTAGATTT	56
Xtxp208	Forward: AAGGCCGTGAGGATG Reverse: AAGCAGCCAAGAGCAG	56.2
Xtxp270	Forward: AGCAAGAAGAAGGCAAGAAGAAGG Reverse: GCGAAATTATTTGAAATGGAGTTGA	62
Xtxp289	Forward: AAGTGGGGTGAAGAGATA Reverse: CTGCCTTTCCGACTC	56
Xtxp283	Forward: CGCCCGAACTCTTCTTAAATCT Reverse: ATTATGCCCTAACTGCCTTTGA	60
Xtxp231	Forward: GGAAATCCAGGATAGGGT Reverse: AGGCAAAGGGTCATCA	57.6
Xtxp230	Forward: GCTACCGCTGCTGCTCT Reverse: AGGGGGCATCCAAGAAAT	57.6
Xtxp295	Forward: AAATCATGCATCCATGTTCGTCTTG Reverse: CTCCCGCTACAAGAGTACATTCATAGCTTA	61

Table 2 Cont'd

Xtxp273	Forward: GTACCCATTTAAATTGTTTGCAGTAG Reverse: CAGAGGAGGAGGAAGAGAAGG	60
Xtxp285	Forward: ATTTGATTCTTCTTGCTTTGCCTTGT Reverse: TTGTCATTTCCCCCTTCTTTCTTTT	59
Xtxp296	Forward: CAGAAATAACATATAATGATGGGGTGAA Reverse: ATGCTGTTATGATTTAGAGCCTGTAGAGTT	60
Xtxp298	Forward: GCATGTGTCAGATGATCTGGTGA Reverse: GCTGTTAGCTTCTTCTAATCGTCGGT	62

Table 3. Major allele frequency, number of alleles, gene diversity, heterozygosity and polymorphism information content for the primers used in this study.

Marker	Major allele frequency	No. of alleles	Gene diversity	Hetero-zygosity	PIC
Kaf2e	0.56	4.00	0.56	0.00	0.49
Xtxp57	0.83	3.00	0.30	0.00	0.28
Xtxp107	0.41	6.00	0.75	0.02	0.71
Xtxp145	0.76	4.00	0.41	0.10	0.38
Xtxp196	0.60	4.00	0.56	0.07	0.51
Xtxp205	0.94	3.00	0.12	0.02	0.11
Xtxp208	0.95	4.00	0.09	0.02	0.09
Xtxp211	0.93	3.00	0.14	0.00	0.13
Xtxp230	0.32	5.00	0.74	0.00	0.70
Xtxp231	0.89	3.00	0.20	0.02	0.19
Xtxp256	0.63	3.00	0.52	0.00	0.46
Xtxp270	0.48	6.00	0.71	0.17	0.68
Xtxp273	0.67	5.00	0.50	0.02	0.46
Xtxp278	0.98	2.00	0.05	0.00	0.05
Xtxp283	0.88	2.00	0.21	0.00	0.19
Xtxp285	0.34	5.00	0.77	0.05	0.73
Xtxp289	0.44	6.00	0.67	0.05	0.62
Xtxp295	0.34	6.00	0.76	0.05	0.73
Xtxp296	0.56	3.00	0.56	0.00	0.48
Xtxp298	0.37	5.00	0.73	0.00	0.68
Xtxp319	0.27	7.00	0.80	0.05	0.78
Xtxp321	0.73	3.00	0.41	0.00	0.36
Mean	0.63	4.18	0.48	0.03	0.44

relatedness between the two accessions. 'Dua-G' clustered with 'Buyele_Kadapale' and 'Kalazie' at coefficient of 0.95. 'Ayu' also clustered with 'Buyele_Kadapale', 'Kalazie' and 'Dua-G'. 'Belko-peelik' then clustered with 'Ayu', 'Buyele_Kadapale', 'Kalazie' and 'Dua-G' at similarity coefficient of 0.86. The third sub-group had 'GO-2' and 'Kundabua', which were 90% similar and also clustered with 'Kapagninzie' at similarity coefficient of 0.85. The fourth sub-group contained 'Chodiri', 'Kazegu', 'Edipii' and 'Amoro-2'. 'Edipii' and'Kazegu' were also 90% similar, indicating they are closely related genotypes. The first group contained only one accession 'Edepipii', which was least, related to the other genotypes at similarity coefficient value of 0.67. The second group included 'Baninga' at one end and 'Kapiale' at the other end. Furthermore, a high level of genetic

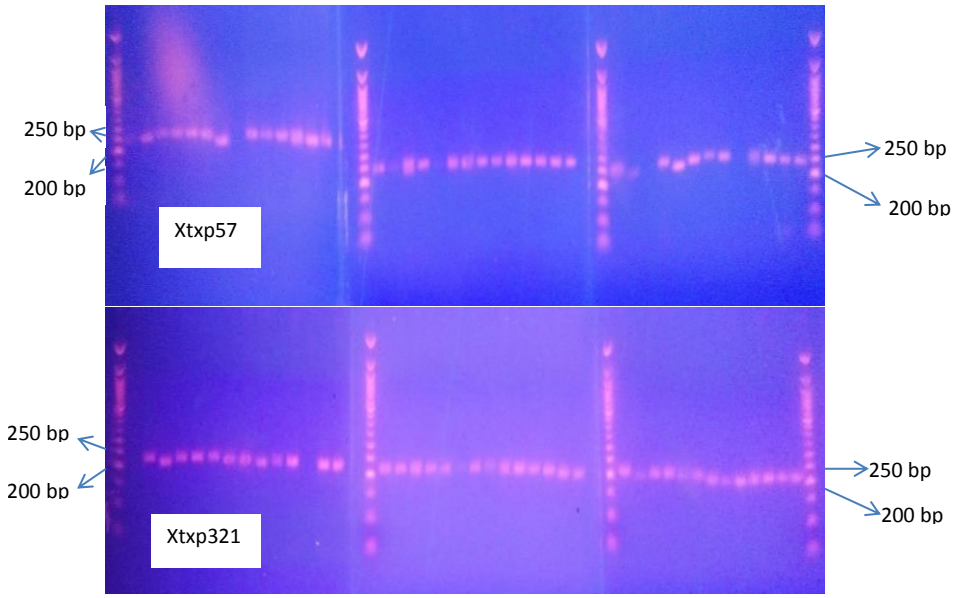

Figure 1. SSR markers profile among sorghum accessions generated using primers *Xtxp57* and *Xtxp321*.

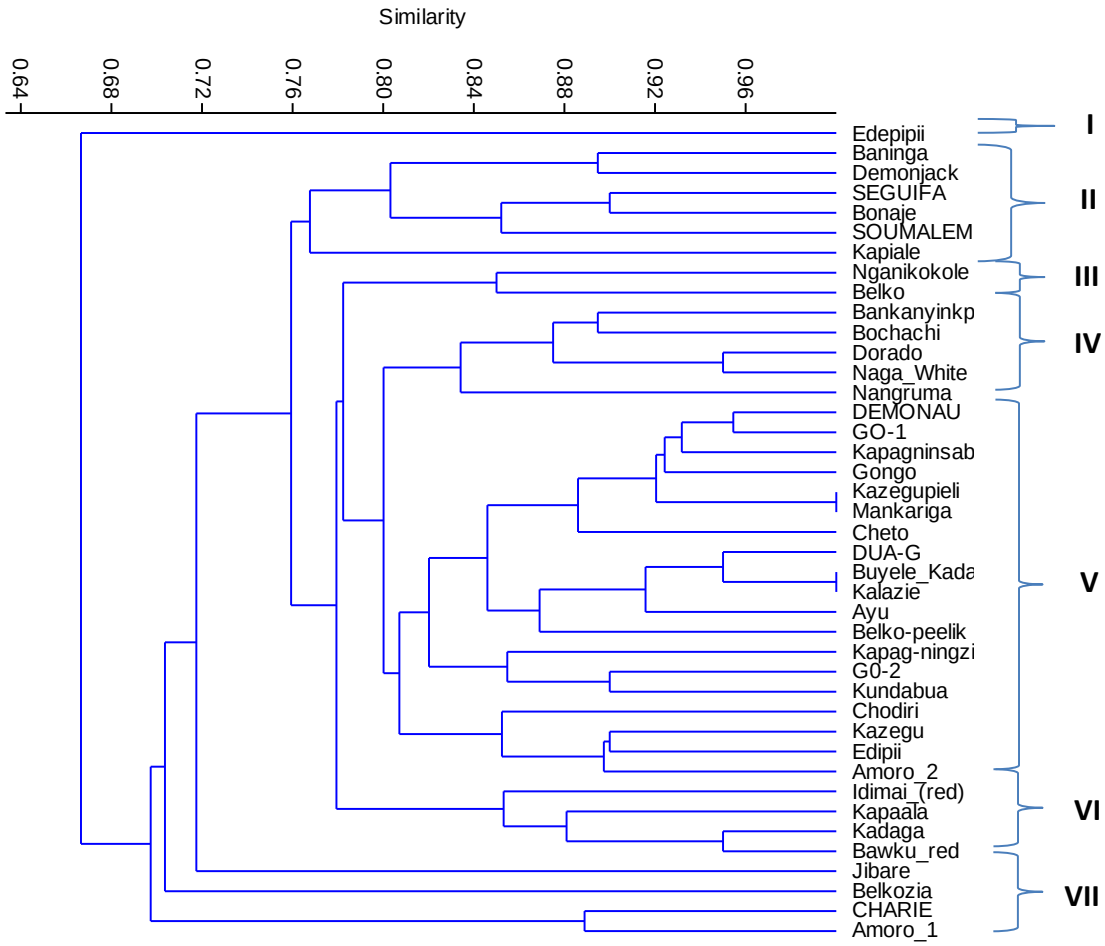

Figure 2. Genetic relationship among the 41 sorghum lines using PCR products of the 22 SSR primer pairs. The dendrogram was constructed based on Unweighted Paired Group Method using the Arithmetic Average (UPGMA) clustering algorithm from Jaccard's pairwise matrix of genetic similarities.

similarity of 0.89 and 0.9 was observed for ‘Baninga’ and ‘Demonjack’ (0.89) and also for ‘Seguifa’ and ‘Bonaje’ (0.90). ‘Soumalemba’ was 85% similar to ‘Baninga’ and ‘Demonjack’. The third group had only two genotypes, ‘Nganikokole’ and ‘Belko’, which were also 85% similar. The fourth group had three genotypes comprising ‘Dorado’, ‘Naga White’ and ‘Nangruma’. ‘Dorado’ and ‘Naga White’ were 0.94 similar. Group six consisted of 4 genotypes, namely ‘Idimai Red’, ‘Kapaala’, ‘Kadaga’ and ‘Bawku Red’, which were closely similar. ‘Kadaga’ and ‘Bawku Red’ differed by just 5% while ‘Kapaala’ was 12% dissimilar to ‘Kadaga’ and ‘Bawku Red’. ‘Idimai Red’ was 85% similar to ‘Kapaala’, ‘Kadaga’ and ‘Bawku Red’. In group seven, ‘Charie’ and ‘Amoro 1’ were clustered together with a coefficient similarity of 0.88 and both of them mature late, while the other two genotypes, ‘Jibare’ and ‘Belkozia’, were remotely related, showing distinct genetic characteristics compared to the rest of the group seven genotypes (Figure 2).

Genetic distance (GD

Euclidean distances of 150 to 650 were observed in the pair-wise combinations, indicating that the cultivars were diverse for the genotypic characters measured, while the cophenetic correlation coefficient (CCC) was 0.64. The minimum genetic distance of 150 was recorded between cultivars ‘Buyele_Kadapula’ and ‘Kalazie’. The highest genetic distance of 650 was recorded between cultivar ‘Edepipii’ and the rest of the cultivars, indicating that this line was different from the other cultivars (Figure 3).

The dendrogram grouped the 41 sorghum lines into six main clusters and two singletons. The first main cluster was formed between a genetic distance of 250 and 520, and these included the cultivars ‘Kapagninsablinli’, ‘Kapag-ningzie’, ‘Bankanyinkpe’, ‘Bochachi’, ‘Dorado’, ‘Nangruma’, ‘Naga White’ and ‘Jibare’ (Figure 3).

Cultivar ‘Edepipii’ was remotely related to the rest at a genetic distance of 640 followed by ‘Belkozia’ at 610 and ‘Jibare’ at a genetic distance of 520. Both ‘Nangruma’ and ‘Naga White’ were associated at a genetic distance of 250 while ‘Kapagninsablinli’ and ‘Kapag-ningzie’ were associated at a distance of 360. ‘Bochachi’ and ‘Dorado’ clustered at a genetic distance of 300. The second cluster was formed at a genetic distance of 330 and comprised of only cultivars ‘Kundabua’ and ‘GO-2’. The third cluster was the largest group with twelve genotypes with a genetic distance of 150 between ‘Kalazie’ and ‘Buyele_Kadapula’, the most closely related lines followed by ‘Edipii’ and ‘Amoro_2’ with a distance of 280.

‘Nganinkokole’ and ‘Belko’ were separated from the rest by a genetic distance of 420 indicating genetic dissimilarity with the rest of the cultivars in the cluster. ‘Chodiri’ and ‘Bonaje’ were related at a genetic distance of 410.

The other members of this cluster were ‘Dua-G’, ‘Ayu’, ‘Belko peelik’ and ‘Kazegu’. The fourth cluster consisted of eight cultivars with ‘Demonau’ at one end and ‘Mankariga’ at the other end. ‘Kazegupieli’ and ‘Mankariga’, the most closely related in this group, were associated at distance of 180 while ‘Gongo’ and ‘GO-1’ were at a distance of 240 (Figure 3). ‘Demonau’ and ‘Cheto’ also were related at a genetic distance of 260. Other members in this group included ‘Baninga’ and ‘Kapaala’. The fifth cluster consisted of four cultivars, with ‘Kadaga’ and ‘Bawku Red’ at a distance of 280, while ‘Idimai Red’ and ‘Demonjack’ were at distances of 420 and 360, respectively. Cultivars ‘Belkozia’ and ‘Edepipii’ did not cluster with any of the other 41 lines but stood distinctly individually, indicating that they were genotypically dissimilar from the other sorghum lines. The sixth cluster consisted of five cultivars (‘Charie’, ‘Amoro 1’, ‘Seguifa’, ‘Soumalemba’ and ‘Kapiale’) with varied genetic distances (380 to 510) between them (Figure 3).

DISCUSSION

Analysis of the extent and distribution of genetic variation in a crop is essential in understanding the evolutionary relationships between accessions and sampling genetic resources in a more systematic fashion for breeding and conservation purposes (Ejeta et al., 2000). Menkir et al., (1997) have argued that molecular markers, in particular genetic distance estimates determined by molecular markers, are suitable for assessing genetic diversity and identifying diverse sources in crop germplasm collections. The SSR markers used in this study revealed a wide variation between the 41 genotypes evaluated. Interestingly, the stay-green sources were very variable based on the dendrogram from SSRs associated with the stay-green trait in DO and KP (Figure 2). This agrees with the theory that different sources of stay-green can be under different genetic control (Thomas and Smart, 1993).

The amplification of 22 microsatellite loci in the 41 sorghum accessions in this study revealed that all the loci were polymorphic with a total of 92 alleles (Table 3). The number of alleles per locus ranged from 2 (*Xtxp278* and *Xtxp283*) to 7 (*Xtxp319*) and averaged 4.2 alleles. Galyuon et al. (2016) assessed 66 SSR loci in 28 sorghum accessions and detected 419 alleles with a mean of 6.2 alleles per locus. In their study, the number of alleles ranged from 1 for Xtxp94 to 14 for Xtx88. One of the reasons for variation in number of alleles obtained per locus could be due to differences in number of mutations per locus since mutation rates tend to be locus specific (Estoup et al., 2002). Similar SSR polymorphic levels and ranges of fragment size of alleles have been reported from earlier studies (Brown et al., 1996; Shehzad et al., 2009).

The expected heterozygosity (H_e) of cultivated sorghum found in this work across the 22 SSR loci (H_e = 0.03, N = 41) was much lower than that found for cultivate

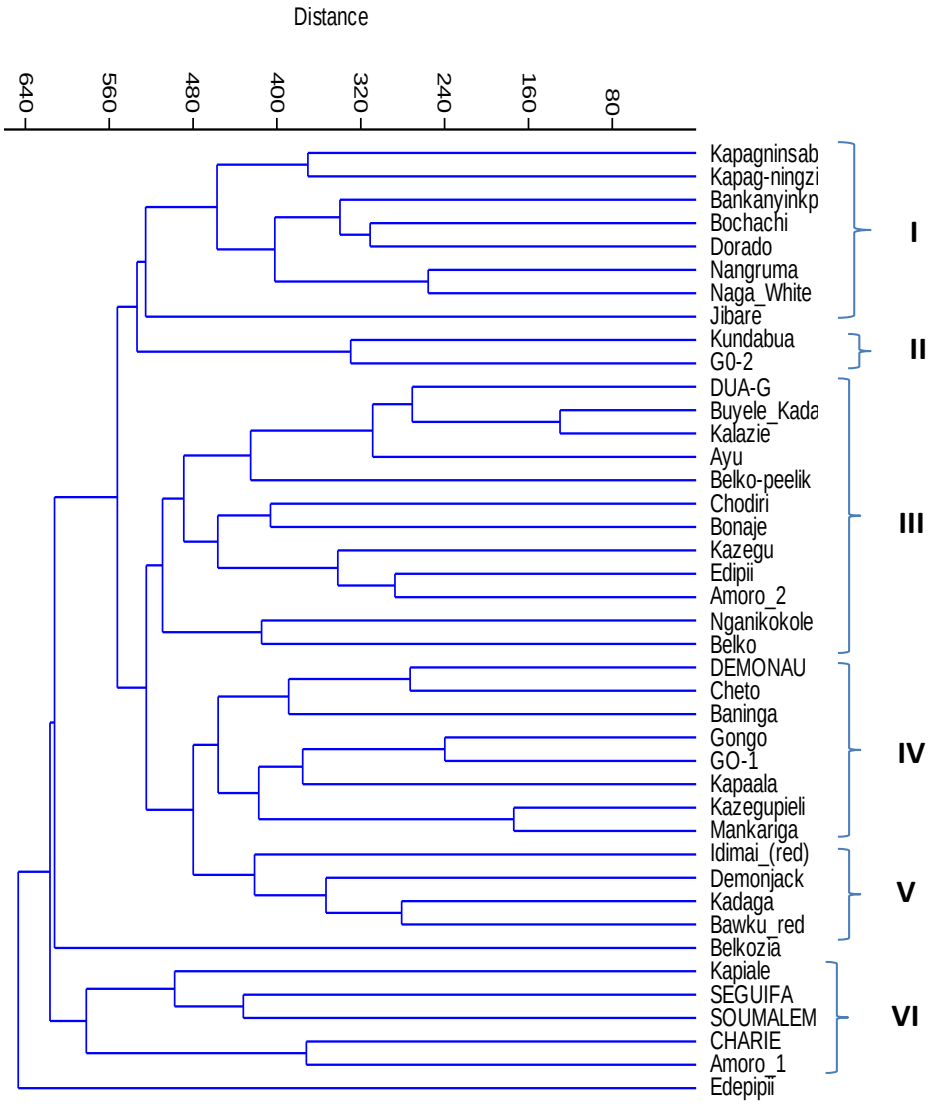

Figure 3. Genetic distances among the 41 sorghum lines using the 22 SSR primer pairs. The dendrogram was constructed using Unweighted Paired Group Method using the Arithmetic Average (UPGMA) clustering algorithm from Euclidean's pairwise matrix of genetic distances.

sorghum in Kenya (H_e = 0.59, N = 439) across 24 microsatellites (Mutegi et al., 2011) and Niger (H_e = 0.61, N = 472) across 28 microsatellites (Deu et al., 2008), and again lower than that found in Burkina Faso (H_e = 0.37, N = 124) across 29 microsatellites (Barro-Kondombo et al., 2010). The explanation put forward by Barro-Kondombo et al., (2010) for the low level of diversity found in Burkina Faso, compared with other studies, is the low amount of sorghum landrace or racial diversity present in Burkina Faso. The amount of heterozygosity across loci, which is synonymous with allelic variation, indicates the amount of genetic variability, which has a bearing on the survival of a species and allows organisms to adapt to changing environments provided that some loci have adaptive values (Ng'uni et al., 2011). In the current study, the observed heterozygosity ranged from 0 to 0.17 with an average of 0.03 for the sorghum accessions. The low level of observed heterozygosity maybe more attributable to the predominantly inbreeding nature of sorghum other than samples size used. Indeed, when a bottleneck occurs in a population, allelic diversity is reduced faster than is heterozygosity (Nei et al., 1975), which is a result of loss of rare alleles from the population contributing little to the overall heterozygosity (Muraya et al., 2010). Sorghum is a self-pollinating crop, although a wide range of outcrossing rates of 7-30% or higher have been reported (Dje et al., 2004; Barnaud et al., 2008). Cleistogamy (flowers remain enclosed) in sorghum due to very long glumes prevent pollen movement and thus strongly promoting selfing (Barnaud et al., 2008). The

predominantly selfing nature of the species explains the observed lower genetic variation within than among accessions in this study. Low levels of genetic variation among self-pollinated plants are attributed to limited movement of genes via pollen, which also results in greater differentiation among populations (Hamrick, 1983). The other plausible reason may be that farmers obtain seed from the same sources or exchange seed for planting. In such situation, the genetic base becomes narrow, hence low heterozygosity.

Gene diversity varied from 0.05 (*Xtxp278)* to 0.8 (*Xtxp319)* with an overall mean of 0.48. A number of factors, such as agronomic, economic and cultural practices in the traditional farming systems, have been reported to impact on levels of genetic diversity in sorghum (Chakauya et al., 2006; Mutegi et al., 2011). Following the plant domestication stage, artificial selection has been identified as one of the factors contributing to the reduced genetic diversity of crops (Gepts, 2004). In most cases, traditional farmers maintain more than one distinct local variety selected for particular characteristics of interest to them and specific use. These landraces are perpetuated as farmer varieties from generation to generation. The driving forces behind the practice of maintenance of two or more sorghum landraces per household involve the farmers selecting landraces that could cope with local environmental factors such as duration of rainy season. Therefore, early maturing local varieties are usually planted by most households to provide food early in the season and thus ensuring attainment of household food security.

The lowest genetic similarity (0.85) (Figure 2) was obtained between cultivars Nganikokole and Belko in this study. Agrama and Tuinstra (2003) have found a genetic similarity value of 0.44 among 22 sorghum genotypes, using SSR markers, which is lower than the values obtained in the current study. Selection of the parents, based on genetic distance information, could provide a basis for choosing parents for crossing programmes (Zhong-hu, 1991). High correlation between and among characters may show that the characters share some common genetic and geographical information (Thorpe, 1976; Ayana and Bekele, 2000) as well as pleiotropic and linkage of genes governing the traits. Ayana (2001) reports that correlations among characters are of interest to plant breeders because they help in the identification of easily measured characters that could be used as indicators of more important (but more complex to score) characters. They are also useful in selection of desirable traits (Amurrio et al., 1992; Ayana and Bekele, 2000). Chozin (2007) has argued that evaluation of the patternof variation and genetic relationship among breeding material can facilitate precise identification of genetic divergence and reliable classification of specific heterotic groups, which will be particularly useful in planning crosses.

In this study, the major allele frequency was between 0.27 (Xtxp319) and 0.98 (Xtxp278) with a mean of 0.63 (Table 3). The distance in gene frequency between parental genotypes is important because the higher the difference in gene frequency, the higher the amount of heterosis which indicates larger the distances lead to larger heterosis and vice-versa (Carrera et al., 1996). Genetic distances among progeny confirm their origin and the genetic relationships between them and their parents (Carrera et al., 1996). Efficient identification and selection of the desirable genotypes largely depend on a comprehensive understanding of the genetic relatedness and variation present within the crop and its closely related wild species (Muench et al., 1991; Kearsey, 1993). Information concerning genetic relatedness is crucial, for it indicates the rate of adaptive evolution and the extent of response in crop improvement (Vega, 1993). Furthermore, it is essential as a guideline in the choice of parents for breeding programmes (McNaught, 1988; Loarce et al., 1996), to detect the genetic duplicates in germplasm collections and implementing an effective genetic conservation programme (Frankel and Brown, 1984; Muench et al., 1991).

Cluster analysis of the 41 accessions, based on the Jaccard similarity coefficient, revealed Buyele Kadapale and Kalazie were the most closely related accessions. Similarly, accessions Kazegupiele and Mankanga were highly similar. The other accessions, such as Nganikokole, Belko Edipipii, Jibare and Belkozia, were clearly distinct from the rest. The clustering of accessions based on their genetic similarity in this study has indicated that some could be employed as parental lines for breeding and selection programmes for superior hybrids (Jeya Prakash et al., 2006). Indeed, SSR-based analysis of 40 sorghum landraces from Tanzania based on their area of collection sites and pedigree of relationships was able to reveal variation and diversity among landraces Bucheyeki et al. (2009). According to Barnaud et al. (2008), Bucheyeki et al. (2009) and Muray et al. (2010), gene flow plays a large role in structuring the genetic variability within and among sorghum populations. Manzelli et al. (2007) similarly have reported continuous exchanges of genes between sorghum population results in genetic diversity. SSR markers have been used to group sorghum genotypes based on their geographical origin (Abu Assar et al., 2005; Vittal et al., 2010). In this study, however, clustering did not always follow the sorghum race classification (or country of origin) particularly as a number of the advanced breeding lines examined have more than one race in their genetic background. This has also been found in other genetic diversity studies in sorghum (Kebede, 1991; Ayana and Bekele, 2000; Menz et al., 2004; Chozin, 2007; Bucheyekei et al., 2009). In earlier studies Taramino et al., (1997), Smith et al. (2000), Uptmoor et al. (2003) and Menz et al. (2004) comparisons were made between R-lines and B-lines or were based on region of origin. The current study was not based on any of these classifications; however, clusters were not always made up of only lines from the same region or race. For

example, Seguifa (Mali, Sahelian) and Baninga (Ghana, Guineans) from different geographical regions or races belonged to the same cluster. Similarly, Dua-G (Mali, North Guinean) and Kalazie (Ghana, Caudatum) also belonged to same cluster, while Dua-G and Soumalemba did not cluster together even though both originated from Mali.

Genetic diversity is influenced by gene flow, which encompasses several mechanisms of gene exchange among populations, including movement of gametes, seed, individuals or groups of individuals from one place to another (Slatkin, 1987). The high genetic similarity observed in the current study could result from seed exchange practices between communities as this is usual practice with peasant farmers in Ghana.

Overall, the studied sorghum accessions showed significant genetic variations, indicating that the accessions could be employed in the development of new genotypes of desired traits through breeding and selection programmes.

Conclusion

The 22 SSR loci generated 92 alleles with a mean of 4.2 and were able to group the 41 sorghum cultivars into seven clusters. Edepipii was the most divergent compared to the other cultivars. The most genetically distinct varieties were Edepipii, Jibare and Belkozia, which did not cluster with any other line, indicating no similarity among these varieties and could be employed as parental lines for breeding and selection programmes for superior hybrids. The mean gene diversity (0.48), heterozygosity (0.03), PIC (0.44) and mean number of alleles (4.2) suggest that the genetic base of local sorghum germplasm is narrow and there may be the need to introduce exotic cultivars to increase the genetic base. This notwithstanding, there is the potential to use the sorghum cultivars in Ghana and Mali to breed and select for more resilient and high yielding hybrids, which could be used to improve yields and economic gains of peasant farmers in northern Ghana.

CONFLICT OF INTERESTS

The authors have not declared any conflict of interests.

REFERENCES

Abu Assar AH, Uptmoor R, Abdelmula AA, Salih M, Ordon F, Friedt W (2005). Genetic variation in sorghum germplasm from Sudan, ICRISAT, and USA assembled by simple sequence repeats (SSRs). Crop Science 45(4):1636-1644.

Africa Harvest (2007). The African Biofortified Sorghum Project: midterm report. Nairobi: Africa Harvest Biotech Foundation International (AHBFI), p. 40.

Agrama HA, Tuinstra MR (2003). Phylogenetic diversity and relationships among sorghum accessions using SSRs and RAPDs. African Journal Biotechnology 2(10):334-340.

Ali ML, Rajewski JF, Baenziger PS, Gill KS, Eskridge KM, Dweikat L (2008). Assessment of genetic diversity and relationship among a collection of US sweet sorghum germplasm by SSR markers. Molecular Breeding 21(4):497-509.

Amurrio JM, de Ron AM, Escribano MR (1992). Evaluation of *Pisum sativum* landraces from the Northwest of Iberian Peninsula and their breeding value. Euphytica 66(1):1-10.

Anderson JA, Churchill GA, Autrique JE, Tanksley SD, Sorrells ME (1993). Optimizing parental selection for genetic linkage maps. Genome 36(1):181-186.

Ayana A (2001). Genetic diversity in sorghum (*Sorghum bicolor* (L.) Moench) germplasm from Ethiopia and Eritrea. PhD Thesis, Addis Ababa University, Addis Ababa, Ethiopia.

Ayana A, Bekele E (2000). Geographical patterns of morphological variation in sorghum (*Sorghum bicolor* (L.) Moench) germplasm from Ethiopia and Eritrea: Quantitative characters. Euphytica 115(2):91-104.

Barnaud A, Trigueros G, McKey D, Joly HI (2008). High outcrossing rates in fields with mixed sorghum landraces: how are landraces maintained? Heredity 101(5):445-452.

Barrett BA, Kidwell KK (1998). AFLP based genetic diversity assessment among wheat cultivars from Pacific North West. Crop Science 38(5):1261-1271.

Barro-Kondombo C, Sagnard F, Chantereau J, Deu M, vom Brocke K, Durand P, Goze E, Zongo JD (2010). Genetic structure among sorghum landraces as revealed by morphological variation and microsatellite markers in three agroclimatic regions of Burkina Faso. Theoretical and Applied Genetics 120(8):1511-1523.

Brown SM, Hopkins MS, Mitchell SE, Senior ML, Wang TY, Duncan RR, Gonzalez-Candelas F, Kresovich S (1996). Multiple methods for the identification of polymorphic simple sequence repeats (SSRs) in sorghum [*Sorghum bicolor* (L.) Moench]. Theoretical and Applied Genetics 93(1-2):190-198.

Bucheyekei TL, Gwanama C, Mgonja M, Chisi M, Folkertsma R, Mutegi R (2009). Genetic variability characterisation of Tanzania sorghum landraces based on Simple Sequence Repeats (SSR) molecular and morphological markers. African Crop Science Journal 17(2):71-86.

Carrera AD, Poverene MM, Rodriguez RH (1996). Isozyme variability in *Helianthus agrophyllus*. Its application in crosses with cultivated sunflower. HELIA-NOVI SAD-, 19:19-28.

Chakauya E, Tongoona P, Matiburi EA, Grum M (2006). Genetic diversity assessment of sorghum landraces in Zimbabwe using microsatellites and indigenous local names. International Journal of Botany 2(1):219-222.

Chozin M (2007). Characterization of sorghum accessions and choice of parents for hybridization. Journal Akta Agrosia Edisi Khusus 2:227-232.

Cox TS, Murphy JP, Rodgers DM (1986). Changes in genetic diversity in the red winter wheat regions of the United States. Proceedings of National Academy of Science, USA 83(15):5583-5586.

Deu M, Sagnard F, Chantereau J, Calatayud C, Hérault D, Mariac C, Pham JL, Vigouroux Y, Kapran I, Traore PS, Mamadou A, Gerard B, Ndjeunga J, Bezançon G (2008). Niger-wide assessment of in situ sorghum genetic diversity with microsatellite markers. Theoretical and Applied Genetics 116(7):903-913.

Dje Y, Heuertz M, Ater M, Lefèbvre C, Vekemans X (2004). *In situ* estimation of outcrossing rate in sorghum landraces using microsatellite markers. Euphytica 138(3):205-212.

Ejeta G, Goldsbrough PB, Tuinstra MR, Grote EM, Menkir A, Ibrahim Y, Cisse N, Weerasuriya Y, Melak-Berhane A, Shaner CA (2000). Molecular marker applications in sorghum. In: Haussmann BIG, Geiger HH, Hess DE, Hash CT, Bramel-Cox P (eds) Application of molecular markers in plant breeding. Training manual for a seminar held at IITA, Ibadan, Nigeria, from 16-17 August 1999, ICRISAT, Patancheru 502324, Andhra Pradesh, India, pp. 81-89.

Estoup A, Jarne P, Cornuet JM (2002). Homoplasy and mutation model at microsatellite loci and their consequences for population genetics analysis. Molecular Ecology 11(9):1591-1604.

Foley JA, Ramankutty N, Braumann KA, Cassidy E, Gerber JS, Johnston M, Mueller ND, O'Connell C, Deepak KR, Zaks DPM

(2011). Solutions for a cultivated planet. Nature 478(7369):337-342.
Frankel OH, Brown AHD (1984). Plant genetic resources today: a critical appraisal. In: Holden JHW Williams JT (eds) Crop genetic resources: Conservation and evaluation, George Allen and Unwin, London, pp. 249-259.
Galyuon IKA, Madhusudhana R, Borrell AK, Hash TC, Howarth CJ (2016). Genetic diversity of stay-green sorghums and their derivatives revealed by microsatellites. African Journal of Biotechnology 15(25):1363-1374.
Gepts P (2004). Crop domestication as a long-term selection experiment, Volume 24, Part 2: Long-term selection: crops, animals, bacteria. In: Jannick J (ed) Plant Breeding Reviews. New York: Wiley.
Hamrick JL (1983). The distribution of genetic variation within and among natural plant populations. In: Schoewald-Cox CM, Chamber B, MacBoyde WL, Thomas (eds) Genetics and Conservation. Menlopark: Benjamin Cummings. pp 501-508.
Haub C (2013). 2013 World population data sheet. http://www.prb.org/pdf13/2013-population-data-sheet_eng.
IPCC (Intergovernmental Panel on Climate Change) (2014). Climate Change 2014: Impacts, Adaptation, and Vulnerability. Working Group II. Cambridge, UK: Cambridge University Press.
Jeya Prakash SP, Biji KR, Gomez SM, Murthy KG, Babu RC (2006). Genetic diversity analysis of sorghum [*Sorghum bicolor* (L.) Moench] accessions using RAPD markers. Indian Journal of Crop Science 1(1-2):109-112.
Kearsey MJ (1993). Biochemical genetics in breeding. In: Hayward MD, Bosemark NO, Romagosa I (eds) Plant Breeding Principles and Prospects. Chapman and Hall, London, pp. 103-183.
Kebede Y (1991). The role of Ethiopian germplasm resources in the national breeding programme. In: Engles JM, Hawkes JG, Worede M (eds.) Plant genetic resources of Ethiopia. Cambridge University Press, Cambridge, UK, pp 315-322.
Lee M (1995). DNA markers and plant breeding programs. Advance Agronomy 55:265-343.
Loarce Y, Gallego R, Ferrer E (1996). A comparative analysis of the genetic relationships between rice cultivars by RAPD markers. Horticultural Science 31:127-129.
Manzelli M, Pileri L, Lacerenza N, Benedettelli S, Vecchio V (2007). Genetic diversity assessment in Somali sorghum (*Sorghum bicolor* (L.) Moench) accessions using microsatellite markers. Biodiversity and Conservation 16(6):1715-1730.
McNaught SJ (1988). Diversity and stability. Nature 333:204-205.
Menkir A, Goldsbrough P, Ejeta G (1997). RAPD based assessment of genetic diversity in cultivated races of sorghum. Crop Science 37(2):564-569.
Menz MA, Klein RR, Unruh NC, Rooney WL, Klein PE, Mullet JE (2004). Genetic diversity of public inbreds of sorghum determined by mapped AFLP and SSR markers. Crop Science 44(4):1236-1244.
Mohammadi SA, Prasanna BM (2003). Analysis of genetic diversity in crop plants-salient statistical tools and considerations. Review and interpretation. Crop Science 43(4):1235-1248.
Muench DG, Slinkard AE, Scales GJ (1991). Determination of genetic variation and taxonomy in lentils (*Lens miller*) species by chloroplast DNA polymorphism. Euphytica 56(3):213-218.
Muray MM, Geiger HH, Mutegi E, Kanyenji BM, Sagnard F, de Villiers SM, Kiambi D, Parzies HK (2010). Geographical patterns of phenotypic diversity and structure of Kenyan wild sorghum populations (*Sorghum spp.*) as an aid to germplasm collection and conservation strategy. Plant Genetic Resources: Characterisation and Utilization 1-8. doi 10.1017/S1479262110000225.
Muraya M, Sagnard F, Parzies HK (2010). Investigation of recent population bottlenecks in Kenyan wild sorghum populations (*Sorghum bicolor* (L.) Moench ssp. verticilliflorum (Steud.) De Wet) based on microsatellite diversity and genetic disequilibria. Genetic Resources and Crop Evolution 57(7):995-1005.
Mutegi E, Sagnard F, Semagn K, Deu M, Muraya M, Kanyenji B, de Villiers S, Kiambi D, Herselman L, Labuschagne M (2011). Genetic structure and relationships within and between cultivated and wild sorghum (*Sorghum bicolor* (L.) Moench) in Kenya as revealed by microsatellite markers. Theoretical and Applied Genetics 122(5):989-1004.
Nei M (1973). The theory and estimation of genetic distance. In: Genetic Structure of Populations. Morton NE (ed) University Hawaii Press, Honolulu. pp. 45-54.
Nei M, Lei WH (1979). Mathematical model for studying genetic variation in terms of restriction endonucleases. Proceedings of National Academy of Science 76(10):5269-5273.
Nei M, Maruyama T, Chakraborty R (1975). The bottleneck effect and genetic variability in populations. Evolution 29(1):1-10.
Ng'uni D, Geleta M, Bryngelsson T (2011). Genetic diversity in sorghum (*Sorghum bicolor* (L.) Moench) accessions of Zambia as revealed by simple sequence repeats (SSR). Hereditas 148(2):52-62.
Pei Z, Gao J, Chen Q, Wei J, Li Z, Luo F, Shi L, Ding B, Sun S (2010). Genetic diversity of elite sweet sorghum genotypes assessed by SSR markers. Biologia Planetarium 54(4):653-658.
Sanchez AC, Subudhi PK, Rosenow DT, Nguyen HT (2002). Mapping QTL associated with drought resistance in sorghum (*Sorghum bicolor* (L.) Moench). Plant Molecular Biology 48(5-6):713-726.
Shehzad T, Okuizumi H, Kawase M, Okuno K (2009). Development of SSR based sorghum (*Sorghum bicolor* (L.) Moench) diversity research set of germplasm and its evaluation by morphological traits. Genetic Resources and Crop Evolution 56(6):809-827.
Slatkin M (1987). Gene flow and the geographic structure of natural populations. Science 236(4803):787-792.
Smith JSC (1984). Genetic variability within U.S. hybrid maize: Multivariate analysis of isozyme data. Crop Science 24(6):1041-1046.
Smith JSC, Kresovich S, Hopkins MS, Mitchell SE, Dean RE, Woodman WL, Lee M, Porter K (2000). Genetic diversity among elite sorghum inbred lines assessed with Simple sequence repeats. Crop Science 40(1):226-232.
Smith OS, Smith JSC (1992). Measurement of genetic diversity among maize hybrids. A comparison of isozymic, RfLP, pedigree, and heterosis data. Maydica 37:53-60.
Sneath PHA, Sokal RR (1973). Numerical taxonomy: the principles and practice of numerical classification. San Francisco: Freeman. p. 573.
Taramino G, Tarchini R, Ferrario S, Lee M, Pe ME (1997). Characterization and mapping of simple sequence repeats in sorghum. Theoretical and Applied Genetics 95(1-2):66-72.
Thomas H, Smart CM (1993). Crops that stay-green. 27 Nov. - 2 Dec. 1983. ICRISAT, Patancheru, A.P., India. Annals of Applied Biology 123:193-219.
Thompson JA, Nelson RL, Vodkin LO (1998). Identification of diverse soybean germplasm using RAPD markers. Crop Science 38(5):1348-1355.
Thorpe RS (1976). Biochemical analysis of geographical variation and racial affinities. Biology Review 51(4):407-452.
UNDP (2012). Africa Human Development Report 2012 Towards a Food Secure Future, United Nations Development Programme. New York, USA: United Nations Publications.
Uptmoor R, Wenzel W, Friedt W, Donaldson G, Ayisi K, Ordon F (2003). Comparative analysis on the genetic relatedness of *Sorghum bicolor* accessions from Southern Africa by RAPDs, AFLPs and SSRs. Theoretical and Applied Genetics 106(7):1316-1325.
Vega MP (1993). Biochemical characterization of populations. In: Hayward MD, Bosemark NO, Romagosa I (eds) Plant Breeding: Principles and Prospects. Chapman and Hall, London, pp. 184-200.
Vittal R, Ghosh N, Weng Y, Stewart BA (2010). Genetic diversity among *Sorghum bicolor* (L.) Moench genotypes as revealed by prolamines and SSR markers. Journal of Biotechnology Research 2:101-111.
Zhihong X, Jiayang L, Yongbiao X, Weicai Y (2008). The Africa biofortified sorghum project–applying biotechnology to develop nutritionally improved sorghum for Africa. Springer, Netherlands.
Zhong-hu H (1991). An investigation of the relationship between the F1 potential and measures of genetic distance among wheat lines. Euphytica 58(2):165-170

Vol. 18(27), pp. 603-611, July, 2019
DOI: 10.5897/AJB2019.16859
Article Number: 39428A261411
ISSN: 1684-5315

http://www.academicjournals.org/AJB

ACADEMIC JOURNALS
expand your knowledge

African Journal of Biotechnology

Full Length Research Paper

Effective method to control *Vibrio mimicus* infection in channel catfish *Ictalurus punctatus*

Yan-Wei Li, Xiang Zhang, Yi-Jie Cai, Shu-Yin Chen, Hong-Yan Sun[#] and Xue-Ming Dan[#*]

College of Marine Sciences, South China Agricultural University, 483 Wushan Street, Tianhe District, Guangzhou 510642, Guangdong Province, PR China.

Received 14 May, 2019; Accepted 27 June 2019

Recently, a skin ulcerative disease caused by *Vibrio mimicus* has led to heavy economic losses in catfish, including yellow catfish, southern catfish, and Zhengchuan catfish in China. Currently, there was no effective method of controlling the outbreak of this disease. In this study, the bacterial isolates were obtained from dying channel catfish and identified as *V. mimicus*, which consist of formalin-inactivated *V. mimicus* (antigen). After first immunization, four weeks later, fishes were exposed to *V. mimicus* and the immune response was analyzed: Fish survival, respiratory burst activity of blood leukocytes, serum agglutination titers, and lysozyme activity, every week (during four weeks). Survival was up 90%. Respiratory burst activity of blood leukocytes, serum agglutination titers, and lysozyme activity were determined at 1, 2, 3, and 4 weeks after primary immunization. Immunization of channel catfish protected hosts against *V. mimicus* infection with a survival percentage of more than 90%. Respiratory burst activity of blood leukocytes was not affected by vaccination. Serum agglutination titer and lysozyme activity were significantly increased after immunization, in comparison with un-vaccinated control fish. The obtained results indicated that vaccination is an effective method to control the outbreaks of *V. mimicus* through regulation of the humoral immune response.

Key words: *Vibrio mimicus*, catfish, skin ulcer, vaccine.

INTRODUCTION

Vibrio mimicus, a Gram-negative bacteria similar to *Vibrio cholerae*, has been identified as a causative agent of human gastroenteritis, which is characterized by watery to dysentery-like diarrhea (Davis et al., 1981; Takahashi et al., 2007). *V. mimicus* is a natural inhabitant of aquatic environments, including freshwater, brackish water, and saltwater. *V. mimicus* has been isolated from water samples (Adeleye et al., 2010; Chowdhury et al., 1989), sediments (Adeleye et al., 2010), aquatic plants (Li et al., 2005), snails (Li et al., 2005), oysters (Li et al., 2005), crayfish (Eaves and Ketterer, 1994), turtle eggs (Campos et al., 1996), shrimp (Guardiola-Avila et al., 2016; Thune

*Corresponding author. E-mail: dxm72@scau.edu.cn.

[#]These authors contributed equally to this study.

et al., 1991; Wang et al., 2003; Wong et al., 1995), crabs (Li et al., 2005), fish (Li et al., 2005).

V. mimicus has been reported to be responsible for ascites disease in aquatic animals (Cen et al., 2013).

Recently we and others have reported that *V. mimicus* is also a pathogenic agent causing skin ulcerative disease in freshwater catfish species, including yellow catfish (*Pelteobagrus fulvidraco*) (Geng et al., 2014), southern catfish (*Silurus soldatovi meridionalis*, Chen) (Geng et al., 2014), and Zhengchuan catfish (*Silurus soldatovi meridionalis*, Chen ♂× *Silurus asotus* ♀) (Zhang et al., 2014). The most evident clinical symptoms of this skin ulcerative disease is the presence of regularly-shaped ulcers with clear boundaries. This disease has resulted in more than 70% cumulative mortality of freshwater fish farms, and has led to severely economic losses to aquaculture in south China according to the data from Guangdong Provincial center for disease control and prevention.

Antibiotics are a suitable strategy often used to control *V. mimicus* infection in aquaculture animals. However, the excessive use of antibiotics has led to the emergence of antibiotic-resistant bacteria (Liu et al. 2015), and to environmental deterioration (Nugroho and Fotedar, 2013). Therefore, other eco-friendly environment methods are needed to prevent outbreaks of this disease.

Recent studies have indicated that dietary supplementation with mannan oligosaccharide, with customized probiotics, or with organic selenium improved the resistance of marron *Cherax tenuimanus* (Ambas et al., 2013; Nugroho and Fotedar, 2013) to *V. mimicus* (Sang et al., 2009). In addition, Cen et al. (2013) and Zhang et al. (2014) have produced a vaccine based on outer membrane protein U (OmpU), protecting carp *Ctenopharyngodon idella* against *V. mimicus* infection. Despite the heavy economic losses due to catfish infection with *V. mimicus* in recent years, no prophylactic method has been developed to provide protection against *V. mimicus* infection, until now.

Channel catfish (*Ictalurus punctatus* Rafinesque) is an economically important fish species, reared in southern China, in places such as Guangdong and Sichuan. In recent years, a disease characterized by skin ulcers (Figure 1A) has been prevalent in farmed channel catfish. This symptom has been observed by Geng et al. (2014) and Zhang et al. (2014) in catfish infected by *V. mimicus*. Thus the aim of the present study was to isolate *V. mimicus* bacteria from dying channel catfish, develop an effective prophylaxis method, a formalin-inactivated *V. mimicus* vaccine. Results of this study will be of immense value to the aquaculture industry in southern China.

MATERIALS AND METHODS

Fish

Dying channel catfish were brought to our laboratory for pathogen detection from a channel catfish aquaculture farm (Foshan, Guangdong Province, southern China). Healthy channel catfish were purchased from an aquaculture farm (Guangzhou, Guangdong Province). Fish were acclimatized in tanks for more than 14 days at 28±1°C, and fed daily with a commercial feed. Prior to experiments, five fish were randomly selected to confirm that they had not been infected with bacteria. Using conventional microbiological methods, such as 16S rDNA identification and tissue section, and no signs of bacterial infection were observed in any of the fish samples tested.

Isolation and identification of bacteria

For bacterial isolation, samples from brain, liver, spleen and kidney of the moribund catfish were taken using disposable inoculation loops, and inoculated immediately onto blood agar plates (Huankai, Guangzhou, southern China) or thiosulfate citrate bile salts sucrose(TCBS) agar plates (Huankai). The plates were incubated at 28°C for 48 h. Single colonies from plates were then selected and re-streaked on the same media. The isolates were stored in brain heart infusion (BHI) medium (Huankai) containing 20% (v/v) glycerol in liquid nitrogen.

After samples were prepared with the standard methods as described previously (Sun et al., 2009), the morphology of bacteria was observed under light microscopy, scanning electron microscopy and transmission electron microscopy. The biochemical characterization of bacterial isolates was performed using the VITEK2 Compact microbial identification system (BioMerieux, Lyon, France). Additionally, 16S rDNA and three housekeeping genes encoding recombination repair protein (recA), urydilate kinase (pyrH) and RNA polymerase α-chain (rpoA) were selected to identify the bacterial species using the method described by Zhang et al. (2014). Table 2

Immunization and sampling

To prepare inactivated *V. mimicus*, the NH isolate was cultivated overnight in 5 ml BHI broth at 28°C with shaking at 150 rpm, allowing bacteria to reach the logarithmic growth phase. One milliliter sample of the culture was transferred into 100 ml fresh BHI broth, and cultivated at 28°C with shaking at 150 rpm for 48 h. The culture was then inactivated with 1% formalin at 4 °C for 24 h. The inactivated cells were harvested by centrifugation at 8000×*g* for 5 min, washed three times with phosphate-buffered saline (PBS) and then adjusted to a suitable concentration with PBS. The suspension of *V. mimicus* was mixed with an equal volume of Freund's complete or incomplete adjuvant (Sigma, Missouri, USA).

Fish (33.8±3.7 g) were divided into three groups (85 fish each). Fish were left untreated (control), or injected intra-peritoneal with 0.1 ml vaccine in Freund's complete adjuvant, containing 2×10^8 colony forming units (CFU) (Group I) or 2×10^5 (GroupII) CFU inactivated *V. mimicus*. Two weeks after primary immunization, vaccinated fish were boosted with the same dose of bacteria in Freund's incomplete adjuvant. Control fish were injected intra-peritoneal with 0.1 ml of PBS. At week 1, 2, 3 and 4 post primary immunization, heparin-treated or normal blood was collected from the tail vein of five fish in each group. Heparin-treated blood was used to measure respiratory burst activity of blood leukocytes. Normal blood was stored at room temperature for 1 h and then at 4 °C for 5 h. Serum was the collected by centrifugation at 12,000 rpm for 5 min to determine the agglutination antibody titer and lysozyme activity.

Challenge

The NH isolate was cultured in BHI broth at 28°C for 24 h and

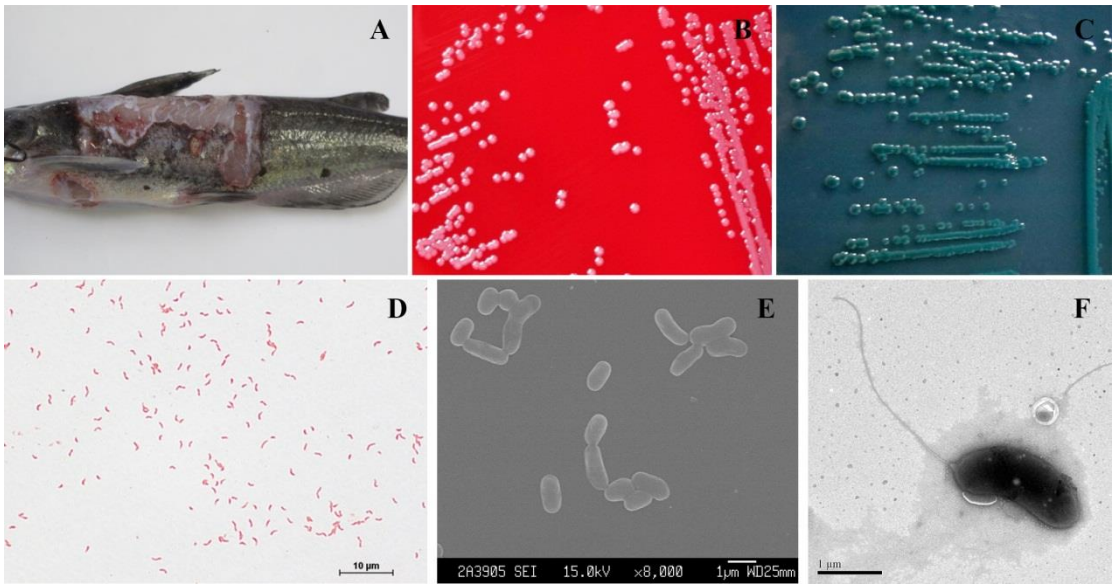

Figure 1. Clinical signs of dying channel catfish (A). Colonies of bacterial isolates grown on blood agar (B) or TCBS agar (C). Bacterial morphology under light microscopy (D), under scanning electron microscopy (E), or under transmission electron microscopy (F).

harvested by centrifugation at 5000 rpm for 5 min. Bacteria were washed three times, suspended in sterile PBS, and then adjusted to suitable concentration. We then evaluated the virulence of the NH isolate to channel catfish that were not vaccinated. Fish (15.1±1.8 g) were randomly divided into seven groups (one control group and six infection groups; 20 fish in each group). For infection, fish were injected intra-peritoneal with 0.1 ml of the bacterial suspension, at a concentration of 4.3×10^2, 4.3×10^3, 4.3×10^4, 4.3×10^5, 4.3×10^6, or 4.3×10^7 CFU/ml. Control fish were injected intra-peritoneal with 0.1 ml of PBS. Fish mortality was recorded daily for 14 days after inoculation. The median lethal dose (LD50) values were calculated using the trimmed Spearman–Karber method (Hamilton et al., 1977).

To evaluate the vaccine's immune protection, four weeks after the primary immunization, 60 fish from each group were randomly selected and injected intra-peritoneally with 0.1 ml of the bacterial cultures containing 5.6×10^5 CFU of *V. mimicus*. Fish mortality was recorded daily for 14 days after the infection, the relative percentage survival (RPS) was calculated using the formula: (1-mortality of immunized fish/control fish mortality) × 100%.

Respiratory burst activity

Blood leukocyte respiratory burst activity was measured according to the method described by Anderson and AK (1995). Briefly, 0.1 ml of 0.2% nitro blue tetrazolium buffer was added to 0.1 ml anticoagulated blood, and the mixture was incubated at room temperature for 30 min. Next, 0.05 ml of the mixture were added into 1 ml dimethylformamide, and the mix was then centrifuged at 3000×g for 5 min. The supernatant was collected, and the absorbance value was detected at 540 nm. Dimethylformamide alone was used as a negative control.

Agglutination antibody titer

Serum agglutination antibody titers were determined in 96-well microplates with round bottoms. Heat-inactivated serum (50 µl) was added to each well in serial two-fold dilution. PBS was used as negative control. An equal volume of inactivated *V. mimicus* was added to each well containing serum samples. Microplates were incubated at 28°C overnight. The maximum dilution factor of the solutions that caused complete clumping of bacteria was considered the agglutination antibody titer.

Lysozyme activity

Serum lysozyme activity was detected using an LZM test kit (Nanjing Jiancheng Bioengineering Institute, Nanjing, China). In brief, 100 ml of distilled water, standard liquid (supplied by the kit), or serum samples were added to 1 ml of a bacterial solution. After mixing and incubating at 37°C for 15 min, the mixture was transferred to an ice bath for 3 min. The suspension was transferred into a 0.5 cm optically clear colorimetric dish for transmittance (T15) determination at 530 nm. Transmittance of the distilled water at 530 nm was adjusted to 100% before measurements. Lysozyme content of the samples was calculated according to the following formula: Lysozyme content (U/ml) = $(UT_{15}\text{-}OT_{15})/(ST_{15}\text{-}OT_{15})$ × standard concentration (200 U/ml) × sample dilution factor where UT_{15} is test tube transmittance, OT_{15} is blank tube transmittance, and ST_{15} is standard tube transmittance.

Statistical analysis

Data are expressed as mean ± standard error. Significance of differences between samples was determined using Duncan's test. The level of statistical significance was set at $P < 0.05$.

Ethical considerations

The authors agree upon standards of expected ethical behavior.

Table 1. Biochemical characteristics of the isolate were detected by VITEK2 Compact microbial identification system.

Characteristics	Results	Characteristics	Results
Ala-Phe-Pro-arylamidase	-	Saccharose/Sucrose	-
Adonitol	-	D-tagatose	-
L-pyrrolydonyl-arylamidase	+	D-trehalose	+
L-arabitol	-	Citrate (Sodium)	-
D-cellobiose	-	Malonate	-
β-galactosidase	+	5-keto-D-gluconate	-
H_2S production	-	L-lactate alkalinisation	+
β-N-acetyl-glucosaminidase	+	α-glucosidase	-
GlutamylarylamidasepNA	-	Succinate alkalinisation	+
D-glucose	+	β-N-acetyl-galactosaminidase	+
γ-glutamyl-transferase	-	α-galactosidase	-
Fermentation/Glucose	-	Phosphatase	+
β-glucosidase	-	Glycine arylamidase	-
D-maltose	+	Ornithine decarboxylase	-
D-mannitol	+	Lysine decarboxylase	-
D-mannose	-	L-histidine assimilation	-
β-xylosidase	-	Courmarate	+
β-alanine arylamidasepNA	-	β-glucoronidase	-
L-prolinearylamidase	-	O/129 RESISTANCE	-
Lipase	-	O/129 Resistance (comp.vibrio.)	-
Palatinose	-	Glu-Gly-Arg-arylamidase	-
Tyrosine arylamidase	-	L-malate assimilation	+
Urease	-	Ellman	-
D-sorbitol	-		

Notes: "-" negative, "+" positive.

RESULTS

Identification of bacterium

Bacteria were isolated from the tissues of dying catfish, and the bacterial colonies were orbicular, smooth and white on blood agar, or green on TCBS agar (Figure 1B and C). Isolated bacteria were Gram-negative, curved rod-shaped, and had a single polar flagella (Figure 1D and F). BioMerieux VITEK system identified the bacterial isolates as *V. mimicus,* with 99% probability (Table 1). In addition, phylogenetic analysis of the 16S rDNA sequence showed that the NH strain clustered with *V. cholerae* CECT514^T and *V. mimicus* ATCC33653^T into the same group (Figure 2A). However, the phylogenetic analysis, based on the concatenated sequence of three housekeeping genes rpoA, recA, and pyrH, showed that the NH strain had a closer relationship to *V. mimicus* ATCC33653^T than to *V. cholerae* CECT514^T (Figure 2B).

Virulence of the isolate

The NH strain caused death of healthy channel catfish from day 1 post infection. Most deaths were observed at day 3 (~40%) and 4 (~100%) post infection. Infected fish exhibited the typical symptom of skin ulcers. Moreover, *V. mimicus* could be recovered from dead fish. The LD50 value of the isolate to catfish was 3.42×10^5 CFU per fish.

Vaccine protection

After *V. mimicus* infection, 56 fish (100%) died in the control group. However only one (Group I) and three (Group II) fish died in the vaccinated groups. The RPS of group I and group II were 98.2 and 94.6%, respectively.

Respiratory burst activity

After immunization, the respiratory burst activity of blood leukocyte increased slightly, but there were no significant differences between the immunization groups and the control group at each time point (Figure 3).

Agglutination antibody titer

As shown in Figure 4, the serum agglutination antibody

Table 2. *Vibrio* type strains and accession numbers included in the multilocus sequence analysis.

Species	16SrDNA	rpoA	recA	pyrH
Vibrio cholerae	X76337	HE805630	FM204835	FM202582
V. alginolyticus	X56576	KC954203	KC954188	JN408273
V. brasiliensis	AEVS01000097	HM771384	HM771379	HM771374
V. campbellii	CP000789	AJ842564	AJ842377	EF596641
V.coralliilyticus	ACZN01000020	JN039157	JN039156	JN039155
V.diazotrophicus	X74701	AJ842598	AJ842411	HE805632
V.ezurae	BATM01000062	BATM01000005	BATM01000003	BATM01000001
V.fluvialis	X76335	AJ842606	AJ842419	JN426808
V.furnissii	ACZP01000015	AJ842614	AJ842427	JF316672
V.halioticoli	BAUJ01000001	BAUJ01000003	BAUJ01000053	BAUJ01000014
V.harveyi	X74706	KC954196	KC954182	KC954172
V.kanaloae	AJ316193	AJ842637	AJ842450	FN908851
V.mimicus	X74713	EF643486	EF643485	EU118242
V.mytili	X99761	AJ842657	AJ842472	GU266287
V.neptunius	AJ316171	JN039153	AJ842478	GU266291
V.parahaemolyticus	X56580	AJ842677	AJ842490	GU266286
V.rotiferianus	AJ316187	AJ842688	AJ842501	EF596722
V.tubiashii	X74725	AJ842734	AJ842518	JF316670
Photobacterium kishitanii	AY341439	EF415588	EF415552	EF415536

titer was significantly increased at week 1 post immunization, and increased continuously until 4 weeks after immunization. The agglutination antibody titer was not significantly different between vaccinated fish of Group I or II. In un-vaccinated fish no agglutination was detected during the course of experiment.

Lysozyme activity

Similar to serum agglutination, serum lysozyme activity was significantly up-regulated at week 1 post immunization, and it continuously increased until the end of the experiment (Figure 5). The lysozyme activity did not change significantly between the two immunization groups (that is, Group I and II). There were small changes in lysozyme activity in the control group during the experiment, but differences were not significant.

DISCUSSION

V. mimicus can cause human gastroenteritis, ear infections, and severe cholera-like diarrhea (Austin 2010; Hasan et al., 2010). *V. mimicus*is is also associated with disease in aquatic animals, which are potential sources of infection to humans after ingestion (Miyoshi et al., 2014). Effective prophylaxis methods are needed to control *V. mimicus* epidemics. In this study, *V. mimicus* was isolated from dying channel catfish, and an effective prophylaxis method, a formalin-inactivated *V. mimicus* vaccine was developed.

According to the bacterial morphology and the character of gene sequences, the bacteria isolates were identified as *V. mimicus*. Subsequently, the virulence of the isolates obtained: *V. mimicus* exhibited high virulence to healthy channel catfish with a LD50 value of 3.42×10^5 CFU per fish. Then, we used formalin-inactivated *V. mimicus* as vaccine, which provided catfish with over 90% RPS. Similarly, in carp *Cyprinus carpio*, an inactivated *V. mimicus* vaccine (Zhang et al., 2014), and an OmpU-based vaccine (Cen et al., 2013), was also shown to protect against *V. mimicus* infection. These results indicate that immune prophylaxis is an effective method to control the disease caused by *V. mimicus* in both fish species, and maybe in other siluriformes species, such as yellow catfish *P. fulvidraco* (Geng et al., 2014), southern catfish *S. soldatovi meridionalis* (Geng et al., 2014), and Zhengchuan catfish *S. soldatovi meridionalis* (Zhang et al., 2014), which are also susceptible species.

Compared to the control group, the respiratory burst activity of blood leukocyte in the immunization groups increased slightly, but there were no significant differences between ($P>0.05$); the serum agglutination antibody titer significantly increased since immunization. After immunization with inactivated *V. mimicus*, serum agglutination antibody titer and lysozyme activity (but not the respiratory burst) increased significantly. Adaptive immunity is the basis for vaccine development, and antibodies play a crucial role in it. Fish can produce

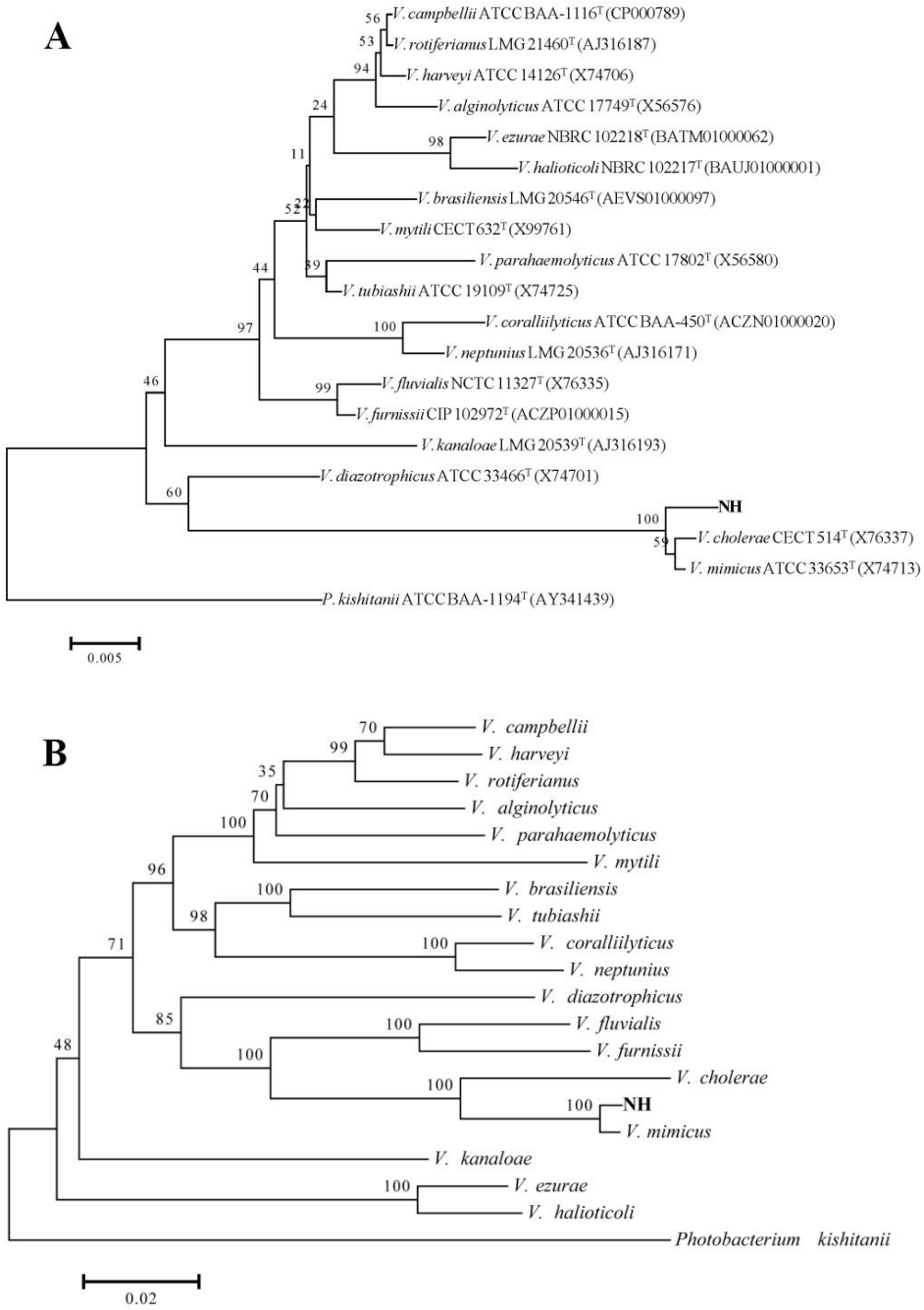

Figure 2. Phylogenetic tree of the NH isolate based on the 16S ribosomal DNA sequences (A) and on concatenated sequences of three housekeeping genes rpoA, recA, and pyrH (B), using the neighbor-joining method. Numbers at the nodes indicate the levels of bootstrap support, based on data for 1,000 replicates. The NCBI accession numbers are listed in Table 2.

specific antibodies after immunization with inactivated *V. mimicus* (Zhang et al., 2014), or with a vaccine based on OmpU subunit (Cen et al., 2013). Li et al. (2016) observed a positive correlation between the antibody titer and immune protection. Similar results were also reported in grouper immunized with *V. harveyi* (Nguyen et al., 2017), in tilapia vaccinated with *Streptococcus iniae* or with *S. agalactiae* (Li et al., 2016; Zou et al., 2011), and in rainbow trout *Oncorhynchus mykiss* immunized with live attenuated *Flavobacterium psychrophilum* (Sudheesh and Cain, 2016), to name a few examples.

Lysozyme is an important component of innate immunity involved in host protection against microbial

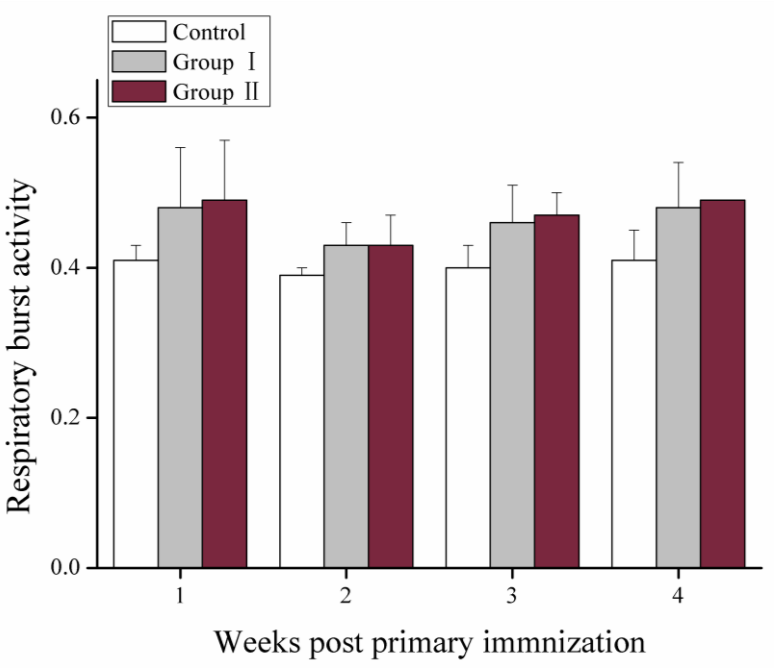

Figure 3. Respiratory burst activity of blood leukocytes after immunization. Data are expressed as mean ± SD (n=3); P<0.05 was considered significant. Asterisks (*) represent significant differences between fish of the un-vaccinated group and fish of the immunization groups.

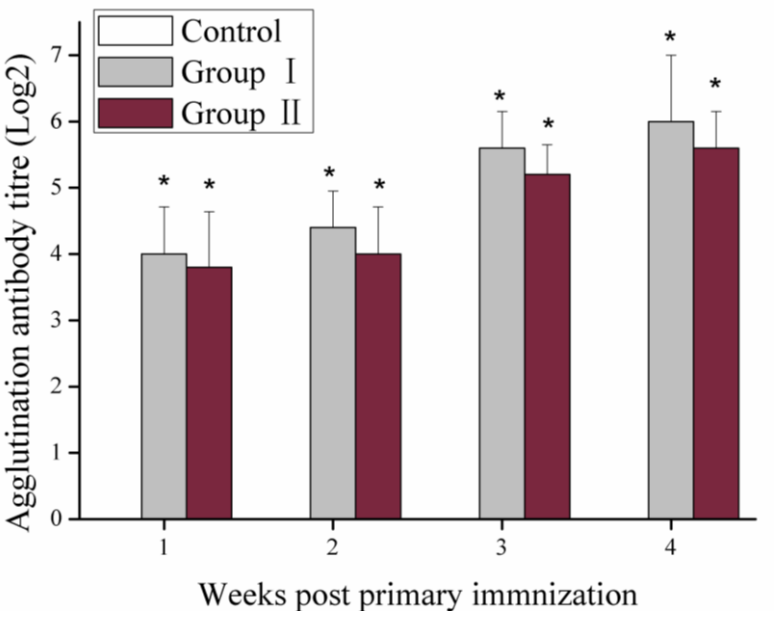

Figure 4. Antibody agglutination titer after immunization. Data are expressed as mean±SD (n=3); P<0.05 was considered significant. Asterisks (*) represent significant differences between fish of the un-vaccinated group and fish of the immunization groups.

infection (Saurabh and Sahoo, 2008). Lysozyme is normally used as an indicator to evaluate the effect of vaccination on the humoral immune responses of fish. In the present study, serum lysozyme activity of immune *I.*

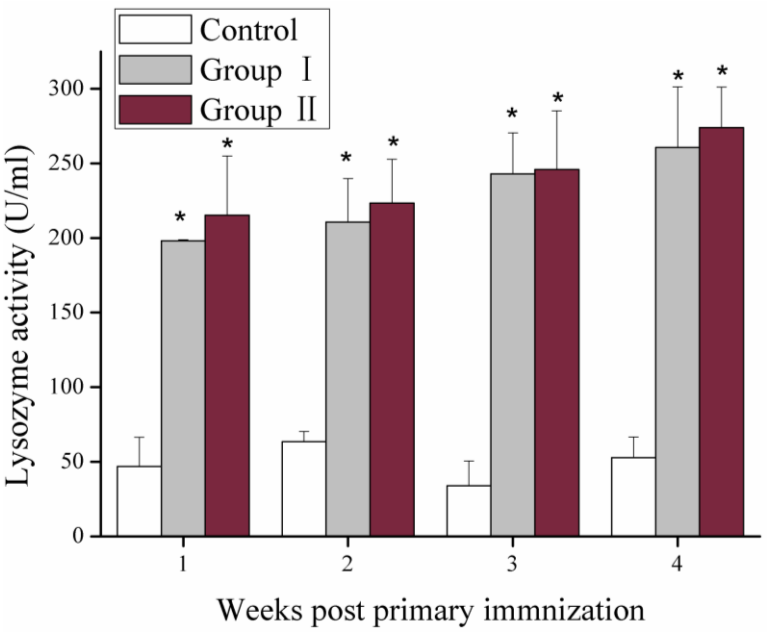

Figure 5. Serum lysozyme activity post immunization. Data are expressed as mean ± SD (n = 3); P<0.05 was considered significant. Asterisks (*) represent significant differences between fish of the un-vaccinated group and fish of the immunization groups.

punctatus was significantly up-regulated post immunization, and similar results were found in *Scortum barcoo* (Liu et al., 2014), and *Anguilla rostrata* (SongLin et al., 2015), indicating that lysozyme activity is up-regulated after immunization.

In conclusion, our results indicate that the RPS observed after vaccination is highly correlated to the agglutination titer of serum antibodies and lysozyme activity, but not to respiratory burst activity of blood leukocytes. Serum antibodies and lysozyme activity may play an important role in catfish immunity against *V. mimicus* infection.

CONFLICT OF INTERESTS

The authors have not declared any conflict of interests.

ACKNOWLEDGEMENTS

The authors appreciate the support of the Special Funds for Marine Fishery Science and Technology Promotion Project of Guangdong Province (Grant No. YCN (2017)17H) given to Dr. Hong-Yan Sun.

REFERENCES

Adeleye IA, Daniels FV, Enyinnia VA (2010). Characterization And Pathogenicity of Vibrio spp. Contaminating Seafoods In Lagos, Nigeria. Internet Journal of Food Safety 12:1-9.

Ambas I, Suriawan A, Fotedar R (2013). Immunological responses of customised probiotics-fed marron, *Cherax tenuimanus*, (Smith 1912) when challenged with *Vibrio mimicus*. Fish and Shellfish Immunology 35:262-270.

Anderson DP, AK S (1995). Basic hematology and serology for fish health programmes. In: Shariff M, Arthur JR, Subasinghe RP, editors. Disease in Asian aquaculture. Manila: Fish Health Section of Asian Fisheries Society, pp. 185-202.

Austin B (2010). Vibrios as causal agents of zoonoses. Veterinary Microbiology 140:310-317.

Campos E, Bolaños H, Acuña MT, Díaz G, Matamoros MC, Raventós H, Sánchez LM, Sánchez O, Barquero C (1996). *Vibrio mimicus* diarrhea following ingestion of raw turtle eggs. Applied and Environmental Microbiology 62:1141-1144.

Cen J, Liu X, Li J, Zhang M, Wang W (2013). Identification and immunogenicity of immunodominant mimotopes of outer membrane protein U (OmpU) of *Vibrio mimicus* from phage display peptide library. Fish and Shellfish Immunology 34:291-295.

Chowdhury MA, Yamanaka H, Miyoshi S, Aziz KM, Shinoda S (1989). Ecology of *Vibrio mimicus* in aquatic environments. Applied and Environmental Microbiology 55:2073-2078.

Davis BR, Fanning GR, Madden .M, Steigerwalt AG, Bradford HB, Jr Smith HL, Jr Brenner DJ (1981). Characterization of biochemically atypical *Vibrio cholerae* strains and designation of a new pathogenic species, *Vibrio mimicus*. Journal of Clinical Microbiology 14: 631-639.

Eaves LE, Ketterer PJ (1994). Mortalities in red claw crayfish *Cherax quadricarinatus* associated with systemic *Vibrio mimicus* infection. Diseases of Aquatic Organisms 19:233-237.

Geng Y, Liu D, Han S, Zhou Y, Wang KY, Huang XL, Chen DF, Peng X, Lai WM (2014) Outbreaks of vibriosis associated with *Vibrio mimicus* in freshwater catfish in China. Aquaculture 433:82-84.

Guardiola-Avila I, Acedo-Felix E, Sifuentes-Romero I, Yepiz-Plascencia G, Gomez-Gil B, Noriega-Orozco L (2016). Molecular and genomic characterization of *Vibrio mimicus* isolated from a frozen shrimp processing facility in Mexico. PloS One 11:e0144885.

Hamilton MA, Russo RC, Thurston RV (1977). Trimmed Spearman-Karber method for estimating median lethal concentrations in toxicity

bioassays. Environmental Science and Technology 11:714-719.
Hasan NA, Grim CJ, Haley BJ, Chun J, Alam M, Taviani E, Hoq M, Munk AC, Saunders E, Brettin TS, Bruce DC, Challacombe JF, Detter JC, Han CS, Xie G, Nair GB, Huq A, Colwell RR (2010). Comparative genomics of clinical and environmental *Vibrio mimicus*. PNAS 107:21134-21139.
Li JN, Li YY, Hu SK, Li L, Fang B, Yu WY, Zhang XH (2005). Analysis on pathogen producing ascitic fluid disease of *Eriocher sinensis*. Journal of Fishery Sciences of China 12:267-274.
Li W, Wang HQ, He RZ, Li YW, Su YL, Li AX (2016). Major surfome and secretome profile of *Streptococcus agalactiae* from Nile tilapia (*Oreochromis niloticus*): Insight into vaccine development. Fish and Shellfish Immunology 55:737-746.
Liu L, Li YW, He RZ, Xiao XX, Zhang X, Su YL, Wang J, Li AX (2014). Outbreak of *Streptococcus agalactiae* infection in barcoo grunter, *Scortum barcoo* (McCulloch & Waite), in an intensive fish farm in China. Journal of Fish Diseases 37:1067-1072.
Liu X, Gao H, Xiao N, Liu Y, Li J, Li L (2015). Outer membrane protein U (OmpU) mediates adhesion of *Vibrio mimicus* to host cells via two novel N-terminal motifs. PloS One 10:e0119026.
Miyoshi SI, Ikehara H, Kumagai M, Mizuno T, Kawase T, Maehara Y (2014). Defensive effects of human intestinal antimicrobial peptides against infectious diseases caused by *Vibrio mimicus* and *V. vulnificus*. Biocontrol Science 19:199-203.
Nguyen HT, Thu Nguyen TT, Tsai MA, Ya-Zhen E, Wang PC, Chen SC (2017). A formalin-inactivated vaccine provides good protection against *Vibrio harveyi* infection in orange-spotted grouper (*Epinephelus coioides*). Fish and Shellfish Immunology 65:118-126.
Nugroho RA, Fotedar R (2013). Dietary organic selenium improves growth, survival and resistance to *Vibrio mimicus* in cultured marron, *Cherax cainii* (Austin, 2002). Fish and Shellfish Immunology 35:79-85.
Sang HM, Ky LT, Fotedar R (2009). Dietary supplementation of mannan oligosaccharide improves the immune responses and survival of marron, *Cherax tenuimanus* (Smith, 1912) when challenged with different stressors. Fish and Shellfish Immunology 27: 341-348.
Saurabh S, Sahoo PK (2008). Lysozyme: an important defence molecule of fish innate immune system. Aquaculture Research 39:223-239.
SongLin G, PanPan L, JianJun F, JinPing Z, Peng L, LiHua D (2015). A novel recombinant bivalent outer membrane protein of *Vibrio vulnificus* and *Aeromonas hydrophila* as a vaccine antigen of American eel (*Anguilla rostrata*). Fish and Shellfish Immunology 43:477-484.
Sudheesh PS, Cain KD (2016). Optimization of efficacy of a live attenuated *Flavobacterium psychrophilum* immersion vaccine. Fish and Shellfish Immunology 56:169-180.
Sun HY, Noe J, Barber J, Coyne RS, Cassidy-Hanley D, Clark TG, Findly RC, Dickerson HW (2009). Endosymbiotic Bacteria in the Parasitic Ciliate *Ichthyophthirius multifiliis*. Applied and Environmental Microbiology 75:7445-7452.
Takahashi A, Miyoshi S, Takata N, Nakano M, Hamamoto A, Mawatari K, Harada N, Shinoda S, Nakaya Y (2007). Haemolysin produced by *Vibrio mimicus* activates two Cl- secretory pathways in cultured intestinal-like Caco-2 cells. Cell Microbiology 9:583-595.
Thune RL, Hawke JP, Siebeling RJ (1991). Vibriosis in the red swamp crawfish. Journal of Aquatic Animal Health 3:188-191.
Wang GL, Zheng TL, Jin S, Lu TX (2003). Preliminary studies on pathogen of ascites disease of cultured *Sparus macrocephelus*. Chinese Journal of Veterinary Science 23:33-35.
Wong FYK, Fowler K, Desmarchelier PM (1995). Vibriosis due to *Vibrio mimicusin* Australian freshwater Crayfish. Journal of Aquatic Animal Health 7:284-291.
Zhang X, Li YW, Mo ZQ, Luo XC, Sun HY, Liu P, Li AX, Zhou SM, Dan XM (2014). Outbreak of a novel disease associated with *Vibrio mimicus* infection in fresh water cultured yellow catfish, *Pelteobagrus fulvidraco*. Aquaculture 432:119-124.
Zhang YQ, Zhang TT, Li JN, Liu XL, Li L (2014). Design and evaluation of a tandemly arranged outer membrane protein U (OmpU) multi-epitope as a potential vaccine antigen against *Vibrio mimicus* in grass carps (*Ctenopharyngodon idella*). Veterinary Immunology and Immunopathology 160:61-69.
Zou LL, Wang J, Huang BF, Xie MQ, Li AX (2011). MtsB, a hydrophobic membrane protein of *Streptococcus iniae*, is an effective subunit vaccine candidate. Vaccine 29:391-394.

Vol. 18(27), pp. 612-621, July, 2019
DOI: 10.5897/AJB2019.16801
Article Number: CDB10F461413
ISSN: 1684-5315

http://www.academicjournals.org/AJB

ACADEMIC JOURNALS
expand your knowledge

African Journal of Biotechnology

Full Length Research Paper

Morphological and molecular screening of rice accessions for salt tolerance

Uyoh E. A.[1*], Ntui V. O.[1,2], Umego C.[1], Ita E. E.[1,3] and Opara C.[1]

[1]Department of Genetics and Biotechnology, Faculty of Biological Sciences, University of Calabar, Calabar, Nigeria.
[2]International Institute of Tropical Agriculture, Nairobi, Kenya.
[3]Laboratory of Plant Cell Technology, Graduate School of Horticulture, Chiba University, Japan.

Received 15 March, 2019; Accepted 27 June, 2019

The ever-increasing demand for rice raises the need to increase productivity by using salt tolerant varieties on saline soils. In this study, 12 rice accessions were screened for tolerance to salt at seedling stage using morphological and molecular methods. The study was carried out in a hydroponic system using Hoagland solution. Scoring was done using the modified standard evaluation score (SES) system after 14 days of treatment. Salt tolerance indices were estimated from shoot length, root length and total biomass. For molecular studies, ten Simple Sequence Repeats (SSR) primers linked with salt tolerance Quantitative Trait Loci (QTL) were used. Results showed greater reductions in biomass and shoot growth of susceptible accessions compared to the tolerant ones. The effect of salt stress on root length showed variability among accessions as well as concentrations. UPIA 1, UPIA 2, FARO 52, FARO 61, TOG 5681 and FARO 44 had similar banding patterns with POKALLI (check variety) suggesting that they may contain salt tolerance genes. Of these accessions, only POKALLI and UPIA 2 survived all levels of salt concentration tested and thus got the highest SES score of one. Both accessions also had the highest overall mean salt tolerance indices. In conclusion, based on SES scores, salt tolerance indices and SSR data, POKALLI and UPIA 2 were identified as highly tolerant, FARO61, FARO 52, UPIA 1 and TOG 5980A as tolerant while WITA 12, CG12, TOG1670, TOG 5681 and TOG 5485 were highly susceptible. Such information will be useful in the selection of parents as breeding lines for salt tolerance.

Key words: Rice, seedling stage, hydroponics, salt tolerance index, simple sequence repeats (SSR) primers.

INTRODUCTION

Rice (mainly *Oryza sativa* L. and *Oryza glaberrima* Steud.) is one of the most important and universally accepted food crops, providing over 20% of human dietary energy and serving as a staple crop for millions of people globally (Calpe, 2006). Its production is limited by salinity, which has been recognized as the second most widespread soil problem in rice growing countries, after drought (Gregorio et al., 1997). The young seedling and

*Corresponding author. E-mail: gen_uyoh@yahoo.com.

Table 1. Identification of rice varieties used for the study and their improved traits.

Code	Species	Characteristics	Country
WITA 12	*O. sativa*	-	Ivory Coast
FARO 44	*O. sativa*	**Long grain, optimum production under low management.	Taiwan
FARO 52	*O. sativa*	**High yielding, tolerant to iron toxicity and drought	Nigeria
TOG 16704	*O. glaberimma*	-	Ivory Coast
UPIA 1	*O. sativa*	**Early maturity, high yielding, long grain, tolerance to iron toxicity and African gall midge.	Nigeria
TOG 5485	*O. glaberimma*		Nigeria
UPIA 2	*O. sativa*	**High yielding, long grain, tolerance to iron toxicity and African gall midge.	Nigeria
POKALLI	*O. sativa*	**Tolerant to salt toxicity	Sri Lanka
FARO 61	*O. sativa*	**Early germination, high yielding and tolerant to anaerobic germination	Nigeria
TOG 5980A	*O. glaberimma*		Nigeria
TOG 5681	*O. glaberimma*	*Drought tolerant	Nigeria
CG14	*O. glaberimma*	***Tolerant to iron toxicity	Senegal

Source: * Ndjiondrop et al. (2012); ** Nigerian Seed Portal Initiatives (Crops). www.seedportal.org.ng . Released and Registered Crops in Nigeria-Rice. (Accessed 10th June 2019);*** Sarla and Mallikarjuna Swamy (2005)

reproductive stages are more vulnerable to salinity stress in contrast to vegetative stage (Singh et al., 2016).

Several agronomic practices like improved field drainage through maintenance of adequate amount of water (2-3 cm height) until early production stage (De Costa et al., 2012), establishment of crop by transplanting (Sirisena et al., 2010) and use of organic fertilizer, are often used to address the issue of salinity. These practices are, however, inefficient, not cost effective, and not affordable for a long-term solution. Hence, the need to explore the tremendous variation in salt tolerance reported to exist within rice species for a long-term solution (Sabouri and Biabani, 2009).

Screening for salt tolerance was previously based on morphological features alone, which are not very reliable since they may be affected by environmental factors. Progress in the breeding for salt tolerance has been made after the discovery of Quantitative Trait Loci (QTL) underlying salinity stress. Islam et al. (2015) used 3 SSR markers (RM3412, RM510 and RM 336) to identify 5 tolerant rice varieties out of the 25. Ali et al. (2014) identified 4 true salt tolerant rice land races out of 33 using both morphological (shoot length, root length and plant biomass) and simple sequence repeats (SSR) markers (RM8046, RM336, RM8094). Searching for DNA markers closely linked to traits related to salt tolerance has become a key objective in most breeding programs and various reports are available (Kanawapee et al., 2012; Dahanayaka et al., 2015; Pires et al., 2015; Krishnamurthy et al., 2016; Sakina et al., 2016; Reddy et al., 2017). However, there is still much to be done considering the increasing number of new rice cultivars and Quantitative Trait Loci yet to be screened (Islam et al., 2015). The present study was undertaken to screen 12 rice varieties for tolerance to salt stress using both morphological and molecular methods.

METHODOLOGY

Twelve (12) varieties of rice (Table 1) obtained from the Africa Rice Centre, Ibadan, Oyo State, Nigeria were screened for tolerance to salinity at the seedling stage. The experiment was carried out in the greenhouse and molecular biology laboratory of the Department of Genetics and Biotechnology, University of Calabar, Calabar, Nigeria.

Morphological studies

The rice seeds were dehusked and surface-sterilized in 70% ethanol for 1 min and in 2.5% commercial bleach solution for 15 min. The seeds were rinsed several times with sterile water and kept in the dark for 48 h for germination. The pre-germinated seeds were transferred to petri dishes containing half-strength liquid Murashige and Skoog (MS) medium (Murashige and Skoog, 1962) and incubated for one week. The 1-week-old seedlings were transferred into falcon tubes containing 50 ml of half-

Table 2. Modified standard evaluation score (SES) of visual salt injury.

Score	Observation	Tolerance level
1	*Normal growth, no leaf symptoms*	Highly tolerant
3	Nearly normal growth, but leaf tips of few leaves are whitish and rolled	Tolerant
5	Growth severely retarded; most leaves rolled; only a few elongating	Moderately tolerant
7	Complete cessation of growth; most leaves dry; some plants dying	Susceptible
9	Almost all plants dead or dying	Highly susceptible

Source: Gregorio et al. (1997).

Table 3. Microsatellite (SSR) primers used for the molecular screening.

S/N	Primer code	Forward sequence	Reverse sequence
1	RM8094	AAGTTTGTACACATCGTATACA	CGCGACCAGTACTACTACTA
2	RM336	CTTACAGAGAAACGGCATCG	GCTGGTTTGTTTCAGGTTCG
3	RM8046	AGTACGATTTCTGTCAGCGTTGCTTAGT	GGATGAAGTTGATGGATGATCTACTTGTT
4	RM493	TAGCTCCAACAGGATCGACC	GTACGTAAACGCGGAAGGTG
5	RM3412	AAAGCAGGTTTTCCTCCTCC	CCCATGTGCAATGTGTCTTC
6	RM8095	TTCCGTGGACATGATGAATC	AAGGTTTAGAACATACACACCGTT
7	RM7075	TATGGACTGGAGCAAACCTC	GGCACAGCACCAATGTCTC
8	RM253	TCCTTCAAGAGTGCAAAACC	GCATTGTCATGTCGAAGCC
9	RM436	ATTCCTGCAGTAAAGCACGG	CTTCGTGTACCTCCCCAAAC
10	RM8053	TCTAAAAGAGACATTGCCGATGATA	CATACTCAAAGTCACGGAAAGTACC

strength modified Hoagland nutrient solution and grown for another one week before salt treatment. The nutrient solution consisted of 5.6 mM NH_4NO_3, 0.8 mM $MgSO_4.7H_2O$, 0.8 mM K_2SO_4, 0.18 mM $FeSO_4.7H_2O$, 0.18 mM $Na_2EDTA.2H_2O$, 1.6 mM $CaCl_2.2H20$, 0.8 mM KNO_3, 0.023 mM H_3BO_3, 0.0045 mM $MnCl_2.4H_2O$, 0.0003 mM $CuSO_4.5H_2O$, 0.0015 mM $ZnCl_2$, 0.0001 mM $Na_2MoO_4.2H_2O$ and 0.4 mM $K_2HPO_4.2H_2O$. After 1 week of culture, the salt treatment was added as 0, 50, 100 and 150 mM of NaCl to the tubes according to the experimental design. The pH of the solution was maintained between 5.0 and 5.5 throughout the experiment for better nutrient availability (Bhowmik et al., 2009; Ali et al., 2014) and the solutions were replaced every 3 days until data were collected. The experiment was set up as a 12 × 4 factorial, laid out using the completely randomized design (CRD) with 3 replications giving a total of 144 experimental units. Factor 1 was rice accessions with 12 levels while Factor 2 was salt concentration with four levels. Growth conditions in the greenhouse were temperature: 28-30°C, Humidity: 65-70%, Light: Natural light, 12 h light: 12h dark.

Data collection and analysis on morphological parameters

Salt evaluation scores were estimated for each rice accession by scoring the seedlings for visual symptoms of salt injury 14 days after commencement of salt treatment using the modified standard evaluation score system given by Gregorio et al. (1997) (Table 2). The mean performance of each variety across the different salt concentration levels was used. Varieties that survived all the 4 salt concentration levels were rated as highly tolerant and given the lowest score (1) while those that did not survive beyond the first salt level got the highest (7). Data were also collected on shoot length (cm), root length (cm), and plant biomass (g) for each variety under different salt concentrations and used to estimate salt tolerance indices by dividing the mean value for the three traits under a given salinity level by the mean value for those traits under control (Zeng et al., 2002). Thus:

Salt Tolerance Index (STI) = Mean performance under stress condition/Mean performance under normal condition (1)

Cluster analysis based on salt tolerance indices was used to group the accessions (Islam et al., 2015).

Molecular screening for salinity tolerance

Genomic DNA was extracted from healthy three-week old leaf samples of the 12 rice varieties using the modified Cetyl Trimethyl Ammonium Bromide (CTAB) method of Dellaporta et al. (1983). The extracted DNA was quantified using a nano-spectrophotometer (JenWay, Genova Nano) and diluted to a final concentration of 250 ng/µl. The samples were screened using a total of 10 SSR markers (Table 3) reported by previous workers to be linked with salt tolerance quantitative trait loci (QTL) in other rice cultivars. A 20 µl PCR reaction mixture containing 1 µl of genomic DNA template, 0.1 µl of Taq polymerase, 0.4 µl of 10 mM dNTPs, 0.5 µl of forward primer, 0.5 µl of reverse primer, 2 µl of 10X PCR buffer and 15.5 µl distilled water was prepared. PCR program was maintained as initial denaturation at 95°C for 5 min followed by 35 cycles of: Denaturation for 30 s at 95°C, primer annealing at 53°C for 30 s, primer extension at 72°C for 30 s, and final extension at 72°C for 5 min. 10 µl of amplified PCR products were mixed with 1.5 µl of loading dye, resolved by electrophoresis in 1% agarose gel and stained with ethidium bromide (Islam et al., 2015).

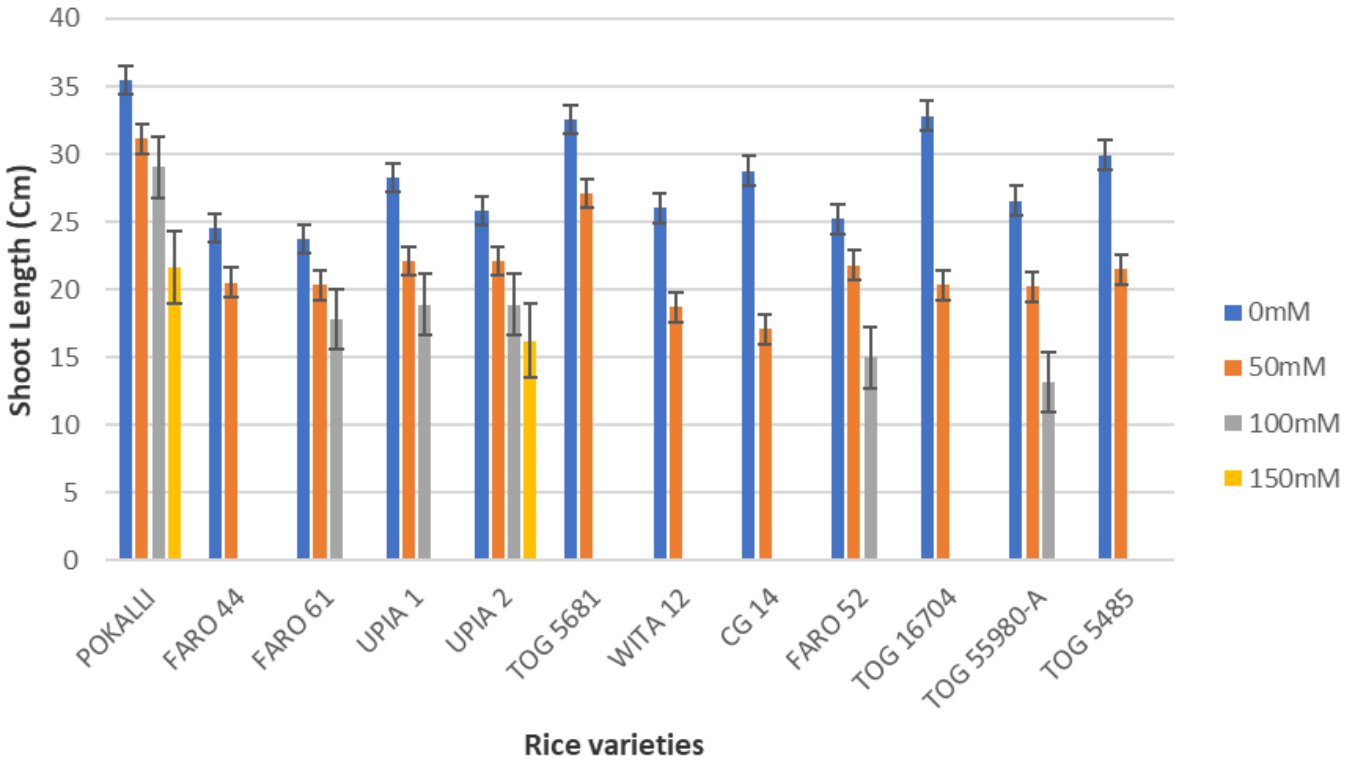

Figure 1. Mean effect of different salt concentrations on shoot length of 12 rice varieties at 14 days of treatment.

Scoring and analysis of amplified fragments

The well separated amplified DNA fragments were carefully scored on a presence/absence matrix, with 1 representing presence and 0 representing absence. The data were analyzed for polymorphic information content (PIC) and allele frequency using the Microsoft Excel workbook software. In each of the primers tested, rice varieties that had similar banding pattern with Pokkali (standard) was regarded as an indication that such varieties may contain the genes for salt tolerance. Results from both morphological and molecular analyses were taken into consideration in the final classification of tolerant and susceptible accessions.

RESULTS

Effect of different salinity levels on seedling growth

The mean effects of the different salt concentrations on shoot length, root length and biomass for all the twelve rice accessions are as shown in Figures 1 to 3. Generally, shoot length and biomass decreased with increasing salt concentrations in most of the accessions. On the other hand, root length increased with salt concentration in all accessions except for POKALLI, UPIA 1, UPIA 2, FARO 52 TOG 55980-A and TOG 16704 where it showed irregular variations across the salt concentrations. Salt sensitive accessions showed greater reduction in these parameters compared to the tolerant ones (Figures 1 and 3).

Standard evaluation score and salt tolerance indices

Only POKALLI and UPIA 2 survived all levels of salt concentration and thus scored highest with an SES score of 1. This was followed by FARO 61, UPIA 1, FARO 52 and TOG 5980A all of which showed good tolerance but did not survive beyond 100 mM of salt concentration. They earned an SES score of 3. FARO 44 showed moderate tolerance to salt with retarded growth and rolled leaves and thus got a score of 5. TOG 5681, WITA 12, CG 14, TOG 1670A, and TOG 5485 were all observed to be susceptible with most leaves dried up, and thus scored 7 (Table 4).

The mean salt tolerance indices for the twelve (12) rice accessions at the three (3) salinity levels are shown in Table 5. POKALLI and UPIA 2 showed the highest overall mean salt tolerance indices of 0.82 and 0.67, respectively while TOG 16704 showed the least with 0.3.

Cluster analysis

Cluster analysis based on data on salt tolerance indices grouped the rice accessions into 3 clusters (Figure 4). Cluster 1 had the following accessions: CG14, TOG5485, FARO44, TOG16704, TOG5681 and WITA12. Cluster 2 was made up of the following accessions: UPIA1, TOG5980-A, FARO61 and FARO52. Cluster 3 was made

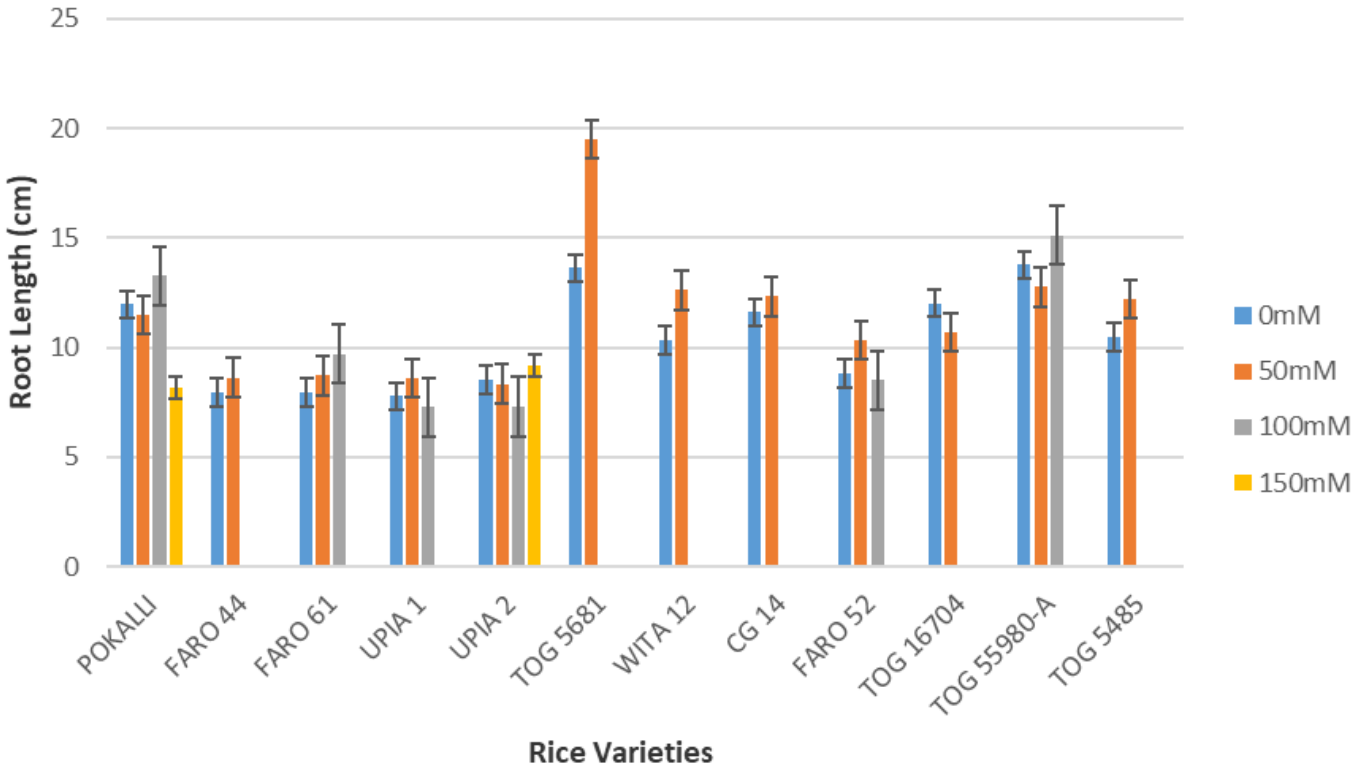

Figure 2. Mean effect of different salt concentrations on root length of 12 rice varieties at 14 days of treatment.

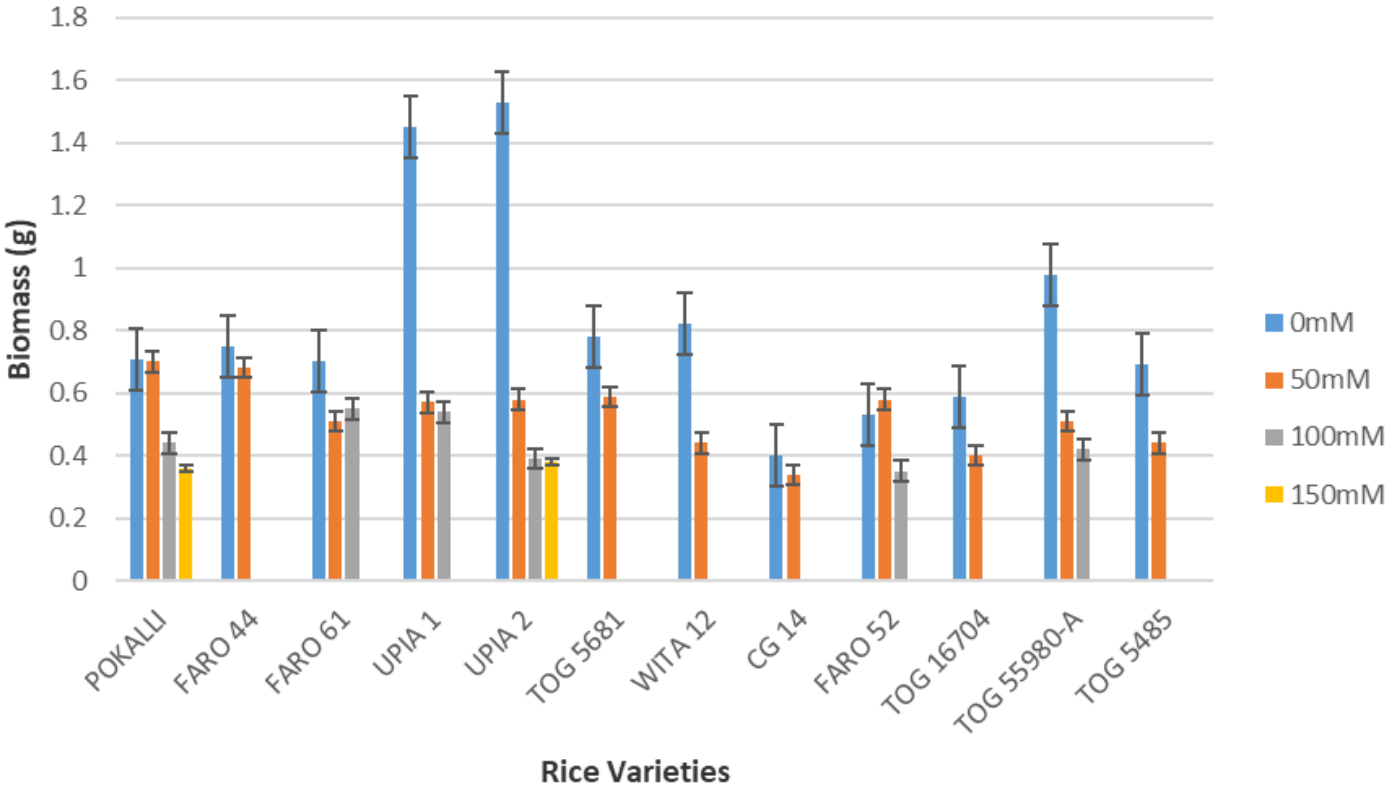

Figure 3. Mean effect of different salt concentrations on biomass of 12 rice varieties at 14 days of treatment.

Table 4. Standard evaluation scores of the rice varieties studied.

S/N	Variety	Score	Tolerance degree
1	POKKALI	1	Highly Tolerant
2	FARO 44	5	Moderately Tolerant
3	FARO 61	3	Tolerant
4	UPIA 1	3	Tolerant
5	UPIA 2	1	Highly Tolerant
6	TOG 5681	7	Susceptible
7	WITA 12	7	Susceptible
8	CG 14	7	Susceptible
9	FARO 52	3	Tolerant
10	TOG 1670A	7	Susceptible
11	TOG 5980A	3	Tolerant
12	TOG 5485	7	Susceptible

Table 5. Mean* salt tolerance indices for 12 rice varieties at 3 salinity levels.

Accession	50 mM	100 mM	150 mM	X
POKKALI	0.94	0.85	0.66	0.82
FARO 44	0.95	0.00	0.00	0.32
FARO 61	0.89	0.75	0.00	0.55
UPIA 1	0.75	0.66	0.00	0.47
UPIA 2	0.74	0.61	0.65	0.67
TOG 5681	1.00	0.00	0.00	0.33
WITA 12	0.83	0.00	0.00	0.28
CG14	0.83	0.00	0.00	0.28
FARO 52	0.87	0.74	0.00	0.54
TOG 16704	0.73	0.00	0.00	0.24
TOG5980A	0.74	0.68	0.00	0.47
TOG5485	0.89	0.00	0.00	0.30

*Values are means for root, shoot and biomass. X = Overall mean for each variety.

up of POKALLI and UPIA2. Members of cluster 1 were highly susceptible to salt conditions; members of cluster 2 were tolerant, while members of cluster 3 were highly tolerant to varying salt conditions.

Molecular studies

Of the ten (10) SSR markers screened, primers RM336, RM493 and RM3412 which ranged in PIC from 0.486 in primer RM336 to 0.626 in primers RM493 and RM3412 gave the clearest polymorphic band patterns, with amplicon sizes ranging from 80 to 300 bp. For primer RM336, banding patterns similar to POKALLI were observed in UPIA 1, UPIA 2 and FARO 52. Primer RM493 produced similar banding patterns for Pokalli and FARO 44. Similar banding patterns in RM3412 were also observed for POKALLI, FARO 44, FARO 61 and UPIA 2. Amplification profiles as revealed by RM336, RM493, and RM3412 across all 12 accessions used are depicted in Plates 1 to 3. A total of 30 alleles were detected across the three primers used, with 3 alleles per locus, giving 0.333 as the average number of alleles per locus. The allele frequencies produced by different markers per locus ranged from 8.3 to 67% (Table 6).

DISCUSSION

The capacity to tolerate salinity is a key factor in plant productivity (Momayezi et al., 2009). In the present study, all the rice accessions grew robustly and showed uniform green colour and height in the non-stressed conditions. However, in the presence of salt stress, the accessions showed variation in vigor in terms of morphological traits and growth attributes and their cumulative effect on plant

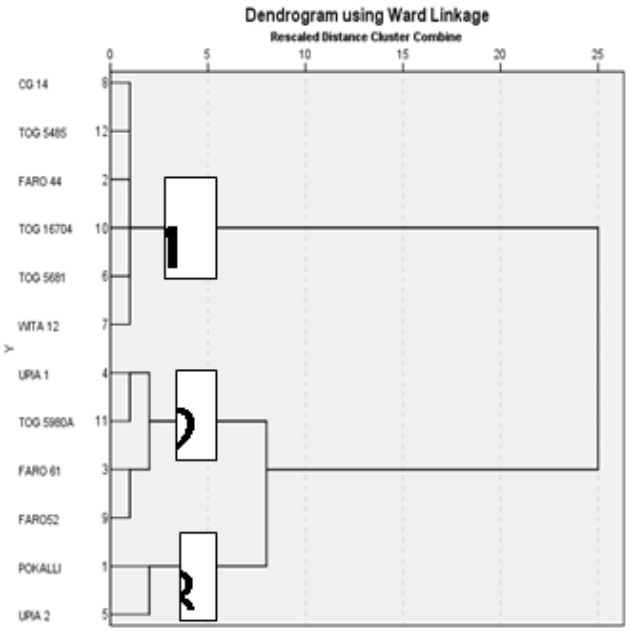

Figure 4. Cluster pattern for salt tolerance indices in 12 rice varieties generated from hierarchical cluster analysis using Ward's method.

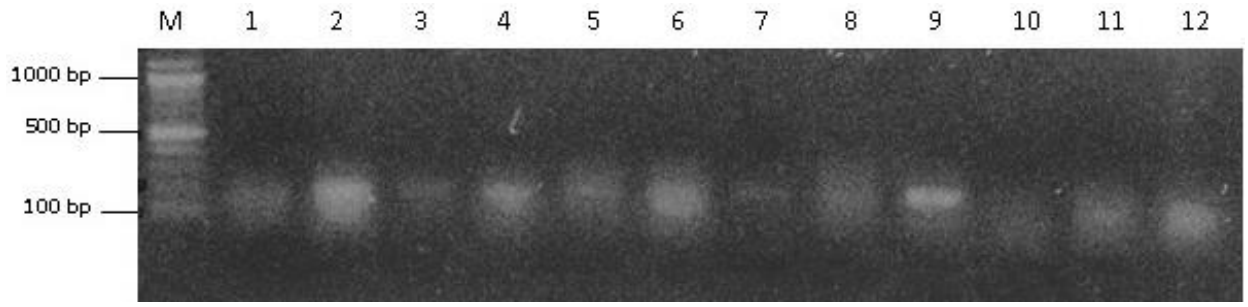

Plate 1. SSR profiles of 12 rice varieties based on the molecular marker RM336. M= Size marker, 1=POKALLI, 2=FARO 44, 3=FARO 61, 4=UPIA 1, 5=UPIA 2, 6=TOG 5681, 7=WITA 12, 8=CG 14, 9=FARO 52, 10=TOG 16704, 11=TOG 5980-A, 12=TOG5485, PRIMER 2 = RM336.

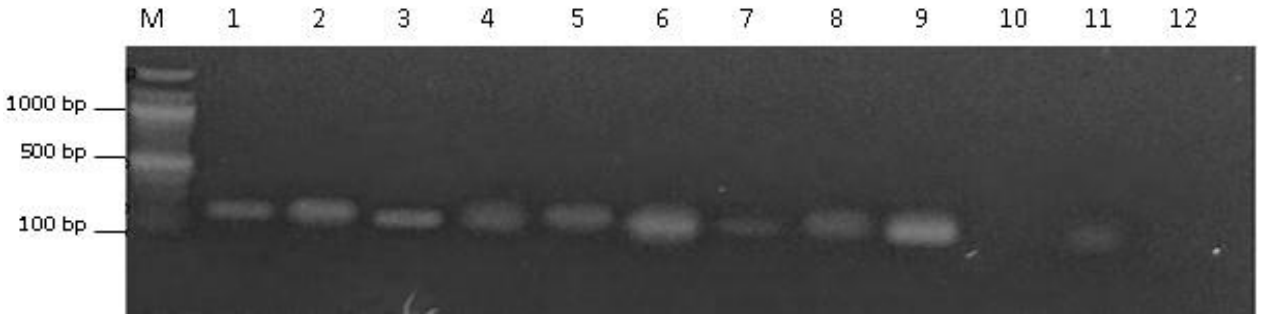

Plate 2. SSR profiles of 12 rice varieties based on the molecular marker RM493M= Size marker, 1=POKALLI, 2=FARO 44, 3=FARO 61, 4=UPIA 1, 5=UPIA 2, 6=TOG 5681, 7=WITA 12, 8=CG 14, 9=FARO 52, 10=TOG 16704, 11=TOG 5980-A, 12=TOG5485, PRIMER 4 = RM493.

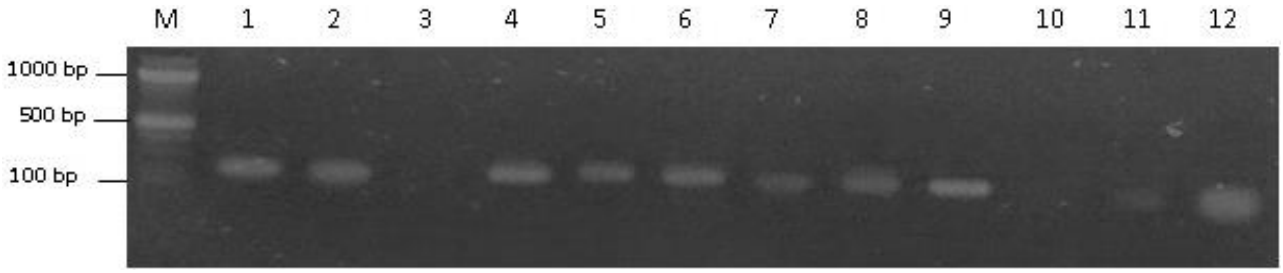

Plate 3. SSR profiles of 12 rice varieties based on the molecular marker RM 3412. M= Size marker, 1=POKALLI, 2=FARO 44, 3=FARO 61, 4=UPIA 1, 5=UPIA 2, 6=TOG 5681, 7=WITA 12, 8=CG 14, 9=FARO 52, 10=TOG 16704, 11=TOG 5980-A, 12=TOG5485, PRIMER 5= RM 3412.

Table 6. Data on allele size range, number of alleles, allele frequencies, and Polymorphic Information Content (PIC).

Locus	Allele size range (bp)	No. of alleles	Allele frequencies	PIC
RM336	100-250	3	0.083 0.25 0.667	0.486
RM493	100-200b	3	0.25 0.5 0.25	0.626
RM3412	110-260	3	0.25 0.25 0.5	0.626

health. Susceptible accessions exhibited varied symptoms of salt injury such as yellowing of leaves, reduction in biomass and shoot growth, and ultimately death of seedlings at vegetative growth stage. Similar results were reported by Mansuri et al. (2012) and Sakina et al. (2016). Generally, salt affects the growth of crop plants by limiting the absorption of water through the root which ultimately affects the metabolic processes of the plant. It has an immediate effect on cell growth and enlargement, and high concentration of salt can be very toxic (Munns and Tester, 2008).

Various plant traits such as shoot and root growth as well as biomass, are reported to be associated with salt tolerance at early growth stage and thus can be used as selection criteria for salt tolerance (Ashraf et al., 1999; Sakina et al., 2016). The present results showed reductions in biomass and shoot growth relative to the controls in all accessions when exposed to salinity stress. It is known that plants, especially those of drought or salt-tolerant species, tend to propagate their roots deeper to absorb more water during osmotic stress (Sakina et al., 2016). This may have been the case in some of the studied accessions. Other root parameters such as root biomass and root surface area could be used along with root length for a better understanding of the effect of salinity on root growth. Indeed, Robin et al., (2016) had reported that reduction in root surface area is a major component of salinity damage in wheat.

Standard evaluation score of visual salt injury is a widely used screening technique for salinity tolerance in rice. In the present study, the rice accessions were classified as highly tolerant (POKALLI and UPIA2), tolerant (FARO61, UPIA1, FARO52 and TOG5980-A), moderately tolerant (FARO44 and TOG5681) and susceptible (TOG16704, CG14, TOG 5485 and WITA12), on the basis of Standard Evaluation score. Analysis based on Salt Tolerance Indices gave similar results except that FARO 44 and TOG 5681 were grouped together with the 4 accessions that were regarded as susceptible, giving only 3 classes (Figure 4). The other 2 groups (Highly Tolerant and Tolerant) retained the same members in both evaluation methods.

The SSR markers used for this study proved to be a viable tool for discriminating between salt tolerant and susceptible varieties. Interestingly, UPIA 2 was consistently associated with POKALLI (tolerant check) in both the morphological and molecular screening techniques, which suggests that UPIA 2 can be

considered as a true salt tolerant variety. It also buttresses the findings of the morphological screening in this study which ranked both genotypes as highly tolerant based on the SES scores and salinity indices. In addition, it was observed that 80% of the accessions that had similar banding pattern with POKKALI, namely, UPIA 1, UPIA 2, FARO 52 and FARO 61 showed good degree of tolerance to salt with Standard Evaluation Scores ranging between 1 (Highly tolerant) and 3 (Tolerant), which may indicate some correlation between these methods. Although different screening methods may not always agree completely in cases like these, the differences do not necessarily signify a limitation in screening method but could be due to differences at the molecular level which may not be expressed at the morphological level (Karhu et al., 1996; Roldán-Ruiz et al., 2001) or vice versa. In addition, this variation could be because of variety-environment interaction. Hence, to overcome this problem, the number of molecular markers should be increased reasonably and the morphological traits studied must contain all possible parameters (Ali et al., 2014).

Conclusion

The present study has used Standard Evaluation Score, Salt Tolerance indices and SSR markers to identify UPIA 2 as a true, highly salt tolerant variety. It has also identified UPIA 1, FARO 52, FARO 61 and TOG 5980-A as fairly salt tolerant while TOG 16704, TOG 5485, CG 14 and WITA 12 are highly susceptible. Such information will be useful in the selection of parents as breeding lines for salt tolerance.

ACKNOWLEDGEMENTS

The authors are grateful to Bill Gates Foundation for providing an enabling environment in the University of Calabar for the molecular studies and to Africa Rice Center, Ibadan, Oyo State for providing the seeds used for this study.

CONFLICT OF INTERESTS

The authors have not declared any conflict of interests.

REFERENCES

Ali N, Yeasmin L, Gantait S, Goswami R, Chakraborty S (2014). Screening of rice landraces for salinity tolerance at seedling stage through morphological and molecular markers. Journal of Physiological and Molecular Biology in Plants 20:411-423.

Ashraf MY, Waheed RA, Bhatti AS, Sarwar G, Aslam Z (1999). Salt tolerant potential in different *Brassica species*, growth studies. In: Halophyte uses different climates. Handy A, Leith H, Todorovic M, Moscheuko, M (II eds). Backhuys Pubs, Leiden, The Netherlands, pp. 119-125.

Bhowmik SK, Titov S, Islam MM, Siddika A, Sultana S, Haque MDS (2009). Phenotypic and genotypic screening of rice genotypes at seedling stage for salt tolerance. African Journal of Biotechnology 8(23):6490-6494.

Calpe C (2006). Rice international commodity profile. Food and Agriculture Organization of the United Nations Markets and Trade Division (2006) 23. http://www.fao.org/fileadmin/templetes/est/COMM_MARKETS_MONITORING/Rice/Documents/Rice_profile_Dec-06.pdf. As accessed on 13th July 2015.

Dahanayaka BA, Gimhani DR, Kottearachchi NS, Samarasighe WLG (2015). Assessment of salinity tolerance and analysis of SSR markers linked with *Saltol* QTL in Sri Lankan rice (*Oryza sativa*) genotypes. American Journal of Experimental Agriculture 9(5):1-10.

De Costa WAM, Wijeratne MAD, De Costa DM (2012). Identification of Sri Lanka rice varieties having osmotic and ionic stress tolerance during the first phase of salinity stress. Journal of National Science Foundation of Sri Lanka 40(3):251-280.

Dellaporta SL, Wood J, Hicks JB (1983). A plant DNA mini-preparation: Version II. Plant Molecular Biology Reporter 1:19-21.

Gregorio GB, Senadhira D, Mendoza RD (1997). Screening rice for salinity tolerance. Vol 22. IRRI Discussion Paper Series. International Rice Research Institute.

Islam MM, Islam SN, Alam MS (2015). Molecular Characterization of Selected Landraces of Rice for Salt Tolerance Using SSR Markers. International Journal of Innovation and Scientific Research 17(1):206-218.

Kanawapee N, Sanitchon J, Lontom W, Theerakulposut P (2012). Evaluation of salt tolerance at the seedling stage in rice genotypes by growth performance, ion accumulation, proline and chlorophyll content. Plant Soil 358:235-249.

Karhu A, Hurme P, Karjalainen M, Karvonen P, Kärkkäinen K, Neale D, Savolainen O (1996). Do molecular markers reflect patterns of differentiation in adaptive traits of conifers? Journal of Applied and Theoretical Genetics 93:215-221.

Krishnamurthy SL, Gautan RK, Sharma PC, Sharma DK (2016). Effect of different salt stress on agro-morphological traits and utilization of salt stress indices for reproductive stage salt tolerance in rice. Field Crops Research 190:26-33.

Mansuri SM, Jelodar NB, Bagheri N (2012). Evaluation of rice genotypes to salt stress in different growth stages via phenotypic and random amplified polymorphic DNA (RAPD) marker assisted selection. African Journal of Biotechnology 11:9362-9372.

Momayezi MR, Zaharah AR, Hanafi MM, Mohd-Razi I (2009). Agronomic characteristics and proline accumulation of Iranian rice genotypes at early seedling stage under sodium salt stress. Malaysian Journal of Soil Science 13:59-75.

Murashige T, Skoog F (1962). A revised medium for rapid growth and Bioassays with tobacco tissue culture. *Physiologia plantarum*. Wiley Online library.

Munns R, Tester M (2008). Mechanisms of salinity tolerance. Annual Review of Plant Biology 59:651-681.

Nigerian Seed Portal Initiatives (Crops). www.seedportal.org.ng . Released and Registered Crops in Nigeria-Rice. (Accessed 10th June 2019)

Pires IS, Negrão S, Oliveria MM, Purugganan MD (2015). Comprehensive phenotypic analysis of rice (*Oryza sativa*) response to salinity stress. Physiologia Plantarum 155(1):43-54.

Reddy INL, Kim SM, Kim BK, Yoon IS, Kwon TR (2017). Identification of rice accessions associated with K+/Na+ ratio and salt tolerance based on physiological and molecular responses. Rice Science 24(6):360-364.

Robin AHK, Mathew C, Uddim JM, Bayazid KN (2016). Salinity-induced reduction in root surface area and changes in major root and shoot traits at the phytomer level in wheat. Journal of Experimental Botany 67(12):3719-3729.

Roldán-Ruiz I, Van Euwijk FA, Gilliland TJ, Dubreuil P, Dillmann C, Lallemand J, De Loose M, Baril CP (2001). A comparative study of molecular and morphological methods of describing relationships between perennial ryegrass (*Lolium perenne* L.) varieties. Journal of

Applied and Theoretical Genetics 103:1138-1150.
Sabouri H, Biabani A (2009). Toward the mapping of agronomic characters on rice genetic map: Quantitative trait loci analysis under saline condition. Biotechnology 8(1):144-149.
Sakina A, Ahmed I, Shahzad A, Iqbal M, Asif M (2016). Genetic variation for salinity tolerance in Pakistani rice (*Oryza sativa* L.) germplasm. Journal of Agronomy and Crop Science 202:25-36.
Singh D, Singh B, Mishra S, Singh AK, Sharma TR, Singh NK (2016). Allelic diversity for salt stress responsive candidate genes among Indian rice landraces. Indian Journal of Biotechnology 15:25-33.
Sirisena DN, Rathnayake WMK, Herath HMA (2010). Productivity enhancement of saline paddy fields in Angiththamkulam Yala, Sri Lanka, a case study. Pedologist, pp. 96-100.
Zeng I, Shannon MC, Grieve CM (2002). Evaluation of salt tolerance in rice genotypes by multiple agronomic parameters. Euphytica 127:235-245.

Vol. 18(27), pp. 622-631, July, 2019
DOI: 10.5897/AJB2019.16852
Article Number: 97B0DAB61415
ISSN: 1684-5315

http://www.academicjournals.org/AJB

ACADEMIC JOURNALS
expand your knowledge

African Journal of Biotechnology

Full Length Research Paper

Enhancement of phytoremediation efficiency of *Acacia mangium* using earthworms in metal-contaminated soil in Bonoua, Ivory Coast

BONGOUA-DEVISME Affi Jeanne[1*], AKOTTO Odi Faustin[1], GUETY Thierry[1], KOUAKOU Sainte Adélaïde Ahya Edith[1], NDOYE Fatou[2] and DIOUF Diégane[2]

[1]Département des Sciences du Sol, UFR Sciences de la Terre et des Ressources Minières, Université Felix Houphouët-Boigny, Cocody, 22 BP 582 Abidjan 22, Côte d'Ivoire.
[2]Centre de Recherche de Bel Air, Laboratoire Commun de Microbiologie, BP 1386, 18524 Dakar, Sénégal.

Received 29 April, 2019; Accepted 27 June, 2019

In this paper, the impact of *Pontoscolex corethrurus* on *Acacia mangium* growth and its phytoremediation efficiency in metal-contaminated soils were studied in a greenhouse pot culture under four treatments: non contaminated soil-non inoculated, control (C); non contaminated soil-inoculated (NcI); contaminated soil-non inoculated (CNi); contaminated soil-inoculated (CI). The results showed that *A. mangium* growth performance and its Pb, Ni and Cr uptake were significantly (P<0.05) increased under CI treatment. Under CNi treatment, *A. mangium* uptake more Ni and Cr content in root tissue than in shoot tissue. But for Pb, the greater content was noted in shoot tissue. *A. mangium* non-inoculated preferentially promoted the phytoimmobilization process for Cr and Ni and the phytoextraction process for Pb. However, under CI treatment, the greater content of potential toxic elements (Cr, Ni and Pb) was observed in roots tissue and *A. mangium* inoculated promoted the phytoimmobilization process for Cr, Ni and Pb. In addition, the phytoextraction efficiency (PEE) of *A. mangium* increase (ranged 0.1% under CNi to 14% under CI treatment. This study indicates that earthworms can be used to enhance the phytoremediation efficiency of metal-tolerant plant species in contaminated soil.

Key words: *Acacia*, heavy metal, phytoextraction, potential toxic element, *Pontoscolex corethrurus,* inoculation.

INTRODUCTION

In Ivory Coast, the continuous accumulation of municipal solid waste from different sources causes an undesirable enrichment of heavy metals or metalloids in dumpsite areas (Bongoua-Devisme et al., 2018a, b). This is the case for the dumpsite soil of M'Plouessoue Park, where the soils are contaminated with heavy metals such chromium (Cr), lead (Pb) and nickel (Ni) (Bongoua-Devisme et al., 2018a, b). These potential toxic elements

*Corresponding author. E-mail: bongoua_jeanne@yahoo.fr.

(PTEs) can enter the soil and groundwater resources and, consequently, pose severe threats to the food chain, human health and soil ecosystems. Thus, it is necessary to develop a remedial approach to remove heavy metals from contaminated soils. One of the established approaches is through phytoremediation strategies.

Phytoremediation is a new technology that utilizes plant to extract heavy metals from the contaminated ground, accumulating these metals in roots, stems and branches. Many studies have been conducted in this field over the last two decades, and various phytoremediation approaches (phytostabilization, phytoimmobilization and phytoextraction) have been successfully performed (Favas et al., 2019). However, the success of this new technology depends on the plant species, which must be able to tolerate and accumulate high concentrations of metals in shoots, undergo rapid growth and show high biomass production potential (Mohd et al., 2013).

Acacia mangium Wild. is a tropical plant which has the capacity to improve soil fertility by enhancing nutrient cycling, higher nutrient availability and microbial activities (Koutika, 2019). Moreover, this plant is rapidly growing and developing very fast. They can also grow in extreme conditions. It is also plant owing to its remarkable capacity to extract metal from polluted soils. The phytoremediation potential of *A. mangium* was been previously reported in numerous studies (Majid et al., 2012; Mohd et al., 2013). In fact, Majid et al. (2012) demonstrated that *A. mangium* can accumulate 93.5 mg kg^{-1} of copper (Cu) and 79 mg kg^{-1} of zinc (Zn) in its biomass and was able to tolerate high concentration of cadmium (Cd). Mohd et al. (2013) reported that *A. mangium* requires 5 and 17 years to remove 79.8 $kgha^{-1}$ of Zn and 47 $kgha^{-1}$ of Cu, respectively.

In contrast, many works have demonstrated that the success of phytoremediation may not solely depend on the plant itself but also on the interaction of plant roots with soil microorganism and fauna and the amount of heavy metals accumulated soil, because the interaction between plants and beneficial rhizosphere micro-organisms can enhance biomass production and the tolerance of plants to heavy metals (Ma et al., 2015).

Hence, another promising approach that has recently been employed to improve plant growth is the application of soil fauna such as earthworms. Earthworms are generally described as ecosystem engineers that greatly impact the physical, chemical and biological properties of soil by affecting the availability of nutrients and organic compounds for other organisms, and significantly increasing plant production (Blouin et al., 2013).

Pontoscolex corethrurus, an endogeic earthworm is one of the most widespread peregrine earthworms which is commonly found in humid tropics (Taheri et al., 2018; De Novais et al., 2018). It shows a very broad tolerance to various environmental conditions (Taheri et al., 2018). It is used in ecotoxicological studies and has also been recommended as a bioindicator for the assessment of soil quality and ecosystem disturbances (Taheri et al., 2018). For instance, it was used for the remediation of polluted sites (Duarte et al., 2014) and the improvement of phytoextraction treatments (Jusselme et al., 2015). Moreover, many studies have demonstrated that *P. corethrurus* species offers a more relevant alternative than the current use of *Eisenia fetida* or *Eisenia andrei* for ecotoxicological tests (Buch et al., 2013).

Thus, it is of interest to study the conjugated actions of *P. corethrurus* earthworm and of a metal tolerant plant such as *A. mangium* in the remediation of metal-contaminated soil. The principal aims of this research were to evaluate the effects of *P. corethrurus* on Pb, Cr and Ni phytoremediation efficiency of *A. mangium* in contaminated soil.

MATERIALS AND METHODS

Soil sampling and analysis

The contaminated soils were sampled from the abandoned dumping site located in M'Ploussoue Park, Bonoua, Ivory Coast, at latitude 5°16' N and longitude 3°36' W, where the potential toxic elements (PTEs) concentration exceeded environmental law screening values (Bongoua-Devisme et al., 2018a,b). Soil samples were collected at 18 different points from the surface (0-30 cm) to cover the entire study area according to the random sampling technique. Non-contaminated soil (control) situated at 5 km of contaminated site at latitude 5°15' N and longitude 3°35' W was used as a control medium. The characteristics of contaminated soil and non-contaminated soil are described in Table 1.

In each site, soil samples were air-dried and sieved to 2 mm to remove various types of wastes (paper, used batteries, electronic goods, wood, plastic paper, straws, buckets, tin cans, sacks, clothes, glass bottles, cotton wool, food wastes, leaves, fruit wastes, medicine bottles, foams, ashes, water sachet, card board and human excreta), then were mixed and homogenized to obtain a composite sample. The composite sample was transferred to the laboratory for various analyses. The composite sample was also used for a pot experiment.

Biological material

Seeds of *A. mangium* were obtained from the Centre National of Research Agronomy (CNRA) at Oume, Ivory Coast. Seeds were treated with concentrated sulfuric acid (95%) before pregermination, as described by Diouf et al. (2005). The treated seeds were pregerminated in a Petri dish containing 0.8% water-agar medium (w/v) and sterilized for 30 min at 110°C. Then, the Petri dish was stored at room temperature (30°C) in the dark for 72 h, after packing with aluminium paper. Before pregermination in the Petri dish, three pregerminated seedlings were transplanted into polyethylene plastic nursery bags (15 × 40 × 150 cm) filled with contaminated and non-contaminated soil sieved at 2 mm. One month after the transplantation in the plastic nursery bags, seedlings of uniform size were individually transferred into perforated pots filled with 5 kg of dry soil sieved at 2 mm.

Earthworms (*P. corethrurus*) were hand-collected from Felix Houphouet-Boigny University, Cocody, Abidjan, Ivory Coast, which had not been contaminated with trace metal elements. The earthworms were then kept in plastic boxes filled with water for one

Table 1. Physico-chemical properties of contaminated and non-contaminated soil used in pot experiment (Bongoua-Devisme et al., 2018a).

Site	pH	Particle Size (%)			C	N	MO	Heavy Metal (mg.kg^{-1} dry soil)		
		Clay	Silt	Sand	(g.kg^{-1} dry soil)			Pb	Ni	Cr
Contaminated	6.9±0.2	21.3±2	1.6±0.3	77.1±5	22.6±0.09	2.4±0.02	38.9±0.20	118±19	119±13	130.1±16
Non-contaminated	5.8±0.3	18±3	3±1	79.2±9	13.6±0.05	1.3±0.01	23.4±0.09	5.4±0.2	3.2±0.3	0.23 ±0.01

week to monitor their health before starting the experiment. For the treatment with earthworms, five adult earthworms (±5 g) were placed in the perforated pot after transplantation of the seedling.

Experimental design

A greenhouse pot culture experiment was conducted at Felix Houphouet-Boigny University, Cocody, Abidjan, Ivory Coast to study the effect of the *P. corethrurus* earthworms on the growth and phytoremediation capacity of *A. mangium*. The average temperatures in the greenhouse were 26, 38 and 32°C for morning, afternoon and evening, respectively. The experiment was carried out using four treatments:

(1) non contaminated soil-non inoculated, control (C);
(2) non contaminated soil-inoculated (NcI);
(3) contaminated soil-non inoculated (CNi);
(4) Contaminated soil-Inoculated (CI).

The experiment was conducted for 90 days, and each treatment was carried out in triplicate. Before filling the pot with the soil, it was perforated to allow aeration and then covered with a perforated net to prevent the earthworms from escaping. The pots were placed in a factorial arrangement based on a completely randomized block design. The seedlings were watered daily with deionized water to maintain the moisture content at approximately 60% water-holding capacity of the soil.

Plant harvest and analysis

At the end of the experiment (90 days), plant in the pot for each treatment was removed. The rhizosphere soil (RS), which was defined as the soil that remained attached to the roots after gentle shaking (Tan et al., 2017) and the drilosphere soil (DS), which was the portion of soil influenced by earthworm secretions, burrowing and castings, were collected. Growth parameters such as shoot length, fresh weight and dry weight of the plants were measured. The height of *Acacia* was measured for each treatment and each replicate. Shoots (leaves and stems) were harvested, and roots were carefully removed from the soil, rinsed with tap water, and washed three times with deionized water; nodules were detached and counted. The fresh weight was determined for each plant part (shoots and roots) and then the plant part was dried at 60°C for 72 h, weighed and stored for analysis. The total dry weight of biomass (shoots + roots) of each plant per pot was determined. Rhizobial infection was evaluated by counting the number of nodules per plant. All the different soil compartments were air-dried and stored prior to the analyses. The earthworms were hand-collected, counted and weighed. The PTEs such as Ni, Cr and Pb concentrations in plant shoots (leaves and stems) and roots were dosed but for the different soil compartments (RS and DS) only their concentrations were determined in the contaminated soil treatments, using an inductively coupled plasma atomic emission spectrometer (ICP-AES).

The ability of the plant to accumulate metals from the soil and transfer metals from the roots to the shoots was estimated by the bioconcentration factor (BCF) and translocation factor (TF), respectively, as described by Majid et al. (2012). BCF is the ratio of the metal concentration in the shoots of plants to that in the soil. TF is the ratio of the metal concentration in the shoots to that in the roots of plants.

Bioconcentration factor (BCF):

$$BCF_{ETM} = \frac{[ETM]Plant}{[ETM]soil} \quad (1)$$

Translocation factor (TF):

$$FT_{ETM} = \frac{[ETM]\,Shoots}{[ETM]\,Roots} \quad (2)$$

According to Buscaroli (2017), plants with both factors (TF and BCF) > 1 are suitable for phytoextraction, while plants with both factors < 1 are suitable for phytoimmobilization. For Majid et al. (2012), plants with TF > 1 promote the phytoextraction process, while plants with TF< 1, plant are suitable for phytoimmobilization process. Moreover, plants with BCF > 1 are qualified as a hyperaccumulator.

The phytoextraction efficiency (PEE) by *Acacia* under different treatments was calculated as suggested by Yang et al. (2017):

$$(PEE\%) = \frac{[ETM]_{\text{in plant tissue}}\,(mgkg^{-1}) \times W_{\text{plant dry weight}}\,(g)}{[ETM]_{\text{in soil}}\,(mgkg^{-1}) \times W_{\text{soil used to fill into pot}}(g)} \times 100 \quad (3)$$

where $[ETM]_{\text{in plant tissue}}$ = metal (Pb, Ni or Cr) concentration in plant tissue ($mgkg^{-1}$), $W_{\text{plant dry weight}}$ = total plant dry biomass (g), $[ETM]_{\text{in RS and DS soil compartments}}$ = metal (Pb, Ni or Cr) concentration in RS and DS soil compartment ($mgkg^{-1}$), and $W_{\text{soil used to fill into pot}}\,(g)$ = Weight of soil used to fill the pot (g)

Statistical analysis

The data were subjected to statistical analysis using 7.1 Statistica software. Significant differences between different treatments (non contaminated soil-non inoculated, control, (C); non contaminated soil-inoculated (NcI); contaminated soil-non inoculated (CNi); contaminated soil-inoculated (CI)) in terms of height, biomass production, nodule numbers, and heavy metal contents in plant biomass, shoot tissue, root tissue and different compartments RS and DS were performed using the Student-Newman-Keuls (SNK) test at 0.05 probability level.

RESULTS AND DISCUSSION

Plant growth performance under different treatments

Throughout the experimental period (90 days), regardless

of treatments applied, no visible heavy metal morphological toxicity symptoms, such as leaf chlorosis and root browning, appeared when *Acacia* was planted in contaminated soil under greenhouse conditions (Figure 1). This result revealed that *Acacia* is able to grow in metal-contaminated soils and is a metal-tolerant plant species, as suggested by Majid et al. (2012).

The significantly ($P < 0.05$) lowest height (Figure 2a), total dry weight biomass (Figure 2b) and nodule number (Figure 2c) were obtained under the contaminated soil-non inoculated (CNi) treatment, with 25.7 cm, 31 g and 5 nodules/plant, respectively (Figure 2). However, the presence of the earthworms resulted in a significant ($P<0.05$) increase in height (ranging from 25.7 to 51.5 cm), total dry biomass weight (ranging from 31 to 101 g) and nodule numbers (ranging from 5 to 9 nodules/plant) of the plant under CI treatments (Figure 2). Furthermore, the same increase in height (ranging from 40.5 to 55.3 cm), total dry biomass weight (ranging from 89 to 125 g) and nodule numbers (ranging from 19 to 100 nodules/plant) was noted under non-contaminated soil in the presence of earthworm (NcI) (Figure 2). This phenomenon was probably due to the action of *P. corethrurus* earthworms, which can improve the condition of the contaminated soil, enhance nutrient cycling, increase soil nutrient availability, and as a result, facilitate plant growth and biomass production. Furthermore, most previous studies have justified this finding by the fact that earthworms have the potential to modify edaphic parameters such as soil structure, organic matter decomposition and indirectly facilitate the uptake of many important nutrients by plant and consequently promote plant growth. In addition, the enhancement of *Acacia* growth performance can be attributed to the fact that some earthworms species can decrease the content of potential toxic elements (PTEs) in metal contaminated soil through the accumulation potential toxic elements (PTEs) in their tissues and consequently promote plant growth, as demonstrated in many studies (Lemtiri et al., 2016; Sizmur et al., 2011; Boughattas et al., 2018) in the presence of different species of earthworms (*E. fetida*, *Lumbricus terrestris, P. corethrurus*). A similar finding has been documented by Jusselme et al. (2015) who showed that the presence of *P. corethrurus* could enhance the biomass of *Lantana camara L.* by approximately 1.5-2-fold under Pb stress.

Earthworms can be used to improve phytoremediation efficiency by *Acacia* because of their ability to promote plant growth and biomass production and also because the morphological parameters of *Acacia* are not affected in contaminated soil.

Phytoremediation potential of *A. mangium* in contaminated soil

Cr, Ni and Pb contents are below the detection limit under non contaminated soil-non inoculated (C) and non contaminated soil-inoculated (NcI) treatments (Figure 3). In contaminated soil, the contents of Cr and Ni in plant biomass were significantly greater under inoculated (CI), with 2.4 $mg.kg^{-1}$ for Cr and 2.5 $mg.kg^{-1}$ for Ni, than non inoculated (CNi) treatments, with 1.33 $mg.kg^{-1}$ for Cr and 2 $mg.kg^{-1}$ for Ni. However, the content of Pb was lowest under inoculated (CI), with 3.4 $mg.kg^{-1}$, than non inoculated (CNi) treatment, with 3.8 $mg.kg^{-1}$ (Figure 3). In addition, the repartition of metal in different parts of plant tissue (root and shoot) showed that under CNi treatment, excepted for Pb content (which was 1.5-fold greater in shoot tissue (2.3 $mg.kg^{-1}$) than in roots tissue (1.5 $mg.kg^{-1}$)), Cr and Ni contents were very highly significant ($P<0.001$), 3 to 4-fold greater in roots tissue, with 1.04 $mg.kg^{-1}$ for Cr and 1.6 $mg.kg^{-1}$ for Ni, than in shoot tissue, with 0.3 $mg.kg^{-1}$ for Cr and 0.44 $mg.kg^{-1}$ for Ni (Figure 4). The results indicated that in the absence of earthworm, *Acacia* preferentially uptake Cr and Ni in its roots and Pb in its shoots (Figure 4). Moreover, the translocation factors ([metal]shoot/[metal]root), indicator of the effectiveness of the plant to translocate metals from roots to shoots of *Acacia* species, was $TF < 1$ for Cr and Ni, and $TF > 1$ for Pb under CNi treatment but under CI treatment, whatever metal dosed $TF < 1$ (Table 2). This emphasizes that *Acacia* may possess metal exclusion strategy, which probably depend to the nature of the metal. The bioconcentration factors (BCF) ([metal]plant biomass/[metal]soil) were BCF <0.1 under CNi and CI treatments (Table 2), which were indicated that *Acacia* are not hyperaccumulator plant as demonstrated by Cipriani et al. (2013). The findings did not differ from those of various studies indicating that *Acacia* is able to tolerate and uptake heavy metal in its tissues and therefore could be suitable for phytostabilization of metal-contaminated sites (Majid et al., 2012; Mohd et al., 2013). Ang et al. (2010) observed a higher accumulation of Pb in the shoots of *A. mangium* compared with the roots as the present finding. Furthermore, Cr, Ni and Pb phytoextraction efficiency (PEE) of *A. mangium* was 2, 16.9 and 9.8%, respectively, under CNi treatment (Table 2) and varied according to the nature of metal, which could be attributed to the form of the metal in the soil rhizosphere. Thus, it appeared that, according to the nature of the heavy metal in contaminated soil, *Acacia* could have different phytoremediation processes (phytoimmobilization and phytoextraction) when it was none inoculated with *P. corethrurus*. But this phytoremediation process of *Acacia* seems to depend on the nature and the mobile form of metal in the rhizosphere soil.

However, under inoculated treatment (CI), Cr, Ni and Pb contents were very highly significant ($P<0.001$), 2 to 10-fold greater in roots tissue, with 1.6 $mg.kg^{-1}$ for Cr, 1.9 $mg.kg^{-1}$ for Ni and 3.1 $mg.kg^{-1}$ for Pb, than in shoot tissue, with 0.8, 0.63 and 0.3 $mg.kg^{-1}$, respectively (Figure 4). In addition, under CI treatment, PEE >10%, irrespective of

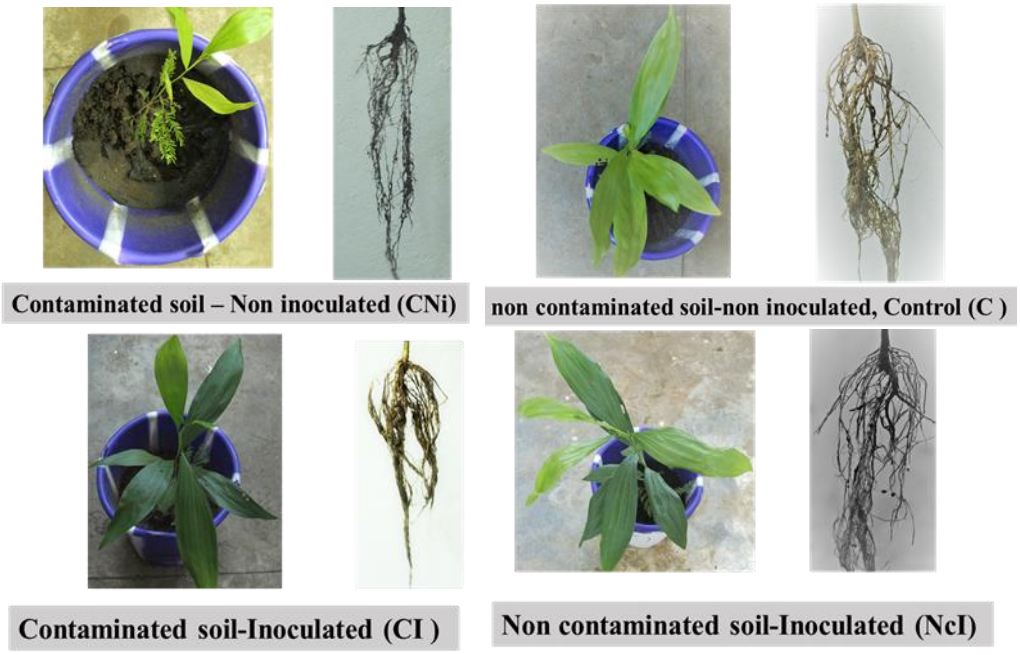

Figure 1. *Acacia mangium* growth performance (number of leaves, length of stem, root system development) under different treatments.

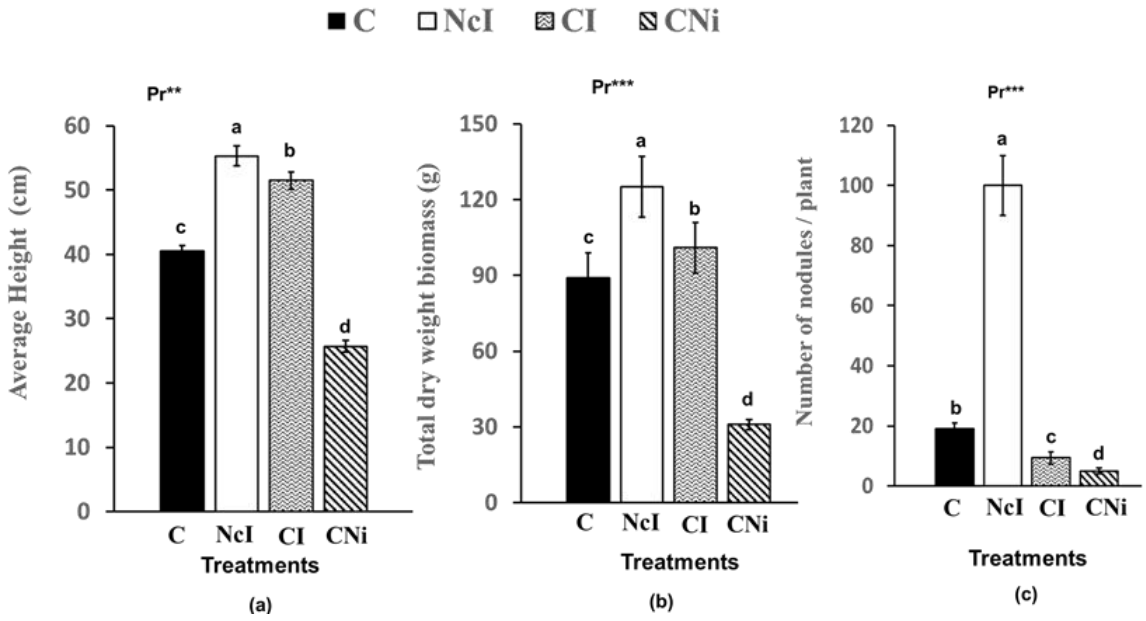

Figure 2. Effect of different treatments (non-contaminated soil-non inoculated control (C); non-contaminated soil-inoculated (NcI); contaminated soil-non inoculated (CNi); contaminated soil-inoculated (CI)) on plant height, total dry weight biomass and number of nodule/plant of *Acacia manguim*. Histogram with the same letters (a, b, c, d) indicated no significant differences between treatments. ***Very highly significant at 0.001 probability level, **highly significant at 0.01 probability level according to Student-Newman-Keuls test.

the heavy metal dosed (Table 2), with 10.4% for Cr, 48.5% for Ni and 70% for Pb. This finding indicated that the inoculation of *A. mangium* with earthworm significantly increase the uptake and transport of Cr, Ni and Pb from

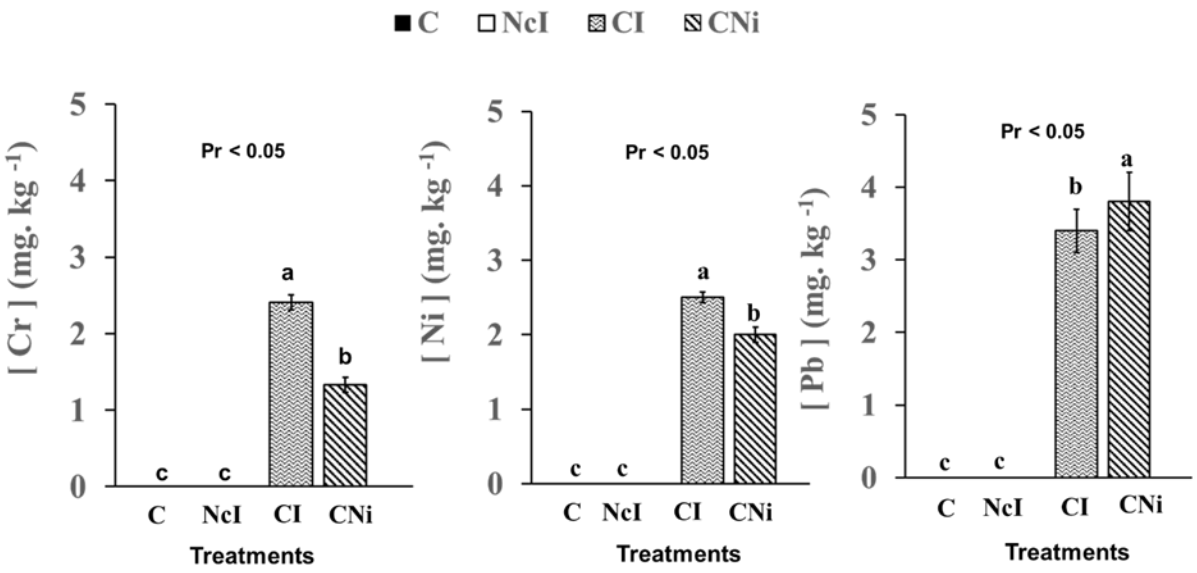

Figure 3. Chromium (Cr), nickel (Ni) and lead (Pb) content (mg.kg^{-1}) in *Acacia manguim* total biomass under different treatments (non-contaminated soil-non inoculated control (C); non-contaminated soil-inoculated (NcI); contaminated soil-non inoculated (CNi); contaminated soil-inoculated (CI)). Histogram with the same letters (a, b, c) indicate no significant differences between treatments. P<0.05 significant probability according to Student-Newman-Keuls test.

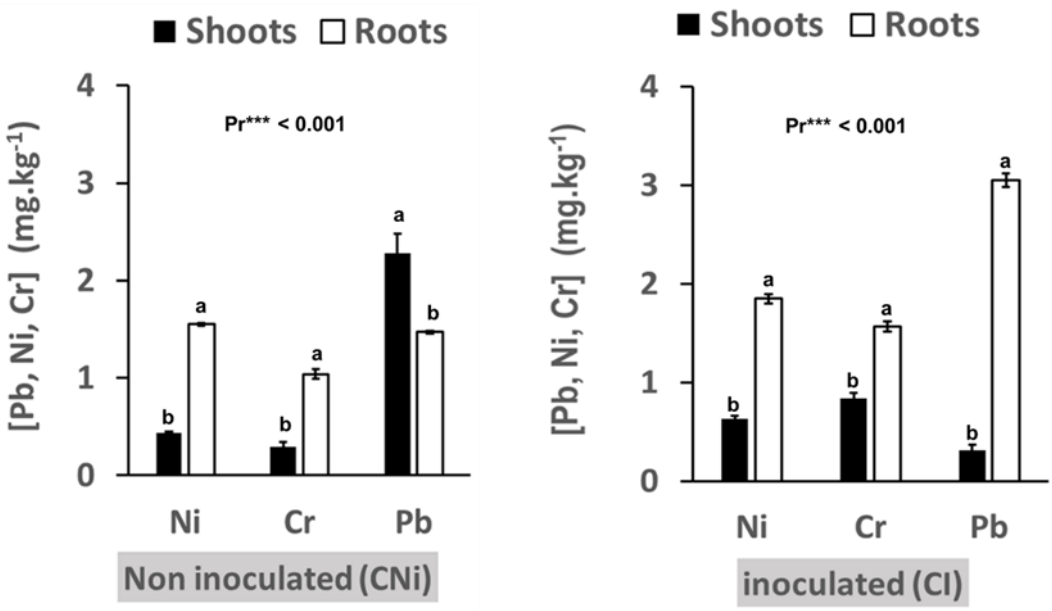

Figure 4. Chromium (Cr), nickel (Ni) and lead (Pb) contents (mg.kg^{-1}) in *Acacia mangium* shoot and root tissues in contaminated soil under different treatments: contaminated soil-non inoculated (CNi); contaminated soil-inoculated (NI). Histogram with the same letters (a, b) indicate no significant differences between Cr, Ni or Pb contents in shoot and root tissues under. ***Very highly significant at 0.001 probability level, according to Student-Newman-Keuls test.

the soil environment to *A. mangium* biomass particularly in its roots tissue, and also its phytoextraction efficiency (PEE). This increase of potential toxic elements in *Acacia* biomass may have been caused by the earthworm activities, as suggested previous studies (Sizmur et al., 2011), which demonstrated an increase in the

Table 2. Bioaccumulator (BCF), translocation factors (TF) and phytoextraction efficiency (PEE) of Cr, Ni and Pb in *Acacia mangium* biomass in contaminated soil under different treatments: contaminated soil-non inoculated (CNi); contaminated soil-inoculated (CI).

Heavy metal	BCF		TF		PEE (%)	
	CNi	CI	CNi	CI	CNi	CI
Cr	0.01	0.02	0.3	0.5	2.1	10.4
Pb	0.03	0.03	1.6	0.1	9.8	70.3
Ni	0.02	0.02	0.3	0.3	16.9	48.5

bioavailability of metal in the presence of earthworm. Earthworms influence metal bioavailability in soil through the mixing and comminution of soils and by the humic materials and detritus contained in the earthworm gut (Sizmur et al., 2011). Furthermore, similar effect has been noted by Wang et al. (2006) which reported that *Pheretima* species could enhance zinc (Zn) accumulation in ryegrass. Moreover, the sequestration of Cr, Ni and Pb into the root parts of *A. mangium* in the presence of *P. corethrurus* earthworms probably could be related to the plant physiological attributes, such as root structure and function and also to the fractional distribution of heavy metals in metal contaminated soil, as well as their phytoavailability. Furthermore, in the presence of *P. corethrurus* earthworms, the phytoimmobilization potential of uninoculated *A. mangium* for Cr and Ni was not modified, whereas for Pb, the phytoextraction potential of uninoculated *A. mangium* was modified into phytoimmobilization potential.

The repartition of Cr, Ni and Pb contents in the different soil compartments such as rhizosphere soil (RS) and drilosphere soil (DS) compartments, under earthworm treatment, indicated that only the content of Cr (29 $mgkg^{-1}$ dry soil) was significantly ($P < 0.05$) higher in the rhizosphere soil (RS) than in drilosphere soil (DS) compartments with 18 $mgkg^{-1}$ Cr dry soil (Table 3). The highest content of Cr and Pb in the RS than in the DS compartment under earthworm treatment and the highest content of Cr (1.5 $mgkg^{-1}$) and Pb (3.1 $mgkg^{-1}$) in plant roots suggested that Cr and Pb mobilized by earthworm in their structures (burrows and casts) were transferred to RS compartment, which acted as sinks for these element (Brown et al., 2004), and subsequently transferred to root tissue. In contrast, despite the highest content of Ni in the DS compartment (5.6 $mgkg^{-1}$ Ni dry soil) under earthworm treatment, the content of Ni was higher in the root parts than in the shoot part, which suggested that Ni mobilized in the DS compartment in their structures (burrows and casts) was stored in these structure, and temporarily transferred to RS compartment and subsequently transferred to root tissue. In addition, despite the significant accumulation of metal in RS (4.7-28.6 $mg.kg^{-1}$) and DS (4.7-17.8 $mg.kg^{-1}$) soil compartments, the content of metal in *Acacia* tissue was below 4 $mg.kg^{-1}$. Thus, it appears that DS soil compartment was used by the plant as a sink of metal element but their content in plant tissue seems to be regulated by the plant itself, contrary to Kaur et al. (2018) studies, which demonstrated that Cd content in *Brassica juncea* was regulated by earthworms in the drilosphere.

This work suggested that *A. mangium* could have different phytoremediation process which was probably related to the form in which metal can be absorbed by the plant and also to the function of the rhizosphere.

P. corethrurus earthworm and *A. mangium* interaction on phytoremediation process

Previous studies have reported the interactive role of earthworms in improving plant growth in non-contaminated soils (Braga et al., 2016). In addition to this, the benefit effect of earthworms in the remediation of metal contaminated soil has been very well demonstrated in numerous research (Boughattas et al., 2017, 2018; Lv et al., 2016; Lemtiri et al., 2016), but only few studies have been conducted to assess their role in improving plant metal uptake during phytoremediation in contaminated soils (Kaur et al., 2017).

The findings of the present study have shown that the inoculation of *Acacia* with *P. corethrurus* resulted in a highly to very highly significant increase ($P<0.01$) in plant height, total dry weight and metal concentration in plant biomass compared with the uninoculated treatment (Table 4). Thus, *Acacia* appeared to exhibit rapid growth and high biomass production when earthworms were present.

This increase can been due to the interactive action between *A. mangium* and *P. corethrurus*. In fact, the character specific of the plant (*Acacia*) used, which is a leguminous and have the capacity to form symbiotic association with rhizosphere microorganism, such as N-fixing bacteria and arbuscular mycorrhizal fungi, and consequently influence positively plant P nutrition and growth, and then soil microbial activities (Jusselme et al., 2015), can improve the uptake of metal in contaminated soil. For Kabas et al. (2017), the increase of plant growth and metal uptake by *Acacia* may be due to the secretion of organic acids from root exudation. They demonstrated that some species such as *Acacia* spp. secrete different

Table 3. Content of chromium, nickel and lead (mg.kg^{-1} dry soil) in different soil compartments: Rhizosphere Soil (RS) and Drilosphere Soil (DS).

Metal	Different Compartments	Treatments	
		CNi	CI
Chromium	RS	13.8	28.6^{a}
	DS	n.d	17.8^{b}
Lead	RS	8.4	4.9^{a}
	DS	n.d	4.7^{a}
Nickel	RS	2.6	4.7^{b}
	DS	n.d	5.6^{a}

n.d (none determined) under different treatments: contaminated soil-non inoculated (CNi); contaminated soil-inoculated (CI). Values with the same letters (a, b) indicated no significant difference between the content of Cr, Ni and Pb in RS and DS at 0.05 probability level according to Student-Newman-Keuls test.

Table 4. Statistical difference between different treatments (contaminated soil-non inoculated (CNi); contaminated soil-inoculated (CI)) on plant height, dry weight biomass, number of nodule and metal content in plant biomass.

Parameter	Treatments	Mean	Probability
Plant height	CNi	25.7^{d}	**P < 0.01
	CI	51.5^{b}	
Dry weight biomass	CNi	31^{d}	***P < 0.001
	CI	101^{b}	
Number of nodules	CNi	5^{d}	**P < 0.01
	CI	9^{c}	
Chromium content	CNi	1.3^{b}	**P < 0.01
	CI	2.4^{a}	
Nickel content	CNi	2^{b}	*P < 0.05
	CI	2.5^{a}	
Lead content	CNi	3.8^{a}	*P < 0.05
	CI	3.4^{b}	

***Very highly significant at 0.001 probability level; **highly significant at 0.01 probability level, *significant at 0.05 probability level according to Student-Newman-Keuls test.

types and quantities of organic acids into the rhizosphere, which may enhance the mobility of metals and their uptake by roots, explaining the immobilization of Cr, Ni and Pb in plant biomass. In addition, the higher content of Cr and Pb in RS and Ni in DS than in plant biomass could be related to the physiological character of *Acacia* spp., which here seems to exclude a metal in its shoot tissue (Kabas et al., 2017; Majid et al., 2012; Mohd et al., 2013; Cipriani et al., 2013).

The higher significant (P<0.05) content of Pb in shoot tissue under CNi treatment, that was modified under CI, could be attributed to the form of the metal in the soil rhizosphere, which can change in the presence of earthworm. De Novais et al. (2018) justified this by the fact that the main source of organic matter used by *P. corethrurus* comes from the rhizosphere. So, by decomposing different types of root exudates and organic acids secreted by *A. mangium* into the rhizosphere, *P.*

corethrurus can probably reduce the mobile form of metal while increase its stable form in the rhizosphere (Lemtiri et al., 2016, Boughattas et al., 2017). Boughattas et al., (2018) justified the decrease of Pb concentration in *Acacia* biomass under earthworm treatment by the fact that earthworm can reduced the amount of Pb associated with the soluble and exchangeable fraction.

These results suggest that, although earthworms have the potential to improve the efficiency of plant phytoremediation in metal-contaminated soils, its effectiveness depends on the nature of the plant, its behavior towards metals, rhizosphere function, and metal speciation in different soil compartments involved in the phytoremediation process.

CONCLUSION AND RECOMMENDATION

In the presence of earthworms, the present results revealed the beneficial effects of *P. corethrurus* earthworms on *A. mangium* growth and its Pb, Ni and Cr uptake. However, the work further demonstrated that the presence of *P. corethrurus* earthworm affected the phytoremediation potential of *A. mangium* in different manners. In the control treatment, uninoculated *A. mangium* preferentially promoted the phytoextraction process for Pb and the phytoimmobilization process for Cr and Ni, qualifying it as a metal-tolerant plant. Furthermore, in the presence of *P. corethrurus*, *A. mangium* promoted the phytoimmobilization process for Ni, Cr and Pb. The experiments highlight the importance of biological soil parameters on the phytoremediation efficiency. It appears that earthworms have the potential to enhance the phytoremediation efficiency of plants in metal-contaminated soil but its effectiveness depends on the nature of the plant, its behavior towards metals, rhizosphere function, and metal speciation in different soil compartments involved in the phytoremediation process

CONFLICT OF INTERESTS

The authors have not declared any conflict of interests.

ACKNOWLEDGEMENTS

The authors sincerely thank the Education and Research Ministry of Ivory Coast, as part of the Debt Reduction-Development Contracts (C2Ds) managed by IRD for the financial support rendered to carry out the project on ReSiPol research. They also thank the Bonoua City Hall for permission to carry out the studies at the dumpsites.

REFERENCES

Ang LH, Tang LK, Ho WM, Hui TF, Theseira GW (2010). Phytoremediation of Cd and Pb by four tropical timber species grown on an Ex-tin mine in peninsular Malaysia. Studies. International Journal of Environmental, Chemical, Ecological, Geological and Geophysical Engineering 4(2):70-74.

Blouin M, Hodson ME, Delgado EA, Baker G, Brussaard L, Butt KR, Brun J-J (2013). A review of earthworm impact on soil function and ecosystem services. European Journal of Soil Science 64(2):161-182.

Bongoua-Devisme AJ, Gueable YKD, Balland Bolou Bi C, Bolou Bi BE, Kassin KE, Adiaffi B, Yao-Kouame A, Djagoua EMV (2018a). Hazardous impacts of open dumpsite of municipal solid wastes on soil: case of M'Ploussoue Park dump at Bonoua in Ivory Coast. International Journal of Sciences 7(5):32-38.

Bongoua-Devisme AJ, Bolou Bi BE, Kassin KE, Balland Bolou Bi C, Gueable YKD, Adiaffi B, Yao-Kouame A, Djagoua EMV (2008b). Assessment of heavy metal contamination degree of municipal open-air dumpsite on surrounding soils: Case of dumpsite of Bonoua, Ivory Coast. International Journal of Engineering Research and General Science 6(5):28-42.

Boughattas I, Hattab S, Alphonse V, Livet A, Giusti-Miller S, Boussetta H, Bousserrhine N (2018). Use of earthworms *Eisenia andrei* on the bioremediation of contaminated area in north of Tunisia and microbial soil enzymes as bioindicator of change on heavy metals speciation. Journal of Soils and Sediments 19(1):296-309.

Boughattas I, Hattab S, Boussetta H, Banni M, Navarro E (2017). Impact of heavy metal contamination on oxidative stress of *Eisenia andrei* and bacterial community structure in Tunisian mine soil. Environmental Science and Pollution Research 24(22):18083-18095.

Brown G, Edwards CA, Brussaard L (2004). How earthworm affect plant growth: burrowing into the mechanisms. In: Edwards, C.A. (Ed.), Earthworm Ecology. CRC Press, Boca Raton, USA pp.13-49

Buch AC, Brown GG, Niva CC, Sautter KD, Sousa JP (2013). Toxicity of three pesticides commonly used in Brazil to *Pontoscolex corethrurus* (Müller, 1857) and *Eisenia andrei* (Bouché, 1972). Applied Soil Ecology 69:32-38.

Buscaroli A, (2017). An overview of indexes to evaluate terrestrial plants for phytoremediation purposes (Review). Ecological Indicators 82:367-380.

Cipriani HN, Dias LE, Costa MD, Campos NV, Azevedo AA, Gomes RJ, Fialho IF, Amezquita SP (2013). Arsenic toxicity in Acacia mangium willd. and mimosa Caesalpiniaefolia benth. Seedlings. Revista Brasileira de Ciência Do Solo 37(5):1423-1430.

De Novais CB, de Oliveira JR, Siqueira JO, de Faria SM, da Silva EMR, Aquino AM, Saggin Júnior OJ (2018). Trophic relationships between the earthworm *Pontoscolex corethrurus* and three tropical arbuscular mycorrhizal fungal species. Applied Soil Ecology 135:9-15.

Diouf D, Duponnois R, Tidiane Ba A, Neyra M, Lesueur D (2005). Symbiosis of *Acacia auriculiformis* and *Acacia mangium* with mycorrhizal fungi and *Bradyrhizobium* spp. improves salt tolerance in greenhouse conditions. Functional Plant Biology 32(12):1143-1152.

Duarte AP, Melo VF, Brown GG, Pauletti V (2014). Earthworm (*Pontoscolex corethrurus*) survival and impacts on properties of soils from a lead mining site in Southern Brazil. Biology and Fertility of Soils 50(5):851-860.

Favas PJC, Pratas J, Paul MS, Prasad MNV (2019). Remediation of Uranium-Contaminated Sites by Phytoremediation and Natural Attenuation. Phytomanagement of Polluted Sites pp. 77-300.

Jusselme MD, Poly F, Lebeau T, Rouland-lefèvre C, and Miambi E (2015). Effects of earthworms on the fungal community and microbial activity in root-adhering soil of *Lantana camara* during phytoextraction of lead. Applied Soil Ecology 96:151-158.

Kabas S, Saavedra-Mella F, Huynh T, Kopittke PM, Carter S, Huang L (2017). Metal uptake and organic acid exudation of native Acacia species in mine tailings. Australian Journal of Botany 65:357-367.

Kaur P, Bali S, Sharma A, Vig AP, Bhardwaj R (2017). Effect of earthworms on growth, photosynthetic efficiency and metal uptake in *Brassica juncea L.* plants grown in cadmium-polluted soils. Environmental Science and Pollution Research 24(15):13452-13465.

Kaur P, Bali S, Sharma A, Kohli SK, Vig AP, Bhardwaj R, Ahmad, P. (2018). Cd induced generation of free radical species in Brassica juncea is regulated by supplementation of earthworms in the drilosphere. Science of The Total Environment 655:663-675.

Koutika L-S (2019). Afforesting savannas with Acacia mangium and

eucalyptus improves P availability in Arenosols of the Congolese coastal plains. Geoderma Regional e00207.
Lemtiri A, Liénard A, Alabi T, Brostaux Y, Cluzeau D, Francis F, Colinet G (2016). Earthworms *Eisenia fetida* affect the uptake of heavy metals by plants Vicia faba and Zea mays in metal-contaminated soils. Applied Soil Ecology 104:67-78.
Lv B, Xing M, Yang J (2016). Speciation and transformation of heavy metals during vermicomposting of animal manure. Bioresource Technology 209:397-401.
Ma Y, Oliveira RS, Nai F, Rajkumar M, Luo Y, Rocha I, Freitas H (2015). The hyperaccumulator Sedum plumbizincicola harbors metal-resistant endophytic bacteria that improve its phytoextraction capacity in multi-metal contaminated soil. Journal of environmental management 156:62-69.
Majid NM, Islam MM, Mathew L (2012). Heavy metal uptake and translocation by mangium (Acacia mangium) from sewage sludge contaminated soil. Australian Journal of Crop Science 6(8):1228-1235.
Mohd SN, Majid N M, Shazili N A M, Abdu A (2013). Growth performance, biomass and phytoextraction efficiency of *Acacia mangium* and *Melaleuca cajuputi* in remediating heavy metal contaminated soil. American Journal of Environmental Sciences 9(4):310-316.
Sizmur T, Palumbo-Roe B, Watts M J, Hodson ME (2011). Impact of the earthworm *Lumbricus terrestris* (L.) on As, Cu, Pb and Zn mobility and speciation in contaminated soils. Environmental Pollution 159(3):742-748.
Taheri S, Pelosi C, Dupont L (2018). Harmful or useful? A case study of the exotic peregrine earthworm morpho-species *Pontoscolex corethrurus*. Soil Biology and Biochemistry 116:277-289.
Tan Y, Cui Y, Li H, Kuang A, Li X, Wei Y, Ji X (2017). Rhizospheric soil and root endogenous fungal diversity and composition in response to continuous *Panax notoginseng* cropping practices. Microbiological Research 194:10-19.
Wang D, Li H, Wei Z, Wang X, Hu F (2006). Effect of earthworms on the phytoremediation of zinc-polluted soil by ryegrass and Indian mustard. Biology and Fertility of Soils 43(1):120-123.
Yang Y, Ge Y, Zeng H, Zhou X, Peng L, Zeng, Q (2017). Phytoextraction of cadmium-contaminated soil and potential of regenerated tobacco biomass for recovery of cadmium. Scientific Reports 7:1.

Vol. 18(27), pp. 632-639, July, 2019
DOI: 10.5897/AJB2019.16850
Article Number: AB3C16661445
ISSN: 1684-5315

http://www.academicjournals.org/AJB

ACADEMIC JOURNALS
expand your knowledge

African Journal of Biotechnology

Review

Review of microfluidics approaches to mimic the kidney

Zach Odeh[1,2] and Hongli Lin[1,2*]

[1]Graduate School of Dalian Medical University, No. 9 Western Section Lvshun South Road, Lvshun 116044, China.
[2]Center for Kidney Diseases and Translational Medicine, Department of Nephrology, 1st Affiliated Hospital of Dalian Medical University, Liaoning Province, No. 222 Zhongshan Road, Dalian, 116044, China.

Received 28 April, 2019; Accepted 27 June, 2019

The use of microfluidics and nanotechnology in bioscience is gaining favor among the next generation of bioscience and clinical researchers, and this field has expanded to include organ-specific applications and modeling. While certain organ-specific microfluidic chips/applications, such as those in the heart and liver, are ubiquitous in the peer-reviewed literature, the kidneys require more focus and attention to drive innovation. This review is a comprehensive overview of kidney microfluidic bio-applications and includes the current challenges and limitations that should be the focus of research efforts. More specifically, previous research efforts focused on glomerular or tubule segments of the kidney, but never both anatomical regions. This is due, in part, to the complexity of reconstituting the kidney complete with all its variable mechanical and biochemical functions.

Key words: Kidney, organs and organ systems, microfluidics.

INTRODUCTION

Research on body organs has produced new perceptions on tissue engineering, providing a framework that enables cells to preserve their phenotypic features during this process and to advance within the mesh of available proteins (Paoli and Samitier, 2016). Despite these improvements in technology, there are still challenges that need to be addressed, for example, monitoring the positions of the cells and harvesting them later for biochemical or functional analysis. Although decellularization involves a three-dimensional scaffold that provides specific essential information on the cells, including their topography and stiffness, mechanical stimuli present in the cellular microenvironment have not been elucidated in this framework. Thus, in finding solutions to this limitation, biologists, physicians, engineers, and physicists have worked together to develop unique methods of solving this problem.

Microfluidics is a field of science involving the use of technological systems to manipulate the behavior of fluids in micrometer channels (Saliterman, 2006). A microfluidic chip refers to an arrangement of microchannels that can be incised or notched. The microenvironment is linked to the network on the microfluidic chip through numerous varying dimensions that exist throughout the microfluidic disk (Li, 2004). Specifically, the patched holes create a pathway through which fluids enter or exit the chip. The fluids are then processed, which entails mixing, separating, and

*Corresponding author. E-mail: hllin@dlmedu.edu.cn. Tel: +86-411-83635963/3007. Fax: +86-411-83633689.

manipulating the liquid to achieve multiplexing and a mechanization system (Li, 2004). Precise and accurate management of the microchannels require essential elements that are sometimes embedded within or outside (pressure controllers) the microfluidic chip. For example, the microchannel network on the chip must be able to perform processes such as electrophoresis and DNA analysis.

Microfluidic devices (MDs) examine the chemical and physical features of fluids on the micro-scale and are better than conventional macro-scale systems in several ways. For example, MDs allow the use of lower volumes of samples and reagents, thereby reducing costs (Nguyen and Werely, 2002). MDs can also perform multiple operations simultaneously due to their compact size, which shortens the experiment time due to experimental replications and other factors surrounding this experiment (Li, 2004). Further, they offer high-quality data with significant parameter control (Saliterman, 2006).

This paper reviewed the available literature on microfluidic chips/devices focused on nephrology and the kidney. Microfluidic chips can be used in this organ must address all or any of the physiological functions, which include blood filtration to remove waste and excess fluid, limiting toxins in the bloodstream, electrolyte homeostasis, and filtrate drainage. This comprehensive review uses academic publications from the last 18 years. Publications with overly simplistic designs, such as the use of mere wells, were excluded, since they cannot mimic key physiological functions or structural aspects.

Terms used in the study

The term microfluidics refers to both a science and a technology. The scientific field of microfluidics involves the study of liquid flow in devices. As a technology, microfluidics involves the micro-scale engineering (range from 200 microns to 100 nm) of fluid flow on a substrate that contains micro-features to transport liquids like blood, bacterial suspensions, reagents, and buffers as well as to control flow, heat transfer, and mass transport. Microfluidic devices use microfluidics concepts to stimulate various controlled physiologic environments or to mimic organ functions like the kidney-on-a-chip (Sia and Whitesides, 2003). Liquids are introduced or removed from microfluidic devices using syringes or tubing (Sia and Whitesides, 2003). Flow in microfluidic devices is normally laminar but turbulent or transitional flow or a combination of both can also exist.

KIDNEY ORGAN SYSTEMS AND MICROFLUIDIC CHIPS

Microfluidic technology offers an explicit, economical, reliable, combined, and controlled environment to perform essential tasks, and microsystems can replace traditional biological laboratory methods. Microfluidic cell culture is used in diagnostics, tissue engineering, drug screening, cancer research, immunology, and stem-cell propagation. MDs offer active cell culturing within micro-perfusion arrangements to supply continuous nutrients for cell culture in the long-term. Microfluidics has the potential to reproduce the cell-extracellular matrix and cell-cell relationships in tissues through the formation of gradient solutions of biochemical indicators such as development factors, chemokines, and hormonal conditions (Perestrelo et al., 2015). Some of the areas where cell cultivation in a microfluidic system is useful include high-resolution cell design on an altered substrate using epoxy resin designs and the rebuilding of complex tissue architecture.

The initial trial to replicate the functional aspects of the kidney using an MD occurred in 2001 (Attanasio et al., 2016). Essig et al. (2001) considered the flow-prompted consequences of the proximal tubular (PT) phenotype both *in vitro* and *in vivo* (IV) by subjecting PT cells to varying flow levels. Laminar flow prompted a reformation of the actin cytoskeleton (AC) and considerably decreased the plasminogen activator level (Essig et al., 2001). *In vivo*, nephrectomy reduced the actions of fibrinolytic renal cells within the proximal tubules and strengthened the apical AC domain, which was analyzed using immunofluorescence. These effects were avoided *in vitro* when cytochalasin D was used to block AC reorganization. These findings illustrate that tubular flow affects the composition of the renal epithelial cells (ECs). Essig et al. (2001) showed how tubular flow changes the structure of renal ECs and suggested that mechanical stretching in an induced flow may contribute to interstitial tubule lacerations when renal illnesses develop. The technology or device used for this study was a modest set up, involving the assembly of slides (two) to form an analogous platter chamber, followed by the application of laminar flow (Essig et al., 2001).

Baudoin et al. (2007) established a poly-dimethylsiloxane device that could maintain cells within microchambers linked to a microfluidic system, enabling constant renal tubular (RT) nourishment and by-product elimination. This device has two layers, each 100 mm deep, where the first layer is composed of a series of microchambers and microchannels and the second is a network of microchannels that serve as an inlet and a chamber to circulate the culture medium.

Weinberg et al. (2008) established a calculative scheme for the development of a typical nephron-on-chip device using existing microfabrication technologies comprising three divisions that replicated the tubular area, the loop of Henle, and the glomerulus, which can be made of different renal cell types. Building a bioartificial loop of Henle requires a regulator with diffusion scale features. Further, using the model described earlier, this author generated a design with

transport properties, including solute and flow, that were similar to those of human nephrons. This model had functional scope for channels in every division, and the calculated flow rates were similar to practical values. However, this research was restricted to mathematical simulations of water reabsorption, and there has been no other use of the model in previous studies (Weinberg et al., 2008).

Jang and Suh (2010), developed a modest multi-layer MD by assimilating polydimethylsiloxane (PDMS), a porous tissue substrate and microfluidic channel, to culture and analyze the RT cells. Using this, they cultured a rat inner medullary collecting duct (IMCD) in a conduit. To generate IV-like tubular conditions, fluid shear stress (FSS) of 1 dyn/cm^2 was applied for 5 h. This led to the formation of an optimum fluidic environment for the developed cells, as confirmed by improved cytoskeleton reorganization, cell polarization, and molecular transport through hormone-initiated stimulation. It was concluded that MDs can effectively mimic an IV renal tubule system, a process that could be applied in advanced tissue engineering and drug screening (Jang and Suh, 2010).

An artificial kidney made of a microfluidic chip includes circulation and has two compartments. The first compartment is the top channel, which resembles the urinary lumen and has a fluid flow, and the second is the bottom chamber, which resembles the interstitial space. The compartment is filled with fluid, which is the media through which materials are transported in and out of the chip (Kim and Takayama, 2015).

During drug development, it is common to receive reports on kidney toxicity based on tissue culture and non-representative animal studies. Thus, a better approach to restoring kidney function *in vitro* is required. Jang et al. (2013) designed an MD lined with living kidney ECs, which was exposed to fluid flow imitating the vital functions of the proximal tubule of the human kidney.

Wilmer et al. (2016) showed the need for enhanced design systems to predict the efficiency of new and existing drugs by focusing on drug interactions, and drug-induced kidney injury (DIKI). Such predictions were accomplished using the most appropriate *in vitro* arrangement technology, organ-on-a-chip, because it mimics the three-dimensional microenvironment (Wilmer et al., 2016). Specifically, kidney-on-a-chip is able to reproduce the technical, organizational, transportation, reabsorption, and functional properties of the human kidney. Wilmer et al. (2016) investigated the state-of-the-art microfluidic culture systems and focused on kidney PT culturing. The kidney PT is a good model for identifying biomarkers that indicate drug relationships and DIKI. Moreover, Wilmer et al. (2016) used high-throughput screening and *in vitro* experiments for IV extrapolation.

The primary kidney ECs that are secluded from a human PT are present on the top part of the extracellular exterior and matrix-coated permeable tissue, which separates the device's primary channel into two adjacent channels: a basal interstitial channel and an apical luminal canal. Moreover, exposing the single epithelial layer to apical fluid stress improves the epithelial cell polarity and forms the primary cilia. The cells in these conditions exhibit advanced features such as the ability to transport albumin, enhanced glucose reabsorption, and increased enzyme phosphatase activity. Measuring the level of cisplatin toxicity and P-glycoprotein 1 (P-gp) efflux on-chip closely mimics the IV responses compared to the outcomes from cells kept under traditional culture conditions. Zhou et al. (2014) first investigated kidney tubular cells under flow and claimed that this is a necessary condition, since the *in vivo* microenvironment is characterized by urine flow, a stimulus that is constantly present along the epithelial brush border. These authors developed a microfluidic model that reconstitutes the renal tubular flow environment to investigate renal interstitial fibrosis by focusing on the epithelial-to-mesenchymal transition (EMT) in the proximal tubule (Zhou et al., 2014). In particular, they showed cell morphological changes and migration during the EMT of human proximal tubular epithelial cells (PTECs) (HK-2) (Zhou et al., 2014). PTEC transition is related to renal interstitial fibrosis and ultimately, proteinuria. Last, Jang et al. (2013) presented primary findings on kidney toxicity through the utilization of human PTECs in a microfluidic organ-on-a-chip micro-device.

The "kidney-on-a-chip" has different possible applications. The transfer of both AC and aquaporin-2 in the kidney-on-a-chip is likely to stress devices using cultured IMCD cells in the rat kidney (Choi et al., 2015). The condition serves as an excellent illustration of the physiological experiments performed using the kidney-on-a-chip model (Jang et al., 2011).

Fluidic studies investigate the impact of fluid shear stress (FSS) on the morphology alterations and the role of the cells in the RT. Duan et al. (2008) showed that FSS causes cytoskeletal restructuring and rectification in the renal PTECs, which may be the primary indication of FSS-prompted proximal tubule bicarbonate transportation and liquid and sodium reabsorption. Other studies have suggested that FSS-prompted cytoskeletal reorganization could be done from a device that controls cytoskeleton-related protein transportation in the tubular ECs. Jang et al. (2011) used a modest multilayer fluidic chip to show that luminal FSS improves aquaporin-2 transfer to the cells through the plasma tissue (IMCD) (Choi et al., 2012). This condition is linked to the F-actin depolymerization in the basal and apical areas of the cells, regardless of the availability of the stimulus arginine vasopressin (AVP).

There are functional limitations of the current hemodialysis method in addition to the patient being ineligible for renal transplant. A bioartificial tubule device was invented to provide metabolic function. This advancement includes the embedding of renal ECs into hollow tubes to increase the chance of survival for acute

kidney injury patients (Bonnans et al., 2014). Different cells interacting alongside extracellular matrices are mostly composed of collagen and laminin; these surround the ECs in a healthy kidney (Gattazzo et al., 2014). Huang et al. (2013) developed a microfluidic co-culture stage to increase the epithelial functioning of the cell in bioartificial microenvironments along with compound microfluidic mediums microfabricated by the use of polydimethylsiloxane. The encapsulated collagen containing the adipose-derived stem cells was then injected. Moreover, Madin-Darby canine kidney (MDCK) cells were infused; these were re-suspended in budding channels to form a single epithelial layer. In contrast to the different co-culture cells which used the commercial trans-well system, the recent work of Huang et al. (2013) on the co-culture device enabled the observation of the MDCK cell epithelial monolayer as well as CG-ASC samples in a three-dimensional microenvironment. In this experiment, the height of the cells increased because of the columnar outlines by MDCK cells.

For co-cultured MDs, ion translocation in the MDCK follows cilia formation. During fluid flow, intracellular protein undercurrents can be observed with confocal microscopy. Therefore, MD co-culture offers renal EC morphological and functional enhancements that may be essential for the development of bioartificial renal chips (Tehranirokh et al., 2013).

GLOMERULUS-ON-A-CHIP

Due to the complexity of the kidney and its variable physiological functions, kidney-on-a-chip studies have mainly been performed on proximal tubular epithelial cell barriers. However, glomerulus-on-a-chip studies have also recently been reported. The glomerulus is a vital segment of the kidney, because it is the main anatomical site for blood filtration and is akin to the blood-brain barrier, albeit in the micron range as opposed to the nano-scale. This makes it essential for drug development and toxicity investigations and a solid foundation for a variety of kidney disease models.

Wang et al. (2017) developed a novel microfluidic chip that does not mimic a single glomerulus, but rather, represents many glomerular microtissues using a series of crescent microstructures to stimulate multiple glomerular microenvironments. Their rationale was to create a system that enabled the investigation of multiple glomeruli microenvironments to establish a better *in vitro* disease model for diabetic nephropathy. The middle channel of their chip contains the glomerulus inlet where the multiple glomeruli tumble eventually settles in the crescent-shaped microfeatures to form an array that lines the parallel channels filled with 3D Matrigel (Corning, Tewksbury, MA, USA) (Figure 1) (Wang et al., 2017). According to their design, the inlet of the glomeruli flow represents the capillary lumen, and the gel channels represent the glomerular basement membrane (GBM) (Figure 1) (Wang et al., 2017). The 3D Matrigel enhances the adhesion of the arrayed glomeruli and provides a natural barrier. The gel channels are flanked by collection channels that contain the glomerular filtration barrier (GFB) filtrate and represent the Bowman's capsule (Figure 1) (Wang et al., 2017). These multiple glomeruli microfluidic approaches have been effective in mimicking endothelial and podocyte phenotypes and can demonstrate morphological changes and GFB dysfunction under high glucose scenarios.

Musah et al. (2017) chose a minimalist design but with a different bio-application than that of Wang et al. (2017). They used two linear microchannels (replicating capillary and urinary compartments) superimposed over one another and parted by flexible PDMS tissue. This membrane is flanked by vacuum channels to permit stretching and cyclic strain to better reconstitute *in vivo* physiological conditions. Musah et al. (2017) used human glomerular endothelial cells (facing the capillary compartments) and human induced pluripotent stem (hiPS) cells that differentiate into podocytes with primary and secondary processes (facing the urinary compartment). These could create a tissue-to-tissue boundary exchange that controls for selective permeability (Musah et al., 2017). The major innovation in this study, however, is not the microfluidic design, but rather, their method of directing the differentiation of hip cells into highly functional human podocytes with more than 90% efficiency. Previous attempts to differentiate these cells were restricted by heterogeneity and immature phenotypes. The differential clearance efficacy of the glomerular basement membrane was verified with only 5% inulin filtration to the urinary side and capillary retention of larger proteins such as albumin with 99% efficiency (Musah et al., 2017).

This efficiency outperformed conventional cell-line culturing which cannot recreate an endothelial/podocyte interface to study flow. This feature is essential, because the mechanical cues provided by this barrier enhance podocyte differentiation and maturation. The new model is suitable for drug toxicity investigation and renal injury models and is preferable to animal studies, which may over- or under-estimate human physiological responses. Microfluidic models allow for single organ investigation in isolation of the entire human vascular circuit, which helps to eliminate confounding factors.

Conversely, Ashammakhi et al. (2017) argued that this system could eventually be integrated into a human-on-a-chip system to investigate the effects of drugs, toxicity, and multi-factorial effects. They argued that it could replace animal testing and even dialysis. Ashammakhi et al. (2017) made another valid argument that medicine could be personalized using stem cells with patient involvement. This could replace previous less efficient methods using partially differentiated renal cells from either the Bowman's capsule or podocytes from amniotic

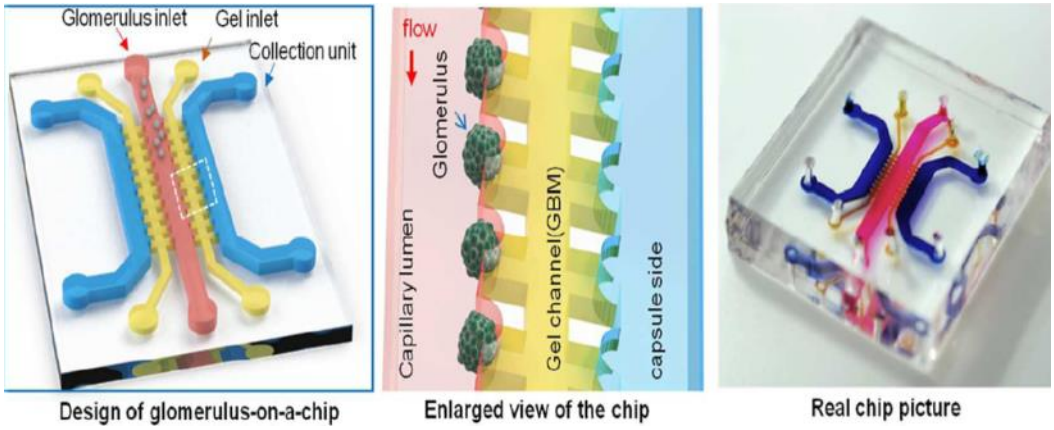

Figure 1. Real design of multiple-glomeruli-on-a-chip.
Source: Reproduced with permission from Lab Chip, 2017, DOI: 10.1039/C7LC00134G.

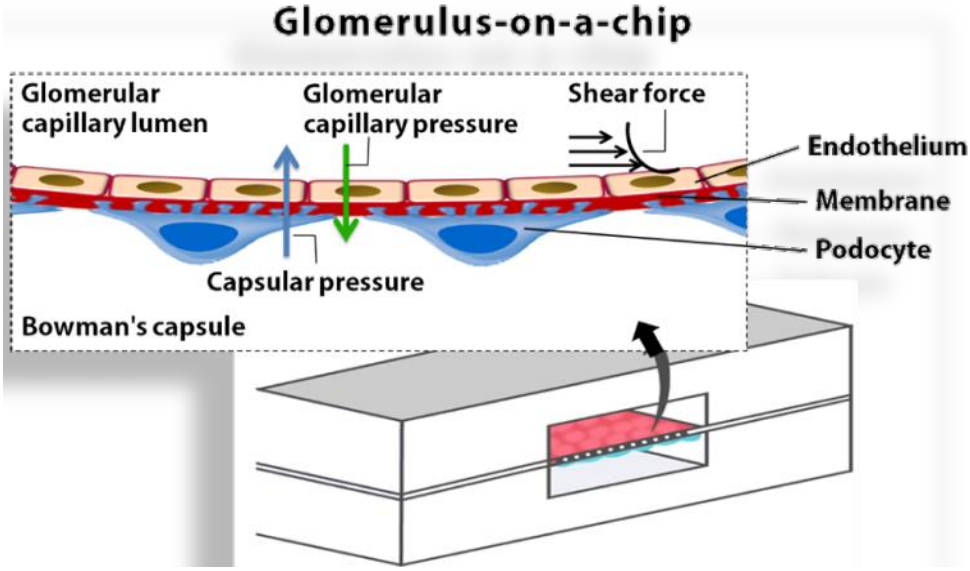

Figure 2. Schematic of endothelium and podocyte cell placement.
Source: Reproduced with permission from Scientific Reports | 6:31771 | DOI: 10.1038/srep31771.

fluid stem cells (Xinaris et al., 2016), or partially differentiated renal cells from either the Bowman's capsule (Lasagni et al., 2010) or urine (Lazzeri et al., 2015).

In a later study, Zhou et al. (2016) designed a novel glomerulus-on-a-chip to model hypertensive nephropathy. More specifically, their design addressed the shortcomings of previous models that did not accurately mimic the mechanical forces present under normal physiological conditions (Zhou et al., 2016). This was necessary because these mechanical and fluid forces can stress or damage cell cytoskeletal structure and rearrangement, especially in patients with diabetic nephropathy and end-stage renal failure. Zhou et al. (2016) used a dual PDMS layer approach (Figure 2) where a 10-micron thick polycarbonate filtration membrane track-etched with 10-micron diameter holes is inserted in the middle, and the three layers are aligned and sealed (Figure 2) (Zhou et al., 2016). The upper PDMS layer contains 16 culture chambers with endothelial cells that line the upper part of the polycarbonate membrane and podocytes that line the opposite side of the membrane (Figure 2) (Zhou et al., 2016). They used various flow rates and found that both 10 and 15 µL/min flow rates damaged the GFM, as reflected by an increase in inulin permeability after 12 h. However, the difference between these flows rates

suggested that the permeability of BSA and IgG occurred in 6 h with 15 µL/min as opposed to 24 h with 10 µL/min. Their chip design explains sclerotic tissue formation in the glomerulus filtration membrane, which is the critical functional site of the glomerulus.

The shear force in the diagram (Figure 2) represents the contraction and relaxation of the membrane. Glomerular capillary pressure regulates the in and out movement of fluids. The endothelium cell is used for the secretion of fluids.

The multi-layer microfluidic device (MMD) was invented by Jang and Suh (2010). The device incorporates polydimethylsiloxane (PDMS), a porous membrane substrate, and a microfluidic channel to analyze and culture renal tubular cells. It was first tested on a rat model through culturing on the inner medullary collecting duct (IMCD). In order to establish a tubular environment for the cell, a 5-h process involving the application of 1 $\mathrm{dyn/cm^2}$ of shear stress was undertaken to establish the optimal fluidic conditions for the cells, cytoskeletal reorganization, molecular transport through hormonal prompts, and boosted polarization.

Most kidney-on-chip devices, including the MMD, are placed below the microchannel and exposed to physiological shear stress. Jang and Suh (2010) established that cell thickness increased, there was Na/K ATPase expression, and cilia development promotion occurred, all of which were likely caused by shear stress through the use of the device. As a result, they noted that when using a suitably controlled shear stress load, it is possible to replicate the physiological behavior of kidney-derived cells.

The MMD uses a two-layered porous membrane to replicate the reabsorption purposes of the renal tubules. Jang and Suh (2010) found that they reproduced physiological responses related to sodium content changes and osmotic pressure of the apical channel through the introduction of hormones like aldosterone and vasopressin to the basal part of the instrument. Consequently, they noted that shear stress could result in various outcomes including the alteration of cell orientation, the promotion of p-glycoprotein expression, the absorption of glucose or albumin, cell growth, and cell polarity expression.

One main challenge related to the viability of the MMD is the podocyte-on-chip mechanism. According to Kim and Takayama (2015), a podocyte, being a glomerular visceral epithelial cell, acts as a size- and charge-selective wall to the plasma protein. Misalignment of the walls can cause harm to the podocytes and can lead to proteinuria. The researchers stated that, over the years, developers have tried to come up with a podocyte-on-a chip mechanism, but little success has been achieved. The main reason for the lack of breakthrough is that the *in vivo* exposure of intentional shear stress to podocyte cells requires innovative culturing conditions.

Practically, Jang and Suh (2010) proved that the MMD could help facilitate the rescue of cells or biomarkers that may have been harmed or lost as a result of shear stress. For instance, the shear stress facilitated the relocation of the actin cytoskeleton in the kidney-on-a-chip through the primary cultured inner medullary collecting duct cells and the translocation of aquaporin-2 on rat kidney cells. The results were a representation of the device's physiological capability. Jang and Suh (2010) established the function by taking into account the fact that renal tubular epithelial cells often experience shifts presented by the extracellular microenvironment, for example, changes in the interstitial or luminal pH and trans-epithelial osmotic gradient.

DISCUSSION

Although organ-on-a-chip systems do not require expensive raw materials, they are associated with high costs due to the development of micro engineering capabilities such as pump and clean rooms. The first challenge is that of bubbles, produced during or before perfusion of fluids, which are hard to remove and can increase the susceptibility of cells in the devices to injury or detachment. Occasionally, however, injuries associated with the air-liquid interface can be physiologically beneficial in, for instance, mimicking kidney injury. Nevertheless, bubbles or dust are generally harmful and ought to be avoided. To prevent them, Weber et al. (2016) recommended using an extracellular matrix coating for the attachment of cells on the membranes.

Second, developers of organ-on-a-chip devices face a noteworthy hindrance in culturing. According to Weber et al. (2016), prolonged culturing can degrade the matrix, affecting the viability of the cells. Moreover, it can be challenging to establish steady cell seeding and prevent microbes from being contaminated, because most experiments require long culturing periods. There is also the concern that, thus far, most of the devices' systems are yet to adequately account for certain elements such as complex system-level behavior, adaptive immune responses, nervous or skeletal systems, adaptive immune responses, and chronic disease modeling. Although the use of various kinds of attaching cells can be easy, culturing suspending cells remains a major challenge in organ-on-a-chip developments.

Previous research studies in this area have involved small-scale experiments. In order to improve future findings, greater sample sizes are required. One area that could benefit from improved research is fluid flow control. According to Kim and Takayama (2015), greater understanding of fluid flow control could enable developers to enhance the differentiation, functionality, and viability of their devices. Moreover, the enhancement of the synthetic culture system could enable different parameters to be controlled, for example, the mechanical forcing regimens, flow patterns and levels, and oxygen, molecular, and trans-cellular chemical gradients.

Weber et al. (2016) also believed that incorporating a cell culture in a 3D form could lead to more precise illustrations in *in vivo* studies. Thus far, most 3D culture methodologies have been assessed under static conditions as opposed to the recommended dynamic settings. Weber et al. (2016) noted that the use of 3D cell culture in organ-on-a-chip models could present an optimal cell culture for simulating an *in vivo*-like microenvironment.

Assuming, the challenge of developing a novel 3D biomimetic microfluidic model has been fully addressed, the focus of attention can shift to include pathological scenarios that negatively affect fluid flow and filtration. More specifically, Aghajani et al. (2019) suggested that the *Brucella* bacteria, acquired from unpasteurized milk and uncooked meat, is a major contributor to acute tubular necrosis since it can decrease blood flow and increase interstitial fluid in the kidneys.

CONCLUSION

The mimicking of organ systems through microfluidic approaches is gaining great significance within the fields of bioscience and clinical research. Attempts to emulate kidney function are within the laws of physics and fluid mechanics that mimic pathological microenvironments. The key benefit of microfluidics is the use of simple materials, which has increased the interest of current clinical researchers in this area. This review presented a comprehensive overview of kidney microfluidic bio-applications, including current challenges and limitations that should be addressed in future research efforts.

Currently, none of these organ-on-a-chip approaches are intended to replace the tissue engineering of an entire fully-functional living kidney. Rather, studies have attempted to mimic critical physiological functions of major biochemical operational units including the glomerulus or tubular epithelial cell barriers. This reconstitution of vital processes can be used instead of animal models or cell cultures. Microfluidic devices have also significantly contributed to the body-on-a-chip approach, which seeks to develop high-performing devices.

The significance of microfluidic research for clinical practice cannot be underestimated. Research has created a platform and a biomedical tool for use in everyday healthcare practice, which is especially useful for monitoring and predicting diseases. Medical diagnostics will become more affordable and faster, as microfluidics will help to reconstruct a damaged organ or tissue that has lost its functionality. Although the drawback of this method is that these man-made tissues cannot effectively work in the same ways as the natural organs of the human body, the increased complexity of the experiments has a critical effect in comparison to the petri dish. This complexity could see the development of more bio-applications, including those related to the physiological functions of major biochemical operational units such as the glomerulus or the tubular epithelial cells.

Microphysiological systems currently in production mainly include devices that use a single type of cell. Advancements in this area could incorporate prototypes that can further the capability to include, for instance, the necessary steps for secretion in the proximal tubule *in vivo*. These steps could focus particularly on the solutes' passage across the modified vascular endothelium into the tubular epithelium and interstitial matrix. Such ingenuity could act as a tight barrier to allow trans-cellular solute diffusion into the tubule lumen. For human kidney diseases, biomimetic micro-physiologic systems could help in the identification of effective and safe therapeutics (Weber et al., 2016).

The development of biomimetic microfluidic systems has indisputably provided the research community with a unique opportunity to contribute to the field of healthcare and science in general. Future researchers should continue with the quest to come up with better mechanisms that address unexplored areas, like the development of screening tools for modeling diseases affecting humans and the production of novel treatments. Furthermore, future designs could create efficient systems that can mimic vascular, interstitial, and proximal tubule characteristics including the integration of myofibroblasts, pericytes, and immune cells. Such advancements would contribute significantly to improvements in kidney physiologic function, drug development and discovery, and overall organ-on-chip technology.

CONFLICT OF INTERESTS

The authors have not declared any conflict of interests.

ACKNOWLEDGEMENTS

This research was funded by the Key Project of National Natural Science Foundation of China (NSFC No. 81530021), the General Project of the National Natural Science Foundation (NSFC No. 81770694), the Guidance and Planning Program for Key Research and Development of Liaoning Province (No. 2018225052), and the Support Program of Liaoning Distinguished Professor.

REFERENCES

Aghajani A, Mortazav SA, Yazdi FT, Zenosian MS, Asl MR (2019). Color, microbiological and sensory properties of low–fat probiotic yogurt supplemented with Spirulina platensis and Ferulago angulata hydroalcoholic extracts during cold storage. Banat's Journal of Biotechnology 10(19):20-34.

Ashammakhi N, Elkhammas EA, Hasan A (2017). Glomerulus-on-a-chip. Life up. Transplantation 101(11):e343-e344.

Attanasio C, Latancia MT, Otterbein LE, Netti PA (2016). Update on renal replacement therapy: implantable artificial devices and bioengineered organs. Tissue Engineering Part B: Reviews 22(4):330-340.

Baudoin R, Corlu A, Griscom L, Legallais C, Leclerc E (2007). Trends in the development of microfluidic cell biochips for in vitro hepatotoxicity. Toxicology *in Vitro* 21(4):535-544.

Bonnans C, Chou J, Werb Z (2014). Remodelling the extracellular matrix in development and disease. Nature Reviews Molecular Cell Biology 15(12):786-801.

Choi H-J, Jung HJ, Kwon T-H (2015). Extracellular pH affects phosphorylation and intracellular trafficking of AQP2 in inner medullary collecting duct cells. American Journal of Physiology-Renal Physiology 308(7):F737-F748.

Choi H-J, Yoon Y-J, Kwon Y-K, Lee Y-J, Chae S, Hwang D, Hwang G-S, Kwon T-H (2012). Patterns of gene and metabolite define the effects of extracellular osmolality on kidney collecting duct. Journal of Proteome Research 11(7):3816-3828.

Duan Y, Gotoh N, Yan Q, Du Z, Weinstein AM, Wang T, Weinbaum S (2008). Shear-induced reorganization of renal proximal tubule cell actin cytoskeleton and apical junctional complexes. Proceedings of the National Academy of Sciences of the United States of America 105(32):11418-11423.

Essig M, Terzi F, Burtin M, Friedlander G (2001). Mechanical strains induced by tubular flow affect the phenotype of proximal tubular cells. American Journal of Physiology-Renal Physiology 281(4):F751-F762.

Gattazzo F, Urciuolo A, Bonaldo P (2014). Extracellular matrix: a dynamic microenvironment for stem cell niche. Biochimica et Biophysica Acta (BBA) - General Subjects 1840(8):2506-2519.

Huang H-C, Chang Y-J, Chen W-C, Harn HIC, Tang M-J, Wu C-C (2013). Enhancement of renal epithelial cell functions through microfluidic-based coculture with adipose-derived stem cells. Tissue Engineering Part A 19(17-18):2024-2034.

Jang K-J, Cho HS, Kang DH, Bae WG, Kwon T-H, Suh K-Y (2011). Fluid-shear-stress-induced translocation of aquaporin-2 and reorganization of actin cytoskeleton in renal tubular epithelial cells. Integrative Biology 3(2):134-141.

Jang K-J, Mehr AP, Hamilton GA, McPartlin LA, Chung S, Suh K-Y, Ingber DE (2013). Human kidney proximal tubule-on-a-chip for drug transport and nephrotoxicity assessment. Integrative Biology 5(9):1119-1129.

Jang K-J, Suh K-Y (2010). A multi-layer microfluidic device for efficient culture and analysis of renal tubular cells. Lab on a Chip 10(1):36-42.

Kim S, Takayama S (2015). Organ-on-a-chip and the kidney. Kidney Research and Clinical Practice 34(3):165-169.

Lasagni L, Ballerini L, Angelotti ML, Parente E, Sagrinati C, Mazzinghi B, Peired A, Ronconi E, Becherucci F, Bani D, Gacci M, Carini M, Lazzeri E, Romagnani P (2010). Notch activation differentially regulates renal progenitors proliferation and differentiation toward the podocyte lineage in glomerular disorders. Stem Cells 28(9):1674-1685.

Lazzeri E, Ronconi E, Angelotti ML, Peired A, Mazzinghi B, Becherucci F, Conti S, Sansavini G, Sisti A, Ravaglia F, Lombardi D, Provenzano A, Manonelles A, Cruzado JM, Giglio S, Roperto RM, Materassi M, Lasagni L, Romagnani P (2015). Human urine-derived renal progenitors for personalized modeling of genetic kidney disorders. Journal of the American Society of Nephrology 26(8):1961-1974.

Li D (2004). Electrokinetics in Microfluidics, 1st ed. Elsevier, Amsterdam.

Musah S, Mammoto A, Ferrante TC, Jeanty SSF, Hirano-Kobayashi M, Mammoto T, Roberts K, Chung S, Novak R, Ingram M, Fatanat-Didar T, Koshy S, Weaver JC, Church GM, Ingber DE (2017). Mature induced-pluripotent-stem-cell-derived human podocytes reconstitute kidney glomerular-capillary-wall function on a chip. Nature Biomedical Engineering 10069.

Nguyen NT, Werely ST (2002). Fundamentals and Applications of Microfluidics. Artech House, Boston, MA.

Paoli R, Samitier J (2016). Mimicking the kidney: a key role in organ-on-chip development. Micromachines 7(7):126.

Perestrelo A, Águas A, Rainer A, Forte G (2015). Microfluidic organ/body-on-a-chip devices at the convergence of biology and microengineering. Sensors 15(12):31142-31170.

Saliterman SS (2006). Fundamentals of BioMEMS and Medical Microdevices. SPIE, Bellingham.

Sia SK, Whitesides GM (2003). Microfluidic devices fabricated in poly(dimethylsiloxane) for biological studies. Electrophoresis 24(21):3563-3576.

Tehranirokh M, Kouzani AZ, Francis PS, Kanwar JR (2013). Microfluidic devices for cell cultivation and proliferation. Biomicrofluidics 7(5):051502.

Wang L, Tao T, Su W, Yu H, Yu Y, Qin J (2017). A disease model of diabetic nephropathy in a glomerulus-on-a-chip microdevice. Lab on a Chip 17(10):1749-1760.

Weber EJ, Chapron A, Chapron BD, Voellinger JL, Lidberg KA, Yeung CK, Wang Z, Yamaura Y, Hailey DW, Neumann T, Shen DD, Thummel KE, Muczynski KA, Himmelfarb J, Kelly EJ (2016). Development of a microphysiological model of human kidney proximal tubule function. Kidney International 90(3):627-637.

Weinberg E, Kaazempur-Mofrad M, Borenstein J (2008). Concept and computational design for a bioartificial nephron-on-a-chip. The International Journal of Artificial Organs 31(6):508-514.

Wilmer MJ, Ng CP, Lanz HL, Vulto P, Suter-Dick L, Masereeuw R (2016). Kidney-on-a-chip technology for drug-induced nephrotoxicity screening. Trends in Biotechnology 34(2):156-170.

Xinaris C, Benedetti V, Novelli R, Abbate M, Rizzo P, Conti S, Tomasoni S, Corna D, Pozzobon M, Cavallotti D, Yokoo T, Morigi M, Benigni A, Remuzzi G (2016). Functional human podocytes generated in organoids from amniotic fluid stem cells. Journal of the American Society of Nephrology 27(5):1400-1411.

Zhou M, Ma H, Lin H, Qin J (2014). Induction of epithelial-to-mesenchymal transition in proximal tubular epithelial cells on microfluidic devices. Biomaterials 35(5):1390-1401. https://doi.org/10.1016/j.biomaterials.2013.10.070

Zhou M, Zhang X, Wen X, Wu T, Wang W, Yang M, Wang J, Fang M, Lin B, Lin H (2016). Development of a functional glomerulus at the organ level on a chip to mimic hypertensive nephropathy. Scientific Reports 6(1):31771.

Vol. 18(27), pp. 640-646, July, 2019
DOI: 10.5897/AJB2019.16851
Article Number: AFD1D0661449
ISSN: 1684-5315

http://www.academicjournals.org/AJB

ACADEMIC JOURNALS
expand your knowledge

African Journal of Biotechnology

Full Length Research Paper

Role of mucous cell and p53 protein in gastroprotective activity of methanolic extracts of *Ageratum conyzoides* Linn in rats

Omotoso D. R.[1*], Ajeigbe K. O.[2], Owonikoko W. M.[2], Okwuonu U. C.[1], Akinola A. O.[3], Daramola O. O.[2], Adagboyin O.[1] and Bienonwu E. O.[1]

[1]Department of Anatomy, College of Health Sciences, Igbinedion University, Okada, Edo State, Nigeria.
[2]Department of Physiology, College of Health Sciences, Igbinedion University, Okada, Edo State, Nigeria.
[3]Department of Physiology, College of Health Sciences, University of Medical Sciences, Ondo City, Ondo State, Nigeria.

Received 29 April, 2019; Accepted 12 June, 2019

***Ageratum conyzoides* Linn is a medicinal plant used for diverse ethnomedicinal applications including anti-ulcer treatment. Usually, protection of gastric mucosa from injury or ulceration is dependent on the efficacy of intrinsic or induced protective factors against erosive effects of aggressive factors. In this study, our aim was to ascertain the gastroprotective activity of methanolic leaf extracts of *A. conyzoides* L. and assess the associated roles of gastric mucous cells and p53 protein. This study involved 25 adult male Wistar rats divided into five groups (A-E). Groups A and E were used as normal and test controls while B-D were administered with extracts at 100, 300 and 500 mg/kg body weight for 28 days. Gastric mucosal injury was induced via pyloric ligation method. Gastric tissues were processed, stained with periodic acid-Schiff and immunostained for p53 protein (using monoclonal antibody). Stained sections were quantified using image-J software, data obtained were statistically analyzed. The results showed significant increase ($p<0.05$) in mucous cell population but no significant increase in p53 protein expression in gastric tissues of treated animals. This implied that increase in mucous cell count and down-regulation of p53 protein in gastric tissues play key role in gastroprotective activity of methanolic extracts of *A. conyzoides* L.**

Key words: Ageratum conyzoides, mucous cell, p53 protein, gastroprotection, rats.

INTRODUCTION

Ageratum conyzoides Linn (Asteraceae) is a medicinal, tropical plant commonly found in West Africa and parts of Asia and South America. It is an annual herbaceous plant not usually eaten by humans largely because of the characteristics bad odour, likened to the smell of a male goat but has an age-long record of diverse traditional medicinal uses in several countries (Ming, 1999; Okunade, 2002; Shekhar and Anju, 2012). Historically, it is popularly known for its usage in treatment of burns, wounds, infectious diseases, arthritis and fever (Kamboj and Saluja, 2008). The study by Elisabetsky and Wannmacher (1993) and Ming (1999) reported the

*Corresponding author. E-mail: dayohmts@gmail.com. Tel: +2348034779886.

application of *A. conyzoides* L. extracts as anti-inflammatory agent, analgesic and for treatment of malaria and yellow fever. The study by Dung and Loi, (1991) and Sharma and Sharma (1995) described the application of whole plant of *A. conyzoides* L. as antiallergic agent and also for treatment of gynaecological diseases. Further studies by Perumal-Samy et al., (1999) and Ayyanar and Ignacimuthu, (2005) reported the application of *A. conyzoides* L. leaf extracts as coagulant and in treatment of diarrhea. The study by Sofowora (1993) reported the application of *A. conyzoides* L. leaf extracts to treat conjunctivitis; otitis and head ache in some parts of Cameroon. In Madagascar, Novy (1997) described the application of juice extracted from *A. conyzoides* L. leaves as a coagulant and for treatment of diarrhoea. Another study by Gurib-Fakim et al., (1993) in Mauritius, reported the medicinal application of *A. conyzoides* L. leaves to cure diarrhoea, skin infection and as diuretic in urinary diseases. In some parts of Kenya, leaves and roots of *A. conyzoides* L. are used for treatment of stomach ache while the seeds are used for treatment of epilepsy in Tanzania (Geissler et al., 2002; Moshi et al., 2005). The study by Mahmood et al., (2005) reported the anti-ulcer effects of leaf extracts of *A. conyzoides* L. in ethanol-induced gastric ulceration in rats. However, with several reported and documented pharmacological uses of *A. conyzoides* L., there remains a conspicuous dearth of explanation of the mechanisms of its numerous pharmacological applications. This study was therefore carried out to ascertain gastroprotective activity of methanolic leaf extracts of *A. conyzoides* L. and to determine the role of gastric mucous cells and tumor suppressor (p53) protein during the activity in male Wistar rats treated with the extracts prior to induction of gastric mucosal injury through pyloric-ligation method.

MATERIALS AND METHODS

Plant material

Fresh whole plant of *A. conyzoides* L. was identified at the Herbarium of Department of Plant Biology and Biotechnology, University of Benin, Nigeria and documented with a voucher number 344.

Method of extraction

The leaves of plant were detached, air-dried and pulverised into powdered form using mechanical grinder. 1000 g of the powdered leaves was dissolved in 5 L of methanol for 72 h. Thereafter, the preparation was filtered and the filtrate evaporated to dryness by using rotary evaporator. The residue obtained was cooled at room temperature, weighed and used as the methanolic extracts for this study.

Animal used

This study involved 25 male Wistar rats weighing between 180-200 g and divided into five groups (A -E) comprising 5 animals per group (that is, n = 5).

Experimental design

Group A animals were given distilled water (5 mls/kg body weight). This group represented normal control that was not treated and not induced by pyloric ligation.
Group B animals were given 100 mg/kg methanolic extracts of *A. conyzoides* L.
Group C animals were given 300 mg/kg methanolic extracts of *A. conyzoides* L.
Group D animals were given 500 mg/kg methanolic extracts of *A. conyzoides* L.
Group E animals were given distilled water (5 mls/kg body weight). This group represented test control that was not treated but induced by pyloric ligation.

Period and mode of study

The treatment period of this study was 28 consecutive days and all treatments were done orally using a flexible orogastric gavage.

Induction of gastric mucosal injury using pyloric ligation method

The animals were fasted for 24 h in separate cages but allow free access to water. Animals were anesthetized by intraperitoneal injection of Ketamine/Xylazine (50 mg/kg at 1:1). A small midline incision was made on the abdomen of animals to access pyloric part of the stomach. The pyloric end of stomach was gently pulled up, ligated and gently returned into the abdominal cavity and the abdomen was closed. After an observatory period of 5 h, the animals were sacrificed and stomach tissue harvested and prepared for tissue processing (Shay et al., 1945).

Tissue processing

The tissues were fixed in 10% neutral buffered formalin, dehydrated using ascending grades of alcohol (two changes each of 70 and 90%, respectively, and absolute alcohol for 30 min each), cleared in xylene for 30 min and embedded in molten paraffin and allowed to cool to form tissue blocks.

Sectioning

Blocks of tissue were cut into sections at 3 and 5 µ thickness by using rotary microtome and mounted on microscope slides.

Staining:

The 3 and 5 µ tissue sections were used for the histochemical (Periodic acid–Schiff) staining and immunohistochemical (Horseradich-peroxidise-3, 3-Diaminobenzidine) staining respectively.

Periodic acid–Schiff (PAS) staining

Sections were deparaffinised in xylene 15 min, hydrated from absolute alcohol to distilled water, immersed in 0.5% periodic acid solution at room temperature for 5 min, rinsed in several changes of

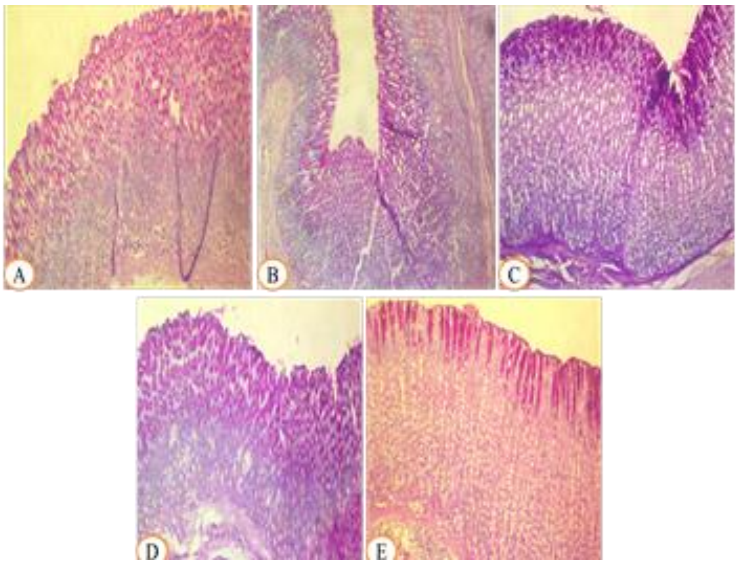

Figure 1. Photomicrograph of tissue sections of experimental animals showing distribution of mucous cells in the gastric mucosa of experimental animals (PAS X100). A: Normal control group; B – D: Treated groups administered with 100, 300 and 500 mg/kg methanolic extracts of *A. conyzoides* L. respectively and E: Test control group.

distilled water, immersed in Schiff's reagent at room temperature for 15 min, washed in running tap water, counterstained in Mayer's Haematoxylin solution for 3 min, rinsed in running tap water, dehydrated in alcohol, cleared in xylene and mounted with DPX.

Horseradich-peroxidise-3, 3-Diaminobenzidine (HRP-DAB) immunostaining for *p53* protein (using monoclonal antibody)

Sections brought to water, antigen retrieval performed by using citric acid solution (pH 6.0) in a microwave at power 100 Watts for 15 min, equilibrated by gently displacing hot citric acid with running tap water for 3 min, endogenous peroxidases blocked using peroxidase block for 15 min, sections washed in phosphate buffer saline (PBS) mixed with Tween 20 for 3 min, protein blocked with Nevocastra protein block for 15 min, sections washed with PBS for 3 min, sections incubated in primary antibody (1 in 100 dilution ratio) for 45 min, washed with PBS for 3 min, secondary antibody added and allowed for 15 min, sections washed with PBS for 3 min, polymer added and allowed for 15 min, sections washed twice with PBS and treated with 3, 3-Diaminobenzidine (DAB) substrate for 5 min each (DAB was prepared in 1/100 dilution ratio with the DAB substrate), washed with water and counterstained with Haematoxylin for 2 min, washed in water, dehydrated in alcohol, cleared in xylene and mounted with DPX.

Photomicrography

Photomicrographs were generated from stained microscope slides using 10 MP digital camera for microscope.

Analysis of photomicrographs

All photomicrographs were analyzed using the image-J software to quantify mucous cell population in PAS sections and distribution of *p53* protein in HRP-DAB sections. All values obtained were recorded.

Statistical analysis

The recorded data were analyzed using IBM-SPSS (version 20) and presented as mean ± SEM. Relevant statistical values were derived using *T*-test and one-way analysis of variance (ANOVA). ($P<0.05$ was considered as statistically significance level).

RESULTS

Histochemical results

The PAS-stained tissue sections showed the distribution of mucous cell population in the gastric mucosa of experimental animals in normal control group A, treated groups B-D and test control group E (Figures 1 and 2).

Immunohistochemical results

The immunostained gastric tissue sections showed the distribution of p53 protein in the gastric mucosa of experimental animals in normal control group A, treated groups B-D and test control group E (Figure 3).

DISCUSSION

The protection of gastric mucosa integrity is usually a

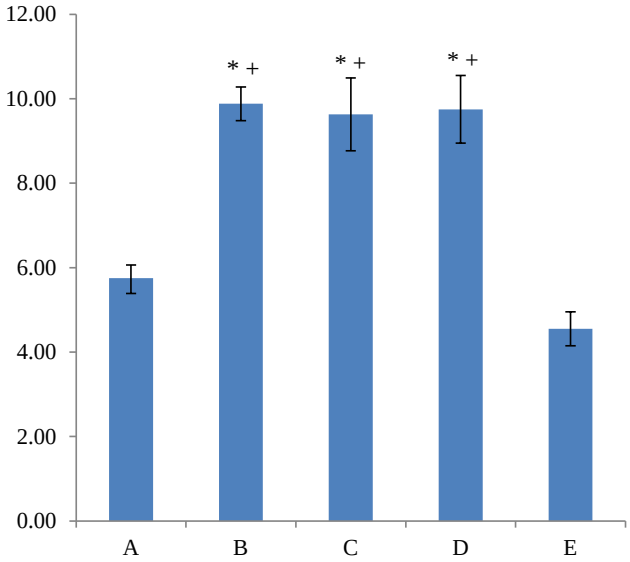

Figure 2. Chart showing the mean mucous cell count in the gastric mucosa of experimental animals. A: Normal control group; B-D: Treated groups administered with 100, 300 and 500 mg/kg methanolic extracts of *A. conyzoides* L. respectively and E: Test control group.

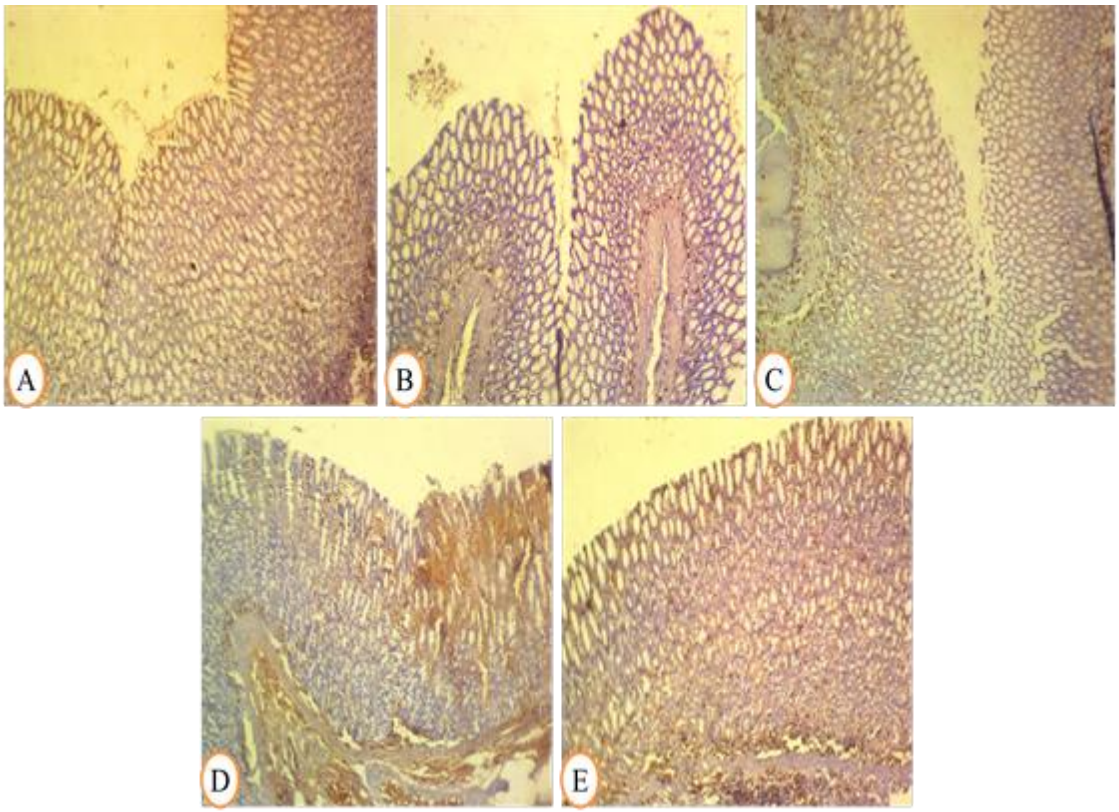

Figure 3. Photomicrograph of immuno-stained tissue sections of experimental animals showing p53 protein distribution in gastric mucosa indicated by dark-brown coloration (HRP-DAB X100). A: Normal control group; B – D: Treated groups administered with 100, 300 and 500 mg/kg methanolic extracts of *A. conyzoides* L. respectively and E: Test control group.

Table 1. Mean and standard error of mean (SEM) of mucous cell count in gastric tissues of experimental animals in control groups A and E and treated groups B-D.

Groups	Mean ± SEM
A	5.75 ± 0.31
B	9.88 ± 0.40*+
C	9.63 ± 0.86*+
D	9.75 ± 0.80*+
E	4.55 ± 0.40

function of equilibrium between protective and aggressive factors or their stimulators and inhibitors. Among the primary protective factors of gastric mucosa is the mucus produced by mucous cells (Johnson, 2003). From the histochemical result of this study, there was observable prominence of mucous cell population in gastric tissues of treated groups B-D (Figure 1) and there was corresponding significant increase ($P<0.05$) in the mucous cell count in gastric tissues of animals in all treated groups compared to the control groups (Figure 2). According to Table 1, the values of mucous cell count for treated groups B (9.88 ± 0.40), C (9.63 ± 0.86), and D (9.75 ± 0.80) were significantly ($P<0.05$) higher compared to the control groups A (5.75 ± 0.31) and E (4.55 ± 0.40). The increased gastric mucous cell population implied increased secretion of viscous and alkaline mucus which constitutes a vital part of primary gastric mucosal protective factors. The mucus forms a protective layer of gel on gastric mucosal surface which protects it against the digestive action of pepsin and erosive effect of acidic gastric juice (Sembulingam and Sembulingam, 2010). There are two types of mucus secreted by mucous cells of gastric mucosa. These include soluble mucus secreted by neck mucous cells which help to neutralize gastric contents and insoluble mucus secreted by surface mucous cells after exposure to chemical or physical irritants (Rhoades and Tanner, 2004; Sembulingam and Sembulingam, 2010). The study by Olaibi et al., (2014) identified one mechanism of gastric mucosal injury to involve disruption of mucus production by gastric mucous cells. The result of their study also showed that preservation of these mucus secreting cells in stomach tissue is vital in gastric mucosal protection. Another study by Ige et al., (2016) reported that increase in mucus secretion (by gastric mucous cells) is one mechanism of protecting gastric mucosa from effects of aggressive factors gastric mucosal injury. In this study, the gastroprotective activity of methanolic extracts of *Ageratum conyzoides* L. may result from significant increase in mucous cell population.

Moreover, factors that shift the equilibrium between protective and aggressive factors positively towards cell survival or negatively toward cell death will either maintain or disrupt the gastric mucosal integrity respectively. One factor that projects cell toward cell death is the tumor suppressor (p53) protein. The immunohistochemical result of this study revealed a staining intensity which range from moderate immuno-staining in normal control group A and treated group B to mild or concentric immunostaining in treated groups C and D but intense or widespread staining in test control group E (Figure 3). Consequently, the distribution of p53 protein was not markedly increased in all treated groups compared to the normal control group A. However, there was a spike in the p53 protein expression in test control group E due to exposure to the aggressive factor (acidic gastric juice) (Figure 4). From Table 2, the values of p53 distribution obtained among the treated groups B (16.67 ± 1.20), C (14.00 ± 2.08) and D (14.67 ± 0.88) were not significantly different from the value in normal control group (16.33 ± 0.88) but was significantly increased in test control group E (32.00 ± 3.03). The p53 is a nuclear protein commonly described as guardian of the genome due to its vital regulatory role during different events of cell cycle which include DNA damage repair, cellular division and cell death (Kern et al., 1991; Lane, 1992; Volgelstein and Kinzler, 1992). It is a tumor suppressor protein which plays an important role in cell proliferation and apoptosis (Alshenawy and Alshafey, 2012). In a stable or unstressed tissue, p53 protein exhibits low level of expression and its short half-life is due to continuous ubiquitination via an inhibitory interaction with MDM-2 and degradation by 26S proteasome (Brooks and Gu, 2004; Yang et al., 2004; Bond et al., 2006). As a guardian of the genome, the p53 is expressed as an important inducer of apoptosis especially in condition of irreparable genomic alterations, over-expression of oncogenes or other cellular stresses which may be caused by exposure of cells to cytotoxic agents (Brooks and Gu, 2004; Yang et al., 2004). The study by Teh et al., (2002) reported the critical role that p53 protein plays during initiation of apoptosis such that the mutation of p53 gene or inactivation of wild-type p53 protein cause unregulated gastric epithelial plasticity. The study by Arab et al., (2015) opined that gastroprotective mechanisms involve down-regulation of apoptotic triggers such as p53 protein expression so as to shift the balance of gastric mucosal cells toward survival. From this study, the

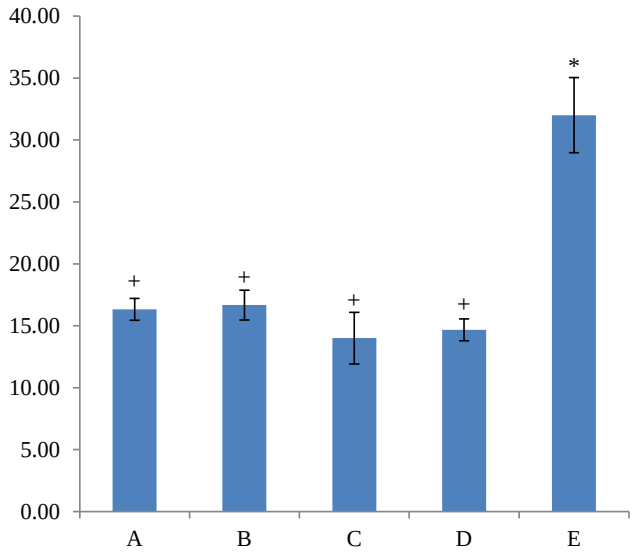

Figure 4. Chart showing the mean p53 distribution count in the gastric mucosa of the experimental animals A: Normal control group; B – D: Treated groups administered with 100mg/kg, 300mg/kg and 500mg/kg methanolic extracts of *A. conyzoides* L. respectively and E: Test control group.

Table 2. Mean and standard error of mean (SEM) of p53 distribution in gastric tissues of experimental animals in control groups A and E and treated groups B- D.

Groups	Mean ± SEM
A	16.33 ± 0.88
B	16.67 ± 1.20^{+}
C	14.00 ± 2.08^{+}
D	14.67 ± 0.88^{+}
E	32.00 ± 3.03*

* P< 0.05 was accepted as significant relative to group A
$^{+}$ P< 0.05 was accepted as significant relative to group E.

exposure to methanolic extracts of *A. conyzoides* L. have resulted into gastroprotective activity in the experimental animals also through suppression of pro-apoptotic signals generated by p53 protein which may follow exposure to gastric mucosal aggressive factors.

Conclusion

The methanolic extracts of *A. conyzoides* L. exhibited potent gastroprotective activity against exposure to aggressive factors of gastric mucosal injury at all the dosage levels in this study. The identified mechanisms of gastroprotective activity of methanolic extracts *A. conyzoides* L. include increase in mucous cell population leading increase in protective mucus secretion and down-regulation of p53 protein expression leading to suppression of pro-apoptotic signals that follows exposure to the aggressive factors.

RECOMMENDATIONS

The methanolic extracts of *A. conyzoides* L. is a potent gastroprotective agent. However, further studies are recommended to identify other mechanisms of its gastroprotective activity and veracity of its potency against other aggressive factors.

CONFLICT OF INTERESTS

The authors have not declared any conflict of interests.

ACKNOWLEDGEMENTS

Authors appreciate the efforts of the following during the tissue processing and staining: Mrs Okoro, Histopathology Department, University of Benin Teaching Hospital, Benin city, Nigeria and Mr Jonathan, Histopathology Department, National Hospital, Abuja, Nigeria.

REFERENCES

Alshenawy HA, Alshafey AM (2012). Does eradication of *Helicobacter pylori* decreases the expression of p53 and c-Myc oncogenes in the human gastric mucosa? Current Topics in Gastritis DOI:10.5772/53673.

Arab HH, Salama SA, Omar HA, Arafa EA, Maghrabi IA (2015). Diosmin protects against ethanol-induced gastric injury in rats: Novel Anti-ulcer actions. PLoS One 10(3):e0122417 DOI: 10.1371.

Ayyanar M, Ignacimuthu S (2005). Traditional knowledge of Kani tribals in Kouthalai of Tirunelveni Hills,Tamil Nadu, India. Journal of Ethnopharmacology 102(2):246-255.

Bond GL, Hirshfield KM, Kirchhoff T, Alexe G, Bond EE, Robins H, Bartel F, Taubert H, Wuerl P, Hait W, Toppmeyer D, Offit K, Levine AJ (2006). Mdm2 snp309 accelerates tumor formation in a gender-specific and hormone-dependent manner. Cancer Research 66(10):5104-5110.

Brooks CL, Gu W (2004). Dynamics in the p53-mdm2 ubiquitination pathway. Cell Cycle 3(7):895-899.

Dung NX, Loi DT (1991). Selection of traditional medicine for study. Journal of Ethnopharmacology 32(1-3):57-70.

Elisabetsky E, Wannmacher L (1993). The status of ethnopharmacology in Brazil. Journal of Ethnopharmacology 38(2-3):137-143.

Geissler PW, Harris SA, Prince RJ, Olsen A, Odhiambo RA, Oketch-Rabah H, Madiega PA, Anderson A, Molgaard P (2002). Medicinal plants used by Lou mothers and children in Boudo district, Kenya. Journal of Ethnopharmacology 83(1-2):39-54.

Gurib-Fakim AI, Gueho J, Sewraj-Bissoondayal M, Dulloo E (1993). Medical ethnobotany of some weeds of Mauritius and Rodrigues. Journal of Ethnopharmacology 39(3):175-185.

Ige AO, Adewoye EO, Okwundu NC, Alade OE. and Onuobia PC (2016). Oral magnesium reduces gastric mucosa susceptibility to injury in experimental diabetes mellitus. Pathophysiology 23(2):87-93.

Johnson LR (2003). Essential Medical Physiology. Third Edition. Elsevier Academic Press, Carlifonia, USA pp. 502-512.

Kamboj A, Saluja AK (2008). *Ageratum conyzoides* L. – a review of its phytochemical and pharmacological profile. International Journal of Green Pharmacy 2(2):59-68.

Kern SE, Kinzler KW, Bruskin A, Jarosz D, Friedman P, Prives C, Vogelstein B (1991). Identification of p53 as a sequence-specific DNA-binding protein. Science 252(5013):1708-1711.

Lane DP (1992). P-53, Guardian of the genome. Nature 358:15-16.

Mahmood AA, Sidik K, Salmah I, Suzainur KAR, Philips K (2005). Antiulcerogenic activity of *Ageratum conyzoides* leaf extract against ethanol-induced gastric ulcer in rats as animal model. International Journal of Molecular Medicine and Advance Sciences 1(4):402-405.

Ming LC (1999). *Ageratum conyzoides*: a tropical source of medicinal and agricultural products. Perspective on new crops and new uses. J. Janick (ed), *ASHS Press,* Alexandria, Virginia, USA pp. 469-473.

Moshi MJ, Kagashe GAB, Mbwambo ZH (2005). Plants used to treat epilepsy by Tanzanian traditional healers. Journal of Ethnopharmacology 97(2):327-36.

Novy JW (1997). Medicinal plants of the Eastern region of Madagascar. Journal of Ethnopharmacology 55(2):119-126.

Okunade AL (2002). Review: *Ageratum conyzoides* L. (Asteracaea). Fitoterapia 73(1):1-16.

Olaibi OK, Ijomone OM, Olawuni IJ, Adewole SO, Akinsomisoye SO (2014). Mucus secreting activity and nitric oxide concentrations of ethanol-induced pylorus and duodenum of rats pretreated with *Moringa oleifera*. Journal of Experimental and Integrative Medicine 4(2):123-130.

Perumal-Samy R, Ignacimuthu S, Patric-Raja D (1999). Preliminary screening of ethnomedicinal plants from India. Journal of Ethnopharmacology 66(2):235-240.

Rhoades RA, Tanner GA (2004). Medical Physiology. Second Edition. Lippincott Williams and Wilkins pp. 484-488.

Sembulingam K, Sembulingam P (2010). Essentials of Medical Physiology. Fifth Edition. Jaypee Brothers Medical Publishers Ltd, St Louis, USA pp. 218-226.

Sharma PD, Sharma OMP (1995). Natural products chemistry and biological proportions of the *Ageratum* plant. Toxicological and. Environmental Chemistry 50(1):213-232.

Shay JP, Komorov SA, Fels SS, Meranze D, Grunstein M, Simpler H (1945). A simple method for the uniform production of gastric ulceration in the rat. Gastroenterology 5:43-61.

Shekhar TC, Anju G (2012). A comprehensive review on *Ageratum conyzoides Linn* (Goat weed). International Journal of Pharmaceutical and Phytopharmacological Research 1(6):391-395.

Sofowora EA (1993). Medicinal plants and traditional medicine in Africa. Spectrum Books Limited. Ibadan, Nigeria pp. 142-147.

Teh M, Tan KB, Seet BL, Yeoh KG (2002).Study of p53 immunostaining in the gastric epithelium of cagA-positive and cagA-negative *Helicobacter pylori* gastritis. Cancer 95(3):499–505.

Volgelstein B, Kinzler KW (1992). P-53 function and dysfunction. Cell 70(4):523-526.

Yang Y, Li CC, Weissman AM (2004). Regulating the p53 system through ubiquitination. Oncogene 23(11):2096-2106.

Vol. 18(27), pp. 647-658, July, 2019
DOI: 10.5897/AJB2019.16819
Article Number: 4E53BD661452
ISSN: 1684-5315

http://www.academicjournals.org/AJB

ACADEMIC JOURNALS
expand your knowledge

African Journal of Biotechnology

Full Length Research Paper

Modified protocol for RNA isolation from different parts of field-grown jute plant suitable for NGS data generation and quantitative real-time RT-PCR

Rasel Ahmed[1], Md. Sabbir Hossain[1], Md. Samiul Haque[1,2], Md. Monjurul Alam[1,2] and Md. Shahidul Islam[1,2*]

[1]Basic and Applied Research on Jute Project, Bangladesh Jute Research Institute, Dhaka, Bangladesh.
[2]Bangladesh Jute Research Institute, Dhaka, Bangladesh.

Received 31 March, 2019; Accepted 17 June, 2019

High quality RNA extraction from field-grown jute plants can be difficult due to the presence of complex polyphenolic, polysaccharide and waxes. But isolation of RNA in high quality is a basic need in plant genetics, genomics, transcriptomics, molecular biology and related physiological investigations. Here, cetyl trimethyl ammonium bromide (CTAB) based modified RNA isolation protocol suitable for isolating high quality total RNA from different parts of field-grown jute plants was reported. Modifications come with two extra wash with extraction buffer, residual polysaccharides precipitation with absolute ethanol and potassium acetate during phenol:chloroform:isoamyl alcohol (PCI), intermediate pelleting with lithium chloride followed by dissolving the pellet in sodium dodecyl sulfate (SDS). The 28S/18S ratio and RIN of isolated RNA were greater than 2.0 and 7.3 to 8.8, respectively reveal RNA to be high purity. The isolated RNA can be used directly for subsequent downstream applications including cDNA library construction, reverse transcription polymerase chain reaction (RT-PCR) and RNA-Seq raw data generation without further purification. Moreover, this study showed that this method could also be successfully applied to other polyphenols and polysaccharides rich malvaceous plants.

Key words: RNA isolation, *Corchorus*, Jute, quantitative polymerase chain reaction with reverse transcription (RT-qPCR), cDNA library construction, next-generation sequencing (NGS) data generation.

INTRODUCTION

cDNA sequencing (RNA-Seq) technology provides the opportunity to identify all expressed transcripts (Guttman et al., 2010) along with the assessment of different important phenomena such as gene expression levels (Pickrell et al., 2010), differential splicing events (Liu et al., 2012; Wang et al., 2008, 2010) and allele-specific gene expression (Rozowsky et al., 2011). High quality RNA extraction is required for cDNA sequencing which is very challenging for the plants rich in mucilage, polysaccharides and polyphenolic compounds (Mac, 2007). Jute (*Corchorus* species) is an annual, herbaceous bast fibre crop and the second most important natural

*Corresponding author. E-mail: nshahidul@gmail.com or shahidul@jutegenome.org. Tel: +8802-9103148. Fax: +8802-9146134.

fiber after cotton, in terms of production and usage. Fibers are commonly used as filler, or reinforcement; insulation or use as structural elements, and disposable or durable products such as yarns and textiles, ropes, twines, non-woven fabrics, paper and fiber board products, packaging and construction materials, geotextiles and composites and automotive parts (van Dam and Bos, 2004). Jute plant has extremely high contents of acidic and proteinaceous type of mucilage (Stephen et al., 2006) in its various tissues which complicates the isolation of RNA for downstream applications (Rai et al., 2010; Pandey et al., 1996). Elimination of this mucilage is a major challenge for the available protocols of RNA extraction. Moreover, the problem is magnified by conformational changes in mature jute leaves. An irreversible increase in viscosity of the hydrocolloid obtained from leaves occurs during cell lysis at the temperature >60°C (Yamazaki et al., 2009). Standard RNA isolation techniques such as guanidinium-phenol-chloroform extraction (Chomczynski and Sacchi, 1987), TRIZOL and Cetyl Trimethyl Ammonium Bromide (CTAB) methods have failed to isolate adequate and quality RNA from jute leaf (Figure S1 and Table 2). The difficulties of RNA extraction from jute plants have been reported by number of researchers (Khan et al., 2004; Mahmood et al., 2011).

Several protocols (Kumar et al., 2011; Sharma et al., 2003; Hu et al., 2002) are available for isolating RNA from plant tissues containing high levels of polysaccharides and polyphenol compounds. Each of the methods is designed for specific plant species and the nature of the target tissue. Samanta et al. (2011) had established a method for RNA extraction from jute stem only, which employs modified hot borate treatment followed by isopycnic centrifugation. Furthermore, Choudhary et al. (2016) also claimed an RNA isolation procedure from developing jute stem only. But the amount of mucilage, polysaccharides and polyphenolic compounds varies extensively within the developing tissues (Khanuja et al., 1999). Therefore, an efficient protocol is required for isolation of quality RNA from all parts of full grown jute plant. Here, a robust plant RNA isolation protocol, suitable for different types of tissue of jute ranging from root to developing fruits, derived from CTAB method was described (Doyle and Doyle, 1987).

MATERIALS AND METHODS

Plant sample

Plants of the tossa jute (*Corchorus olitorius* variety O-4) were grown in an experimental field at Jute Agricultural Experimental Station, Manikganj, Bangladesh. The root, stem, bark, stick and leaf tissues were sampled from 45 days plants. Flowers were collected just after blooming and developing fruits were collected at 15 days post-anthesis. All samples were snap-frozen in liquid N_2 and stored at -80°C. To check the general effectiveness of our protocol, RNA was extracted from the leaves of some other malvaceous plants including *Hibiscus cannabinnas*, *Hibiscus sabdariffa*, *Hibiscus rosa-sinensis,* and *Abelmoschus esculentus* collected from Jute Agricultural Experimental Station, Manikganj, Bangladesh.

Reagents and solutions

Extraction buffer 100 mM Tris-HCl [Invitrogen, USA], pH 8.0; 1.4 M NaCl [Carl Roth, Germany]; 20 mM EDTA [Sigma-Aldrich, Germany], pH 8.0; 2% (w/v) CTAB [Sigma-Aldrich, Germany]; 4% (w/v) Polyvinylpolypyrrolidone (PVPP) [Sigma-Aldrich, Germany]; 2% (w/v) Polyvinylpyrrolidone (PVP) [Sigma-Aldrich, Germany]; 4% (v/v) β-mercaptoethanol [Sigma-Aldrich, Germany] (to be added just before use); Phenol [Carl Roth, Germany]:Chloroform [Sigma-Aldrich, Germany]:isoamyl alcohol [Carl Roth, Germany] (PCI; 25:24:1, v/v; freshly prepared); 10 M LiCl [Sigma-Aldrich, Germany]; 2% SDS [Invitrogen, USA]; 5 M Potassium acetate [Sigma-Aldrich, Germany], pH 4.8; Absolute Ethanol [Merck, Germany]; Isopropanol [Sigma-Aldrich, Germany]; 70% ethanol. The chemicals used were of molecular biology grade and solutions were made with 0.1% v/v diethylpyrocarbonate (DEPC) [Carl Roth, Germany] treated water and consumables were RNase-free as well.

Isolation procedure

One gram frozen tissue of each sample was ground to a very fine powder in liquid nitrogen with a cooled mortar and pestle. The powder was transferred immediately (before thawing) to 20 ml Extraction Buffer (EB) kept in a 50 ml falcon tube which was pre-heated at 65°C in water bath. The sample in extraction buffer was homogenized by vigorous shaking followed by incubation at 65°C for 20 min with occasional shaking. After incubation, the homogenate was centrifuged at 13,000 g for 20 min at room temperature. The supernatant was collected carefully without disturbing the pellet and transferred to 50 ml tube containing 10 ml EB buffer and inverted to mix the contents. After 10 min incubation at room temperature, the content was centrifuged at 13,000 g for 20 min at room temperature and supernatant was collected carefully without disturbing the pellet in 50 ml tube containing 5 ml EB buffer and inverted to mix the contents followed by 10 min incubation at room temperature. Again the content was centrifuged at 13,000 g for 20 min at room temperature. This time the supernatant was collected and kept on ice until further steps. One tenth volume of absolute ethanol and 1/15 volume potassium acetate (5 M, pH 4.8) were added to the tube and mixed by inversion. Then an equal volume of PCI (25:24:1, v/v) was added, shaked vigorously by hand for 10 s and the content was turned into milky white in colour. The mixer was centrifuged at 13,000 g for 20 min at 4°C and the aqueous phase was collected in a 15 ml falcon tube kept on ice. And then, 1/4 volume of 10 M LiC was added, mixed gently, incubated for 1 h at -70°C (at this stage, sample can be stored at -20°C if it is required to perform the rest of the procedure later) and centrifuged at 13,000 g for 20 min at 4°C. The supernatant was discarded and the pellet was dissolved in 1 ml SDS (2%, w/v). An equal volume of PCI (25:24:1, v/v) was added and mixed well by inversion followed by centrifugation at 13,000 g for 20 min at 4°C. The resulting upper aqueous phase was transferred to a 1.5 ml Eppendorf tube. Then, an equal volume of ice-cold 2-propanol was added and mixed well (at this point 2-propanol added sample can be stored at -20°C if it is required to perform the rest of the procedure later). After incubation for 1 h at -70°C, the content was centrifuged at 13,000 g for 20 min at 4°C and the supernatant was discarded. The final RNA pellet was washed twice with 70% ethanol by centrifugation at 13,000 g for 10 min at 4°C. After confirmation of complete removal of ethanol by air-drying, the pellet was dissolved in nuclease free water.

This isolation procedure basically differs from traditional CTAB

based method in such ways: two extra wash with EB buffer, adding absolute ethanol and potassium acetate during first phenol: chloroform:isoamyl alcohol (PCI) step, first precipitation with LiCl followed by dissolving first pellet with SDS. All those modifications were done to reduce the amount of mucilage, polysaccharides and polyphenolic compounds present in different parts of jute plant as well as to ensure the purity of RNA.

Assessment of RNA quantity and integrity

The RNA quantity and purity were checked both spectrophotometrically using NanoDrop® (ND2000c, Thermo Scientific, USA) and by electrophoresis followed by visualization on a denaturing formaldehyde 1.2% agarose gel using Molecular Imager® Gel DOC^{TM} XR+ with Image Lab^{TM} Software (Bio Rad Laboratories, Inc., USA). Quality and integrity of isolated RNA was also verified electrophoretically on an Agilent 2100 Bioanalyzer with RNA 6000 Nano LabChip (Agilent Technologies, CA, USA).

cDNA synthesis and RT-PCR analysis

RNA extracted from the samples was treated with DNase I amplification grade (Sigma-Aldrich, Germany) to remove any traces of genomic DNA according to the manufacturer's instructions. cDNA was synthesized from 1.0 µg of total RNA using the RevertAid First Strand cDNA Synthesis Kit (Thermo Fisher Scientific Inc) containing oligo dT primers according to manufacturer's instructions. Freshly prepared cDNAs were amplified by GAPDH gene specific primers (Forward primer 5'- GAAGGATCGGTAGGTTGGTG -3' and Reverse primer 5'-CCTTGACTTTGAGCTCGTGA -3'). The primer was designed using Genscript primer designing tool with default parameters. PCR reactions were carried out in a final volume of 25 µl reaction mixture containing 10 mM Tris-HCl (pH 8.3), 50 mM KCl, 1.5 mM $MgCl_2$, 200 µM dNTP, 0.2 µM each primer, 2.0 µl cDNA and 0.5 U of Taq DNA polymerase. PCR was performed using thermo cycler condition which was initiated by a hot start at 95°C for 5 min followed by 30 cycles of 95°C for 30 s, 50°C for 30 s and 72°C for 45 s with a 72°C for 5 min final extension. Minus RT control PCR was carried out with 0.5 µg of total RNA instead of cDNA to check DNA contamination. In addition, a H_2O control (without template) was set to check whether the PCR signal is resulting from specific cDNA amplification. The PCR products were resolved on a 1.5% agarose gel and visualized under ultraviolet light.

Quantitative polymerase chain reaction with reverse transcription (RT-qPCR)

RT-qPCR amplification was performed in a LightCycler®480 Instrument II (Roche) using the SYBR Green I Master (Roche) according to manufacturer's instructions. PCR amplification was carried out in a 20-µl volume containing 10-µl of 2X SYBR Green I Master mix, 10 ng cDNA and 0.4 µM of each primer. Thermo cycling conditions were set as an enzyme activation step at 95°C for 5 min followed by 40 cycles consisting of 10 s of denaturation at 95°C, 10 s of annealing at 50°C and 20 s of elongation at 72°C.

NGS data generation from isolated RNA

Sequencing library was prepared using TruSeq Stranded mRNA Library Prep Kit (Illumina Inc., USA) according to manufacturer's instructions. mRNA was isolated from 1 µg of total RNA using poly-T oligo attached magnetic beads with two rounds of purification. The purified mRNA was fragmented and primed with random hexamers. First strand cDNA was synthesized using SuperScript II Reverse Transcriptase followed by the synthesis of second-strand cDNA. After end repair and the ligation of adaptors, the products were enriched and amplified by PCR. The amplified cDNA libraries were purified by Agencourt AMPure XP beads and assessed on an Agilent Bioanalyzer 2100 system. After validation and quantification, the final cDNA libraries were sequenced using an Illumina HiSeq™ 2500 sequencing platform.

Bioinformatic analysis

After the removal of the adapters (by Trimmomatic tool version 0.36 with default parameters) from the raw reads, low quality and duplicate reads were filtered using SICLE (Q30+; Min Len=50 bp). HISAT2 2.1.0 was used to map the filtered reads with reference genome assembly and coding sequences of *C. olitorius* (Wang et al., 2008) with the parameters '--mp 4,1 --sp 1,0.5 --score-min L,0,-0.8'.

Data availability

The RNA-Seq data were deposited in the NCBI Sequence Read Archive (SRA) under SRP049494.

RESULTS

Quality, integrity and quantity of extracted RNA

RNA was isolated from various parts of fully-grown jute plant such as root, stem, bark, stick, leaf, flower and fruit (Figure 1) using the CTAB based RNA extraction protocol. The amount of total extracted RNA varied in different parts ranging from 68.32 to 148.01 µg/g tissue (Table 1). Different amount of water and mucilage in different parts of the plant may cause the variation.

The quality of isolated RNA was assessed by multiple independent methods. The 1.2% agarose gel electrophoresis (Figure 2) showed that the brightness of 28S rRNA was significantly prominent than 18S rRNA. It demonstrates that the extracted RNAs were not degraded and there was no detectable amount of gDNA contamination. In addition, from the Bioanalyzer analysis, it was observed that the ratio of 28S rRNA and 18S rRNA for different samples were between 2.1 and 2.6 which indicates good quality of RNA (Table 1).

The spectrophotometer analysis showed that the A260/280 and A260/230 absorbance ratio of RNA samples are >2.0 and between 1.90 and 2.37, respectively (Table 1). The A260/280 absorbance ratios represent the high purity of isolated RNAs whereas the A260/230 absorbance ratios indicate that RNAs were not contaminated by polyphenolics and polysaccharides. Though A260/230 absorbance ratio of root little bit lower but the other quality parameters such as RNA gel electrophoresis, yield per g tissue and RIN in bioanalyzer analysis were good. RNA extracted with modified method produced better results compared to CTAB, Trizol and GNTC according to spectrophotometrical and agarose gel electrophoresis analysis (Table 2 and Figure S1).

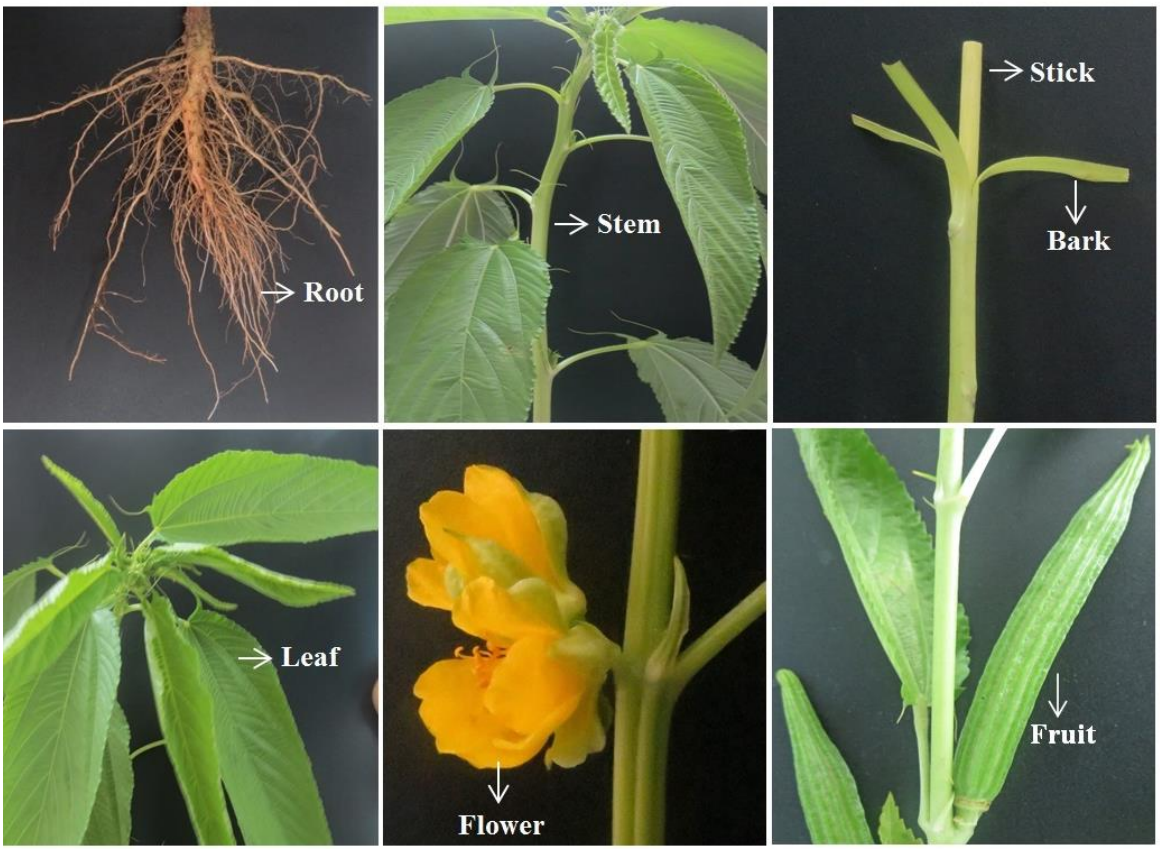

Figure 1. Different parts of jute plant used for RNA isolation.

Table 1. Quantity and quality of RNA extracted from different parts of field grown jute plants

Sample	Yield (µg/g)	A 260/280	A 260/230	RIN	28S/18S
Root	148.01 ± 5.02	2.04 ± 0.02	1.90 ± 0.05	8.8 ± 0.02	2.1 ± 0.02
Stem	108.64 ± 3.33	2.07 ± 0.03	2.36 ± 0.09	8.8 ± 0.01	2.3 ± 0.03
Bark	104.18 ± 4.17	2.05 ± 0.01	2.35 ± 0.06	7.8 ± 0.03	2.6 ± 0.02
Stick	69.74 ± 2.01	2.05 ± 0.04	2.37 ± 0.08	8.2 ± 0.03	2.6 ± 0.01
Leaf	98.99 ± 3.93	2.10 ± 0.03	2.35 ± 0.03	8.7 ± 0.02	2.2 ± 0.01
Flower	107.29 ± 4.32	2.06 ± 0.05	2.33 ± 0.04	8.2 ± 0.01	2.1 ± 0.01
Fruit	68.32 ± 3.79	2.03 ± 0.03	2.34 ± 0.02	7.3 ± 0.01	2.1 ± 0.01

Data represent mean ± SD of three replicates.

The RNA integrity was measured using Bioanalyzer metrics (Agilent Technologies, Santa Clara, California, USA). The obtained RNA Integrity Numbers (RIN) were between 7.3 and 8.8 (Table 1) whereas RNA with a RIN value above 7.0 is considered good enough for next-generation sequencing (Islam et al., 2017). A representative electropherogram of RNA isolated from different parts of jute plant are as shown in Figure 3 with clear peaks of rRNAs, indicating no degradation of the RNAs.

Downstream analysis results

RT-PCR

Single-stranded cDNA was successfully synthesized from extracted RNA samples using the RevertAid First Strand cDNA Synthesis Kit (Thermo Fisher Scientific Inc.) containing oligo dT primer. Glyceraldehyde-3-Phosphate Dehydrogenase (GAPDH) gene was amplified from synthesized cDNA by PCR (Figure 4). Fragments for

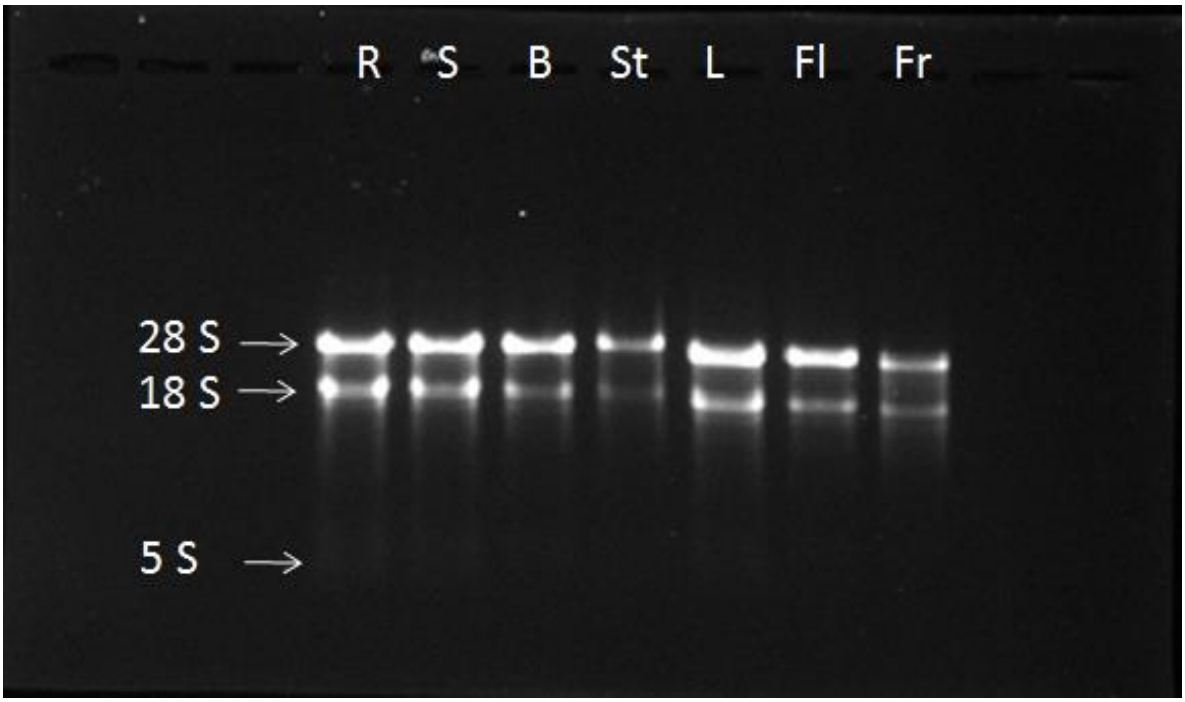

Figure 2. Electrophoresis of RNAs isolated by the CTAB based RNA extraction protocol. Total RNA from different parts of jute plants, resolved by electrophoresis through a formaldehyde-agarose gel and visualized with ethidium bromide staining. R-Root; S-Stem; B-Bark; St-Stick; L- Leaf; Fl-Flower; Fr-Fruit.

Table 2. Quantity and quality of RNA extracted from leaves using different methods.

Method	Yield (µg/g)	A 260/280	A 260/230
GNTC	2.76	1.09	0.92
Trizol	3.18	0.94	0.40
CTAB	12.69	1.61	1.34
Modified	98.99	2.10	2.35

GAPDH were obtained as per designed primer (159 bp) in all of the samples, indicating that the isolated RNA is good enough for RT-PCR. No band associated with genomic DNA contamination was observed when RNA was used as template.

RT-qPCR

qRT-PCR was successfully performed with housekeeping gene, GAPDH for further evaluation of the integrity of extracted RNA. A dissociation curve with single peak ensured that the primers amplified specific fragment (Figure 5). In addition, PCR efficiency of GAPDH was determined from the standard curve based on serial dilution. The efficiency values were from 92.72 to 99.04% with good linear regression (R2>0.99) which indicates that there were no PCR inhibitors present in the RNA samples (Figure S2).

Each PCR reaction included minus RT and H_2O (no template) control to check for potential genomic DNA and reagent contamination. All samples were amplified in technical and biological triplicates.

NGS data generation

A total of ~53 Gbp RNA-seq data were generated from three independent biological replica samples of jute stem using Illumina HiSeq 2500. About 94 and 83% filtered reads were mapped to reference genome and coding sequences, respectively. Among 37,031 predicted genes in *C. olitorius* genome (Islam et al., 2017), 27,500 genes were found in RNA-seq data (Supplementary Table 1).

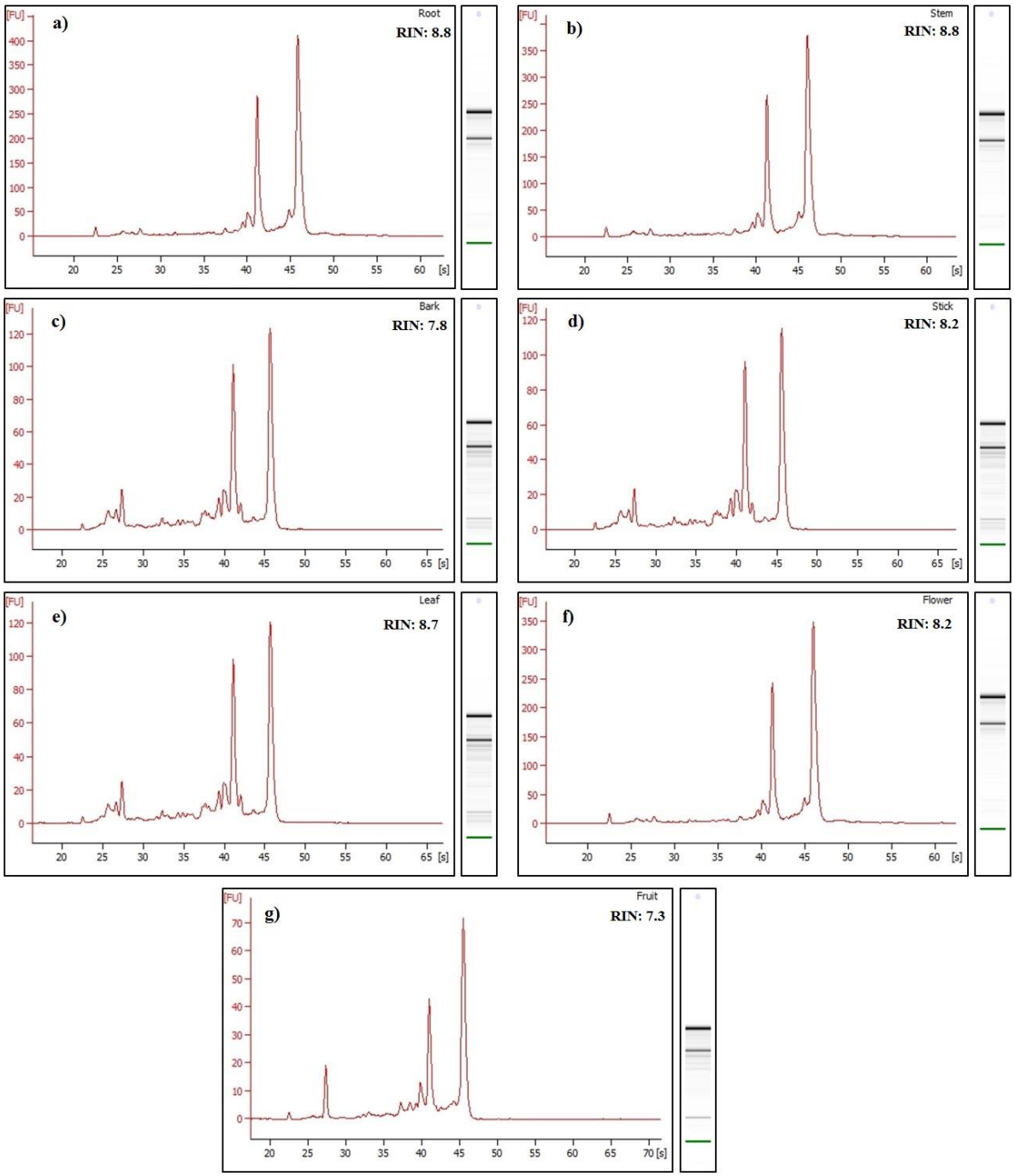

Figure 3. The differences of 18S and 28S ribosomal RNA peak profiles and the RNA integrity numbers (RIN) for different parts of full grown jute plants. a) Root, b) Stem, c) Bark, d) Stick, e) Leaf, f) Flower, and g) Fruit.

Applicability in malvaceous plant species other than jute

The described protocol for RNA isolation can also be applied for various mucilage rich plant species. This protocol was used for four malvaceous plant species, *H. cannabinnas*, *H. sabdariffa*, *H. rosa-sinensis,* and *A. esculentus* and found excellent results (Figure S3 and Supplementary Table 2).

DISCUSSION

Trizol, GNTC protocol and CTAB method were initially tried

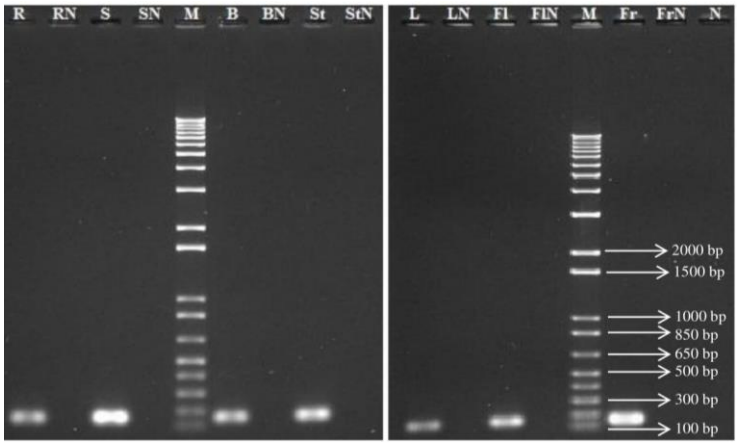

Figure 4. Agarose gel electrophoresis of the RT-PCR from RNAs of different parts of jute plant. RT-PCR amplification of GAPDH gene. R-Root cDNA; RN-Root RNA; S-Stem cDNA; SN-Stem RNA; B-Bark cDNA; BN-Bark RNA; St-Stick cDNA; StN-Stick RNA; L-Leaf cDNA; LN-Leaf RNA; Fl-Flower cDNA; FlN-Flower RNA; Fr-Fruit cDNA; FrN-Fruit RNA and N-H_2O control.

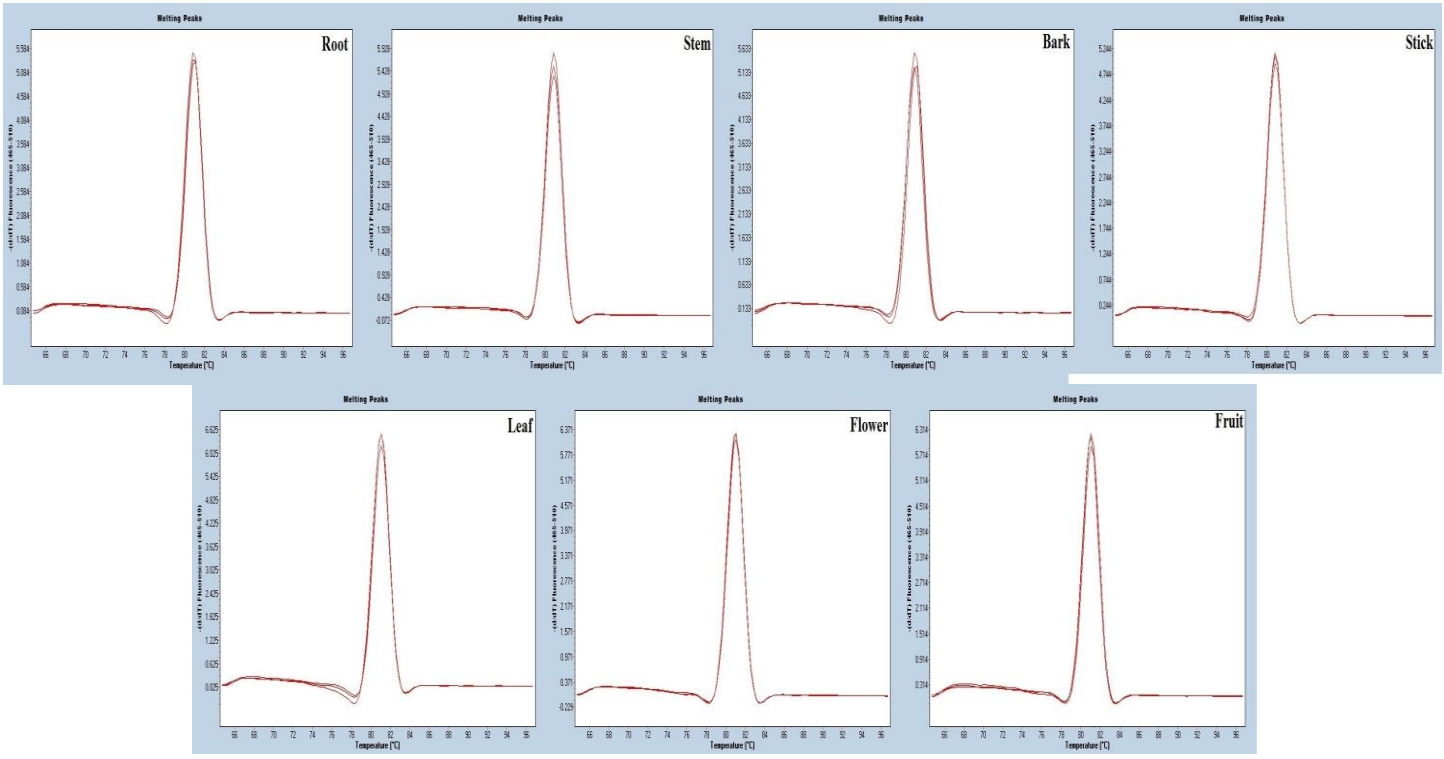

Figure 5. Dissociation curve of GAPDH gene after qRT-PCR reactions using RNAs obtained from different parts of jute plant. X-axis represents temperature (°C) and y-axis represents fluorescence

for RNA extraction from different parts of fully-grown jute plant. Due to presence of high polysaccharide and other viscous materials in the samples, both Trizol and GNTC protocol failed to collect desired supernatant from phase separation step resulting RNA recovery cumbersome. RNA extracted with modified method produced better results compared to CTAB, Trizol and GNTC according to spectrophotometrical analysis (Table 2). Similarly,

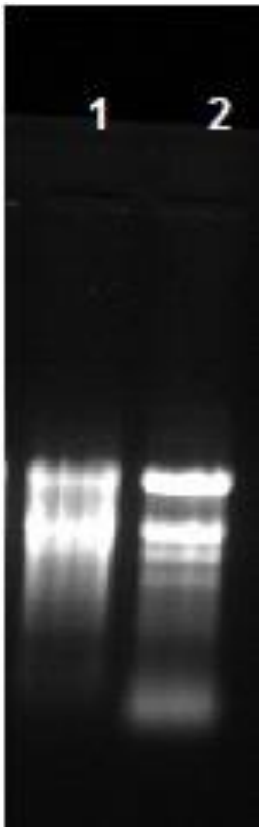

Figure 6. Effect of extra CTAB buffer wash on RNA quality. Lane 1: Single wash; Lane 2: Double wash.

electrophoresis in agarose gel shows that the quality and quantity of RNA obtained from CTAB, Trizol and GNTC method is not adequate enough (Figure S1).

Therefore, the CTAB method was modified. A high-strength CTAB solution was used as a lysis buffer with a higher concentration of PVPP, PVP and β-mercaptoethanol. It ensured rapid removal of phenolic compounds, which otherwise oxidize and bind to RNA molecules. The combination of PVP and PVPP produced top aqueous phase immediately displayed transparency, indicating successful elimination of pigments and most of polyphenolics. In order to reduce the amount of mucilage, two additional CTAB buffer washes were included in our protocol which could successfully eliminate pigments and most polyphenolics (Figure 6). Further, in first purification step of this protocol, 1/10 V absolute ethanol and 1/15 V potassium acetate were added to the supernatant along with phenol: chloroform: isoamyl alcohol (PCI). Absolute ethanol and KAc effectively precipitated residual polysaccharides (Yockteng et al., 2013; Yang et al., 2008). LiCl was used in the first precipitation step of the protocol to reduce co-precipitation of polysaccharides with RNA. It is an important step as LiCl does not precipitate DNA, proteins and phenolic compounds. In addition, 2% SDS was used to dissolve precipitated RNA followed by second PCI extraction as SDS effectively disrupts protein-nucleic acid interaction and protect RNA from ribonucleases. After this disruption, protein was denatured by PCI and became insoluble in aqueous solution (Rio et al., 2010), resulting in good quality RNA with no protein contaminants (Table 1).

There are a limited number of published methods to isolate RNA from jute plant. For instance, Mahmood et al. (2011) reported the procedure to isolate RNA from jute seedling and both Samanta et al. (2011) and Choudhary et al. (2016) illustrated RNA isolation methods from jute stem only. However, the protocol, claimed by Samanta et al. (2011), requires ultra-centrifuge facility, which is a very complex and expensive setup and might not be available in regular laboratories, and costly reagent CsCl for purification of RNA. In contrast, the procedure described here is highly reproducible and easily adoptable in usual laboratory conditions and suitable for isolating RNA from plant species and different tissues rich in polysaccharides and phenolic compounds. To our knowledge, this is the first report of a single method which can be utilized to isolate high quality RNA from different parts of field grown jute plant. Furthermore, using this protocol, high quality RNA has been extracted from different plant species in Malvaceae (*H. cannabinnas*, *H. sabdariffa*, *H. rosasinensis,* and *A. esculentus*) containing abundant polyphenols and polysaccharides.

Conclusion

This method is highly reproducible and easily adoptable in usual laboratory conditions and suitable for isolating RNA from different developing parts of jute plant. The RNA obtained by using this method can be used directly for subsequent downstream applications including cDNA library construction, qRT-PCR and RNA-seq data generation without further purification. The method also applied to other polyphenols and polysaccharides rich malvaceous plant.

ACKNOWLEDGEMENTS

The authors thank Md Sharifur Rahman (Department of Telecommunications, Dhaka 1208, Bangladesh) for critical suggestions and comments on the manuscript. They are grateful to Emdadul Mannan Emdad (Basic and Applied Research on Jute Project, Bangladesh Jute Research Institute, Dhaka 1207, Bangladesh) for technical help. This research was funded by the Government of Bangladesh.

CONFLICT OF INTERESTS

The authors have not declared any conflict of interests.

REFERENCES

Chomczynski P, Sacchi N (1987). Single-step method of RNA isolation by acid guanidinium thiocyanate–phenol–chloroform extraction. Analytical Biochemistry 162:156-159.

Choudhary SB, Kumar M, Chowdhury I, Singh RK, Pandey SP, Sharma HK, Karmakar PG (2016). An efficient and cost effective method of RNA extraction from mucilage, phenol and secondary metabolite rich bark tissue of tossa jute (*C. olitorius* L.) actively developing phloem fiber. 3 Biotech 6:100.

Doyle JJ, Doyle JL (1987). A rapid DNA isolation procedure for small quantities of fresh leaf tissue. Phytochemical Bulletin 19:11-15.

Guttman M, Garber M, Levin JZ, Donaghey J, Robinson J, Adiconis X, Fan L, Koziol MJ, Gnirke A, Nusbaum C, Rinn JL, Lander ES, Regev A (2010). Ab initio reconstruction of cell type-specific transcriptomes in mouse reveals the conserved multi-exonic structure of lincRNAs. Nature Biotechnology 28:503-510.

Hu CG, Honda C, Kita M, Zhang Z, Tsuda T, Moriguchi T (2002). A simple protocol for RNA isolation from fruit trees containing high levels of polysaccharides and polyphenol compounds. Plant Molecular Biology Report 20:69a-69g.

Islam MS, Saito JA, Emdad EM, Ahmed B, Islam MM, Halim A, Hossen QMM, Hossain MZ, Ahmed R, Hossain MS, Kabir SM, Khan MS, Khan MM, Hasan R, Aktar N, Honi U, Islam R, Rashid MM, Wan X1, Hou S, Haque T, Azam MS, Moosa MM, Elias SM, Hasan AM, Mahmood N, Shafiuddin M, Shahid S, Shommu NS, Jahan S, Roy S, Chowdhury A, Akhand AI, Nisho GM, Uddin KS, Rabeya T, Hoque SM, Snigdha AR, Mortoza S, Matin SA, Islam MK, Lashkar MZ, Zaman M, Yuryev A, Uddin MK, Rahman MS, Haque MS, Alam MM, Khan H, Alam M (2017). Comparative genomics of two jute species and insight into fibre biogenesis. Nature Plants 3:16223.

Khan F, Islam A, Sathasivan AK (2004). Rapid method for high quality RNA isolation from jute: *Corchorus capsularis* L. and *Corchorus olitorius* L. Plant Tissue Culture & Biotechnology 14:63-68.

Khanuja SPS, Shasany AK, Darokar MP, Kumar S (1999). Rapid isolation of DNA from dry and fresh samples of plants producing large amounts of secondary metabolites and essential oils. Plant Molecular Biology Report 17:74.

Kumar GRK, Eswaran N, Johnson TS (2011). Isolation of high-quality RNA from various tissues of *Jatropha curcas* for downstream applications. Analytical Biochemistry 413:63-65.

Liu J, Lee W, Jiang Z, Chen Z, Jhunjhunwala S, Haverty PM, Gnad F, Guan Y, Gilbert HN, Stinson J, Klijn C, Guillory J, Bhatt D, Vartanian S, Walter K, Chan J, Holcomb T, Dijkgraaf P, Johnson S, Koeman J, Minna JD, Gazdar AF, Stern HM, Hoeflich KP, Wu TD, Settleman J, de Sauvage FJ, Gentleman RC, Neve RM, Stokoe D, Modrusan Z, Seshagiri S, Shames DS, Zhang Z (2012). Genome and transcriptome sequencing of lung cancers reveal diverse mutational and splicing events. Genome Research 22:2315-2327.

Mac Rae E (2007). Extraction of plant RNA. In 'Methods in molecular biology, Protocols for nucleic acid analysis by nonradioactive probes'. (Eds Hilario E, Mackay J, 2nd ed.) (New Jersey: Humana Press) 353:15-24.

Mahmood N, Ahmed R, Azam MS, Khan H (2011). A simple and swift method for isolating high quality RNA from jute (*Corchorus* spp.). Plant Tissue Culture & Biotechnology 21:207-211.

Pandey RN, Adams RP, Flournoy LE (1996). Inhibition of random amplified polymorphic DNAs (RAPDs) by plant polysaccharides. Plant Molecular Biology Report 14:17-22.

Pickrell JK, Marioni JC, Pai AA, Degner JF, Engelhardt BE, Nkadori E, Veyrieras JB, Stephens M, Gilad Y, Pritchard JK (2010). Understanding mechanisms underlying human gene expression variation with RNA sequencing. Nature 464:768-772.

Rai V, Ghosh SJ, Dey N (2010). Isolation of total RNA from hard bamboo tissue rich in polyphenols and polysaccharides for gene expression studies. Electronic Journal of Biotechnology 13:5.

Rio DC, Ares M Jr, Hannon GJ, Nilsen TW (2010). Purification of RNA by SDS Solubilization and Phenol Extraction. Cold Spring Harbor Protocols. doi: 10.1101/pdb.prot5438

Rozowsky J, Abyzov A, Wang J, Alves P, Raha D, Harmanci A, Leng J, Bjornson R, Kong Y, Kitabayashi N, Bhardwaj N, Rubin M, Snyder M, Gerstein M (2011). AlleleSeq: analysis of allele-specific expression and binding in a network framework. Molecular Systems Biology 7:522.

Samanta P, Sadhukhan S, Das S, Joshi A, Sen SK, Basu A (2011). Isolation of RNA from field-grown jute (*Corchorus capsularis*) plant in different developmental stages for effective downstream molecular analysis. Molecular Biotechnology 49:109-115.

Sharma AD, Gill PK, Singh P (2003). RNA isolation from plant tissues rich in polysaccharides. Analytical Biochemistry 314:319-321.

Stephen AM, phillips GO, williams PA (2006). Food polysaccharides and their applications. 2nd ed. (Boca Raton: CRC Press).

van Dam JEG, Bos HL (2004). The environmental impact of hard fibres and jute in non-textiles industrial application. Consultation of natural fibres. ESC-Fibres consultation No. 04/4. Short version of comprehensive review on the environmental impact of the natural fibres in industrial applications. Agrotechnology and Food Innovations (A & F), Wageningen UR, Wageningen, The Netherlands.

Wang ET, Sandberg R, Luo S, Khrebtukova I, Zhang L, Mayr C, Kingsmore SF, Schroth GP, Burge CB (2008). Alternative isoform regulation in human tissue transcriptomes. Nature 456:470-476.

Wang X, Wu Z, Zhang X (2010). Isoform Abundance Inference Provides a More Accurate Estimation of Gene Expression Levels in RNA-Seq. Journal of Bioinformatics and Computational Biology 8:177-192.

Yamazaki E, kurita O, Matsumura Y (2009). High viscosity of hydrocolloid from leaves of *Corchorus* olitorius L. Food Hydrocolloids 23:655-660.

Yang G, Zhou R, Tang T, Shi S (2008). Simple and Efficient Isolation of High-Quality Total RNA from *Hibiscus tiliaceus*, a Mangrove Associate and Its Relatives. Preparative Biochemistry and Biotechnology 38:257-264.

Yockteng R, Almeida AMR, Yee S, Andre T, Hill C, Specht CD (2013). A Method for Extracting High-Quality RNA from Diverse Plants for Next-Generation Sequencing and Gene Expression Analyses. Applications in Plant Sciences 1:1300070.

Supplementary Table 1. RNA-seq data generated from young stem.

Sample Name	Total reads	Filtered reads	Mapped data		
			Genome (%)	CDs (%)	No. of genes
Young stem 1	2 X 31,730,052	2 X 28,926,178	94.16	83.82	27,866
Young stem 2	2 X 32,276,920	2 X 28,898,789	93.82	83.76	27,759
Young stem 3	2 X 27,897,152	2 X 25,100,964	94.12	83.79	27,801

Supplementary Table 2. Quantity and quality of RNA extracted from leaves of different malvaceous plants.

Sample	Conc (ng/µl)	Yield (µg/g)	A 260/280	A 260/230
Hibiscus cannabinnas	836.6	75.09	2.03	2.42
Hibiscus sabdariffa	571.5	67.14	2.03	2.48
Hibiscus rosa-sinensis	971.8	79.15	2.02	2.44
Abelmoschus esculentus	2224.2	116.72	1.96	2.21

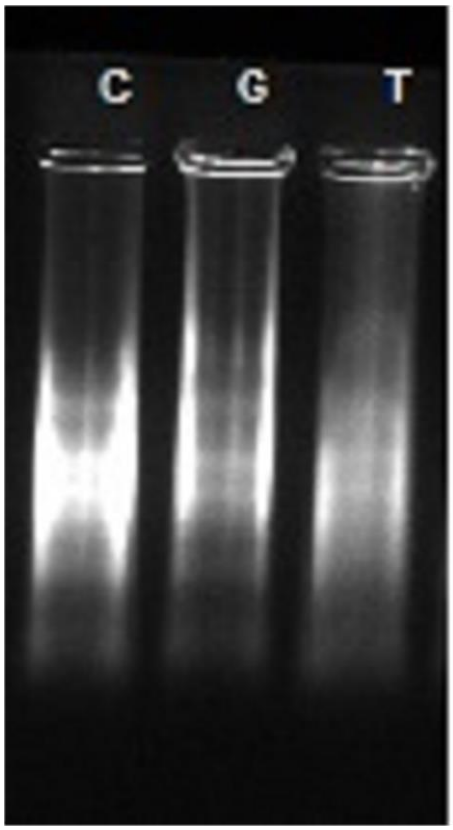

Figure S1 Electrophoresis of RNAs isolated by CTAB, GNTC, TriZol method. C, CTAB; G, GNTC; T, TriZol.

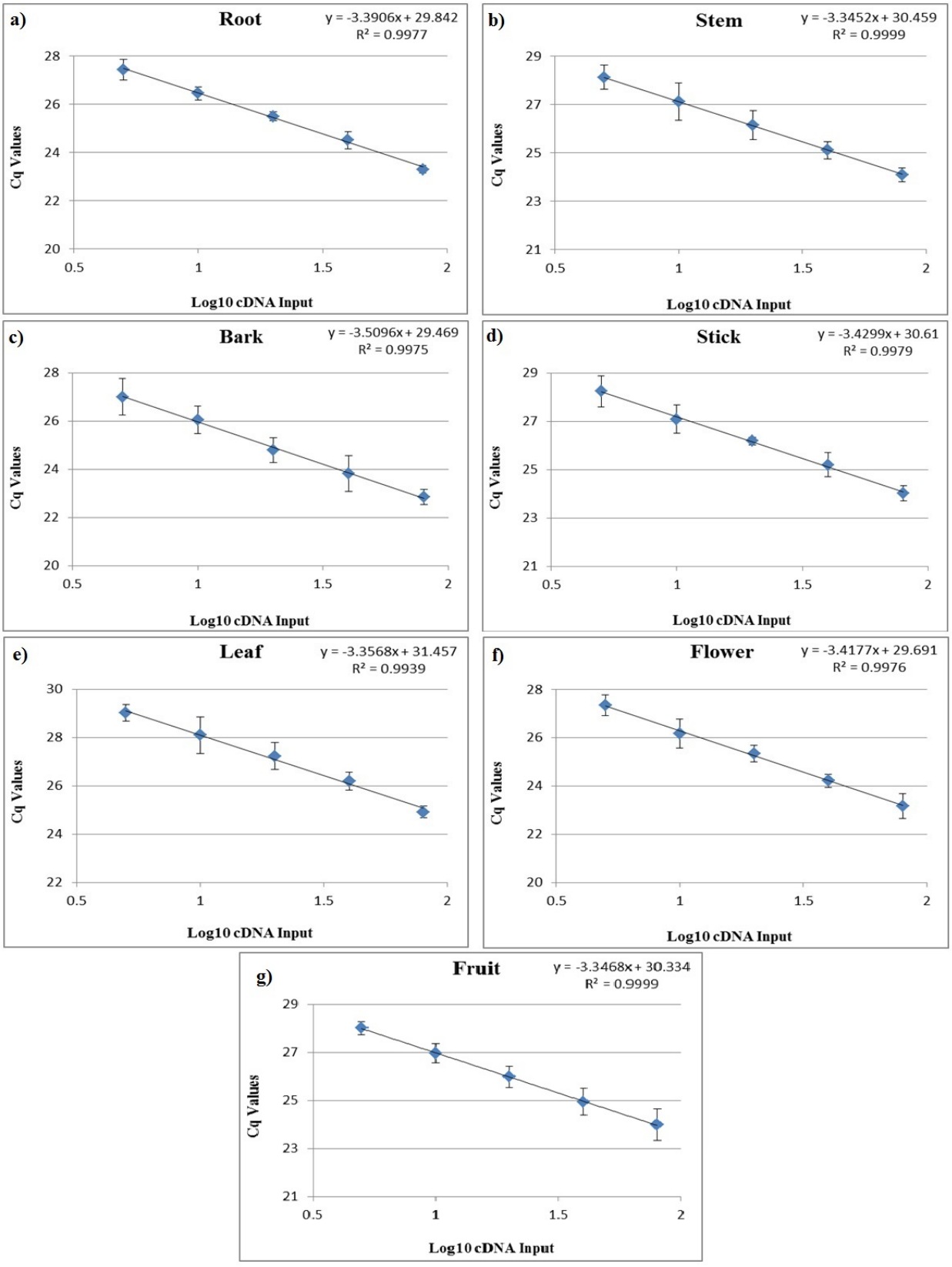

Figure S2 PCR efficiency analysis in qRT-PCR. . a, Root; b, Stem; c, Bark; d, Stick; e, Leaf; f, Flower and g, Fruit.

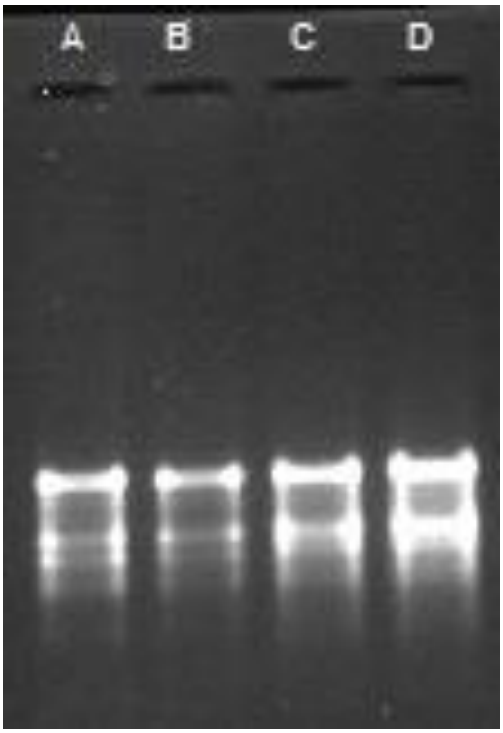

Figure S3 Electrophoresis of RNAs isolated by the modified CTAB method. Total RNA isolated from leaves of different malvaceous plants. A, *Hibiscus cannabinnas*; B, *Hibiscus sabdariffa*; C, *Hibiscus rosa-sinensis*; D, *Abelmoschus esculentus.*

Vol. 18(27), pp. 659-663, July, 2019
DOI: 10.5897/AJB2019.16792
Article Number: 6D45ABF61454
ISSN: 1684-5315

http://www.academicjournals.org/AJB

ACADEMIC JOURNALS
expand your knowledge

African Journal of Biotechnology

Review

DNA barcoding of Ghanaian fish species: Status and prospects

Gyamfua Afriyie[1], Shunkai Huang[1], Zhongdian Dong[1], Yusong Guo[1], Felix K. A. Kuebutornye[2,3], Christian Ayisi Larbi[4], Berchie Asiedu[5] and Zhongduo Wang[1*]

[1]Key Laboratory of Aquaculture in South China Sea for Aquatic Economic Animal of Guangdong Higher Education Institutes, Fisheries College, Guangdong Ocean University, Zhanjiang 524025, China.
[2]Guangdong Provincial Key Laboratory of Pathogenic Biology and Epidemiology for Aquatic Animals, College of Fishery, Guangdong Ocean University, Zhanjiang 524088, China.
[3]Guangdong Key Laboratory of Control for Diseases of Aquatic Economic Animals, Zhanjiang 524088, China.
[4]Department of fisheries and Aquatic Resources Management, University for Development Studies, Tamale, Ghana.
[5]Department of Fisheries and Water Resources, University of Energy and Natural Resources, Sunyani, Ghana.

Received 6 March, 2019; Accepted 30 April, 2019

Ghana's waters are biologically diverse with different fish species due to different ecological habitats and niches harboring several cryptic fish species. However, the fish production has reduced over the past decade; hence an urgent conservation and management strategies are required to save Ghanaian fishery such as accurate identification of species to formulate species-specific conservation and management strategies. Molecular method of fish identification, DNA barcoding, has proven its efficacy in species identification for both freshwater and marine species. In recent years, DNA barcoding has been accepted as a bio-identification system for living organisms globally. This system is fast and produces accurate species identification by using a short DNA sequence marker from a standard region of the DNA sequence of an organism's genome to identify it as belonging to a particular individual or species based on Cytochrome C Oxidase type I (COI/ Cox 1) gene instead of the whole genome. Unfortunately, unlike the developed countries, this molecular method of fish identification is new in Ghana. This review article aims to examine the issues regarding fish identification and the need for DNA barcoding as a tool for taxonomic identification, grouping, and naming of fish species in Ghana. Also, this review takes a look at the current status and future direction of DNA barcoding fisheries in Ghana. In addition, the benefits of DNA Barcoding in fishery management and conservation are discussed.

Key words: DNA barcoding, Ghana, marine species, current status, management, conservation.

INTRODUCTION

Aquatic organisms are the largest and most diverse class of invertebrate and vertebrate species. Recently, the estimated species exceeds 30,000 (Eschmeyer et al., 2010) with an annual description of about 300 new

*Corresponding author. E-mail: aduofa@hotmail.com.

species (Weigt et al., 2012). Hence, taxonomic ambiguity exists for several fish genera and identification (Lakra et al., 2016). The basic research that helps characterize their taxonomic diversity is important for the conservation of these taxa and for improvement of their management and conservation strategies (Wang et al., 2010). Fortunately, they are among the easiest groups of organisms for which to generate DNA barcode data (Weigt et al., 2012).

DNA-based approaches (DNA Barcoding) for taxon diagnosis exploiting DNA sequence diversity among species can be used to identify fishes and resolve taxonomic ambiguity including the identification of new species (Hebert et al., 2003). DNA barcoding is a taxonomic method that uses a short genetic marker from a standard region of the DNA sequence of an organism's genome to identify it as belonging to a particular individual or species (Hebert et al., 2003). This short fragment of mitochondrial (650 base pairs) cytochrome c oxidase subunit I (COI) is used to identify the teleost that has been previously described morphologically (Barros-Garcia et al., 2016). The short fragment (DNA sequence) is made of four nucleotide bases A (Adenine), T (Thymine), C (Cytosine) and G (Guanine) (Kaur, 2015). Apart from facilitating species identification, other benefits of DNA barcoding include highlighting cases of range expansion for known species, flagging previously overlooked species and enabling identifications where traditional methods cannot be applied (Ward et al., 2009).

Previously, Polymerase Chain Reaction (PCR) and hybridization methods such as Random Amplification of Polymorphic DNA (RAPD), probe hybridization, gene-specific primers and PCR- Restriction Fragment Length Polymorphism (RFLP) were used for species identification (Teletchea, 2009). However, these methods of identification lacked a database for reference and universal primer (Vartak et al., 2014). Hebert et al., (2003) proposed that a single gene sequence would be sufficient to differentiate all, or at least the vast majority of animal species, and proposed the use of the mitochondrial DNA gene cytochrome oxidase subunit I (cox1/ COI) as a global bio-identification system for animals. This method has proven its efficacy in fish species identification, both freshwater and marine species. However, due to the lack of reference sequences, there is still a long way to go before we could identify every matured fish, larva, egg or organ by their barcode sequences (Wang et al., 2012).

Ghana's waters, both marine and freshwater serve as habitat for diverse fish species (Dankwa et al., 1999; http://www.fishbase.org). However, the management of these species is challenged by inadequate information on the specific species available which subsequently affects management policies (Ministry of Fisheries and Aquaculture Development (MoFAD), 2015). Traditional method of fish identification based on the morphology is the technique applied in fish identification in Ghana (Dankwa et al., 1999). This review aimed to provide an overview and potentials of Ghana's fishery sector and to access the current and future state of DNA barcoding as a fish identification tool for Ghanaian fish species with a secondary aim to establish a DNA barcode reference library for utilization in biodiversity assessment and conservation for the entire country.

GHANAIAN FISHERY SECTOR

Ghana is a country located in West Africa on the GPS coordinates of latitude: 7° 57' 9.97" N Longitude: -1° 01' 50.56" W (https://latitude.to/map/gh/ghana). The southern part of the country is bordered with the Gulf of Guinea and Atlantic Ocean. The Volta Lake, an artificial lake, is also located in the heart of the country (van Zwieten and Kolding, 2011). These waters, as well as other minor water bodies within the country, serve as sources for capture fisheries.

Based on observation, almost all Ghanaians diets include fish as a source of proteins and micronutrients. Additionally, the fishery sector plays a substantial role in contributing significantly to national economic development objectives related to employment, livelihood support, poverty reduction, food security, foreign exchange earnings and resource sustainability development of Ghana (MoFAD, 2015). The capture fishery industry is based on resources from the freshwater (inland), marine and estuaries (coastal lagoons) sources. According to the MoFAD (2017) report, fish production was about 87.2% for capture fisheries (marine: 71.1% and in-land: 16.1%) and 12.8% for aquaculture. Marine fishery contributes significantly to Ghana's economy, accounting for about 4.5% of the Gross Domestic Product (GDP), 12% of the agriculture GDP and 10% of the workforce (Chauvin et al., 2012). Aquaculture, on the other hand, is still growing as compared to other countries. The capture fisheries sector in Ghana is limited by a number of factors such as seasonal fluctuations of fish abundance; implying that income from fishing is also unstable, poor landing sites, post-harvest losses, poor equipment base and a lack of refrigeration facilities (Gordon et al., 2013), and climate change (Mohammed and Uraguchi, 2013). Other principal concerns are fish stocks overexploitation, leading to the decline of harvests and inadequate information about fish identification, fish biology leading to the formulation of poor conservation and management strategies (Zemlak et al., 2009). Moreover, there is no detailed knowledge about the abundance, diversity, and distribution of fish species in wild Ghanaian waters.

Ghana's waters are biologically diverse environment with different ecological habitats and niches which harbor several different fish species. For marine ecosystem, species are broadly classified in four classes based on

their bathymetric distribution: small pelagic-*Sardinella aurita, Engraulis encrasicolus, Ethmalosa frimbiata*; large pelagic species-*Katsuwonus pelamis, Auxis thazard, Thunnus obesus*; coastal demersal species-*Dantex* species*, Pagellus bellottii, Pagrus ehrenbergi*; and deep-water demersal species-*Sepia officinalis, Epinephelus* species (Ago and Ofori-Adu, 2005). The main commercial species targeted in Ghanaian waters are Clupeid (Sardinellas, Scombridae - chub - mackerels and Engraulidae (anchovies). The large pelagic species represent the Thunidae whereas the demersal species are: Sparidae, Lutjanidae, Mullidae, Pomadasydae, Serranidae, Polynidae and Penaeidae (Mensah et al., 2003).

Within the in-land sector, Volta Lake is the major source of freshwater fish. Other sources are Black Volta River, White Volta River, Lake Bosomtwe, Barekese Reservoir (MoFAD, 2015) and minor water bodies. Common species among the landings are various Tilapia species and *Clarias* species among others. In a study conducted by Dankwa et al. (1999), the Volta Lake hosts about 121 fish species. Common freshwater species landed from the lake are various species of *Tilapia, Chrysichtys, Synodontis, Mormyrids, Heterotis, Clarias, Bagrus, Brychinus, Barbus, Alestes, Labeo, Parailia, Schilbe, Sarotherodon, Distichodus,* and *Citharinus* species and the Nile perch (*Lates niloticus*) (Dankwa et al., 1999). According to FishBase (http://www.fishbase.org), about 491 marine species and 212 freshwater species have been discovered and identified within Ghana waters as at December 2018. Majority of these species are native while few others migrated from neighboring countries.

Irrespective of the many benefits derived from the Ghanaian capture fishery, anthropogenic activities pose a serious threat to its sustainability. This is evidenced by pollution of water bodies, reclamation wetlands due to urbanization, the reduction in catches over the years and the extinction of some species as reported by the local fishers (MoFAD, 2015). Also, taxonomic knowledge is still incomplete and scattered in the scientific literature (Hubert et al., 2015). Therefore, development of new tools such as molecular genetics (DNA barcoding) for species identification is urgently needed to improve the sustainability of the exploitation of the ichthyofauna within Ghana's waters.

SPECIES RECOGNITION, IDENTIFICATION, AND FAMILY GROUPING

Essential for the sustainable development of fish biodiversity for Ghanaians is to generate accurate knowledge of the identity, evolution, and the geographic distribution (Berkes et al., 2000) of Ghana's fish species. Unfortunately, such important information is often only partially or not available for taxonomists and other stakeholders. Ghana's waters are endowed with several species including cryptic species. The documentation and description of these species have significant implications for fishery resource management and conservation. Moreover, cryptic species require special attention in conservation planning, especially for endangered species complex. Because the species that are considered as endangered might be composed of multiple species that are even fewer than previously supposed and different species might require different conservational strategies (Bickford et al., 2007).

DNA barcoding is the system that can provide accurate, fast and automatable species identification by using short and standardized gene regions from a fish species' whole genome (Hebert and Gregory, 2005) using GenBank as a reference.

ISSUES REGARDING FISH IDENTIFICATION IN GHANA AND THE NEED FOR DNA BARCODING

The traditional method of fish identification is based on external morphological features comprising body shape, the pattern of colours, scale size and count, number and relative position of fins, type of fin rays, gill, otoliths and geography (Granadeiro and Silva, 2000). This method of identification has proven not to be effective as it is unable to differentiate a fish species during its egg or larval stages (Zemlak et al., 2009). Even when the undamaged adult sample is available, the morphological characters alone are not enough to identify it sometimes resulting in taxonomic doubt (Lakra et al., 2016). In the event of phenotypic plasticity among fish, morphological based identification may provide a less accurate result (Pavan-Kumar et al., 2016). Moreover, the traditional method does not consider the genetic composition of an organism for the variability of the characters used for species recognition and identification. As a result, species misidentification, an erroneous grouping of different taxa and faulty synonymous taxon names occur. This may lead to paying less attention to species which need immediate conservation strategies. Also, the existing cryptic species are overlooked (Zemlak et al., 2009; Hubert et al., 2012). Furthermore, it results in giving less priority to species which are needed to be conserved and also overlooks morphologically cryptic taxa that are common in many fishes species (Hubert et al., 2008). These associated challenges with the traditional technique of fish identification have resulted in the invention of genetic-based species identification method called DNA barcoding (Mitochondrial DNA).

Grouping of fishes is sustainable in the same species group if their records are not based on inaccurate sub-infra species-level identifications and validation (Halford and Marko, 2004). In a case of large-scale fishery surveys, this issue becomes complicated, many taxonomic experts may be required to identify specimens

from a collection (Ward et al., 2009). In such a situation, it is expensive to assemble and deploy such teams and to distribute specimens for identification. Moreover, it is time-consuming. Also, accessing the historical literature and assessing the validity of species with a controversial taxonomic history are challenging tasks (Ward et al., 2009), even for well-trained taxonomists. For a novice faced with an assemblage of unknown specimens, identification can be challenging and even be close to an impossible task unlike the use of the molecular method. This taxonomic issue generally hinders the assessment, conservation, and management of Ghanaian fish biodiversity.

Again, new species are landed onshore occasionally which require to be identified for scientific study and resource management. This indicates that the application of DNA barcoding is highly required in fisheries sectors for proper species authentication (Rasmussen and Morrissey, 2008).

BENEFITS OF DNA BARCODING IN FISHERY MANAGEMENT AND CONSERVATION

DNA barcoding assists in formulating conservation policies by rapidly assessing the biodiversity at low cost, and this information help prioritize conservation areas or evaluate the success of conservation actions (Krishnamurthy and Francis, 2012). Prioritization of different ecosystems for conservation depends on information of species diversity, its richness and value. Phylogenetic diversity (PD) is an indicator that measures taxonomic divergence between species and an index of phylogenetic diversity can appraise conservation strategies by ignoring tedious species counts and using evolutionary lineages (phylogenies) to boost predictions about biodiversity patterns (Mitchell et al., 2008). Barcoding plays an essential role in terms of phylogenetic (Hajibabaei et al., 2007). Faith and Baker (2010) showed a potential role of DNA barcoding in PD assessments for biodiversity conservation strategies.

CURRENT STATUS AND FUTURE DIRECTION OF DNA BARCODING IN GHANAIAN FISHERIES

With the advent of polymerase chain reaction (PCR) and the reduced cost of DNA barcoding, DNA sequencing has become ubiquitous (Margulies et al., 2005) especially in developed countries. DNA barcoding has gained considerable validation as a key tool for accurate species discovery and identification (Bhattacharya et al., 2015). Moreover, the emergence of different bioinformatics software tools has increased the taxonomic coverage of nucleic acids sequences confined in DNA sequence libraries, also known as GenBank (Bucklin et al., 1999).

Several scientific studies have demonstrated its effectiveness in identifying both marine and freshwater fishes (Eischeid et al., 2016). However, DNA barcoding is still in its new in the third world. Currently, in Ghana, this molecular method of fish identification is in fragments. This can be attributed to the slow pace development in the area of scientific research as a developing country. Again, the lack of resources to carry out such project is another factor hindering molecular method of fish identification. Therefore, Ghanaian waters are fertile grounds for the introduction of DNA barcoding for fish identification and subsequently formulate informed conservation and management strategies to save the deteriorating Ghanaian capture fishery.

As important as DNA barcoding is, there is a need for researchers to consider conducting studies on some of the important fish species in Ghana. For instance, there have been speculations regarding the introduction of tilapia into Ghana believed to have originated from Asia. It will be prudent to conduct studies and characterize the tilapia species in Ghana and generate DNA barcodes for easy identification and comparisons.

CONCLUSION

DNA barcoding has been accepted as a bio-identification system for living organisms globally. It is an essential tool to vouch for species identification and discovery of new species. The COI divergence and species identification success based on DNA barcodes have been previously assessed for many freshwater fish species, for example in Canada (Hubert et al., 2008). This system is fast and produces accurate species identification by using standardized short DNA sequence. It is the simplest way to identify an unknown specimen by comparing its COI sequence generated with the Barcode of Life Database (BOLD) identification engine or data from GenBank (Ward et al., 2009).

Based on successes of studies conducted on DNA barcoding as fish identification, it is the hope to save Ghana's fishery. It has the efficacy to be adopted as a new tool to identify fish to make scientific conservation and management strategies to protect Ghanaian fishery.

ACKNOWLEDGEMENTS

This work was supported by grants from the National Natural Science Foundation of China (31201996, 41806195), Guangdong Talent Project (Yq2013089), and Start-up Fund from GDOU.

CONFLICT OF INTERESTS

The authors have not declared any conflict of interests.

REFERENCES

Ago KE, Ofori-Adu DW (2005). Fishes in the coastal waters of Ghana. Ronna Publisher, pp. 1-112.

Barros-Garcia D, Banon R, Arronte JC, Fernandez L, Garcia R, De Carlos A (2016). DNA barcoding of deep-water notacanthiform fishes (Teleostei, Elopomorpha). Royal Swedish Academy of Sciences 45(3):1-10.

Berkes F, Colding J, Folke C (2000). Rediscovery of Traditional Ecological Knowledge as Adaptive Management. Ecological Applications 10(5):1251-1262.

Bhattacharya M, Sharma AR, Bidhan Chandra Patra BC, Sharma G, Seo EM, Nam JS (2015). DNA barcoding to fishes: current status and future directions. Indian Journal of Marine Sciences, Informa UK Ltd, pp. 1-9.

Bickford D, Lohman JD, Sodhi SN, Ng KLP, Meier R, Winker K, Ingram KK, Das I (2007). Cryptic species as a window on diversity and conservation. Trends in Ecology and Evolution 22(3):148-155.

Bucklin A, Guarnieri M, Hill RS, Bentley AM, Kaartvedt S (1999). Taxonomic and systematic assessment of planktonic copepods using mitochondrial COI sequence variation and competitive, species-specific PCR. Hydrobiologia 401:239-254.

Chauvin DN, Mulangu F, Porto G (2012). Food Production and Consumption Trends in Sub-Saharan Africa: Prospects for the Transformation of the Agricultural Sector. Working Papers 11:76. https://doi: 10.1016/j.foodpol.2013.10.006.

Dankwa HR, Abban EK, Teugels GG (1999). Freshwater fishes of Ghana: identification, distribution, ecological and economic importance. Royal Museum for Central Africa, Vol. 283.

Eischeid AC, Stadig SR, Handy SM, Fry FS, Deeds J (2016). Optimization and evaluation of a method for the generation of DNA barcodes for the identification of crustaceans. LWT- Food Science and Technology 73:357-367.

Eschmeyer W, Fricke R, Fong JD (2010). Marine fish diversity: history of knowledge and discovery (Pisces). *Zootaxa* 2525(1):19-50.

Faith DP, Baker MA (2010). Phylogenetic diversity (PD) and biodiversity conservation : some bioinformatics challenges. Evolutionary Bioinformatics 2:121-128.

Gordon A, Finegold C, Crissman CC, Pulis A (2013). Trade in Sub-Saharan Africa : A Review Analysis. WorldFish, pp. 1-48.

Granadeiro PJ, Silva AM (2000). The use of otoliths and vertebrae in the identification and size-estimation of fish in predator-prey studies. Cybium 24(4):383-393.

Hajibabaei M, Singer GAC, Hebert PDN, Hickey DA (2007). DNA barcoding: how it complements taxonomy, molecular phylogenetics and population genetics. Trends in Genetics 23(4):167-172.

Halford SE, Marko JF (2004). How do site-specific DNA-binding proteins find their targets? Nucleic Acids Research 32(10):3040-3052.

Hebert PDN, Gregory TR (2005). The Promise of DNA Barcoding for Taxonomy. Systematic Biology 54(5):852-859.

Hebert PDN, Ratnasingham S, DeWaard J (2003). The preparation of sterile implants by compression. Pharmaceutisch Weekblad 105(24):681-684.

Hubert N, Hanner R, Holm E, Mandrak EN, Taylor E, Burridge M, Watkinson D, Dumont P, Curry A, Bentzen P, Zhang J, April J, Bernatchez L (2008). Identifying Canadian freshwater fishes through DNA barcodes. PLoS ONE 3(6):1-8.

Hubert N, Meyer CP, Bruggemann HJ, Guerin, F Komeno RJL (2012). Cryptic diversity in Indo-Pacific coral-reef fishes revealed by DNA-barcoding provides new support to the centre-of-overlap hypothesis. PLoS ONE 7(3):28987.

Hubert N, Kadarusman WA, Busson F, Caruso D, Sulandari S, Nafiqoh N, Pouyaud L, Rüber L, Avarre JC, Herder F, Hanner R, Keith P, Hadiaty RK (2015). DNA Barcoding Indonesian freshwater fishes: challenges and prospects. DNA Barcodes 3(1):144-169.

Kaur S (2015). DNA Barcoding and Its Applications. International Journal of Engineering Research and General Science 3(2):602-604.

Krishnamurthy PK, Francis A (2012). A critical review on the utility of DNA barcoding in biodiversity conservation. Biodiversity and Conservation 21(8):1901-1919.

Lakra WS, Singh M, Goswami M, Gopalakrishnan A, Lal KK, Mohindra V, Sarkar UK, Punia PP, Singh KV, Bhatt JP, Ayyappan S (2016). DNA barcoding Indian freshwater fishes. Mitochondrial DNA Part A: DNA Mapping, Sequencing, and Analysis 27(6):4510-4517.

Margulies M, Egholm M, Altman EW, Attiya S, Bader SJ, Bemben AL, Berka J, Braverman SM, Chen YJ, Chen Z, Dewell BS, Du L, Fierro MJ, Gomes VX, Godwin CB, He W, Helgesen S, Ho HC, Begley FR, Rothberg MJ (2005). Genome sequencing in microfabricated high-density picolitre reactors. Nature 437(7057):376-380.

Mensah MA, Koranteng KA, Yeboah D, Bortey A (2003). Study of the impact of Ghana., international trade in fishery products on food security - the case of Ghana.

Mitchell SP, Parkin KR, Kroh ME, Fritz RB, Wyman KS, Pogosova-Agadjanyan LE, Peterson A, Noteboom J, O'Briant CK, Allen A, Lin WD, Urban N, Drescher WC, Knudsen SB, Stirewalt LD, Gentleman R, Vessella LR, Nelson SP, Martin BD, Tewari M (2008). Circulating microRNAs as stable blood-based markers for cancer detection. Proceedings of the National Academy of Sciences 105(30):10513-10518.

Ministry of Fisheries and Aquaculture Development-MoFAD (2015). Fisheries management plan of Ghana; A National Policy for the Management of the Marine Fisheries Sector.

Ministry of Fisheries and Aquaculture Development-MoFAD (2017). Annual Report.

Mohammed EY, Uraguchi ZB (2013). Implications for food security in Sub -Saharan Africa. Nova Science Publishers Inc. pp. 113-135.

Pavan-Kumar A, Gireesh-Babu P, Jaiswar AK, Chaudhari A, Krishna G, Lakra WS (2016). DNA barcoding of marine fishes: Prospects and challenges in DNA Barcoding in Marine Perspectives. Assessment and Conservation of Biodiversity 258-299.

Rasmussen RS, Morrissey TM (2008). DNA Based Methods for the Identification of Commercial Fish and Seafood Species. Comprehensive Reviews in Food Science and Food Safety 7(3):280-295.

Teletchea F (2009). Molecular identification methods of fish species: reassessment and possible applications. Reviews in Fish Biology and Fisheries 19:265-293.

Wang ZD, Guo YS, Liu XM, Fan YB, Liu CW (2012). DNA barcoding South China Sea fishes. Mitochondrial DNA 23(5):405-410.

Wang ZD, Guo YS, Tan W, Lu L I, Tang E (2010). DNA barcoding , phylogenetic relationships and speciation of snappers (genus DNA barcoding , phylogenetic relationships and speciation of snappers (genus Lutjanus). Science China Life Sciences 53(8):1025-1030.

Ward DR, Hanner V, Hebert PD (2009). The campaign to DNA barcode all fishes, FISH-BOL. Journal of Fish Biology 74(2):329-356.

Weigt LA, Driskell AC, Baldwin CC, Ormos A (2012). DNA barcoding fishes'. Methods in Molecular Biology (Clifton, N.J.) 858:109-126.

van Zwieten PAM, Kolding J (2011). The cases of Lake Nasser. Lake Volta and Indo-Gangetic Basin reservoirs', (February 2015).

Vartak VR, Narasimmalu R, Annam PK, Singh DP, Lakra WS (2014). DNA barcoding detected improper labelling and supersession of crab food served by restaurants in India. Journal of the Science of Food and Agriculture 95(2):359-366

Zemlak TS, Ward RD, Connell AD, Holmes BH, Hebert PDN (2009). DNA barcoding reveals overlooked marine fishes. Molecular Ecology Resources 9(s1):237-242.

Vol. 18(27), pp. 664-669, July, 2019
DOI: 10.5897/AJB2019.16827
Article Number: 2EFF37A61507
ISSN: 1684-5315

http://www.academicjournals.org/AJB

ACADEMIC JOURNALS
expand your knowledge

African Journal of Biotechnology

Full Length Research Paper

Genomic sequencing and recombinant expression of proinsulin isolated from cow and buffalo in Pakistan

Farheen Aslam[1*], Hooria Younas[2] and Saima Iftikhar Bajwa[2]

[1]Department of Biotechnology, Lahore College for Women University, Lahore, Pakistan.
[2]School of Biological Sciences, University of the Punjab, Lahore, Pakistan.

Received 8 April, 2019; Accepted 16 May, 2019

This study was conducted to determine the heterologous expression of eukaryotic gene in *Escherichia coli* variable. The expression of Pakistani buffalo (*Bubalus bubalis*) and cow (*Bos taurus*) proinsulin genes in BL21 codon plus cells is 30% of total cellular protein. Total RNA was isolated from pancreatic tissues of local (Pakistani) breeds of buffalo (*B. bubalis*) and cow (*B. taurus*), converted to cDNA and cloned in a T/A cloning vector. There are five silent mutations: one in B-chain, two each in A-chain and C-peptide encoding regions of local Pakistani buffalo proinsulin DNA sequence as compared to the internationally reported cow proinsulin sequence. The DNA sequence of local (Pakistani) cow proinsulin shows there is one nucleotide encodes C-peptide that has mismatch with the reported cow proinsulin sequence but mismatched nucleotide is same between Pakistani cow and Pakistani buffalo proinsulin sequence. This indicates the genetic similarity of Pakistani cow with Pakistani buffalo. Both genes were expressed in BL21 Codon plus (DE3)-RIL cells with 0.2 mM IPTG at 37°C for 6 to 8 h. Proinsulin was expressed as 30% of total cellular proteins as insoluble inclusion bodies.

Key words: *Bubalus bubalis*, *Bos taurus*, cDNA, T/A cloning vector, BL21 Codon plus (DE3)-RIL cells.

INTRODUCTION

Insulin is synthesized as a larger precursor, preproinsulin (Chan et al., 1976), in pancreatic β-cells, which is rapidly cleaved to proinsulin (Patzelt et al., 1978). The proinsulin contains C-peptide connecting the C-terminus of B-chain with the N-terminus of A-chain. The insulin molecule served as a model for studies on the fundamental structure and properties of proteins. Originally, insulin used clinically was derived from cow and pigs because of their close resemblance with the human insulin. Knowing the sequence of bovine insulin (cow and buffalo) of the local breed was important to know the evolutionary aspect behind the two species residing in the same area.

The sequence of cow (*Bos taurus*) preproinsulin was already reported in the literature (accession no. M54979). The sequence of buffalo (*Bubalus bubalis*) proinsulin was not available in the literature because of specific localization of this species in the Indo-Pak region. 97% of the world population of *B. bubalis* resides in Asia with half of the population in the Indian subcontinent (India and Pakistan). Sequencing of the buffalo proinsulin showed

*Corresponding author. E-mail: farheenpu@gmail.com. Tel: +92-42-99203801-9/277.

Table 1. Names, sequences, length, melting temperatures and restriction sites representation in the primers.

Primer name	Primer sequence (5' - 3')	Length	*TM (°C)	Restriction sites
WBI-N (Forward)	GAACATATGTTCGTCAACCAGCATCTGTGTGGC	33	66.6	NdeI
WBI-C (Reverse)	ATCTAGAAGCTTGTCGGGGCAGGCCTAGTTACAG	34	69.0	HindIII

The restriction sites are shown with red color. *TM: Melting temperature.

that there are five nucleotides which cause five silent mutations in the buffalo DNA proinsulin sequence as compared to the sequence reported for cow proinsulin (Younas, 2009). In order to evaluate these differences, the cloning and sequencing of buffalo proinsulin was carried out along with that of the cow prohormone using animals from the same location, Lahore. For this study, total RNA was isolated from buffalo and cow pancreas and converted to cDNA, by using WBI-C as reverse primer. cDNA was then amplified by using WB1-N and WB1-C as forward and reverse primers, respectively. The proinsulin genes from the two species were successfully cloned in pTZ57R/T vector and sequenced.

MATERIALS AND METHODS

The strains used for the cloning and expression of the constructs were *Escherichia coli* DH5α, BL21 Codon plus (DE3)-RIL cells of *E. coli*. All the reagents and chemical were from Sigma, Across and Fisher. Two primers WB1-N and WB1-C (Table 1) were designed with Amplify 1.0 (Bill Engels © 1992, University of Wisconsin, Genetics, Madison, W1 53706) and prepared by GeneLink™.

Isolation of total RNA

The pancreatic tissues of freshly slaughtered buffalo (*B. bubalis*) and cow (*B. taurus*) were cut to a size of approximately 1 cm^2 and total cellular RNA was extracted by acid phenol-guanidinium thiocyanate-chloroform extraction method developed by Sambrook and Russell (2001). Total RNA was visualized on 1.8% agarose gel containing formaldehyde.

RT-PCR of buffalo and cow proinsulin genes

The mRNA of buffalo and cow proinsulin genes were converted to cDNA by using reverse primer WB1-C. In a reaction mixture containing 4.2 µg of total RNA of buffalo or 25.2 and 58.8 µg of cow, 100 pmoles of reverse primer WB1-C was added. The reaction mixture was incubated at 75°C for 5 min, followed by rapid chilling on ice. To the later was added 4 µl of 5X reverse transcriptase buffer, 0.5 mM dNTPs and the mixture was incubated at 37°C for 5 min. Following the addition of 200 units of RevertAid TM M-MuLV reverse transcriptase, the mixture was incubated at 42°C for 60 min and then heated at 70°C for 10 min and chilled on the ice. The cDNA of buffalo was amplified by PCR. The reaction mixture was incubated at 94°C for 3 min then denatured at 94°C for 30 s, annealing at 57°C for 30 s and polymerization at 72°C for 30 s with final incubation at 72°C for 5 min. The PCR products were extracted from the agarose gel by using DNA extraction kit of Fermentas.

Cloning of cow and buffalo proinsulin genes in pTZ57R/T vector

Ligation of the desired PCR product to pTZ57R/T vector was done by using InsTAclone™ PCR cloning kit. The ligated products were used to transform competent cells of *E. coli*. Transformed cells appeared as white colonies whereas non transformed cells appeared as blue colonies. Mini-preparation of plasmid was done by the alkaline lysis method (Bimboim and Doly, 1979). The minipreped samples were restricted with *Nde*1 and *Hind*III to confirm the right sized clones.

Sequence analysis

The sequencing was done by dideoxy chain termination method on Beckman Coulter CEQ™ 8000 DNA sequencer and on applied biosystems 310 DNA sequencer. Gene of interest in pTZ57R/T vector was sequenced through M13 forward and reverse primers. Sequence was aligned on DNA data bank Japan (DDBJ) sequence analysis software ClustalW.

Cloning of cow and buffalo proinsulin genes in pET21a vector

The 264 bp fragment of cow and buffalo proinsulin genes after restriction with *Nde*1 and *Hind*III was ligated to pET21a vector and used to transform BL21 Codon plus (DE3)-RIL cells. The culture was allowed to grow at 37°C for 3 h until the O.D. at 600 nm reached 0.6 to 0.7. Then, 0.2 mM IPTG was added and allowed to grow at 37°C for 6 to 8 h. 1 ml culture of each construct was centrifuged at 5000 rpm for 5 min, the pellet washed with 1 ml of 20 mM Tris pH 8.0 and resuspended in 100 µl of 20 mM Tris pH 8.0. 10 to 20 µl of the resuspended cells mixed with 20 µl of 2X SDS gel loading buffer (100 mM Tris-Cl, pH 6.8, 200 mM DTT, 4% SDS, 0.2% bromophenol blue, 20% glycerol). The induced and uninduced samples were analyzed on 18% SDS-PAGE.

RESULTS AND DISCUSSION

Total cellular RNA was isolated from three different freshly slaughtered pancreatic tissues of buffalo (*B. bubalis*) and two from cow (*B. taurus*) by acid phenol-guanidinium thiocyanate-chloroform extraction method (Chomczynski and Sacchi, 1987), in which guanidinium thiocyanate homogenate is extracted with phenol: chloroform at low pH. The A_{260}/A_{280} ratio of the extracted RNA was 1.2 to 1.27. Of the total cellular RNA, 80 to 85% comprises ribosomal RNA. The analysis of the samples (Figure 1) on agarose gel containing 2.2 M formaldehyde clearly showed two bands of 28S rRNA and 18S rRNA.

Messanger RNA was converted to cDNA using

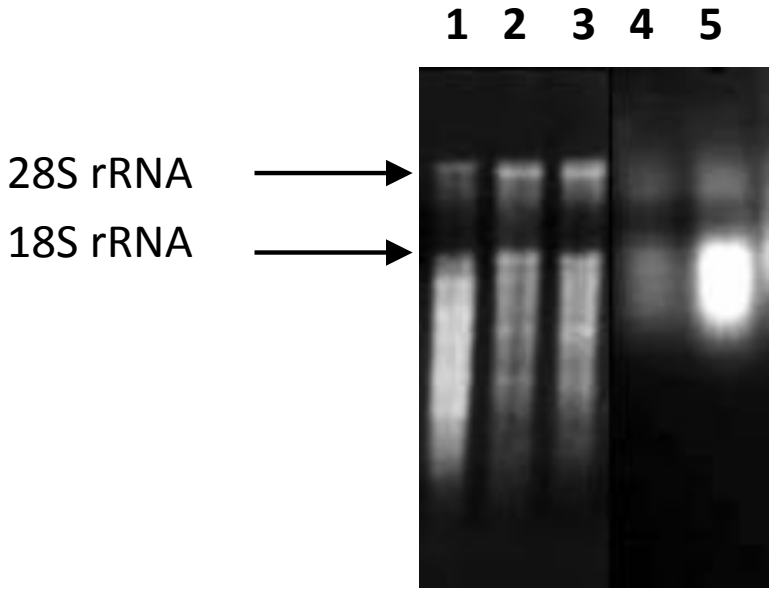

Figure 1. Agarose gel containing 2.2 M formaldehyde after 2 h, showing 28S rRNA (4.8 kb) and 18S rRNA (1.8 kb). Lanes 1, 2, 3: total RNA isolated from three different buffalo pancreatic tissues; Lanes 4, 5: total RNA isolated from cow pancreatic tissues.

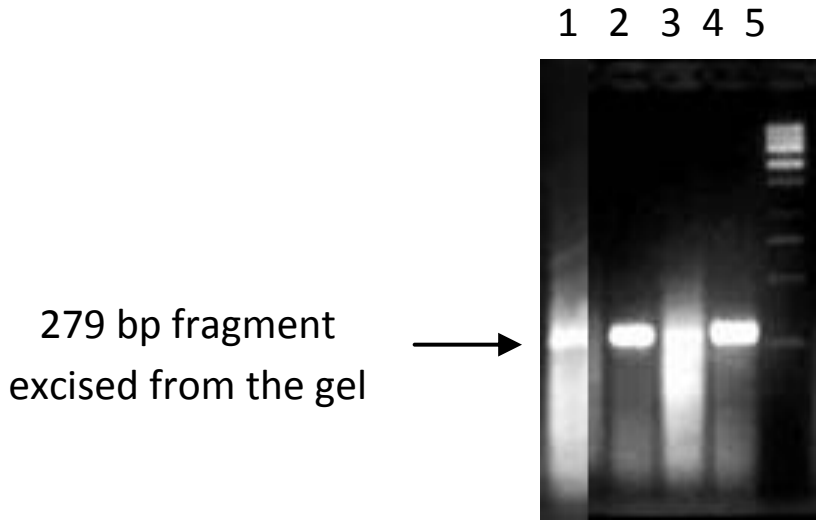

Figure 2. 2% agarose gel of RT-PCR of buffalo and cow proinsulin genes. Lane 1: RT-PCR of buffalo; Lanes 2, 3, 4: RT-PCR of cow; Lane 5: 1 kb DNA ladder (250-10000 bp).

Leukemia Virus reverse transcriptase and WB1-C primer having a *Hind*III site. cDNA was amplified by conventional PCR reaction using WB1-N as forward and WB1-C as reverse primer (Figure 2).

279 bp fragment after RT-PCR of buffalo and cow proinsulin gene was ligated to pTZ57R/T vector and used to transform DH5α cells. Figure 3 shows restriction of plasmid with *Nde*I and *Hind*III.

Buffalo and cow proinsulin genes were sequenced with M13 forward as well as with M13 reverse primer. For the cow DNA sequence (Figure 5), it was found that in the C-peptide 7th amino acid, proline, is encoded by “CCC” in the case of Pakistani cow (*B. taurus*) which is the same codon “CCC” as present in Pakistani buffalo (*B. bubalis*).

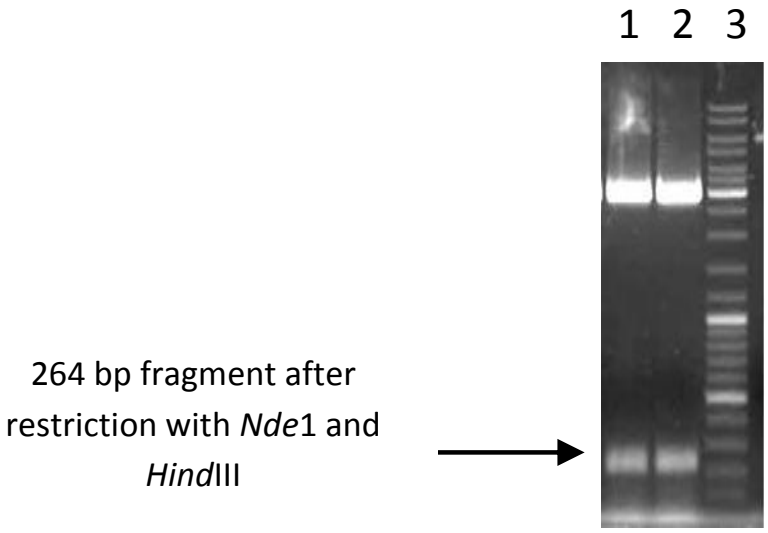

Figure 3. Agarose gel after *Nde*1 and *Hind*III restriction of plasmid from three selected colonies. Lane 1: selected plasmid harboring buffalo proinsulin gene; Lane 2: selected plasmid harboring cow proinsulin gene; Lane 3: DNA ladder (100-10000 bp).

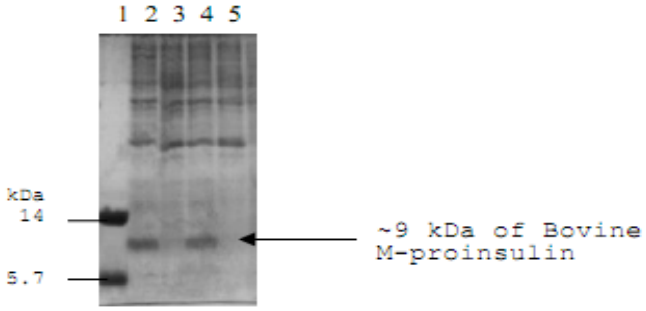

Figure 4. SDS-PAGE analysis of buffalo and cow M-proinsulin expressed in BL21 Codon plus (DE3)-RIL cells. Lanes 2 and 4: induced *E. coli* cells harboring cow proinsulin gene and buffalo proinsulin genes respectively; Lanes 3 and 5: their uninduced counterparts; Lane 1: protein marker, lysozyme (14 kDa) and bovine insulin (5.7 kDa).

However, it is “CCG” in the case of the sequence reported in the database for cow (*B. taurus*). This silent mutation in the proinsulin DNA sequence, indicates the genetic similarity of Pakistani cow with Pakistani buffalo. There is a study which suggests that cows and buffalos are derived from same ancestors (Abdel-Rahman, 2006).

It was found that in buffalo proinsulin sequence, compared to the published cow sequence, there was one mutation in the DNA encoding the B-chain, two in the C-peptide and two in the A-chain encoding regions. The sequence of buffalo proinsulin was submitted to GeneBank (DDBJ/EMBL) with an accession number of AB234871 (Olmos et al., 1994) and the sequence of Pakistani cow proinsulin with an accession number of JX041514 (Aslam et al., 2013).

Many attempts have been made to express insulin and proinsulin in bacterial system using recombinant DNA technology (Olmos et al., 1994).

The buffalo M-proinsulin and cow M-proinsulin were expressed in BL21 Codon plus (DE3)-RIL cells, which were induced with 0.2 mM IPTG. Bacterial cells harboring buffalo and cow proinsulin genes expressed similar amounts of M-proinsulin, that is, approximately 30% of the total cellular proteins (Figure 4).

Insulin used clinically was derived from cow and pigs because of their close resemblance with the human insulin. Knowing the sequence of bovine insulin (cow and buffalo) of the local breed was important to know the

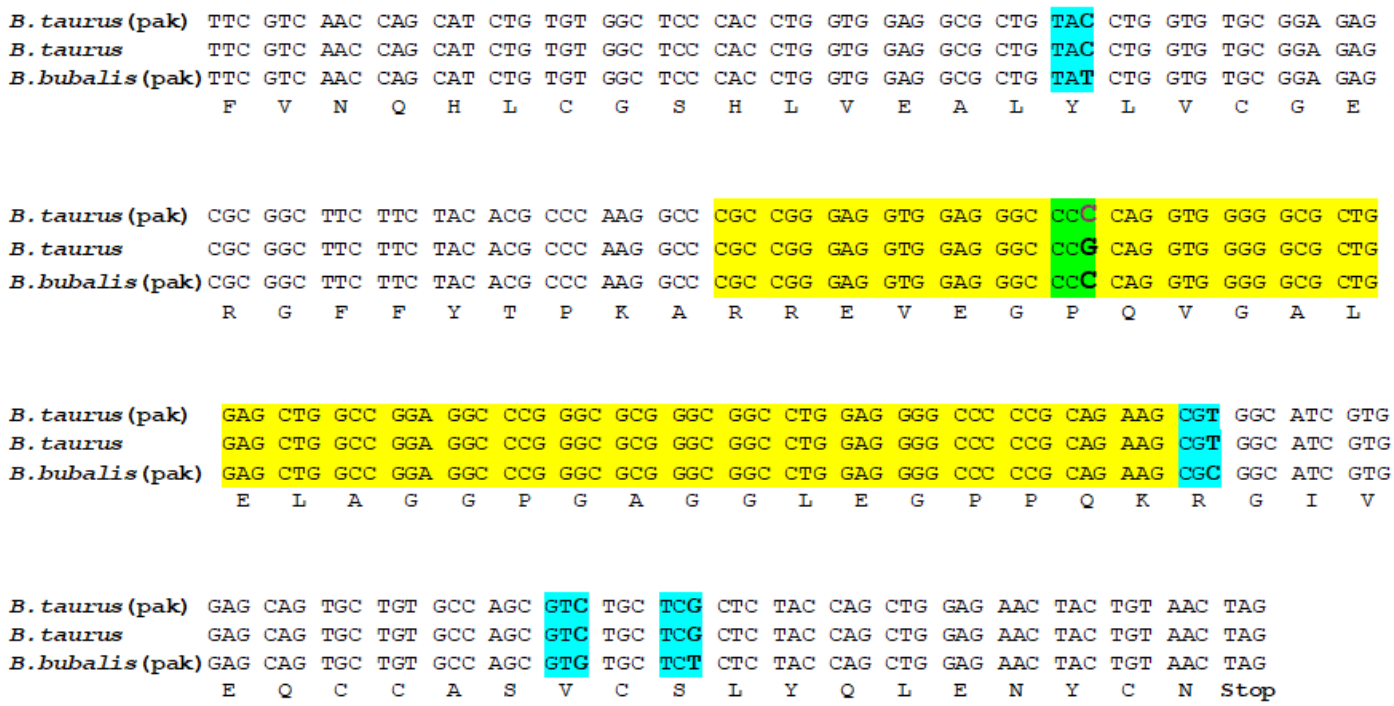

Figure 5. Sequence alignment of Pakistani cow (*B. taurus* pak) with international cow (*B. taurus*) and pakistani buffalo (*B. bubalis* pak). Alignment represents five silent mutations between Pakistani buffalo and international cow, as highlighted in blue and green but Pakistani cow differs at only one nucleotide from international cow at proinsulin level, as highlighted in green.

evolutionary aspect behind the two species residing in the same area. Total RNA was isolated from pancreatic tissues of local (Pakistani) breeds of buffalo (*B. bubalis*) and cow (*B. taurus*), converted to cDNA and cloned in a T/A cloning vector. It was interesting to know that there are five silent mutations: one in B-chain, two each in A-chain and C-peptide encoding regions (Figure 5) of local Pakistani buffalo proinsulin DNA sequence as compared to the internationally reported cow proinsulin sequence. The sequence of *B. bubalis* proinsulin was reported for the first time and was submitted to GeneBank (DDBJ/EMBL) with an accession number of AB234871 (Olmos et al., 1994). The DNA sequence of local (Pakistani) cow proinsulin shows there is one nucleotide encodes C-peptide that has mismatch with the reported cow proinsulin sequence but mismatched nucleotide is same between Pakistani cow and Pakistani buffalo proinsulin sequence. This indicates the genetic similarity of Pakistani cow with Pakistani buffalo. There is a study which suggests that cows and buffalos are derived from same ancestors (Abdel-Rahman, 2006).

Many attempts have been made to express insulin and proinsulin in bacterial system using recombinant DNA technology (Olmos et al., 1994; Aslam et al., 2013). Buffalo and cow M-proinsulin were successfully expressed in BL21 Codon plus (DE3)-RIL cells and produced 30% of total cellular protein which is comparable with the protein expression of different constructs of human proinsulin in BL21 Codon plus cells (Aslam et al., 2013)

CONFLICT OF INTERESTS

The authors have not declared any conflict of interests.

REFERENCES

Abdel-Rahman S (2006). Evidences reveal that cattle and buffalo evolutionary derived from the same ancestor based on cytogenetic and molecular markers. Biotechnology in Animal Husbandry 22(3-4):1-9.

Aslam F, Gardner Q-tAA, Zain H, Nadeem MS, Ali M, Rashid N, Akhtar M (2013). Studies on the expression and processing of human proinsulin derivatives encoded by different DNA constructs. Biochimica et Biophysica Acta (BBA)-Proteins and Proteomics 1834(10):2116-23.

Bimboim H, Doly J (1979). A rapid alkaline extraction procedure for screening recombinant plasmid DNA. Nucleic acids Research 7(6):1513-23.

Bolivar F (1994). Production in Escherichia coli of a rat chimeric proinsulin polypeptide carrying human A and B chains and its preparative chromatography. Journal of biotechnology 38(1):89-96.

Chan SJ, Keim P, Steiner DF (1976). Cell-free synthesis of rat preproinsulins: characterization and partial amino acid sequence determination. Proceedings of the National Academy of Sciences 73(6):1964-8.

Chomczynski P, Sacchi N (1987). Single-step method of RNA isolation by acid guanidinium thiocyanate-phenol-chloroform extraction. Analytical biochemistry 162(1):156-159.

Olmos J, Cruz N, Sánchez M, López M, Balbás P, Gosset G, Valle F, Patzelt C, Labrecque AD, Duguid JR, Carroll RJ, Keim PS, Heinrikson RL, Steiner DF (1978). Detection and kinetic behavior of preproinsulin in pancreatic islets. Proceedings of the National Academy of Sciences 75(3):1260-1264.

Sambrook J, Russell D (2001). Molecular Cloning: A Laboratory Manual. 3rd Ed New York: Cold Spring Harbor Laboratory Press.

Younas H (2009). Studies on recombinant buffalo (*Bubalus bubalis*) proinsulin and its derivatives (Doctoral dissertation, University of Punjab, Lahore).

Vol. 18(27), pp. 670-688, July, 2019
DOI: 10.5897/AJB2019.16827
Article Number: 1768D5461509
ISSN: 1684-5315

http://www.academicjournals.org/AJB

ACADEMIC JOURNALS
expand your knowledge

African Journal of Biotechnology

Full Length Research Paper

Optimization studies of chitin and chitosan production from *Penaeus notialis* shell waste

Amoo K. O., Olafadehan O. A.* and Ajayi T. O.

Department of Chemical and Petroleum Engineering, University of Lagos, Akoka-Yaba, Lagos State 101017, Nigeria.

Received 14 May, 2019; Accepted 26 June, 2019

Optimization studies of extraction of chitin and chitosan from pink shrimp (*Penaeus notialis*) shell waste and of the degree of deacetylation (*DDA*) of extracted chitosan were investigated via the Box-Behnken design of experiments using response surface methodology. Robust quadratic models for predicting the extraction yields of chitin and chitosan and *DDA* of chitosan were obtained. These models were verified by determining their eigenvalues and determinants, thereby revealing the nature of the optimum points and Hessian matrices. The respective modelled optimization conditions for the maximum yields of chitin and chitosan and for the highest *DDA* of chitosan were obtained thus: (3.25 M HCl solution, 19.03 h demineralization time, 2.43 M NaOH solution, and 2.03 h deproteinization time), (50% w/w NaOH solution, 87.9°C deacetylation temperature, and 145.26 min deacetylation time) and (50% w/w NaOH solution, 97.2°C deacetylation temperature, and 90 min deacetylation time). Excellent agreements were achieved between the experimental responses (extraction yields of chitin and chitosan, and *DDA* of extracted chitosan) and their predicted values with % error <5 in all cases.

Key words: Chitin, deproteinization, deacetylation, chitosan, optimization, response surface methodology.

INTRODUCTION

Shrimps are one of the most important seafood worldwide. Industrially, about 45-55% of raw shrimp weight is generated as shell waste during shrimp processing, clean-up and packaging (Hossain and Iqbal, 2014; Lertsutthiwong et al., 2002). These biological wastes can be used to produce value-added products (such as chitin and chitosan) instead of causing major environmental concerns such as air and water pollution (Nouri and Khodaiyan, 2014a, b). On a dry basis, shrimp shell waste contains 30 to 40% w/w protein, 30 to 50% w/w calcium (II) trioxocarbonate (IV) ($CaCO_3$) and 10 to 30% w/w chitin (Hajji et al., 2014; Nithya et al., 2014).

The second most abundant natural bio-polymer after cellulose is chitin, β- (1 → 4) N- acetyl-D-glucosamine, and is one of the chief components of the exoskeleton of crustaceans (crabs, shrimps, krill, barnacles, lobsters, etc.), insects and fungal cell walls. On partial deacetylation of chitin, the cationic amino biopolymer obtained is chitosan, β- (1 → 4) D-glucosamine (Ibitoye et al., 2018). Due to the compact structure of solid state of chitin, it remains insoluble in most solvents and dilute acids. This then usually leads to carrying out a chemical deacetylation of chitin to solve the problem of insolubility and produce the most common derivative (chitosan)

*Corresponding author. E-mail: nsadeghi@sina.tums.ac.ir. Tel: +98-21-66954713. Fax: +098-21-66461178.

(Hajji et al., 2014; Roberts, 1992). Chitin and its derivative, chitosan, can be distinguished mainly by the amount or percentage of the acetyl-glucosamine group present in the bio-polymer. In a case where the acetyl-glucosamine group is > 50%, the bio-polymer is referred to as chitin but if the percentage is < 50%, the bio-polymer is chitosan (Kamboj et al., 2015; Nouri et al., 2016). The structural formulae of chitin and chitosan show the linear chain of acetyl-glucosamine, the removed acetyl groups (CH_3-CO) and the bond types of both biopolymers (Okoya et al., 2016).

Chitin and chitosan are natural, non-toxic, highly stable, and biodegradable polymers, which are difficult to degrade thermally and chemically. They find extensive applications in industries like textiles (Al-Sagheer et al., 2009; Muzzarelli and Peter, 1997), food processing (Ko et al., 2003; Rhoades and Roller, 2000), medicine (Kaya et al., 2014), agriculture (Hirano et al., 2001), and wastewater treatment (Kaya et al., 2016; Rinaudo, 2006). However, the most significant applications in chitin/chitosan technology have been in the area of environmental studies, which include removal of dyes (Kyzas et al., 2017; Szymczyk et al., 2015), polychlorinated biphenyl (PCB) removal (Ikeda et al., 1999), and chemical waste detoxification (Mohanasrinivasan et al., 2014; Wagner and Nicell, 2002). Chitin and chitosan also find applications in water treatment such as filtration (Al-Manhel et al., 2018; Juang and Chiou, 2001), desalination (Arai and Akiya, 1978; Raeiatbin and Acikel, 2017), and flocculation/coagulation (Eikebrokk and Saltnes, 2002; Pontius, 2016; Sudha et al., 2017).

Over the years, chitin has been produced from various crustaceans, the different sources of which affect the production of chitin and in turn of chitosan. Equally, the origin of the source of the crustacean has an influence on the percentage of chitin present in it (Abdou et al., 2008; Muzzarelli and Peter, 1997). Therefore, several works have been reported on the extraction and characterization of chitin and its derivatives from different origins. Limam et al. (2011) investigated the extraction and characterization of chitin and chitosan from two species of crustacean of Tunisian origin. Also, Nouri et al., (2016) isolated chitosan with high functionality from species of Indian white shrimp, *Penaeus indicus*, shell waste. Recently, Ibitoye et al. (2018) examined the physicochemical characteristics of the extracted chitin and chitosan from house cricket and concluded that they compared favourably with the commercial chitin and chitosan.

Despite all these reported works, literature is scanty on the comprehensive optimization studies of the production of chitin and chitosan from crustacean bio-wastes. Chitin sources are abundantly available along river banks and coastal areas (Amos, 2007). The shells of crustaceans are discarded after processing, without proper method of disposal in Nigeria and perhaps in some developing countries thereby constituting environmental pollution and these can be utilized to produce chitin that can be chemically deacetylated to chitosan.

Response surface methodology (RSM) is a useful statistical technique for designing experiments where the number of experimental trials can be reduced, for building models, and for analysing the influences of numerous design variables on the response being investigated, whereby the significant and insignificant factors can be determined. RSM can equally be employed to optimize treatment conditions and processes (Krishnaiah et al., 2015; Younes et al., 2012). This study aims at determining the optimum conditions for the respective extraction yields of chitin and chitosan, and for the degree of deacetylation (*DDA*) of the extracted chitosan from pink shrimp shell waste using RSM via Box-Behnken Design (BBD) of experiments. The chitin and chitosan were extracted and isolated using the chemical processes of demineralization, deproteinization and deacetylation, respectively with high yield and degree of deacetylation (*DDA*).

MATERIALS AND METHODS

Materials and Reagents

Shrimp (*Penaeus notialis*) shell bio-wastes of Nigeria origin were obtained from a fish market in Lagos State, Nigeria. Loose tissue was removed from the shrimp shell, the shell was then washed, and dried. The dried samples were ground in a 500 W-blender and sieved in a 250 µm sieve. At ambient temperature of 28±2°C, the samples were stored in polyethylene bags for further analysis.

NaOH pellets (97%) and HCl (~37%) were purchased from Fischer Scientific Company, USA, while potassium permanganate (99.0%) and oxalic acid dihydrate (99.5%) were purchased from J. T. Baker Company, USA.

Extraction of chitin from *P. notialis* shell waste

The extraction of chitin for *P. notialis* shell waste involved the processes of demineralization, deproteinization, decolourization, and subsequent deacetylation of the extracted chitin to chitosan.

Demineralization

The process of production of chitin from *P. notialis* involved demineralisation with 2 to 4 M hydrochloric acid for 12 to 24 h at ambient temperature of 28±2°C, constant agitation speed of 100 rpm, and solvent to solid ratio of 10:1 (w/v). Separation of the acid-shell mixture was done by vacuum filtration and distilled water was used to wash thoroughly the demineralized shell until a neutral pH was achieved.

Deproteinization

The demineralized shells were deproteinized with 1.5 to 3.5 M NaOH for 1 to 3 h at a temperature of 70±0.5°C, constant agitation speed of 100 rpm and solvent to solid ratio of 15:1 (w/v). The produced heterogeneous mixture was mixed thoroughly to form insoluble particles (chitin) and separated by vacuum filtration. The

Table 1. Coded and uncoded factors of RSM experimental design for chitin extraction.

Variable	Unit	Symbol code	Coded variables level		
			-1	0	+1
			Experimental value		
HCl concentration	mol/L	X_1	2	3	4
Demineralization time	H	X_2	12	18	24
NaOH concentration	mol/L	X_3	1.5	2.5	3.5
Deproteinization time	H	X_4	1	2	3

precipitate was then washed thoroughly with distilled water to a pH of 7.0.

Decolourization

The extracted crude chitin from the treated shrimp shells was decolourised by treating it with 10 g/L potassium permanganate for 1 h and then reacted with 10 g/L oxalic acid for another 1 h. The decolorized chitin was separated from the resulting mixture via vacuum filtration, after which washing with distilled water was performed until pH=7.0. Drying of the sample was carried out at 80°C for 3 h and the dry weight recorded.

Deacetylation of chitin

The deacetylation of chitin produced was carried out via immersion in 30 to 50% w/w of NaOH solution for 1.5 to 4.5 h at a temperature of (60-100)±0.5°C, constant agitation speed of 100 rpm, and solvent to solid ratio of 10:1 (w/v). Vacuum filtration was used to separate the resulting mixture which was thoroughly washed with distilled water until pH was neutral. The solid matter obtained (that is chitosan) was oven-dried at 80°C for 3 h and the dry weight recorded.

Response surface optimization of chitin and chitosan extraction

The optimum conditions for production of chitin and chitosan were determined by using response surface methodology (RSM) in MINITAB 17.1 environment. Design of experiments (DOE) was performed employing three levels and four variables for the chitin extraction process and three levels and three variables for the chitosan extraction process. The optimized conditions obtained from the chitin extraction process were then used for the chitosan production from the shrimp shell wastes. The parameters employed for both extraction processes are shown in Tables 1 and 2.

Analysis of extraction yield

The respective extraction yields of chitin and chitosan from *P. notialis* shell wastes were analysed using Equation 1:

$$Y_j = (W_j / W_s) \times 100, \quad j = ch, cs \tag{1}$$

where ch and cs represent chitin and chitosan, respectively, Y_j represents extraction yield of *j* in %, W_j represents dried extraction weight of *j* in g, W_s represents weight of shrimp shell bio-wastes in g (= 25 and 45 g for chitin and chitosan extraction, respectively).

Determination of the degree of deacetylation (*DDA*) of chitosan

The degree of deacetylation of the chitosan produced from shrimp shell waste was determined by using acid-base titration method of Zhang et al., (2011) with some modification. 0.125 g of chitosan was dissolved in 30 mL of 0.1 M standard HCl aqueous solution, 5 to 6 drops of methyl orange was added as indicator and then stirred for 30 min until total dissolution was observed at room temperature. The resulting red chitosan solution was titrated with 0.1 M NaOH solution until a colour change to orange was observed. The degree of deacetylation of chitosan, *DDA*, in %, was calculated using Equation 2:

$$DDA = \left(\frac{c_1 V_1 - c_2 V_2}{M \times 0.0994} \times 0.016 \right) \times 100 \tag{2}$$

where c_1 and c_2 represent respective concentration of standard HCl and standard NaOH solutions in mol/L, V_1 represents volume of the standard HCl solution used to dissolve chitosan in mL, V_2 represents volume of standard NaOH solution consumed during titration in mL, and *M* represents weight of chitosan in g. The factor 0.016 in Equation 2 is the equivalent weight of NH_2 group in 1 mL of standard 1 M HCl solution, in g, and 0.0994 is the proportion of NH_2 group by weight in chitosan.

Experimental design and statistical analysis

The conventional technique for the optimization of a multi-variable system is to treat one variable at a time (OVAT). However, this technique is time-consuming, not cost efficient, and does not show the interactive and square effects of the factors. A response surface methodology (RSM) in form of a 3^k-Box-Behnken Design (BBD) (k = number of experimental factors) was chosen to statistically optimize the extraction of chitin and chitosan from shrimp shell wastes using four experimental factors (X_1, X_2, X_3, X_4) and three experimental factors (X_5, X_6, X_7), respectively in three factor levels $(-1, 0, +1)$, as shown in Tables 1 and 2. Hence, the chitin extraction optimization required 27 experimental runs while the chitosan production optimization required 15 experimental runs, as determined using Equation 3:

Table 2. Coded and uncoded factors of RSM experimental design for chitosan extraction.

Variable	Unit	Symbol code	Coded variables level		
			-1	0	+1
			Experimental value		
NaOH concentration	% by weight (w/w)	X_5	30	40	50
Reaction temperature	°C	X_6	60	80	100
Reaction time	Min	X_7	90	180	270

$$N = 2k(k-1) + c_p \quad (3)$$

where *N* represents total experimental runs, *k* represents number of variables (=4 for extraction of chitin, and =3 for extraction of chitosan and *DDA* of chitosan), and c_p represents number of central points (=3). Each experimental run was conducted in triplicates and the average value of the experimental response taken.

The Box-Behnken design is a design for fitting response surfaces called response surface designs or designs for quadratic models (Bezerraa et al., 2008). It reveals three levels in order to fit a model that is indicative of the curvature of the response. The quadratic regression model for predicting the response variables is given in Equation 4, which was used to fit the experimental results:

$$Y = \Phi_0 + \sum_{i=1}^{k} \Phi_i X_i + \sum_{i=1}^{k} \Phi_{i,i} X_i^2 + \sum_{1 \le i \le j}^{k} \Phi_{i,j} X_i X_j + \varepsilon \quad (4)$$

where Φ_0, Φ_i, $\Phi_{i,i}$, and $\Phi_{i,j}$ represent regression coefficients of constant, linear, quadratic, and interactions terms, respectively, X_i, X_j represent independent variables, *k* represents number of variables and *Y* represents predicted response (Montgomery, 2001).

The quality and adequacy of the model were evaluated using coefficient of determination, R^2, adjusted R^2 (*adj.* R^2), and predicted R^2 (*pred.* R^2). Analysis of variance (ANOVA) was conducted to show the efficacy of the fitted mathematical model. Three-dimensional response surface plots were used to examine the influence of independent variables on the responses investigated.

Determination and verification of optimum conditions

The optimized conditions for the production of chitin and chitosan and the *DDA* of chitosan were determined by analysing the response surface plots and the composite desirability function, with the objective of finding maximum yield, $(Y)_{\max}$, of both the chitin and chitosan, in %, and the maximum degree of deacetylation, $(DDA)_{\max}$, of the extracted chitosan, in %. The optimized conditions were verified by running the experiments again using the RSM results on MINTAB 17.1 software. The experimental responses were then compared with the predicted values. The optimized response quadratic models were also verified by equating the first derivatives of the mathematical functions to zero. The Hessian matrices were obtained, determinants of the leading principal minors of the Hessian matrices and eigenvalues were calculated to reveal the nature of the optimized variables and those of the Hessian matrices. The quadratic function obtained for *k* number of variables as described in Equation 4 is used to illustrate the necessary and sufficiency conditions needed to determine the nature of extrema points.

$$\frac{\partial \underline{Y}}{\partial \underline{X}} = \underline{0} \text{ at } \underline{X} = \underline{X}^* \quad (5)$$

$$Q = \sum_{i=1}^{k} \sum_{j=1}^{k} h_i h_j \left. \frac{\partial^2 Y}{\partial X_i \partial X_j} \right|_{\underline{X} = \underline{X}^*} \quad (6)$$

$$H(\underline{X})\big|_{\underline{X} = \underline{X}^*} = \left[\left. \frac{\partial^2 Y}{\partial X_i \partial X_j} \right|_{\underline{X} = \underline{X}^*} \right] \quad (7)$$

where $\underline{X}^*$ represents optimum (extremum) point, Q represents quantity of the quadratic form of the Hessian matrix, and $H(\underline{X})\big|_{\underline{X} = \underline{X}^*}$ represents Hessian matrix of the predicted response. Equation 5 shows the necessary condition needed for Equation 4 to calculate optimum of the design variables and Equation 6 is the sufficiency condition needed for the stationary points of Equation 4 to be an extremum (optimum) point.

RESULTS AND DISCUSSION

Development of regression model equations for chitin and chitosan extraction yield and optimization studies

In this investigation, RSM via BBD was employed to determine the optimum combination of parameters for production yield of chitin and chitosan from shrimp shell bio-wastes. The respective observed and predicted yields, $(Y_1)_{\exp}$ in g, and $(Y_1)_{pred}$ in g, for the 27 experimental runs during the chitin extraction are shown in Table 3, where

Table 3. Box-Behnken Design arrangement for the experimental and predicted values for the yield of chitin extraction from shrimp shell waste.

Run order	Symbol code				Yield of chitin		Yield of chitin (%) (g/25 g)	% error, ε_1
	X_1	X_2	X_3	X_4	$(Y_1)_{\exp}$ in g	$(Y_1)_{pred}$ in g		
1	-1	-1	0	0	3.20	3.13000	12.80	2.1875
2	+1	-1	0	0	4.70	4.76833	18.80	1.4539
3	-1	+1	0	0	4.50	4.38500	18.00	2.5556
4	+1	+1	0	0	5.01	5.03333	20.04	0.4657
5	0	0	-1	-1	4.45	4.41000	17.80	0.8989
6	0	0	+1	-1	4.50	4.57667	18.00	1.7037
7	0	0	-1	+1	4.95	4.82667	19.80	2.4916
8	0	0	+1	+1	4.55	4.54333	18.20	0.1465
9	-1	0	0	-1	3.40	3.37792	13.60	0.6495
10	+1	0	0	-1	5.10	4.97125	20.40	2.5245
11	-1	0	0	+1	3.90	4.01958	15.60	3.0662
12	+1	0	0	+1	4.70	4.71292	18.80	0.2748
13	0	-1	-1	0	4.18	4.19958	16.72	0.4685
14	0	+1	-1	0	5.10	5.15458	20.40	1.0703
15	0	-1	+1	0	4.40	4.33625	17.60	1.4489
16	0	+1	+1	0	4.93	4.90125	19.72	0.5832
17	-1	0	-1	0	3.60	3.66042	14.40	1.6782
18	+1	0	-1	0	5.40	5.42875	21.60	0.5324
19	-1	0	+1	0	4.20	4.22708	16.80	0.6448
20	+1	0	+1	0	4.75	4.74542	19.00	0.0965
21	0	-1	0	-1	4.00	4.05208	16.00	1.3021
22	0	+1	0	-1	4.50	4.56208	18.00	1.3796
23	0	-1	0	+1	4.00	3.99375	16.00	0.1563
24	0	+1	0	+1	5.00	5.00375	20.00	0.0750
25	0	0	0	0	6.40	6.39667	25.60	0.0521
26	0	0	0	0	6.42	6.39667	25.68	0.3635
27	0	0	0	0	6.37	6.39667	25.48	0.4186

$$\varepsilon_1 = \frac{(Y_1)_{\exp} - (Y_1)_{pred}}{(Y_1)_{\exp}} \times 100$$

It was observed that the extracted chitin from 25 g of dried shell waste of pink shrimp (*Penaeus notialis*) was in the range of 3.20 to 6.42 g corresponding to yield of 12.80 to 25.68%.

Table 4 shows the results of the 15 experimental runs for the chitosan extraction from the shrimp shell waste, where $(Y_2)_{\exp}$ represents observed extraction yield of chitosan in g, $(Y_{2a})_{pred}$ represents predicted extraction yield of chitosan with both insignificant and significant effects in g, and $(Y_2)_{pred}$ represents predicted extraction yield of chitosan with significant effects only. The percentage yield of chitosan, Y^*, was calculated thus:

$$Y^* = \left(\frac{chitosan\ dry\ weight}{precursor\ dry\ weight} \right) \times 100 \quad (8)$$

In Table 4, it was observed that the extracted chitosan from 45 g of the shrimp shell waste was in the range of 4.27 to 7.52 g corresponding to yield of 9.49 to 16.71%. The resulting quadratic regression equations for estimating the optimal conditions for chitin extraction yield, $(Y_1)_{pred}$ and for chitosan extraction yield, $(Y_2)_{pred}$, from the shrimp shell waste are given in Equations 9 and 10, respectively.

$$\begin{aligned}(Y_1)_{pred} = & -30.6374 + 9.1454X_1 + 1.1535X_2 + 5.3321X_3 + 4.7821X_4 - 1.1X_1^2 - 0.0269X_2^2 \\ & - 0.7813X_3^2 - 1.0262X_4^2 - 0.0413X_1X_2 - 0.3125X_1X_3 - 0.2250X_1X_4 - 0.0162X_2X_3 \\ & + 0.0208X_2X_4 - 0.1125X_3X_4\end{aligned} \quad (9)$$

Table 4. Box-Behnken Design arrangement for the experimental and predicted values for the yield and *DDA* of chitosan extracted from shrimp shell waste.

Run order	X_5	X_6	X_7	$(Y_2)_{\exp}$ in g	$(Y_{2a})_{pred}$ in g	$(Y_2)_{pred}$ in g	Y^* in %	% error, ε_2	$(DDA)_{\exp}$ in %	$(DDA_{is})_{pred}$ in %	$(DDA)_{pred}$ in %	% error, ε_3
1	-1	-1	0	4.27	4.4275	4.4275	9.4889	3.6885	79.25	79.3800	79.3781	0.1616
2	+1	-1	0	5.30	5.2175	5.2175	11.7778	1.5566	84.15	84.1950	84.1931	0.0512
3	-1	+1	0	4.48	4.5625	4.5625	9.9556	1.8415	80.39	80.3450	80.3431	0.0584
4	+1	+1	0	7.39	7.2325	7.2325	16.4222	2.1313	88.11	87.9800	87.9781	0.1497
5	-1	0	-1	5.59	5.4175	5.6375	12.4222	0.8497	81.98	81.8750	81.8769	0.1257
6	+1	0	-1	7.52	7.5875	7.3675	16.7111	2.0279	88.90	88.8800	88.8819	0.0203
7	-1	0	+1	5.16	5.0925	4.8725	11.4667	5.5717	80.79	80.8100	80.8119	0.0271
8	+1	0	+1	6.21	6.3825	6.6025	13.8000	6.3205	86.15	86.2550	86.2569	0.1241
9	0	-1	-1	5.21	5.2250	5.2050	11.5778	0.0960	82.50	82.4750	82.4769	0.0278
10	0	+1	-1	6.17	6.2600	6.2800	13.7111	1.7828	86.05	86.2000	86.2019	0.1766
11	0	-1	+1	4.51	4.4200	4.4400	10.0222	1.5521	82.13	81.9800	81.9819	0.1803
12	0	+1	+1	5.55	5.5350	5.5150	12.3333	0.6306	82.98	83.0050	83.0069	0.0324
13	0	0	0	6.99	7.1200	7.1200	15.5333	1.8598	85.00	84.9033	84.9008	0.1167
14	0	0	0	7.20	7.1200	7.1200	16.0000	1.1111	84.80	84.9033	84.9008	0.1188
15	0	0	0	7.17	7.1200	7.1200	15.9333	0.6974	84.91	84.9033	84.9008	0.0109

$$(Y_2)_{pred} = -20.3650 + 0.2985X_5 + 0.4349X_6 + 0.0180X_7 - 0.0050X_5^2 - 0.0031X_6^2 - 0.0001X_7^2 + 0.023X_5X_6 \quad (10)$$

with % error being

$$\varepsilon_2 = \frac{(Y_2)_{\exp} - (Y_2)_{pred}}{(Y_2)_{\exp}} \times 100 .$$

The positive and negative signs in the models, Equations 9 and 10, signify synergetic and antagonistic effects of the factors, $X_i, i = 1-7$, respectively.

The respective extraction yields of chitin and chitosan varied with all the combinations of conditions during the demineralization, deproteinization, and deacetylation stages of the shrimp shells. The conditions of extraction run 26 (3 M, 18 h, 2.5 M, 2 h) and extraction run 6 (50% w/w, 80°C, 90 min) as shown in Tables 3 and 4 corresponded to the maximum chitin and chitosan yield of 6.42 g (25.68%) and 7.52 g (16.71%), respectively. Furthermore, results obtained showed that the optimal conditions (6.52 g, 26.08%) for chitin preparation from shrimp shells were at 3.25 M HCl solution, 19 h demineralization time, 2.43 M NaOH solution, and 2.03 h deproteinization time, while the optimal conditions (7.62 g, 16.93%) for chitosan extraction yield from shrimp shells were achieved at 50% w/w NaOH concentration, 87.8°C reaction (deacetylation) temperature, and a reaction (deacetylation) time of 145.2 min.

The analysis of variance (ANOVA) and the estimated regression coefficients of each term of the regression models, Equations 9 and 10, are illustrated in Tables 5 and 6. Generally, the smaller and the larger the values of *p* (<0.05) and *t,* respectively, the more significant the corresponding coefficient term is. Based on the results shown in Table 5, the extraction yield of chitin from shrimp shells had significant linear effect, quadratic effect and interaction effect on all

Table 5. Estimated regression coefficients and the Analysis of Variance (ANOVA) for the second-order polynomial model for chitin extraction from shrimp shells (uncoded units).

Chitin extraction yield regression model, $(Y_1)_{pred}$								
Factor/source	***Seq SS***	***DF***	***Adj MS***	***Coef***	***SE Coef***	***F*-value**	***t*-value**	***p*-value**
Regression model	17.2201	14	1.23001	-	-	149.13	-	0.000
Constant	-	-	-	-30.6374	1.08467	-	-28.220	0.000
Linear	5.7748	4	2.24015	-	-	271.60	-	0.000
X_1	3.9216	1	7.18185	9.1454	0.30993	870.75	29.508	0.000
X_2	1.7328	1	4.11338	1.1535	0.05165	498.72	22.332	0.000
X_3	0.0102	1	2.76814	5.3321	0.29105	335.62	18.320	0.000
X_4	0.1102	1	2.50041	4.7821	0.27465	303.16	17.411	0.000
Square	10.4559	4	2.61399	-	-	316.93	-	0.000
X_1^2	1.9802	1	6.45333	-1.1000	0.03933	782.42	-27.972	0.000
X_2^2	1.7016	1	4.99230	-0.0269	0.00109	605.28	-24.602	0.000
X_3^2	1.1572	1	3.25521	-0.7813	0.03933	394.67	-19.866	0.000
X_4^2	5.6170	1	5.61701	-1.0262	0.03933	681.02	-26.096	0.000
Interactions	0.9893	6	0.16488	-	-	19.99	-	0.000
X_1X_2	0.2450	1	0.24503	-0.0413	0.00757	29.71	-5.450	0.000
X_1X_3	0.3906	1	0.39062	-.0.3125	0.04541	47.36	-6.882	0.000
X_1X_4	0.2025	1	0.20250	-0.2250	0.04541	24.55	-4.955	0.000
X_2X_3	0.0380	1	0.03802	-0.0162	0.00757	4.61	-2.147	0.053
X_2X_4	0.0625	1	0.06250	0.0208	0.00757	7.58	2.753	0.018
X_3X_4	0.0506	1	0.05062	-0.1125	0.04541	6.14	-2.477	0.029
Residual error	0.0990	12	0.00825	-	-	-	-	-
Lack of fit	0.0977	10	0.00977	-	-	15.43	-	0.062*
Pure error	0.0013	2	0.0063	-	-	-	-	-
Total	17.3191	26	-	-	-	-	-	-

R^2 99.43%, Predicted R^2 96.73%, AdjustedR^2 98.76%. *S*: Standard deviation (= 0.0908180); PRESS: prediction error sum of squares (= 0.56565); *Coef*: coefficient; *SE Coef*: standard error coefficient; *t*: student test; *p*: probability value; *S*: standard deviation; *insignificant *p* > 0.05 at 95% confidence level; *DF*: degree of freedom; *Seq SS*: sequential sum of squares; *Adj SS*: adjusted sum of squares; *Adj MS*: adjusted mean Square; *F*: Fisher's variance ratio.

the variables ($p < 0.05$; that is, significant at 95% confidence level) while the chitosan extraction yield had insignificant interaction effects of X_5X_7 and X_6X_7 since *p* > 0.05 at 95% confidence level, as presented in Table 6. Le Man et al. (2010) reported that for a regression model to be adequate, the correlation coefficient, R^2, value should not be less than 0.75. Large R^2 value does not usually indicate an acceptable regression model; a similarly high *adj*. R^2 value can be used to arrive at the conclusion of acceptable regression model (Koocheki et al., 2009). The values of *adj*. R^2 for the chitin and chitosan extraction yield from shrimp were 0.9876 and 0.9583, respectively while the respective R^2 values were 0.9943 and 0.9791.

Figure 1a and b shows the respective plots of predicted extracted chitin and chitosan yields by the developed models (Equations 9 and 10) against their corresponding experimental yields.

It was observed that the predicted yields were in consonance with the experimentally obtained yields of chitin and chitosan. Hence, an excellent correlation was achieved between the quadratic models prediction and the observed values. The residual plots for the extracted chitin and chitosan yields from shrimp shell waste are as shown in Figure 2a and b, respectively.

The assumption of normality of error terms is checked by the normal probability plot (Montgomery, 2001). The present results showed that most of the points were clustered around the blue line in Figure 2a and b, which is an indication that the error terms are approximately normal. Thus, the assumption of normality is valid in our investigation. The residuals in Figure 2a and b appear to be normally distributed (shown by the Normal probability

Table 6. Estimated regression coefficients and the Analysis of Variance (ANOVA) for the second-order polynomial model for chitosan extraction yield (uncoded units).

Chitosan extraction yield regression model, $(Y_2)_{pred}$				
Term/Factor	***Seq SS***	***Coef***	***F*-value**	***p*-value**
Regression model	17.3395	-	46.9300	0.0000
Constant	-	-20.3650	-	0.0010
Linear	9.4675	-	25.1800	0.0000
X_5	5.9858	0.2985	7.8700	0.0260
X_6	2.3113	0.4369	67.4000	0.0000
X_7	1.1704	0.0180	11.1200	0.0130
Square	6.9884	-	44.1300	0.0000
X_5^2	0.5230	-0.0050	17.4900	0.0040
X_6^2	5.5423	-0.0031	111.0500	0.0000
X_7^2	0.9231	-0.0001	17.4900	0.0040
Interactions	1.0788	-	10.3200	0.0140
X_5X_6	0.8836	0.0023	16.7400	0.0040
X_5X_7	0.1936	-0.0002	5.5500	0.0650*
X_6X_7	0.0016	0.0000	0.0050	0.8390*
Residual error	0.1743	-	-	-
Lack of fit	0.1485	-	3.8400	0.2140*
Pure error	0.0258	-	-	-
Total	17.7090	-	-	-

R^2 =97.91%, Predicted R^2= 87.62%, Adjusted R^2=95.83%. Standard deviation, *S*=0.229751; Prediction error sum of squares, *PRESS*=2.19155; *Seq SS*: sequential sum of squares; *Coef*: coefficient; *F*: Fisher's variance ratio; *p*: probability value; *insignificant ($p > 0.05$) at 95% confidence level.

and Histogram plots) and generally random (shown by the residuals against their fitted values and observation order) for the extraction yields of chitin and chitosan from shrimp shell waste.

Development of regression model equation for degree of deacetylation of chitosan and optimization studies

The degree of deacetylation of chitosan is one of the factors affecting its solubility, chemical reactivity and biodegradability and thus influences its performance in many applications (Abdel-Salam, 2013). The observed and predicted *DDA*s of chitosan produced from shrimp shell waste for the 15 experimental runs are shown in Table 4, where $(DDA)_{\exp}$ represents observed *DDA* of chitosan in %, $(DDA_{is})_{pred}$ represents predicted *DDA* of chitosan in %, with both insignificant and significant effects, and $(DDA)_{pred}$ represents predicted *DDA* of chitosan in %, with significant effects only. These results indicated that the *DDA* of chitosan ranged from 79.25 to 88.90%. The regression model for estimating the extremum conditions for degree of deacetylation, $(DDA)_{pred}$, of chitosan is given by Equation 11:

$$(DDA)_{pred} = 41.4627 + 0.4623X_5 + 0.5794X_6 + 0.0371X_7 - 0.0044X_5^2 - 0.0037X_6^2 + 0.0035X_5X_6 - 0.0004X_5X_7 - 0.0004X_6X_7 \quad (11)$$

with % error being

$$\varepsilon_3 = \frac{(DDA)_{\exp} - (DDA)_{pred}}{(DDA)_{\exp}} \times 100 .$$

The optimal conditions for the degree of deacetylation, $(DDA)_{pred}$, of chitosan from the precursor shell waste were achieved at X_5 = 50% w/w, X_6 = 97.17°C, and

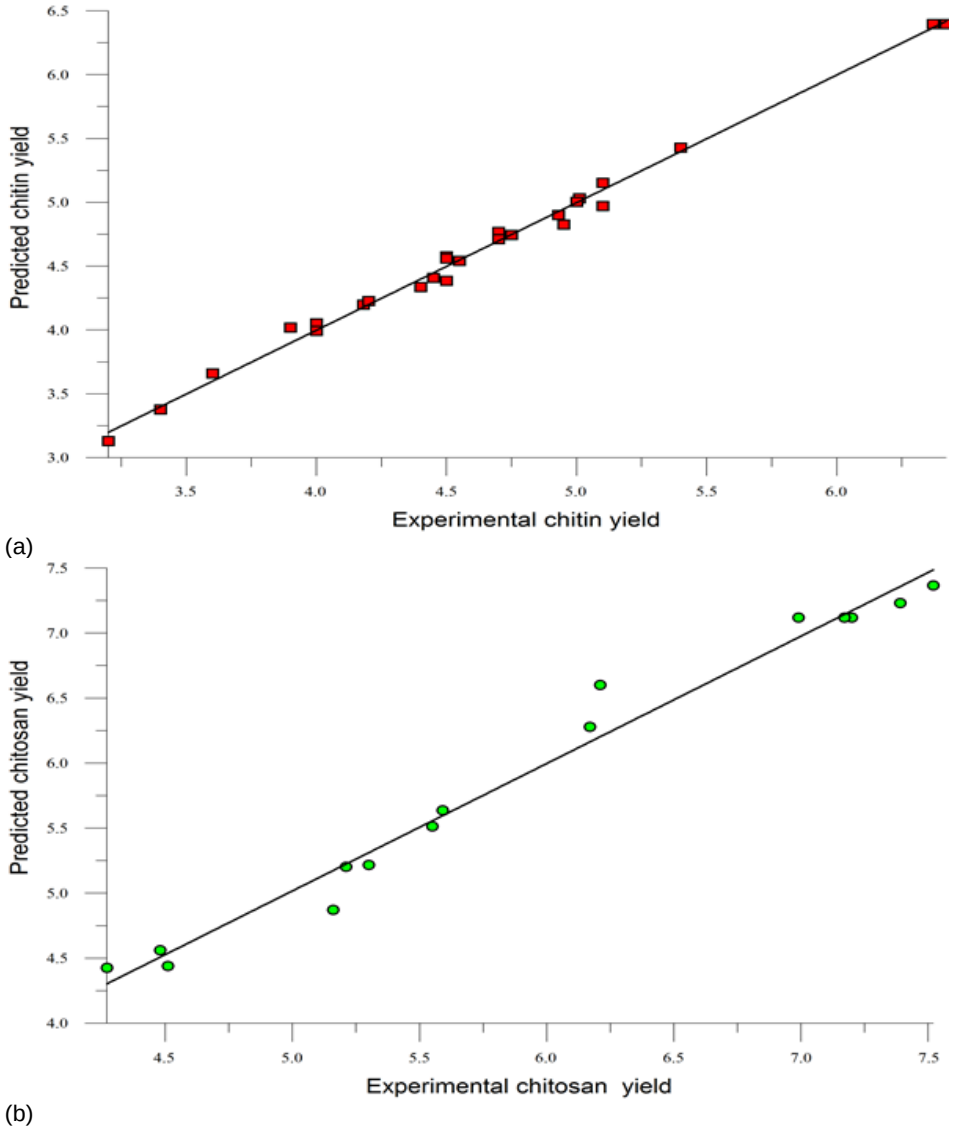

Figure 1. Predicted extraction yields of (a) chitin; (b) chitosan from shrimp shell waste against experimental yields.

X_7 = 90 min using the RSM software of MINITAB 17.1, with $(DDA)_{pred}$ = 89.73%. Figure 3 shows the plot of the predicted *DDA* of chitosan by the developed model (Equation 11) against their corresponding experimental values. Excellent agreement was achieved between the predicted and experimental *DDA* of chitosan. Figure 4 shows the residual plots for the degree of deacetylation of chitosan from shrimp shell waste corroborating the authenticity and robustness of the regression model.

The statistical analyses of the *DDA* of chitosan with significant interaction of design variables are shown in Table 7. Here, the *p*-values and *F*-values were used as tools to check the significance of each of the variables as well as their interactive and quadratic effects. As regards the importance and relationship amongst R^2, *adj*. R^2, and *pred*. R^2, same principle was used for the resulting quadratic regression equation. The values of R^2, *adj*. R^2, and *pred*. R^2 in Table 7 indicated an excellent agreement between $(DDA)_{\exp}$ and $(DDA)_{pred}$ of the chitosan, making the model sufficient for prediction of *DDA* of chitosan in the range of operational/test variables. The significance of the experimental variables for the *DDA* and the summary of analysis of variance (ANOVA) of the regression model of chitosan are shown in Table 7. Here, the ANOVA of the regression model equation revealed that the quadratic model derived from the Box-Behnken Design could adequately be used to predict the response (Table 4) as evident from the high *F*-values and very low *p*-values ($p \leq 0.05$).

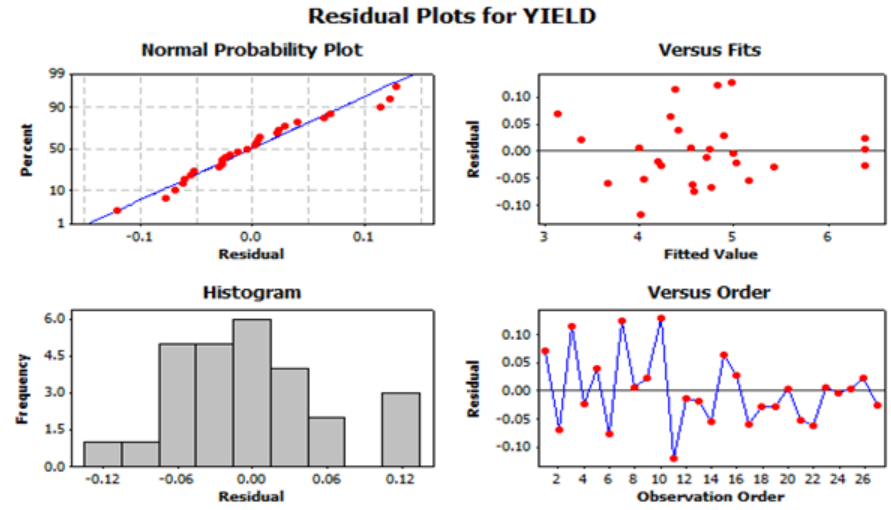

(a)

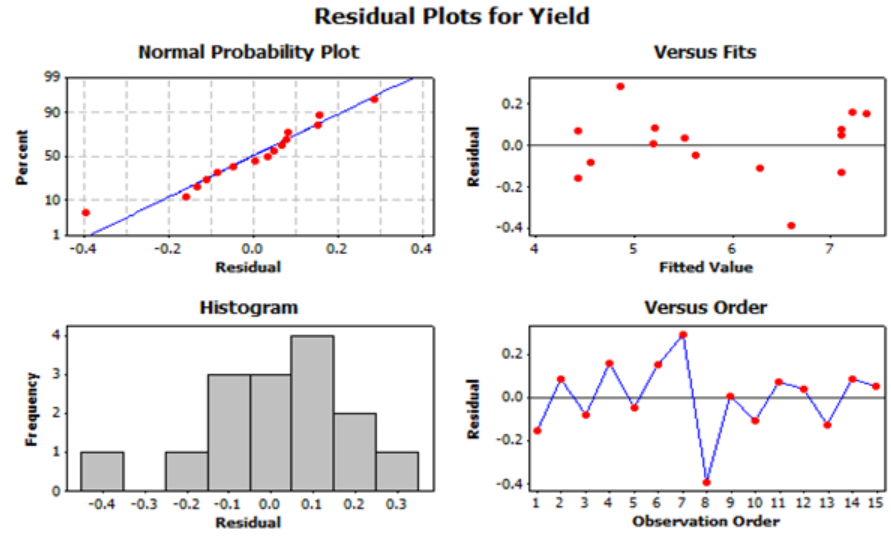

(b)

Figure 2. Residual plots for (a) chitin; (b) chitosan extraction yield from shrimp shells.

Analysis of response surface

Three-dimensional response surface curves and two-dimensional contour plots were depicted to study the interactions between the design variables in the extraction yields of chitin and chitosan, and the degree of deacetylation of chitosan. These plots were used to determine the optimum levels of each factor required to obtain maximum response. The effects of individual factors on the chitin extraction yield from the shrimp shell waste are as shown in Figures 5 and 6. The plots were obtained by holding the third and fourth variables at maximum point (high) values. The surface plots (Figure 5) and contour plots (Figure 6) illustrate the interactive effects of HCl concentration, X_1 in M, time of demineralization, X_2 in h, NaOH concentration, X_3 in M, and time of deproteinization, X_4 in h, on the extraction yield of the chitin. Figures 5i and 6i show the effects of HCl concentration and demineralization time on the extraction chitin yield from shrimp shell waste, maximum yield was likely to occur between 3 to 3.5 M and 18 to 19.5 h; Figures 5ii and 6ii show that maximum response (chitin yield) should be between 3 to 3.5 M and 2 to 2.5 M; while Figures 5iii to vi and 6iii to vi show that maximum extraction chitin yield should be between 3 to 3.5 M and 1.5 to 2.2 h, 18 to 19.5 h and 2 to 2.5 M, 18 to 19.5 h and 1.5 to 2.2 h, and 2 to 2.5 M and 1.5 to 2.2 h, respectively. This is a strong indication of the dependence of the extraction yield of chitin on the HCl concentration, time of demineralization, NaOH concentration and the deproteinization time.

The interactive effects of the NaOH concentration, X_5

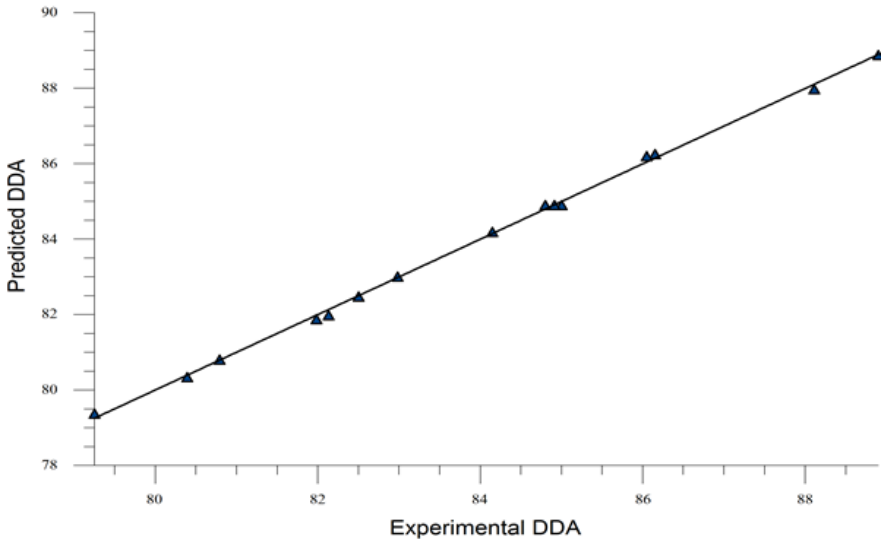

Figure 3. Predicted *DDA* of extracted chitosan from shrimp shell waste against experimental *DDA*.

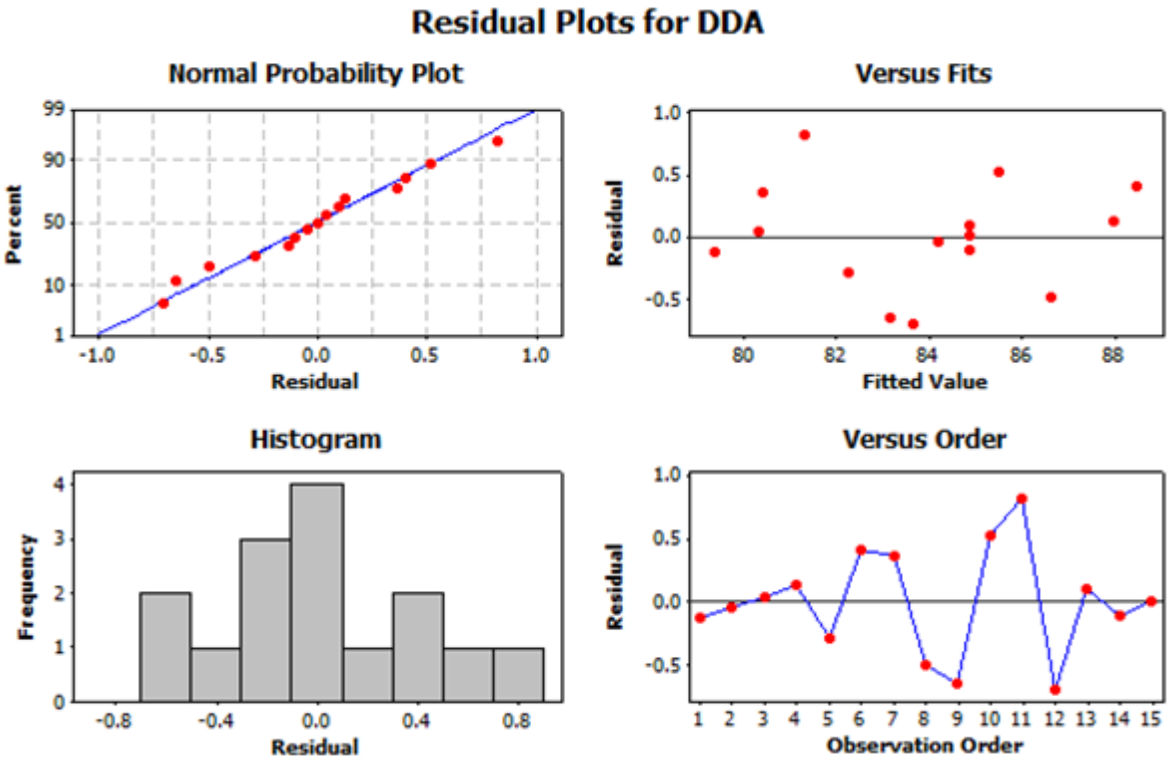

Figure 4. Residual plots for *DDA* of chitosan from shrimp shell waste.

in % w/w, reaction (deacetylation) temperature, X_6 in °C, and reaction (deacetylation) time, X_7 in min, on the extraction yield of chitosan by holding the third variable at mid-point value are as shown in Figures 7 and 8. Figure 7i and ii revealed that as NaOH concentration, deacetylation temperature and deacetylation time increase, the extraction chitosan yield increased to a certain point before evening out. These, therefore, showed positive significant interactions between X_5

Table 7. Estimated regression coefficients and the Analysis of Variance (ANOVA) for the second-order polynomial model for *DDA* of chitosan (uncoded units).

DDA of chitosan regression model, $(DDA)_{pred}$				
Term/factor	***Seq SS***	***Coef***	***F*-value**	***p*-value**
Regression model	108.6140	-	641.0100	0.0000
Constant	-	41.4627	-	0.0000
Linear	95.5910	-	106.6500	0.0000
X_5	77.5010	0.4623	45.1400	0.0010
X_6	11.2810	0.5794	283.6100	0.0000
X_7	6.8080	0.0371	64.7300	0.0000
Square	8.6040	-	203.1200	0.0000
X_5^2	0.4260	-0.0044	34.5500	0.0010
X_6^2	8.1780	-0.0037	386.1200	0.0000
X_7^2	0.0000	0.0000	0.0000	0.9620*
Interactions	4.4190	-	69.5500	0.0000
X_5X_6	1.9880	0.0035	93.8700	0.0000
X_5X_7	0.6080	-0.0004	28.7300	0.0020
X_6X_7	1.8220	-0.0004	86.0500	0.0000
Residual error	0.1270	-	-	-
Lack of fit	0.1070	-	2.6700	2.9100*
Pure error	0.0200	-	-	-
Total	108.7410	-	-	-

R^2 =99.88%, Predicted R^2= 98.93%, Adjusted R^2=99.73%. Standard deviation, *S*=0.145534; Prediction error sum of squares, *PRESS*=1.16407; *Seq SS*: sequential sum of squares; *Coef*: coefficient; *F*: Fisher's variance ratio; *p*: probability value; *insignificant ($p > 0.05$) at 95% confidence level.

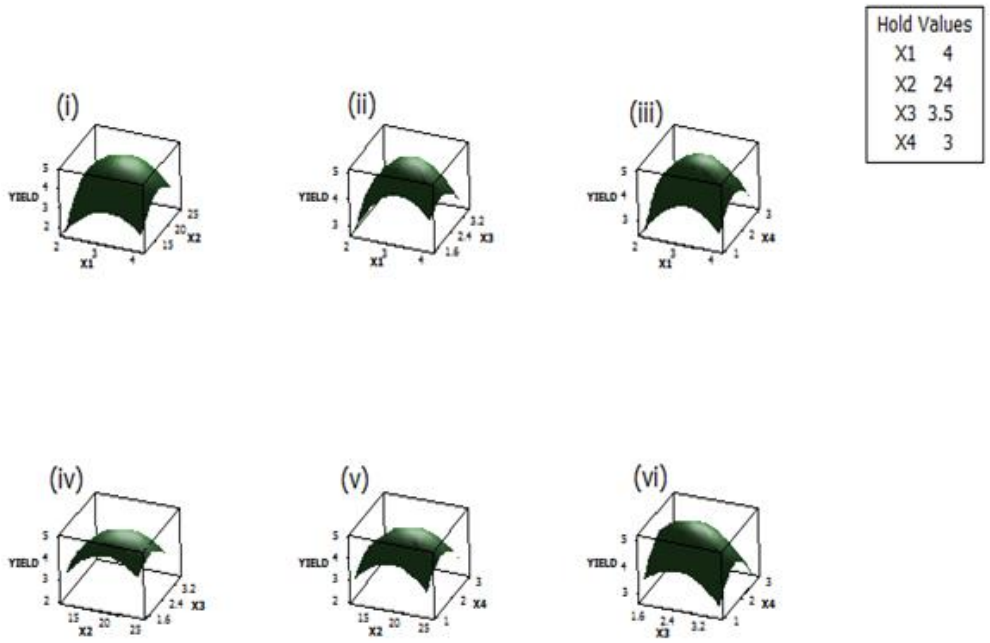

Figure 5. Three-dimensional surface plots of the effects of HCl concentration, X_1 in M, time of demineralization, X_2 in h, NaOH concentration, X_3 in M and time of deproteinization, X_4 in h, on the yield of chitin from shrimp (*Penaeus notialis*) shell waste.

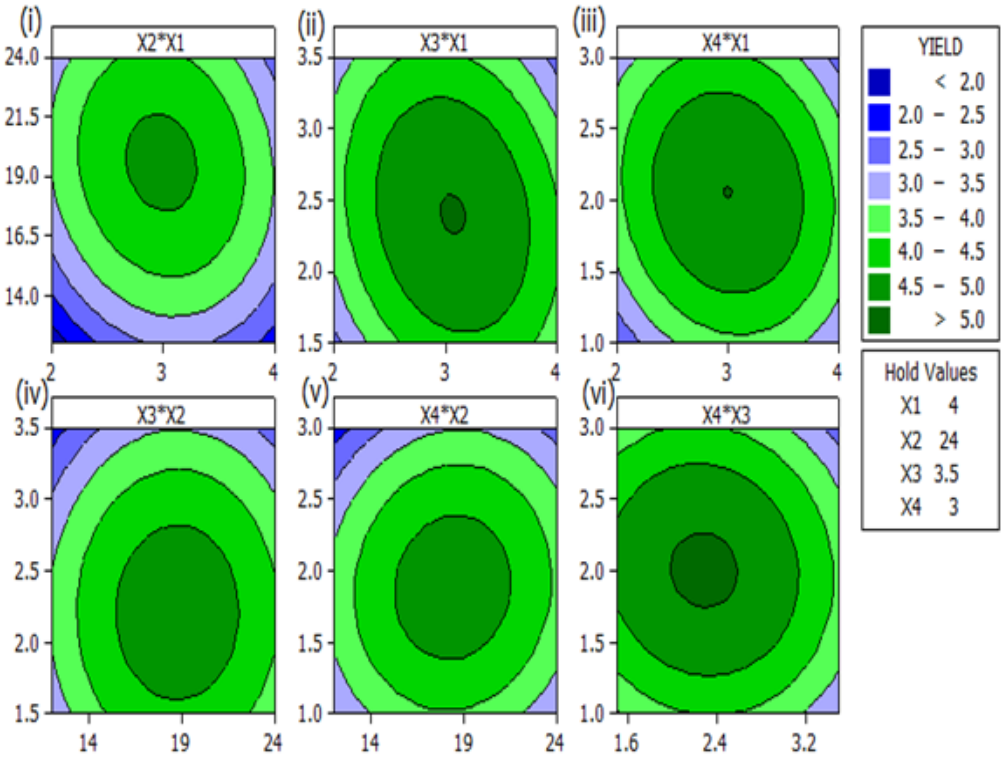

Figure 6. Contour plots of the effects of the HCl concentration, X_1 in M, time of demineralization, X_2 in h, NaOH concentration, X_3 in M, and time of deproteinization, X_4 in h, on the yield of chitin from shrimp (*Penaeus notialis*) shell waste.

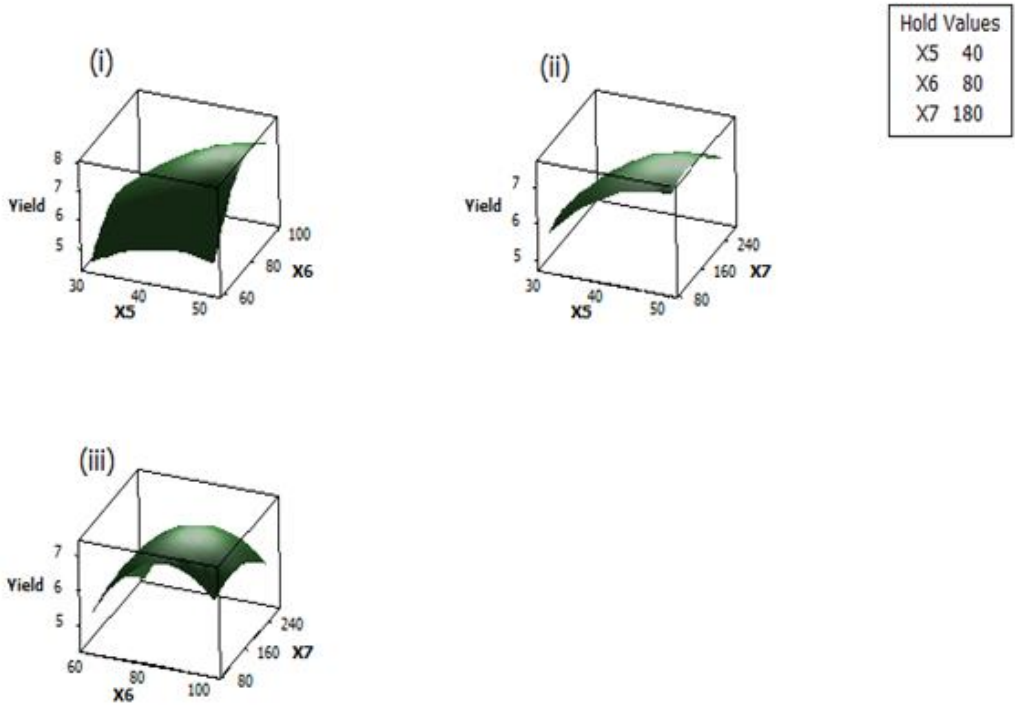

Figure 7. Three-dimensional surface plots of the effects of NaOH concentration, X_5 in % w/w, reaction (deacetylation) temperature, X_6 in °C and reaction (deacetylation) time, X_7 in min, on the yield of chitosan from shrimp (*Penaeus notialis*) shell waste.

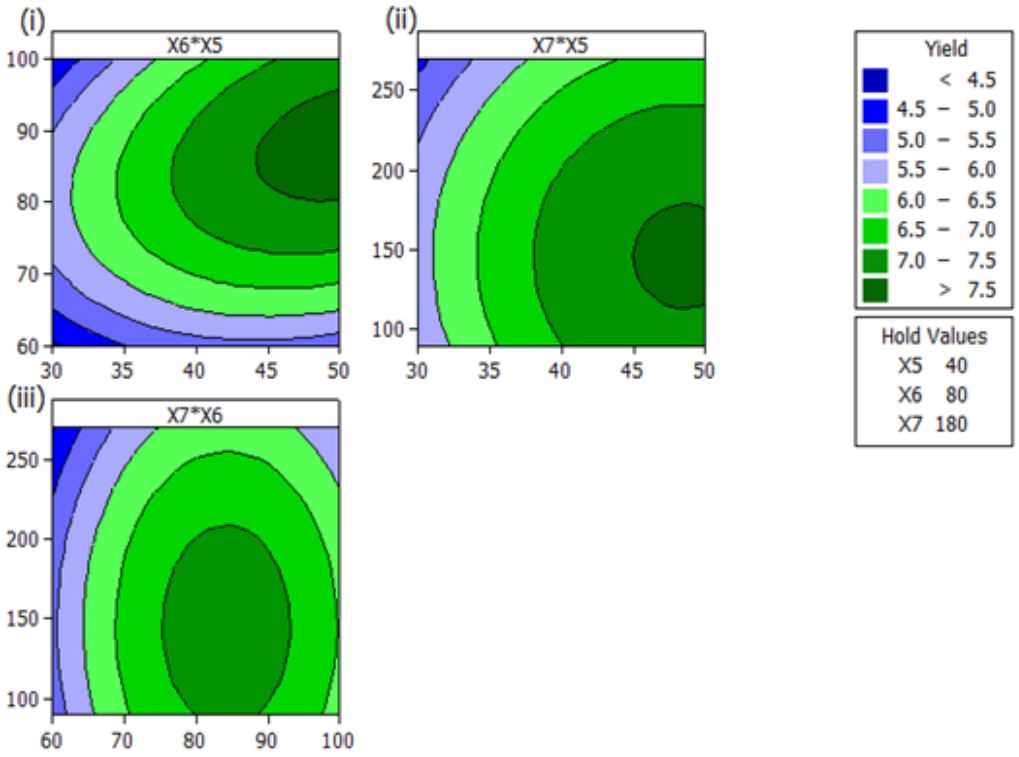

Figure 8. Contour plots of the effects of NaOH concentration, X_5 in % w/w, reaction (deacetylation) temperature, X_6 in °C and reaction (deacetylation) time, X_7 in min, on the yield of chitosan from shrimp (*Penaeus notialis*) shell waste.

and X_6 and $X_5 X_7$. Figure 7iii shows that a mixed and divergent relationship existed between the chitosan yield and input variables (X_6 and X_7); a positive interaction was observed between X_6 and X_7 before experiencing a negative effect after an optimum reaction temperature of approximately 88°C was obtained. Figure 8i to iii shows the effects of NaOH concentration, deacetylation temperature and deacetylation time on the yield of chitosan, indicating that maximum response was likely to occur between 45-50% w/w, 85-90°C and 130-150 min, respectively.

Figures 9 and 10 illustrate the interactive effects of the NaOH concentration, X_5 in % w/w, reaction temperature, X_6 in °C, and reaction time, X_7 in min, on the *DDA* of chitosan produced by holding the third variable at mid-point value. In Figure 9i, the degree of deacetylation was observed to rapidly increase with an increase in the NaOH concentration, X_5, and deacetylation temperature, X_6, while holding the deacetylation time, X_7, constant at a mid-point value of 180 min. This thus confirms the positive significant interaction effect between the NaOH concentration and deacetylation temperature. Additionally, this shows that the degree of deacetylation (*DDA*) of chitosan increases with an increase in NaOH concentration and deacetylation temperature. Figure 9ii and iii shows the effects of the input experimental variables (X_5, X_6 and X_7) on the DDA of chitosan from the *P. notialis* shell waste. The effects indicated a positive interaction between the independent variables (X_5, X_6 and X_7) and the *DDA* of produced chitosan. Figure 10i, ii and iii furthermore shows the effects of the NaOH concentration (X_5), deacetylation temperature (X_6) and deacetylation time (X_7) on the *DDA* of chitosan, illustrating that maximum response should be between 45 to 50% w/w, 80 to 100°C, and 80 to 100 min, respectively.

Verification of optimum conditions and response variables

To obtain the maximum responses, that is, the maximum extraction chitin yield, maximum extraction chitosan yield, and maximum *DDA* of chitosan from the shrimp shell waste, an optimization process was performed using the MINITAB RSM Optimizer® software. The response

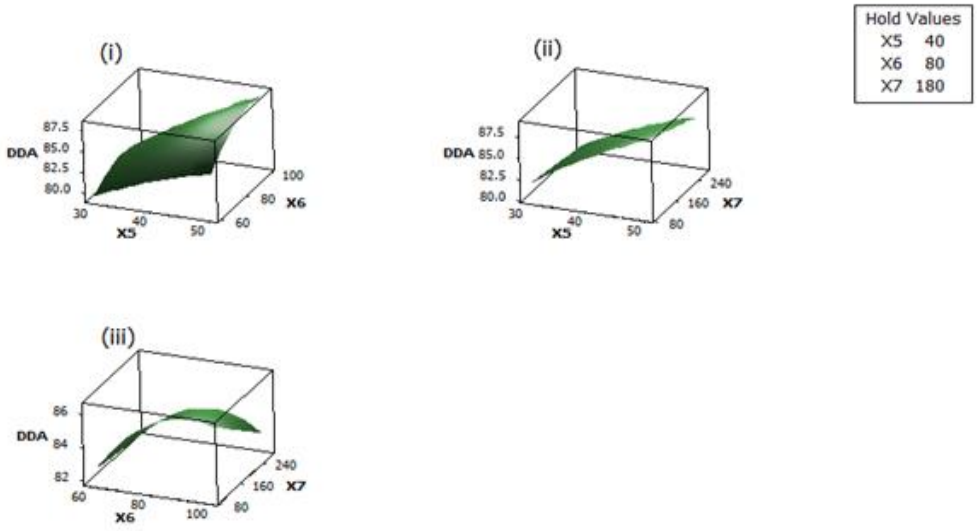

Figure 9. Three-dimensional surface plots of the effects of NaOH concentration, X_5 in % w/w, reaction (deacetylation) temperature, X_6 in °C and reaction (deacetylation) time, X_7 in min, on the *DDA* of chitosan from shrimp (*Penaeus notialis*) shell waste.

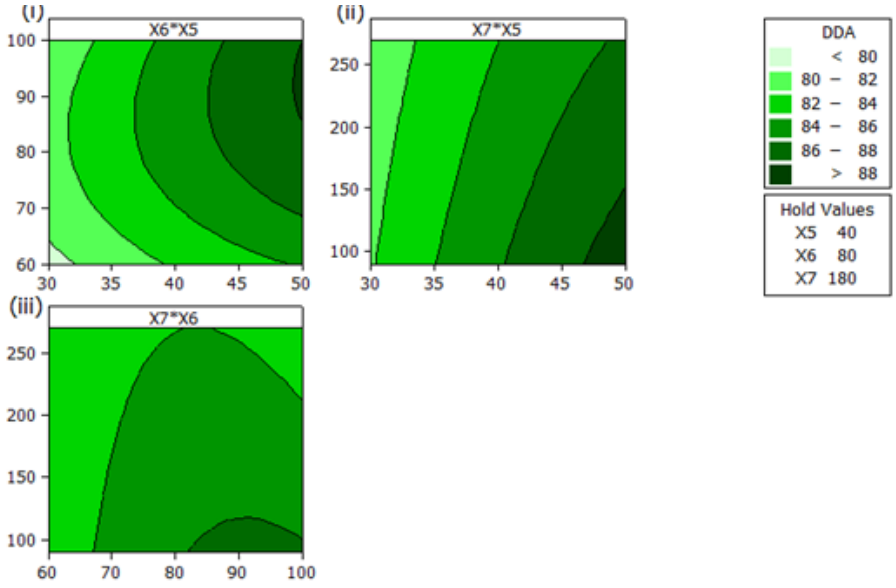

Figure 10. Contour plots of the effects of NaOH concentration, X_5 in % w/w, reaction (deacetylation) temperature, X_6 in °C and reaction (deacetylation) time, X_7 in min, on the *DDA* of chitosan from shrimp (*Penaeus notialis*) shell waste.

optimizer was used to determine the exact optimum values of the design variables (Zainal et al., 2014). The results of the response optimizer at optimum conditions for maximum goals for the extraction chitin yield, extraction chitosan yield, and *DDA* of chitosan were obtained as: (X_1 = 3.25 M, X_2 = 19 h, X_3 = 2.43 M, and X_4 = 2.03 h, $(Y_1)_{pred}$ = 6.5018 g), (X_5 = 50% w/w, X_6 = 87.8°C, and X_7 = 145.2 min, $(Y_2)_{pred}$ = 7.7595 g), and (X_5 = 50% w/w, X_6 = 97.17°C, and X_7 = 90 min, $(DDA)_{pred}$ = 89.9925%), as shown in Figures 11a, 11b and 12, respectively.

Validation experimental runs were conducted using the exact optimum conditions in duplicate and the average values of the responses were obtained as shown in Table 8. It was observed that there was an excellent agreement between the experimental response values and the predicted values based on the regression models.

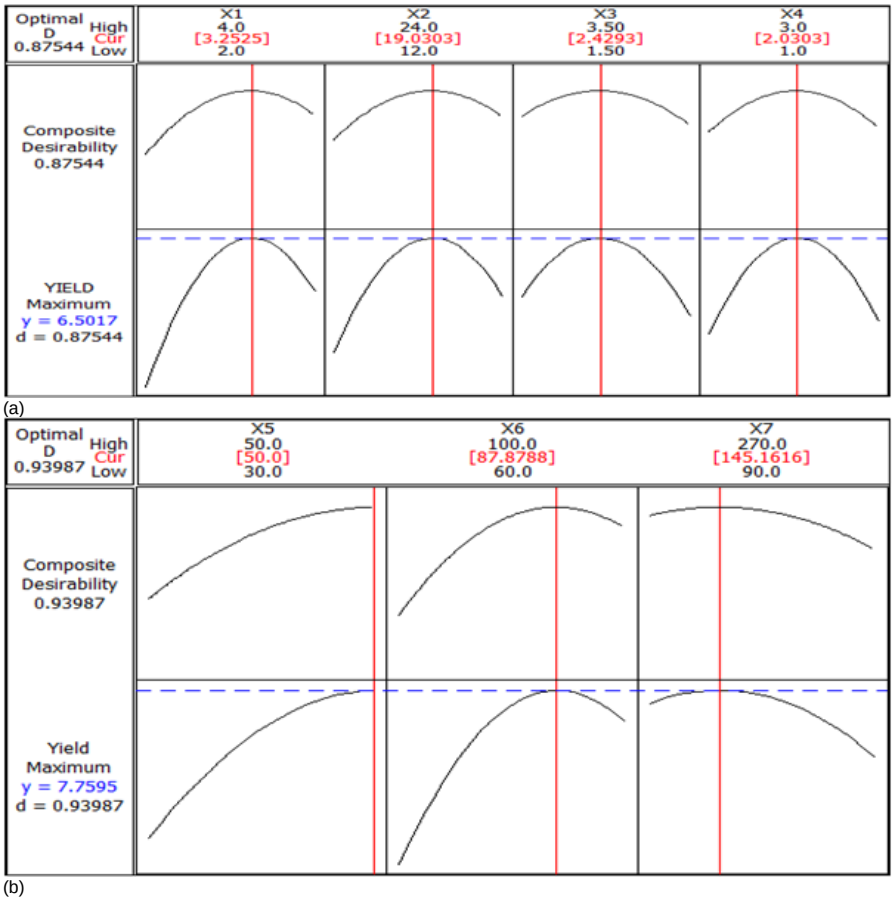

Figure 11. Response optimizer at the optimum conditions for the maximum extraction yields of (a) chitin, and (b) chitosan from shrimp (*Penaeus notialis*) shell waste.

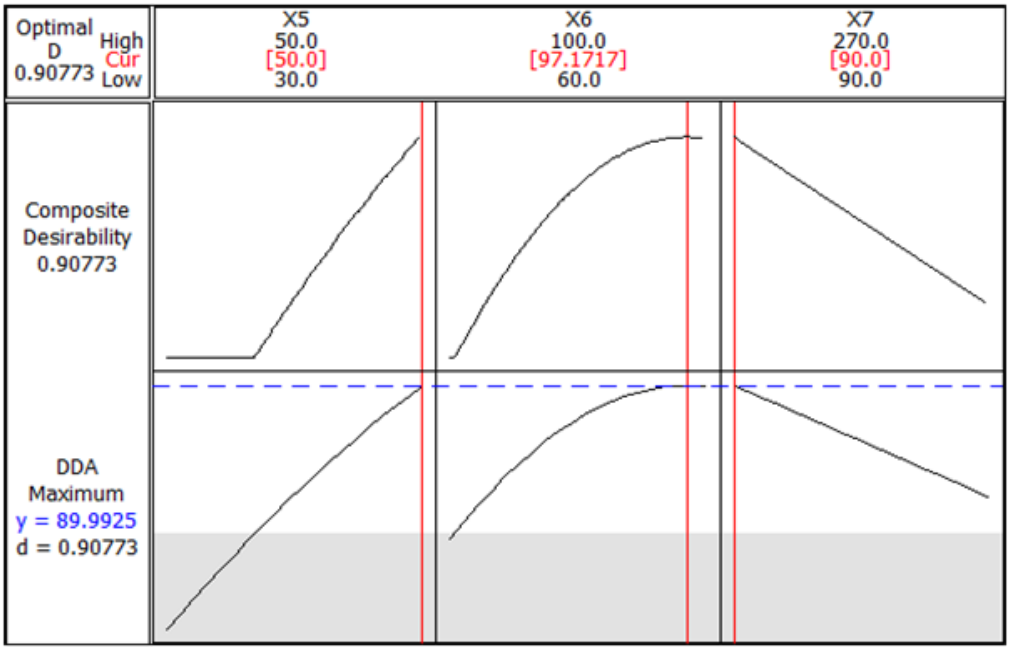

Figure 12. Response optimizer at the optimum conditions for maximum degree of deacetylation (*DDA*) of chitosan from shrimp (*Penaeus notialis*) shell waste.

Table 8. Verification of the optimum conditions of the regression models for the extraction yields of chitin and chitosan, and *DDA* of chitosan from shrimp shell waste.

Equation	Parameter	Response	Calculated optimum point ($\underline{X}^*$)	MINITAB optimum point ($\underline{X}^*$)	Eigenvalues ($\underline{\lambda}$)	Determinant values ($\underline{M}$)	Nature of Hessian matrix $H(\underline{X}^*)$
Equation 9 ($(Y_1)_{pred}$ = g/25 g)	Experimental value (g)	6.52000	X_1^*= 3.24860	X_1^*= 3.2525	λ_1= -2.4765	M_1= -2.2000	Negative definite
	MINITAB value (g)	6.50174	X_2^*= 19.0046	X_2^*= 19.030	λ_2= -1.9054	M_2= +0.1167	
	Calculated value (g)	6.49110	X_3^*= 2.41920	X_3^*= 2.4293	λ_3= -1.4343	M_3= -0.1767	
	-	-	X_4^*= 2.03390	X_4^*= 2.0303	λ_4= -0.0526	M_4= +0.3560	
Equation 10 ($(Y_2)_{pred}$ = g/45 g)	Experimental value (g)	7.62000	X_5^*= 50.0320	X_5^*= 50.000	λ_5= -0.0111	M_5= -0.0100	Negative definite
	MINITAB value (g)	7.75947	X_6^*= 87.5217	X_6^*=87.8788	λ_6= -0.0051	M_6= +5.67×10^{-5}	
	Calculated value (g)	7.74920	X_7^*= 145.981	X_7^*=145.161	λ_7= -0.0002	M_7= -1.134×10^{-8}	
Equation 11	Experimental value (%)	89.7300	X_5^*= 49.9880	X_5^*= 50.000	λ_5= -0.0117	M_5= -0.0088	Negative definite
	MINITAB value (%)	89.9925	X_6^*= 96.8750	X_6^*= 97.172	λ_6= -0.0046	M_6= +5.287×10^{-8}	
	Calculated value (%)	89.9820	X_7^*= 90.0800	X_7^*= 90.000	λ_7= -0.0010	M_7= -3.712×10^{-9}	

The optimum conditions of the regression models, Equations 9 to 11, were also verified by calculating the optimum values of the independent (or design) variables $X_i, i=1-7,$ and then equating the first derivatives of the mathematical functions to zero (necessary conditions), as given in Equation 5. The nature of the test (that is, design) variables and Hessian matrices were also obtained by calculating the eigenvalues ($\underline{\lambda}$) and values of the determinant ($\underline{M}$) of the Hessian matrices (sufficiency conditions), as given in Equation 7. As presented in Table 8, the eigenvalues of $H(\underline{X}^*)$ were all negative, the determinants of the leading principal minors of $H(\underline{X}^*)$ alternated in signs being negative and positive for odd and even values of *i*, that is $M_i\{H(\underline{X}^*)\}<0$ and $M_i\{H(\underline{X}^*)\}>0$, respectively. Hence, the Hessian matrices of the regression models, Equations 9 to 11, were negative definite indicating global (or local) maxima of the optimum points ($\underline{X}^*$). Moreover, the obtained regression models in this study were strictly concave. Table 8 also shows a robust comparison of the calculated optimum points with the optimum points obtained from MINITAB RSM Optimizer® software generated from the regression models and a comparison of the experimental, MINITAB, and calculated responses. Excellent agreements were achieved amongst these responses for extraction yields of chitin and chitosan, and the *DDA* of chitosan.

Conclusion

The extraction of chitin and chitosan from pink shrimp obtained from the coastal area of Lagos State, Nigeria, was investigated. The extraction process was studied via the Box-Behnken Design (BBD) of experiments using response surface methodology. The step-by-step studies showed the input variables that had tremendous influence on the extraction processes. The present study showed that chitin and chitosan could be obtained from the shell waste of pink shrimp (*P. notialis*), with high yield and high degree of deacetylation. It also demonstrated that response surface methodology (RSM) is an advantageous statistical technique for the investigation of the effects of major independent factors on the chitin and chitosan yield, and on the *DDA* of chitosan from

pink shrimp shell waste. Equally, the optimum factors for the extraction yield of the chitin were determined to be 3.25 M HCl, 19.03 h demineralization time, 2.43 M NaOH solution, and 2.03 h deproteinization time with an optimized (maximum) extraction chitin yield of 6.52 g (26.08%). Also, the optimized yield for chitosan extraction was obtained as 7.62 g (16.93%) at optimized conditions of 50% w/w NaOH solution, 87.9°C deacetylation temperature, and 145.26 min deacetylation time while the maximum degree of deacetylation (*DDA*) of chitosan was obtained as 89.73% at optimized conditions of 50% w/w NaOH solution, 97.2°C deacetylation temperature, and 90 min deacetylation time. Analysis of variance (ANOVA) and other statistical tools were used to test the authenticity and robustness of the obtained quadratic regression models, which were found to be very adequate and accurate in predicting the respective responses of the processes.

CONFLICT OF INTERESTS

The authors have not declared any conflict of interests.

REFERENCES

Abdel-Salam HA (2013). Evaluation of nutritional quality of commercially cultured Indian white shrimp Penaeus Indicus. International Journal of Nutrition and Food Sciences 2(4):160-166.

Abdou ES, Nagy KSA, Elsabee MZ (2008). Extraction and characterization of chitin and chitosan from local sources. Bioresource Technology 99(5):1359-1367.

Al-Manhel AJ, Al-Hilphy ARS, Niamah AK (2018). Extraction of chitosan, characterisation and its use for water purification. Journal of the Saudi Society of Agricultural Sciences 17(2):186-190.

Al-Sagheer FA, Al-Sughayer MA, Muslim S, Elsabee MZ (2009). Extraction and characterization of chitin and chitosan from marine sources in Arabian Gulf. Carbohydrate Polymers 77(2):410-419.

Amos TT (2007). Production and productivity of crustacean in Nigeria. Journal of Social Sciences 15(3):229-233.

Arai S, Akiya F (1978). Desalination reverse osmotic membranes and their preparation. US Patent 4111810.

Bezerraa MA, Santelli RE, Oliveira EP, Villar LS, Escaleira LA (2008). Response surface methodology (RSM) as a tool for optimization in analytical chemistry. Talanta 76:965-977.

Eikebrokk B, Saltnes T (2002). NOM removal from drinking water by chitosan coagulation and filtration through lightweight expanded clay aggregate filters. Journal of Water Supply: Research and Technology – AQUA 51(6):323-332.

Hajji S, Younes I, Ghorbel-Bellaaja O, Hajji R, Rinaudo M, Nasri M, Jellouli K (2014). Structural differences between chitin and chitosan extracted from three different marine sources. International Journal of Biological Macromolecules 65:298-306.

Hirano S, Hayashi M, Okuno S (2001). Soybean seeds surface-coated with depolymerised chitins: chitinase activity as a predictive index for the harvest of beans in field culture. Journal of the Science of Food and Agriculture 81:205-209.

Hossain MS, Iqbal A (2014). Production and characterization of chitosan from shrimp waste. Journal of Bangladesh Agricultural University 12:153-160.

Ibitoye EB, Lokman IH, Hezmee MN, Goh YM, Zuki ABZ, Jimoh AA (2018). Extraction and physicochemical characterization of chitin and chitosan isolated from house cricket. Biomedical Materials 13(2):1-12.

Ikeda M, Gotanda T, Imamura Y, Hirakawa C (1999). Method for microbially decomposing organic compounds and method for isolating microorganism, US Patent 5919696.

Juang RS, Chiou CH (2001). Feasibility of the use of polymer-assisted membrane filtration for brackish water softening. Journal of Membrane Science 187(1-2):119-127.

Kamboj S, Singh K, Tiwary A, Rana V (2015). Optimization of microwave assisted Maillard reaction to fabricate and evaluate corn fiber gum-chitosan IPN films. Food Hydrocolloids 44:260-276.

Kaya M, Akyuz B, Bulut E, Sargin I, Eroglu F, Tan G (2016). Chitosan nanofiber production from drosophila by electrospinning. International Journal of Biological Macromolecules 92:49-55.

Kaya M, Baran T, Mentes A, Asaroglu M, Sezen G, Tozak KO (2014). Extraction and characterization of α-chitin and chitosan from six different aquatic invertebrates. Food Biophysics 9(2):145-157.

Ko JA, Park HJ, Park YS, Hwang SJ, Park JB (2003). Chitosan microparticle preparation for controlled drug release by response surface methodology. Journal of Microencapsulation 20(6):791-797.

Koocheki A, Taherian AR, Razavi S, Bostan A (2009). Response surface methodology for optimization of extraction yield, viscosity, hue and emulsion stability of mucilage extracted from Lepidium Perfoliatum seeds. Food Hydrocolloids 23:2369-2379.

Krishnaiah D, Bono A, Sarbatly R, Nithyanandam R, Anisuzzaman SM (2015). Optimisation of spray drying operating conditions of Morinda Citrifolia L. fruit extract using response surface methodology. Journal of King Saud University – Engineering Sciences 27:26-36.

Kyzas GZ, Bikiaris DN, Mitropoulos AC (2017). Chitosan adsorbents for dye removal: A review. Polymer International 66:1800-1811.

Le Man H, Behera SK, Park HS (2010). Optimization of operational parameters for ethanol production from Korean foodwaste leachate. Internationa Journal of Environmental Science and Technology 7(1):157-164.

Lertsutthiwong P, How NC, Chandrkrachang S, Stevens WF (2002). Effect of chemical treatment on the characteristics of shrimp chitosan. Journal of Metals, Materials and Minerals 12(1):11-18.

Limam Z, Selmi S, Sadok S, El Abed A (2011). Extraction and characterization of chitin and chitosan from crustacean by-products: Biological and physiochemical properties. African Journal of Biotechnology 10(4):640-647.

Mohanasrinivasan V, Mishra M, Paliwal J, Singh S, Selvarajan E, Suganthi V (2014). Studies on heavy metal removal efficiency and antibacterial activity of chitosan prepared from shrimp shell waste. 3 Biotechology 4(2):167-175

Montgomery DC (2001). Design and Analysis of Experiments, 5th ed., John Wiley and Sons, New York, NY, USA.

Muzzarelli RAA, Peter MG (1997). Chitin Handbook, 1st ed., European Chitin Society, Atec, Grottammare, Italy.

Nithya A, Jothivenkatachalam K, Prabhu S, Jeganathan K (2014). Chitosan based nanocomposite materials as photocatalyst (A Review). Materials Science Forum 781:79-94.

Nouri M, Khodaiyan F, Razavi HS, Mousavi M (2016). Improvement of chitosan production from Persian Gulf shrimp waste by response surface methodology. Food Hydrocolloids 59:50-58.

Nouri M, Khodaiyan F (2014a). Determination of parameters of chitosan extraction from shrimp shell, in: 1st International Conference on Natural Food Hydrocolloids, Mashhad, Iran.

Nouri M, Khodaiyan F (2014b). Persian Gulf shrimp waste optimization of chitosan extraction condition, in: 1st International Conference on Natural Food Hydrocolloids, Mashhad, Iran.

Okoya AA, Akinyele AB, Amuda OS, Ofoezie IE (2016). Chitosan-grafted carbon for the sequestration of heavy metals in aqueous solution. American Chemical Science Journal 11:1-14.

Pontius FW (2016). Chitosan as a drinking water coagulant. American Journal of Civil Engineering 4(5):205-215.

Raeiatbin P, Acikel YS (2017). Removal of tetracycline ny magnetic chitosan nanoparticles from medical wastewaters. Desalination and Water Treatment 73:380-388.

Rhoades J, Roller S (2000). Antimicrobial actions of degraded and native chitosan against spoilage organisms in laboratory media and foods. Applied and Environmental Microbiology 66(1):80-86.

Rinaudo M (2006). Chitin and chitosan: properties and applications. Progress in Polymer Science 31:603-632.

Roberts GAF (1992). Chitin Chemistry, 1st ed. Macmillan Press, London, United Kingdom.
Sudha PN, Aisverya S, Gomathi T, Vijayalakshmi K, Saranya M, Sangeetha K, Latha S, Thomas S (2017). Application of chitin/chitosan and its derivatives as adsorbents, coagulants, and flocculants, in: Chitosan. Scrivener Publishing LLC pp. 453-487.
Szymczyk P, Fliipkowska U, Jozwiak T, Kuczajowska-Zadrozna M (2015). The use of chitin and chitosan for the removal of reactive black 5 dye. Progress on Chemistry and Application of Chitin and its Derivatives 22:260-272.
Wagner M, Nicell JA (2002). Detoxification of phenolic solutions with horseradish peroxidase and hydrogen peroxide. Water Research 36(16):4041-4052.
Younes I, Ghorbel-Bellaaj O, Nasri R, Chaabouni M, Rinaudo M, Nasri M (2012). Chitin and chitosan preparation from shrimp shells using optimized enzymatic deproteinization. Process Biochemistry 47(12):2032-2039.
Zainal S, Noorul FK, Ri Hanum YS, Rahmah M (2014). Optimization of chitosan extract from cockle shell using response surface methodology (RSM). Asian Journal of Agriculture and Food Science 2(4):314-323.
Zhang AJ, Qin QL, Zhang H, Wang HT, Li X, Miao L, Wu YJ (2011). Preparation and characterisation of good-grade chitosan from housefly larvae. Czech Journal of Food Sciences 29(6):616-623.

Vol. 18(27), pp. 689-694, July, 2019
DOI: 10.5897/AJB2019.16890
Article Number: 810258C61566
ISSN: 1684-5315

http://www.academicjournals.org/AJB

ACADEMIC JOURNALS
expand your knowledge

African Journal of Biotechnology

Full Length Research Paper

Somatic embryogenesis and regeneration of Kenyan wheat (*Triticum aestivum* L.) genotypes from mature embryo explants

Mark Ochieng Adero[1]*, Easter David Syombua[1], Lydia Kwamboka Asande[2], Nelson Onzere Amugune[1], Eliud Sagwa Mulanda[1] and Godwin Macharia[3]

[1]School of Biological Sciences, University of Nairobi, P. O. Box 30197-00100 Nairobi, Kenya.
[2]Department of Plant Sciences, Kenyatta University, P. O. Box 43844-00100 Nairobi, Kenya.
[3]Cereal Breeding and Marker Assisted Selection Laboratory, Kenya Agricultural and Livestock Research Organization, Private Bag, Njoro (20107), Kenya.

Received 14 June, 2019; Accepted 8 July, 2019

Wheat (*Triticum aestivum* L.) improvement *via* genetic transformation depends on an efficient regeneration system for recovery of transgenic events. This study reports a somatic embryogenesis-based regeneration system for two Kenyan wheat genotypes (Eagle 10 and Njoro bread wheat II) from mature embryos. The study investigated the efficiency of mercuric chloride, commercial bleach, and chlorine gas in surface sterilizing explants prior to *in vitro* culture. Callus induction and somatic embryogenesis were done by culturing wheat mature embryos in Murashige and Skoog (MS) medium supplemented with 2, 4-dichlorophenoxyacetic acid (2,4-D) used either singly or in combination with 1-naphthaleneacetic acid (NAA), 4-chlorophenoxyacetic acid (4-CPA) or 6-benzylaminopurine (BAP). Embryo germination and plantlet recovery were done by culturing embryogenic callus in MS medium without plant growth regulators (PGRs). Chlorine gas was significantly (p<0.001) the most effective in surface sterilization and maintenance of explant viability. All 2, 4-D concentrations tested (1, 2, 4 and 8 mg/l) induced embryogenic callus. A significantly higher callus induction rate and callus fresh weight were obtained when 2,4-D was used in combination with either NAA or 4-CPA than when it was used singly. Combining 2,4-D with BAP led to a significantly lower callus induction frequency. Somatic embryo germination was achieved in MS medium without plant growth regulators. These findings have the potential to inform future efforts in the application of modern biotechnology for accelerated wheat cultivar improvement.

Key words: Wheat, somatic embryogenesis, mature embryos.

INTRODUCTION

Wheat (*Triticum aestivum* L.) is among the top five most important food crops in the world, in terms of production and consumption. In Kenya, apart from corn meal ('Ugali'), food products from wheat flour are mostly

*Corresponding author. E-mail: aderomark@gmail.com. Tel: +254711230503.

preferred, making it the second most popular food crop after maize, in terms of consumption. With increasing population especially in Africa, the global demand for wheat is expected to increase by over 60% in 2050. However, due to diseases and climate change stresses, yield is on the decline with estimated projections of 30% over the same period (FAOSTAT, 2017). Notwithstanding that conventional breeding had been achieved, much success in wheat improvement, especially against rust and drought, other biotechnological approaches are needed to handle the challenges. This is especially so because of low frequency of meiotic recombination in the crop which often leads to colossal unwanted linkage drag (Choulet et al., 2014; Darrier et al., 2017). Genetic transformation, for example, is quicker and more precise for improving resistance against diseases in crops. Transgenes or cisgenes can be transferred to elite cultivars in relatively shorter time without compromising on agronomic traits. With emerging technology of genome editing such as CRISPR/Cas 9, it is now possible to up-regulate genes for disease resistance by mutating their specific promoter regions (Dale et al., 2017). Apart from genetic transformation, other alternative approaches include mutation breeding and *in vitro* selection. All these techniques depend on tissue culture as they involve *in vitro* manipulation of wheat axenic cultures. They also require an efficient regeneration system (Miroshnichenko et al., 2016).

Wheat, like many monocots, is recalcitrant to *in vitro* culture and its regeneration and transformation is highly dependent on genotype (Aydin et al., 2011); besides, somatic embryogenesis, which is mostly preferred in genetic transformation procedures, it is difficult to achieve in most cultivars. In fact, genetic transformation of wheat is almost restricted to a few cultivars including 'Bob white' and 'Chinese spring' because of their ease of regeneration. There is need to develop protocols for as many elite cultivars as possible in order to accelerate wheat improvement by modern biotechnology.

Monocots have a limited number of explants which can be regenerated into plants (Repellin et al., 2001). Explants studied so far in wheat include and not limited to immature embryos (Hafeez et al., 2012), mature embryos (Delporte et al*.,* 2001; Filippov et al., 2006), spikes and anthers (Stober and Hessu (1997), and immature inflorescence (Redway et al., 1990; Sharma et al., 1995). However, only immature embryos have been efficient in regeneration (Bouiamrine et al., 2012). The challenge of seasonal availability of immature zygotic embryo explants requires setting up of greenhouses which are expensive to maintain (Zale et al., 2004). In view of this, there is need to optimise regeneration using mature embryos which are independent of season and can be easily conserved and stored for long inside dry seeds. Somatic embryogenesis of Kenyan wheat cultivars has so far not been explored. This is the first report of somatic embryogenesis of wheat genotypes bred in the country.

MATERIALS AND METHODS

Plant material

Two Kenyan wheat varieties, Eagle 10 and Njoro bread wheat II, obtained from the Kenya Agricultural and Livestock Research Organization (KALRO), Njoro, Kenya, were used in the current study.

Explant preparation

Intact mature seeds were used as initial explants for callus induction. Three disinfection methods were investigated for their effectiveness in establishing axenic cultures as well as maintaining explant viability. The first surface disinfection method involved the use of commercial bleach, Jik® (3.85% NaClO). Seeds were first vortexed in 70% ethanol for 3 min followed by three rinses with sterile distilled water. They were then soaked in 100% Jik® plus 2 drops of Teepol detergent, with varying exposure times of 10, 20, 40 and 60 min. The second method involved the use of mercuric chloride. Seeds were first vortexed in 70% ethanol for 3 min then rinsed thrice before being soaked in 0.1% mercuric chloride plus 2 drops Teepol for varying exposure times of 5, 10, 15 and 20 min. The third method involved chlorine gas disinfection in which dry seeds were fumigated with chlorine gas in a closed 8-litre container for 17 h. To generate chlorine gas, varying volumes of concentrated hydrochloric acid (2.5, 3.0, 3.5 and 4.0 ml) were added to 150 ml of Jik®.

Media composition and preparation

The culture media used for callus induction and regeneration were full strength MS (Murashige and Skoog, 1962) basal salts and half strength MS for root induction and proliferation. The medium was obtained from Duchefa Biochemie B.V., Netherlands. After addition of the supplements, and 8 g l^{-1} of agar powder (Thomas Baker), the pH of medium was adjusted to 5.7 ± 0.1 using either 1 N HCl or 1 N NaOH solutions. The medium in volumes of 50 ml was then autoclaved at 1.06 kg cm^{-2} steam pressure (≈ 121 ^{o} C) for 15 min.

Callus induction and maintenance media were supplemented with 2, 4-D in the range of 0.5 to 8 mg/l used either alone or in combination with either 0.2 mg/l of NAA or 4-CPA. These media were also augmented by 300 mg/l casein hydrolysate, 200 mg/l proline and 200 mg/l glutamine. After 4 to 7 days depending on the efficiency of callus induction and growth in different auxin concentrations, endosperm and germinating shoots were cut out and callus fragments were sub-cultured to medium of the same composition but with addition of 10 mg/l silver nitrate for callus maintenance.

Regeneration medium was the same as callus maintenance medium but devoid of plant growth regulators (PGRs). Regenerated plants were transferred to PGR-free ½ MS for root proliferation.

Inoculation and culture conditions

Surface disinfected seeds were aseptically inoculated onto sterile agar medium under a laminar flow cabinet. The cultures were incubated for 30 days in the dark at a temperature of 28±2°C for callus induction and maintenance. Callus initiated was then sub-cultured to regeneration medium and incubated at the same temperature in light of approximately 60 µmole photons m^{-2} $s^{-}1$ and a 16-hour photoperiod.

Table 1. Effect of sterilization treatments on culture contamination levels and viability of wheat seeds.

Disinfection agent	Duration of exposure	% seeds with fungal contamination	% of viable seeds
	Minutes		
	10	100.0±0.0[a]	96.7±2.1[a]
Jik® + 2 drops Teepol®	20	100.0±0.0[a]	93.3±2.1[a]
	40	85.0±4.3[b]	80.0±4.5[a]
	60	73.3±7.2[b]	66.7±3.3[b]
	Minutes		
	5	30.0±4.5[c]	78.3±7.0[a]
$HgCl_2$ + 2 drops Teepol®	10	18.3±3.1[c]	46.7±5.6[c]
	15	16.7±5.6[c]	30.0±5.2[c]
	20	11.7±4.8[c]	16.7±4.9[bc]
Chlorine (volume of HCL (ml))	**Hours**		
2.5	17	23.3±4.2[c]	70.0±8.6[a]
3.0	17	8.3±3.1[c]d	70.0±8.6[a]
3.5	17	6.7±3.3d	58.3±7.0[b]
4.0	17	6.7±4.2d	41.7±6.0[bc]

Data was arcsine transformed before ANOVA. Means followed by the same letters in the same column are not significantly different at p<0.05 according to Tukey's HSD test.

Experimental design and data analysis

Effectiveness of disinfection and severity of the treatment on the seeds were assessed through percentage contamination scores and percentage viability as measured by actual germination scores. For seed disinfection and callus induction experiments, each treatment had 6 replicates with 5 explants per replicate. Each experiment was repeated thrice. A completely randomised design was used in the arrangement of the culture vessels.

Data for percentage callus induction, callus fresh weight, percentage embryogenic callus induction and regeneration were subjected to one-way analysis of variance (ANOVA) and means separated by *Tukey's HSD* test at $p \leq 0.05$. These analyses were completed using GenStat® computer software 15th edition. Prior to ANOVA, arcsine transformation of data (percentages) was done where necessary based on the relation Y = arcsine $\sqrt{p}$, where p = the proportion obtained by dividing the respective percentage value by 100 as described by Rangaswamy (2010).

RESULTS AND DISCUSSION

Explant sterilization

Disinfection of explants is a crucial step in explant preparation prior to *in vitro* culture. Studies have shown that the method applied may have a significant effect on morphogenic responses. This may include variations in callus induction, somatic embryogenesis and regeneration frequencies depending on the disinfectant used (Teng et al., 2002; Çölgeçen et al., 2011). In the present study, preliminary results showed that 50% Jik® produced 100% contamination even when exposure time was extended to one hour. Consequently, full strength Jik® (3.85% NaOCl) was used in subsequent experiments. However, this was still not effective because contamination rates remained at > 70% (Table 1). Mercuric chloride was more effective than Jik® but its phyto-toxicity levels were higher than those of Jik® and this later affected callus induction frequency and vigour. Vapour disinfection by overnight fumigation of seeds with chlorine gas was the most effective surface-disinfection treatment, producing up to 93.3% disinfection (Table 1). The optimal balance between the need for high disinfection and low toxicity was achieved using 3.0 ml HCL in 150 ml Jik, as the source of chlorine gas (Table 1). The results obtained in the present study with respect to commercial bleach and mercuric chloride contrast with those reported by Bi and Wang (2008) and Parmar et al., (2012), who achieved success in using the two disinfectants for disinfection of wheat seeds. This could be due to different environments from which the seeds were obtained. The chlorine vapour disinfection protocol used in this study is adopted from the protocol used by Clough and Bent (1998) in sterilization of arabidopsis seeds. There is no report to date of previous use of this method in wheat seeds.

Callus induction and regeneration

In the present study, callus formation in mature zygotic embryos started on day 2 or 3 depending on the concentration or combination of auxins used. When 2 mg/l 2,4-D was used alone, callus induction started on day three. Augmentation of 2, 4-D with either 0.2 mg/l

Table 2. Callogenesis responses of wheat cv. Njoro BW II and Eagle 10 with different PGRs.

PGRs concentrations(mg)				% callus induction		Callus fresh weight(mg)	
2,4-D	4-CPA	NAA	BAP	Njoro BW II	Eagle 10	Njoro BW II	Eagle 10
1.0	-	-	-	63.3±6.2[a]	53.3±6.7[a]	103.3±8.2[a]	95.5±9.3[a]
2.0	-	-	-	80.0±5.2[a]	83.3±8.0[a]	152.8±4.1[b]	149.3±6.3[b]
4.0	-	-	-	76.7±6.2[a]	86.7±4.2[a]	141.5±4.6[b]	136.0±6.5[b]
8.0	-	-	-	70.0 ±4.5[a]	76.7±6.2[a]	121.2±4.3[a]	128.5±7.8[a]
2.0	0.2	-	-	86.7±6.7[b]	90.0±4.5[b]	161.3±5.4[b]	154.5±8.0[b]
2.0	-	0.2	-	93.3±4.2d	83.3±6.2[a]	158.2±9.4[b]	168.7±7.6[b]
2.0	-	-	0.2	60.0±7.3[ac]	66.7±8.4[a]	121.3±6.3[a]	116.8±6.9[a]

Data was arcsine transformed before ANOVA. Means followed by the same letters in the same column are not significantly different at $p<0.05$ according to Tukey's HSD test.

NAA or 4-CPA reduced the time for initiation of callusing by a day and triggered faster proliferation of callus. Callus fresh masses in augmented media were significantly larger ($p<0.05$) than those in media containing 2,4-D alone after 30 days in culture (Table 2). Embryos which had not formed callus by day seven remained non-responsive throughout the culture period. Callusing also failed to occur in both cultivars in medium containing 0.5 mg/l and lesser 2, 4-D.

Early separation of callusing embryos from the rest of the seed was crucial for further growth and maintenance of the callus probably because it removed the interfering influence of plant growth regulators emanating from the germinating seed. Except for calli from 1 and 2 mg/l 2,4-D alone, which had lots of roots on them by day seven (Day of first subculture), calli from all other treatments were non-morphogenic at this stage, with smooth, less nodular and relatively dry surfaces. Occasionally, watery and spongy calli was observed. Combinations of auxins (2,4-D and 4-CPA) and higher concentrations of 2, 4-D inhibited normal germination and produced callus with no roots. This is consistent with known effects of auxins (Wilkins, 1984). In single-auxin media, 2, 4-D was generally more superior to 4-CPA or NAA in callus induction (data not shown). Similar results have been reported by Hakan and Ismet (2004) and Miroshnichenko et al., (2013). In the study herein, combinations of NAA or 4-CPA with 2, 4-D improved somatic embryogenesis suggesting the importance of combining a superior auxin with less effective ones for synergy. The combination of 2 mg/l 2, 4-D with 0.2 mg/l of either 4-CPA or NAA proved beneficial for callus induction frequency, callus fresh mass, somatic embryogenesis and plant regeneration in both cultivars (Tables 2 and 3). Hakan and Ismet (2004) reported similar synergistic effect with a combination of 2, 4-D and NAA. Filippov et al. (2006) also reported improved somatic embryogenesis when either IAA, IBA or NAA were used in combination with dicamba.

Augmentation of 2 mg/l 2, 4-D with 0.2 mg/l TDZ resulted in browning and necrosis of calli from as early as seven days after subculture. However, the combination of 2 mg/l 2, 4-D with 0.2 mg/l BAP caused a significant reduction in callus induction frequency and fresh mass (Table 2). The inhibitory effects of these cytokinins on callus induction in the present study are in agreement with the findings of Rashid et al., (2002). This combination of BAP and 2, 4-D supported normal germination of seeds which inhibited callus induction.

By day 21, embryogenic callus fragments could easily be distinguished from those that were non-embryogenic. Embryogenic callus had relatively dry and nodular surfaces with visible white embryoids which quickly turned into green spots when the callus was sub-cultured to medium without PGRs (Figure 1a). Non-embryogic callus had watery surfaces without any organized structures (Figure 1b). This type of callus did not give shoots when sub-cultured to regeneration medium, although some turned green. Development of chlorophyll in non-embryonic calli is not unique to this study as similar results had been reported by Parmar et al., (2012). In some cases, a single callus had both embryogenic and non-embryogenic regions.

Frequency of somatic embryogenesis differed depending on the auxin concentration or combination and genotype (Table 3). Within a week of sub-culture of embryogenic calli to medium without PGRs in light, leaf-like structures started to develop from globular protrusions of the callus (Figure 1a). Most of these leaf-like structures did not however develop into plantlets. In fact, a higher percentage of calli which had been identified as embryogenic failed to regenerate any shoot resulting in generally low percentages of plantlet regeneration (Table 3). Regenerated shoot buds (Figure 1c) quickly elongated and developed roots when transferred to ½ MS medium without PGRs (Figure 1d)

Even though both wheat varieties showed a similar pattern of response in all stages of the culture process, genotypic differences were observed in the response to the different PGR concentrations and combinations. When 2,4-D was used alone, callus induction frequency for cv. Eagle 10 was optimum at 4 mg/l 2,4-D while for cv. Njoro BW II the optimum frequency was at 2 mg/l 2,4-D

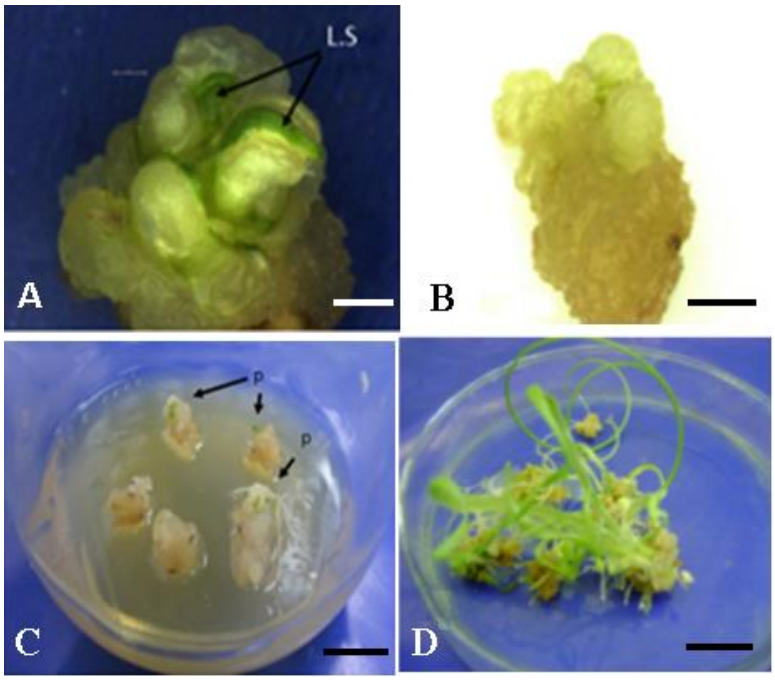

Figure 1. (**A**) compact, dry and friable appearance of embryogenic callus with green leafy structures (L.S) after 21 days of culture, (**B**) succulent and soft appearance of non-embryogenic callus after 21 days of culture. Scale bars = 1 mm. **(C)** shoot buds [p] developing from calli after 13 days of culture **(D)** Elongated shoots and roots after 21 days. Scale bars = 1 cm.

Table 3. Embryogenesis and plant regeneration responses of calli of wheat cv. Njoro BW II and Eagle 10 from different PGRs.

PGRs concentrations(mg/l)				% Embryogenic callus		% plant regeneration on hormone free MS medium	
2,4-D	4- CPA	NAA	BAP	Njoro BW II	Eagle 10	Njoro BW II	Eagle 10
1.0	-	-	-	33.3±9.9^{a}	33.3±6.7^{a}	16.7±6.2^{a}	20.0±5.2^{a}
2.0	-	-	-	40.0±7.3^{a}	43.3±6.2^{a}	30.0±8.6^{a}	33.3±9.9^{a}
4.0	-	-	-	33.3±8.4^{a}	53.3±6.7^{a}	23.3±10.9^{a}	26.7±6.7^{a}
8.0	-	-	-	20.0±7.3^{a}	23.3±6.2^{a}	16.7±6.2^{a}	20.0±10.3^{a}
2.0	0.2	-	-	63.3±6.2^{b}	56.7±6.2^{a}	43.3±6.2^{a}	36.7±9.5^{a}
2.0	-	0.2	-	46.7±8.4^{a}	50.0±11.3^{a}	33.3±9.9^{a}	33.3±8.4^{a}
2.0	-	-	0.2	33.3±6.7^{a}	40.0±10.3^{a}	20.0±7.3^{a}	23.3±9.5^{a}

Data was arcsine transformed before ANOVA. Means followed by the same letters in the same column are not significantly different at $p<0.05$ according to Tukey's HSD test.

(Table 2). Optimal callus fresh mass for both cultivars was in medium with 2 mg/l 2,4-D. When combinations of auxins were used, cv. Eagle 10 showed the best response in terms of callus induction frequency in the combination of 2 mg/l 2, 4-D + 0.2 mg/l 4-CPA while cv. Njoro responded best in the combination of 2 mg/l 2, 4-D and 0.2 mg/l NAA.

There are some previous reports on the unique response of different wheat genotypes to different media (Bi et al., 2007; Aydin et al., 2011; Parmar et al., 2012). The findings of the present study agree with these previous studies.

Conclusion

Combination of auxins was more superior in stimulating callus induction and somatic embryogenesis compared to single auxin treatments. *In vitro* regeneration of wheat is cultivar dependent. There is need for further work to

establish the optimal media and PGRs for other elite wheat cultivars bred in Kenya.

CONFLICT OF INTERESTS

The authors have not declared any conflict of interests.

REFERENCES

Aydin M, Tosun M, Haliloglu K (2011). Plant regeneration in wheat mature embryo culture. African Journal of Biotechnology 10(70):15749-15755.

Bi RM, Kou M, Chen LG, Mao SR, Wang H G (2007). Plant regeneration through callus initiation from mature embryo of Triticum. Plant breeding 126(1):9-12.

Bi R, Wang H (2008). Primary studies on tissue culture from mature embryos in diploid and tetraploid wheat. Frontiers of Agriculture in China 2(3):262-265.

Bouiamrine E, Diouri M, El-Halimi R (2012). Somatic embryogenesis and plant regeneration capacity from mature and immature durum wheat embryos. International Journal of Biosciences 2(9):29-39.

Choulet F, Alberti A, Theil S, Glover N, Barbe V, Daron J, Leroy P (2014). Structural and functional partitioning of bread wheat chromosome 3B. Science 345(6194):1249721. https://doi.org/10.1126/science.1249721

Clough SJ, Bent AF (1998). Floral dip: a simplified method for Agrobacterium-mediated transformation of *Arabidopsis thaliana*. The Plant Journal 16(6):735-743.

Çölgeçen H, Caliskan UK, Toker G (2011). Influence of different sterilization methods on callus initiation and production of pigmented callus in *Arnebia densiflora* Ledeb. Turkish Journal of Biology 35(4):513-520.

Dale J, Paul JY, Dugdale B, Harding R (2017). Modifying bananas: From transgenics to organics? Sustainability 9(3):333.

Darrier B, Rimbert H, Balfourier F, Pingault L, Josselin AA, Servin B, Sourdille P (2017). High-resolution mapping of crossover events in the hexaploid wheat genome suggests a universal recombination mechanism. Genetics 206(3):1373-1388. https://doi.org/10.1534/genetics.116.196014

Delporte F, Mostade O, Jacquemin JM (2001). Plant regeneration through callus initiation from thin mature embryo fragments of wheat. Plant Cell, Tissue and Organ Culture 67(1):73-80.

FAOSTAT (2017). Agriculture data. Available at http://faostat.Fao.org. Accessed on 10th June 2019 http://faostat

Filippov M, Miroshnichenko D, Vernikovskaya D, Dolgov S (2006). The effect of auxins, time exposure to auxin and genotypes on somatic embryogenesis from mature embryos of wheat. Plant Cell, Tissue and Organ Culture 84(2):213-222.

Hafeez I, Sadia B, Sadaqat NA, Kainth RA, Iqbal MZ, Khan IA (2012). Establishment of efficient in vitro culture protocol for wheat land races of Pakistan. African Journal of Biotechnology 11(11):2782-2790.

Miroshnichenko DN, Filippov MV, Dolgov SV (2013). Medium optimization for efficient somatic embryogenesis and *in vitro* plant regeneration of spring common wheat varieties. Russian Agricultural Sciences 39(1):24-28.

Miroshnichenko D, Chernobrovkina M, Dolgov S (2016). Somatic embryogenesis and plant regeneration from immature embryos of *Triticum timopheevii* Zhuk. and Triticumkiharae Dorof. et Migusch, wheat species with G genome. Plant Cell, Tissue and Organ Culture 125(3):495-508.

Murashige T, Skoog F (1962). A revised medium for rapid growth and bioassays with tobacco tissue cultures. Physiologia Plantarum 15(3):473-497.

Parmar SS, Sainger M, Chaudhary D, Jaiwal PK (2012). Plant regeneration from mature embryo of commercial Indian bread wheat (*Triticum aestivum* L.) cultivars. Physiology and Molecular Biology of Plants 18(2):177-183.

Rangaswamy R (2010). A textbook of agricultural statistics. New Age International Publishers, New Delhi 531 p.

Rashid H, Ghani RA, Chaudhry Z, Naqvi SMS, Quraishi A (2002). Effect of media, growth regulators and genotypes on callus induction and regeneration in wheat (*Triticum aestivum*). Biotechnology 1(1):49-54.

Redway FA, Vasil V, Lu D, Vasil IK (1990). Identification of callus types for long-term maintenance and regeneration from commercial cultivars of wheat (*Triticum aestivum* L.). Theoretical and Applied Genetics 79(5):609-617.

Repellin A, Båga M, Jauhar PP, Chibbar RN (2001). Genetic enrichment of cereal crops via alien gene transfer: new challenges. Plant Cell, Tissue and Organ Culture 64(2-3):159-183.

Sharma VK, Rao A, Varshney A, Kothari SL (1995). Comparison of developmental stages of inflorescence for high frequency plant regeneration in *Triticum aestivum* L. and *T. durum* Desf. Plant Cell Reports 15(3-4):227-231.

Stober A, Hessu D (1997). Spike pre-treatments, anther culture conditions and anther culture response of 17 German varieties of spring wheat (*Triticum aestivum* L.). Plant Breeding 116(5):443-447.

Teng WL, Sin T, Teng MC (2002). Explant preparation affects culture initiation and regeneration of Panax ginseng and Panax quinquefolius. Plant Cell, Tissue and Organ Culture 68(3):233-239.

Wilkins BM (1984). Advanced plant physiology. English Language Book Society/Longman. Avon.

Zale JM, Borchardt-Wier H, Kidwell KK, Steber CM (2004). Callus induction and plant regeneration from mature embryos of a diverse set of wheat genotypes. Plant Cell, Tissue and Organ Culture 76(3):277-281.

Related Journals: